Technische Universität Ilmenau

Fakultät für Informatik und Automatisierung

Fachgebiet Regelungstechnik

Dissertation

On-Line Path Planning and Robust Adaptive Path Following for Underactuated Autonomous Underwater Vehicles

zur Erlangung des akademischen Grades Doktoringenieur (Dr.-Ing.)

von

M.Sc. Remon Al Azrak

Gutachter: Prof. Dr.-Ing. Johann Reger
Gutachter: Univ.-Prof. Dipl.-Ing. Dr.techn. Martin Horn
Gutachter: Prof. Dr.-Ing. Robert Seifried

Tag der Einreichung: 08.05.2017
Tag der wissenschaftlichen Aussprache: 18.10.2017

"Give, and it will be given to you. A good measure, pressed down, shaken together and running over, will be poured into your lap. For with the measure you use, it will be measured to you"

Jesus Christ

ZUSAMMENFASSUNG

Autonome Unterwasservehikel (AUV) sind für den Einsatz in maritimen Gebieten mit harschen und lebensbedrohlichen Umgebungsbedingungen sowie langen Missionshorizonten unerlässlich. Die Planung solcher Missionen erfolgt dabei oft über einen übergeordneten Missionsplanungsalgorithmus, der auf Grundlage von Umgebungsdaten, wie z.B. Wetter-, Karten- und Sensordaten, Referenzwegpunkte generiert. Aufgrund zeitlich veränderlicher Missionsziele und dynamisch variierender Hindernisse, wie z.B. andere Seefahrzeuge, ist eine flexible Anpassung dieser Referenzwegpunkte zur Laufzeit unvermeidlich. Da in den meisten Anwendungsfällen eine möglichst genaue Durchquerung der Wegpunkte mit vertretbarem Stellaufwand gewünscht ist, fokussiert diese Dissertation auf die Bahnführung von AUV, die durch eine Kombination aus on-line Bahnplanung und nichtlinearen Folgeregelungskonzepten besteht.

Wegen der Anforderungen von Folgeregelungen an die Glattheit der Referenzbahn (C^2) werden im ersten Teil dieser Arbeit zunächst 3D Bahnplanungsalgorithmen auf Basis von Polynomen 5. Grades vorgestellt, welche die von der Missionsplanung vorgegebenen Wegpunkte interpolieren. Zur Verbesserung der numerischen Eigenschaften sowie der Reduzierung des Rechenaufwands wird dieser Ansatz auf B-Splines übertragen. Durch eine spezielle Pufferung/Fensterung einer bestimmten Anzahl an Wegpunkten wird die zusätzliche Anforderung an die on-line Planung adressiert.

Im zweiten Teil der Arbeit werden ausgehend von einer eingehenden mathematischen Modellbildung von AUVs nichtlineare Folgeregelungskonzepte für den vollaktuierten und den unteraktuierten Fall (mehr Freiheitsgrade als Stellgrößen) entwickelt. Für ersteren wird eine Feedback-Linearisierung mit beobachterbasiertem Ansatz und aktiver Störunterdrückung präsentiert. Für den zweiten Fall wird ein robustes, adaptives Regelgesetz zur Kompensation von Modellunsicherheiten und Störungen entworfen. Wegen der Unteraktuierung des Systems, stellt dies eine anspruchsvolle Aufgabe dar, welche basierend auf der direkten Methode von Lyapunov und adaptiver Backstepping-Verfahren gelöst wird. Zur Robustifizierung des adaptiven Reglers kommen Parameter-Projektions-Techniken zum Einsatz.

Abschliessend werden formale Nachweise der Stabilität der präsentierten Regelungen angeführt und die Leistungsfähigkeit der entwickelten Ansätze anhand von detaillierten Simulationen belegt.

ABSTRACT

Autonomous underwater vehicles (AUVs) are indispensable for use in maritime areas with harsh and life-threatening environmental conditions as well as long mission horizons. The planning of such missions is often carried out via a generic mission planning algorithm. Based on environmental data, e.g. weather, map and sensor data, it generates position reference points or so-called way-points to be followed by the AUV. Due to time-varying mission objectives and dynamically varying obstacles, such as other maritime vehicles, a flexible on-line adaptation of these way-points is unavoidable. In addition, for most applications an accurate crossing of way-points is desirable. Therefore, this dissertation focuses on the path generation and following of AUVs, which consists of a combination of on-line path planning and nonlinear path following concepts.

Due to the special requirements for path following controllers on the smoothness of the reference path (C^2), in the first part of this thesis, we present a 3D path planning algorithm based on degree 5 polynomials which interpolates the way-points given by the mission planning. In order to improve the numerical properties and to reduce the computational effort, this approach is transferred to B-splines. Using a special buffering/windowing of a certain number of way-points, the additional requirement on the on-line planning is addressed.

In the second part of the thesis, mathematical modeling of AUVs is carried out. Based on that, nonlinear path following control concepts for the fully-actuated and the underactuated case (more degrees of freedom than control inputs) are developed. For the former, a feedback linearization controller with an observer-based approach and active disturbance rejection capabilities is presented. For the second case, a robust, adaptive control law is developed for the compensation of modeling uncertainty and disturbances. Owing to the underactuation of the system, the controller design is a challenging task, which is solved based on the direct method of Lyapunov and adaptive backstepping techniques. Moreover, parameter projection is used to robustify the adaptive controller.

Finally, formal proofs of the stability of the presented controllers are provided and the performance of the developed approaches is demonstrated by means of detailed simulations.

DANKSAGUNG

Table of Contents

List of Figures

List of Tables

To Lama, Ralf and my Parents

CHAPTER 1

Introduction

Due to the growing need to explore and operate in risky, dangerous and extreme deep underwater environments, for civil or military purposes, the study of the Autonomous Underwater Vehicles (AUVs) and their related control techniques becomes more and more popular and an attractive research field [1, 2]. The wide range of applications of the AUVs in hard and hazardous environments, such as the exploration of oil and other underwater resources, inspection and studying of the water quality and fish feeding, has increased the effort to study AUVs in robotics and control research in the past two decades [3, 4, 5].

In this chapter, we expose in the first section the state of the art for the path planning and control approaches of the AUVs, then we introduce the main contributions of this thesis, in the last section, we explore the structure of this work.

1.1 State of the Art

The key problem of the AUVs is actually the planning of the path and the associated trajectories. The path following problem can be expressed by means of two tasks: The geometric task, which is concerned with the position of the vehicle, that must track a desired path, which is parametrized by a so-called path variable σ, and the dynamic task, that forces the velocity of the vehicle to converge to a desired velocity profile. The combination of both above mentioned tasks refers to the trajectory tracking. Moreover, the path following approach can be restricted to a trajectory tracking one by predefining the path variable σ as a function of time. Therefore, more flexibility can be gained from utilizing the path following approach compared to trajectory tracking [6, 7, 8].

The AUV path planning problem can be solved off-line if prior information of the underwater environment is available [9, 10]. On the other hand, this problem can be conceived

under lack of information about the environment in which the AUV moves. The path planning algorithm may be adapted to generate the path on-line as in [11, 12].

Due to their optimality, the Dubins curves (interpolations) are widely used in the 3D path planning for the AUVs and UAVs (Unmanned Aerial Vehicles) [13, 14]. Actually, the Dubins curves interpolate a set of data-points by concatenation of circular arcs of maximum curvature (minimum radius) and straight lines (their tangents) [15].

Owing to their simplicity, the polynomial interpolation is wildly used in the path planning, but some downsides come into sight in such polynomials like oscillations, which increase with the degree of the polynomial (related to the number of the interpolated data-points and the boundary conditions), as well the Runge's phenomenon. Those disadvantages can be avoided by utilizing the piecewise interpolation (splines) and the Chebyshev interpolation [16, 17]. Another approach in this field are the Hermite polynomials which represent curves that do not include wiggling or zigzagging since the way-points can only be represented by a non-smooth function [18, 19, 20].

The path following problem in underactuated marine vehicles (ships and submarines) has been researched extensively. For example in ships, despite of availability of just two controls, surge force and yaw moment, the controllers can steer the ship to follow a designed 2D path using two independent aft thrusters or with one main aft thruster and a rudder [21]. The stabilization problem of underactuated ships has been investigated in [22, 23, 24, 25].

Utilizing the feedback linearization, the output tracking controller of ships was designed in [26] and [27]. This controller guarantees the global exponential stability of the reference trajectories. Here, both position variables converge to their reference trajectories while the control of the course angle was not achieved. In [28], the nonlinear ship model is used to design a controller which guarantees the global exponential stability in some arbitrarily small neighborhood about of the desired trajectory for the position as well as for the course angle.

The ship model is transformed into a triangular-like form using a coordinate transformation [21]. That allows to use the integrator backstepping technique to find a tracking controller, which guarantees an exponential stability of the desired trajectory.

In [29] a methodology was presented for integrated design of guidance and control systems for autonomous vessels. This methodology was actually borrowed from the theory of gain-scheduling control and leads to design of a tracking controller for the unmanned

2

aerial vehicles.

For a simplified underactuated ship model, in [30] a feed-forward technique combined with linear quadratic regulator has been introduced to solve the control task. Moreover a nonlinear model predictive controller was designed to obtain local results on "track-keeping".

In [7] a robust recursive controller was developed for uncertain nonlinear plants in the strict-feedback form. The output maneuvering problem was addressed in two tasks. In the first one, the system output is forced to converge to a reference parametrized path and the second is to satisfy a desired dynamic behavior along the path, i.e. the system output has to follow the desired velocity.

In [31] a methodology based on Lyapunov theory and backstepping techniques was proposed to design a 3D path following controller for the AUVs in the Serret-Frenet path frame. The proposed controller guarantees a global convergence to a small arbitrary neighborhood about the desired paths, but not at the origin due to the kinematic singularity at this point.

For fully-actuated and underactuated AUVs the problem of path following was presented in [6]. There, a novel guidance-based approach was used to design a nonlinear controller, which consists of a model-based velocity and an attitude controller.

In the presence of model uncertainties, the problem of position trajectory tracking and path following for underactuated autonomous vehicles was presented in [32] where an adaptive switching and a nonlinear Lyapunov-based tracking controllers were combined to force the position tracking error to converge to an arbitrarily small neighborhood about of the origin.

The Receding Horizon Controller (RHC) of a nonholonomic mobile robots was extended to deal with the tracking control problem of a group of underactuated AUVs in [33].

In presence of the constant ocean current, a control approach was presented in [34] to allow underactuated underwater vehicles to follow a 3D straight line. The proposed controller was designed based on a modified three-dimensional Line-of-Sight (LOS) algorithm with an integral action controller.

The control strategy of AUVs introduced in [35], which is borrowed essentially from [36] and [37], is a combination of the conventional path following and trajectory tracking control. The proposed controller is designed using Lyapunov's direct method to stabilize

the kinematics of the AUV. This controller is extended to control the dynamics of AUVs based on the backstepping technique. The resulting nonlinear control law guarantees a global asymptotic convergence of the AUV to the desired path.

1.2 Contribution of the Dissertation

Since, the guidance and the navigation do not belong to this work, we focus on the path/ trajectories generation based on the data-points (way-points) that are provided from a guidance generator which delivers the way-points on-line according to weather and obstacles information.

The main contributions of this work can be summarized in the following points:

- On-line path planning

  - Polynomial splines: A flexible on-line trajectory planning algorithm is discussed. For dynamically allocated way-points and surge velocities, an on-line algorithm computes polynomials of degree 5 that smoothly link the paths between these way-points. Iteratively, the algorithm interpolates the way-points within a certain window. This window is shifted point by point to cover all of the considered points and generates the desired path.

  - B-splines: To enhance the numerical robustness for the above mentioned algorithm, modifications of B-spline interpolation are employed, which significantly reduce the computational cost.

- Combination of the on-line path planning algorithm with controller for

  - Fully-actuated case: Based on feedback linearization a PD-controller is designed to force the AUV to follow the reference path. For the attenuation of large disturbances a generalized extended state observer (GESO) is employed, that helps improve the tracking performance.

  - Underactuated case: In presence of modeled and unmodeled uncertainties in the AUV, an adaptive robust backstepping controller is designed to steer

the AUV to an arbitrarily small neighborhood about the on-line generated reference path and to force the AUV to move along the path with a desired speed profile. The unknown plant parameters are estimated on-line, to avoid parameter drifts due to the time-varying disturbance. A Lipschitz continuous projection algorithm is used for updating the estimate of the unknown parameters. Figure 1.1 shows the proposed path generation and the control algorithm which are developed in this work. The controller lets the perturbed AUV follow the desired position $\boldsymbol{\eta}_{\mathrm{d}}$ and the desired orientation $\boldsymbol{\gamma}_{\mathrm{d}}$ with desired velocity u_0.
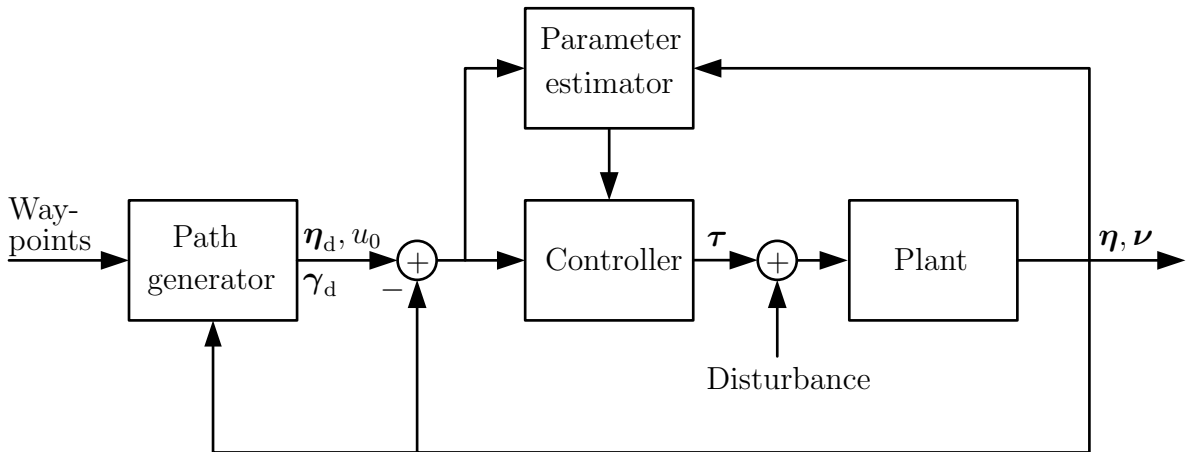
Fig. 1.1: Block diagram of path generator and path following controller

- Mathematically rigorous stability proofs: A main contribution of this work is the formal and detailed proofs of the closed-loop stability, which have not been provided in the literature before.

1.3   Organization of the Dissertation

The dissertation is divided into the following chapters:

- Chapter 1, Introduction: This chapter gives an overview about the existing path planning techniques and path following methods for autonomous vessels.

- Chapter 2, On-Line Path Planning: In this chapter we discuss techniques of generating the reference path for an AUV using the polynomial splines and the B-splines interpolation.

- Chapter 3, Modeling of Marine Vessels: This chapter deals with the kinematics and dynamics of the AUV, and introduces some simplification of dynamic modeling due to the geometric features of the considered underwater vehicle.

- Chapter 4, Previous Approaches for the Fully-Actuated AUVs: In this chapter, we devise a tracking controller which compensates the nonlinearities of the rigid-body dynamics and renders it linear in closed-loop. For the attenuation of large disturbances the generalized extended state observer is employed to improve the tracking performance.

- Chapter 5, Controller Design: This chapter is concerned with the design of a path following controller. The first part of this chapter explains the necessity of using an adaptive feedback control in lieu of the static feedback one and then states the idea of the robust adaptive controller. Hereafter, the second and the third parts illustrate the robust adaptive backstepping technique and the projection operator. In the next part we define the path following problem in the error coordinates. Finally, in the last part of this chapter, relying on the robust adaptive backstepping approach we design a tracking controller for the considered AUV.

- Chapter 6, Stability Analysis: In this chapter we analyze in detail the stability of the complex closed-loop system. To this end, we divide the entire system into subsystems, then we investigate extensively the stability of each regarded subsystem.

- Chapter 7, Simulation Results: We demonstrate the effectiveness of the proposed path planning and control schemes. Moreover, the robustness under modeled and unmodeled uncertainties for on- and off-line path planning is validated.

- Chapter 8, Conclusions: In this chapter we conclude this thesis and list some recommendations for prospective work and future research.

- Chapter 9, Appendix: Finally, simulation studies on real-world vehicle data underscore the usability of the advocated approach for the fully-actuated AUV.

CHAPTER 2

On-Line Path Planning

In way-point guidance systems for marine vessels, depending on the weather and obstacle information, the guidance and navigation systems generate Cartesian way-points to be followed by both ships and underwater vehicles. In this work, we limit ourselves to the path/trajectory generation relying on the way-points, which are supplied on-line from the guidance system.

Owing to its benefit in avoiding the problem of Runge's phenomenon and the undesired oscillations, which can occur between interpolated points if high degree polynomials are used, the spline (piecewise interpolation) is prevalently preferred over the polynomial interpolation. Figure 2.1 exemplifies the overall function $s(\sigma)$ (spline trajectory) of the path variable σ which interpolates $N + 1$ points [38, 39, 40].
Depending on the required degree of continuity of $s(\sigma)$ at the considered points q_k for $k = 1, \ldots, N - 1$, the adequate polynomial degree at each segment between each consecutive two points q_k and q_{k+1} is chosen. In order to obtain the continuity of velocities and accelerations at the σ_k instants, polynomials of degree five must be used.

To this end, we introduce an on-line capable technique which generates an appropriate path of the way-points. The basic idea of our approach is to define a window (buffer) that comprises a certain number of way-points that are interpolated (spline interpolation). Then, the first segment in the window (between first and second point in the window) is dispatched to the control system. Afterwards, in the next step we shift this window by one point and reiterate the process until the very last point in the mission is reached.

For C^2 continuity the polynomial interpolation can be used, but for a high number of way-points, numerical problems may crop up. Therefore, the B-splines (Basis-Splines) can be used to contribute to more numerical robustness and to downgrade the computational cost within calculation of the on-line path.
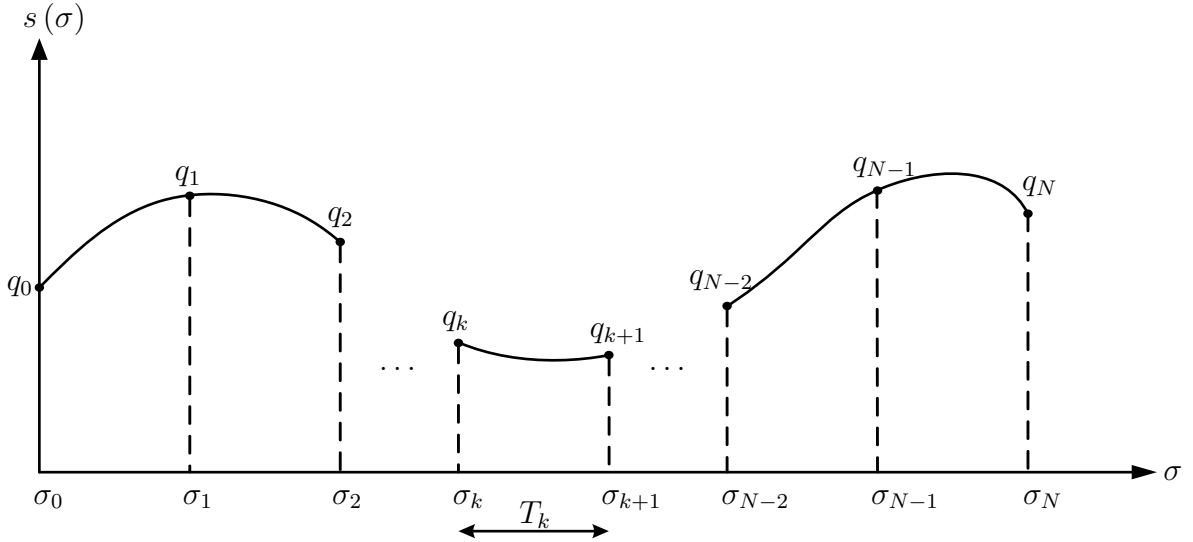
Fig. 2.1: A spline interpolation of $N + 1$ way-points

2.1 On-Line Path Planning using Polynomial

Due to their apparently uncomplicated computational features, piecewise polynomials are widely used to generate the paths for the marine vessels [41]. According to the requirements of our control approach, C^2 continuity is needed in the reference path. Therefore, the use of polynomials with degree five is a convenient choice since we have four boundary conditions at each segment (two for the velocity and two for the acceleration) [42]. Moreover, depending on the generated path and by imposing the desired surge velocity profile u_0, the time dependent reference trajectories on the X, Y and Z axes are created.

The challenge is how to generate an appropriate path when new way-points are subjoined on-line to the predefined way-points, that is, during the mission. Four way-points are considered to generate a twice continuously differentiable function of σ that satisfies the boundary conditions for the velocity and acceleration at the way-points. Therefore, three polynomials with degree five are generated for the considered window where four way-points are regarded in each window. In each iteration (window/buffer), just the first polynomial (between the first and the second way-point) is considered, and the two polynomials (between second way-point and third way-point) as well as the polynomial (between third way-point and fourth way-point) are neglected as long as the fourth way-point is not the last one in the mission. Iteratively, we get a polynomial for each

new added way-point to the path. When the last point in the mission is reached then the three polynomials interpolated between the four considered way-points are taken into account. In other words, for all iterations just the first polynomial (between first and second point in the considered window) is regarded, but for the last iteration all of the three polynomials need to be regarded.

Figure 2.2 illustrates the algorithm for the generation of the polynomial $s(\sigma)$ referring to $N + 1 = 6$ way-points: In the first iteration $j = 1$, merely the polynomial of degree 5 (with its parameter vector $\mathbf{p}_0^1$) is considered, whereas for $j = 2$ just $\mathbf{p}_1^2$ is considered. However in the last iteration $j = 3$ are regarded $\mathbf{p}_2^3, \mathbf{p}_3^3$ and $\mathbf{p}_4^3$ and build together the desired function for this window.

Therefore, the polynomials parameter vectors $\mathbf{p}_0^1, \mathbf{p}_1^2, \mathbf{p}_2^3, \mathbf{p}_3^3$ and $\mathbf{p}_4^3$ construct the entire desired function between q_0 and way-point q_5. Since the vectors $\mathbf{p}_0^1$, $\mathbf{p}_1^1$ and $\mathbf{p}_2^1$ are calculated in the first iteration, thus, the demanded initial velocity and acceleration for the next iteration in the way-point q_1 can be computed. The velocity and acceleration in the first way-point (in the first iteration) is regarded as an initial velocity and acceleration for the second one, and the velocity and acceleration in the first way-point (in the second iteration) is considered as a initial velocity and initial acceleration for the third one, and so forth. This means, that the boundary conditions for velocity and acceleration are guaranteed in each way-point and subsequently, we get a twice continuously differentiable function between the starting way-point q_0 and the final one q_5.
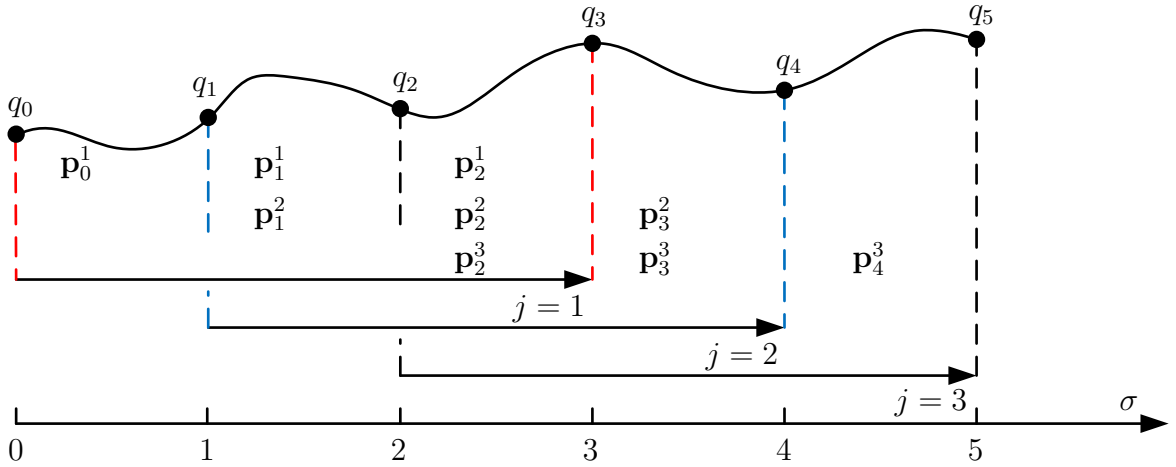
Fig. 2.2: On-line path planning

Generally, we apply the above presented approach for generating a function which interpolates $N+1$ way-points. For this purpose, let us consider that the polynomial between

two successive points for jth window is given through

$$s_i^j(\sigma) = p_{i,5}^j\sigma^5 + p_{i,4}^j\sigma^4 + p_{i,3}^j\sigma^3 + p_{i,2}^j\sigma^2 + p_{i,1}^j\sigma + p_{i,0}^j \tag{2.1}$$

for $i = 0, \ldots, N-1, j = 1, \ldots, N-2$, where N is the number of the polynomials, σ is the path variable and the parameter vector is

$$\mathbf{p}_i^j = \left(p_{i,5}^j, p_{i,4}^j, p_{i,3}^j, p_{i,2}^j, p_{i,1}^j, p_{i,0}^j\right). \tag{2.2}$$

By applying this algorithm we calculate the desired trajectories $x_\mathrm{d}(\sigma), y_\mathrm{d}(\sigma)$ and $z_\mathrm{d}(\sigma)$ of the path variable σ, consequently, we compute on-line the desired 3D underwater path for the AUV. To this end, the functions $x_d(\sigma), y_d(\sigma)$ and $z_d(\sigma)$ can be expressed through the polynomials

$$x_{i,\mathrm{d}}^j(\sigma) = a_{i,5}^j\sigma^5 + a_{i,4}^j\sigma^4 + a_{i,3}^j\sigma^3 + a_{i,2}^j\sigma^2 + a_{i,1}^j\sigma + a_{i,0}^j \tag{2.3}$$

$$y_{i,\mathrm{d}}^j(\sigma) = b_{i,5}^j\sigma^5 + b_{i,4}^j\sigma^4 + b_{i,3}^j\sigma^3 + b_{i,2}^j\sigma^2 + b_{i,1}^j\sigma + b_{i,0}^j \tag{2.4}$$

$$z_{i,\mathrm{d}}^j(\sigma) = c_{i,5}^j\sigma^5 + c_{i,4}^j\sigma^4 + c_{i,3}^j\sigma^3 + c_{i,2}^j\sigma^2 + c_{i,1}^j\sigma + c_{i,0}^j \tag{2.5}$$

with the parameter vectors at the jth iteration

$$\begin{aligned}\mathbf{a}_i^j &= \left(a_{i,5}^j, a_{i,4}^j, a_{i,3}^j, a_{i,2}^j, a_{i,1}^j, a_{i,0}^j\right) \\ \mathbf{b}_i^j &= \left(b_{i,5}^j, b_{i,4}^j, b_{i,3}^j, b_{i,2}^j, b_{i,1}^j, b_{i,0}^j\right) \\ \mathbf{c}_i^j &= \left(c_{i,5}^j, c_{i,4}^j, c_{i,3}^j, c_{i,2}^j, c_{i,1}^j, c_{i,0}^j\right)\end{aligned} \tag{2.6}$$

where i refers to the first way-point of the four considered way-points in the jth iteration, and i starts at the value $i = j - 1$. For example, for second iteration ($j = 2$), the indices of the regarded four way-points are $1, 2, 3$ and 4 (we start at point 1). For each iteration j the four way-points $q_i, q_{i+1}, q_{i+2}, q_{i+3}$ are considered to obtain the coefficients for the three polynomials between those points to incorporate the boundary conditions at each way-point as well as at start and end way-points.

Now, we define the parameter vectors for position, velocity, acceleration, jerk and snap regarding to the path variable σ as

$$\mathbf{p}(\sigma_j) = \left((\sigma_j)^5, (\sigma_j)^4, (\sigma_j)^3, (\sigma_j)^2, \sigma_j, 1\right), \tag{2.7}$$

$$\mathbf{v}(\sigma_j) = \left(5(\sigma_j)^4, 4(\sigma_j)^3, 3(\sigma_j)^2, 2\sigma_j, 1, 0\right), \tag{2.8}$$

$$\mathbf{a}(\sigma_j) = \Big(20(\sigma_j)^3, 12(\sigma_j)^2, 6\sigma_j, 2, 0, 0\Big), \tag{2.9}$$

$$\mathbf{r}(\sigma_j) = \Big(60(\sigma_j)^2, 24(\sigma_j), 6, 0, 0, 0\Big), \tag{2.10}$$

$$\mathbf{s}(\sigma_j) = \Big(120(\sigma_j), 24, 0, 0, 0, 0\Big). \tag{2.11}$$

Then, the procedure of the on-line path planning motioned above can be applied within the jth window, and the coefficients of the regarding parameter vectors $\mathbf{q}^j_{\mathrm{coeff}} = \Big(\mathbf{p}^j_{j-1}, \mathbf{p}^j_j, \mathbf{p}^j_{j+1}\Big)^\top$ are obtained by solving the following linear system:

$$\mathbf{q}^j_{\mathrm{coeff}} = \mathbf{A}^{-1} \mathbf{q}^j_{\mathrm{way}} \tag{2.12}$$

where

$$\mathbf{A}(\sigma_j, \ldots, \sigma_{j+3}) = \left(\begin{array}{ccc}
\mathbf{a}(\sigma_j) & \mathbf{O} & \mathbf{O} \\
\mathbf{v}(\sigma_j) & \mathbf{O} & \mathbf{O} \\
\mathbf{p}(\sigma_j) & \mathbf{O} & \mathbf{O} \\
\hline
\mathbf{p}(\sigma_{j+1}) & \mathbf{O} & \mathbf{O} \\
\mathbf{O} & \mathbf{p}(\sigma_{i+1}) & \mathbf{O} \\
-\mathbf{v}(\sigma_{j+1}) & \mathbf{v}(\sigma_{j+1}) & \mathbf{O} \\
-\mathbf{a}(\sigma_{j+1}) & a(\sigma_{j+1}) & \mathbf{O} \\
-\mathbf{r}(\sigma_{j+1}) & \mathbf{r}(\sigma_{j+1}) & \mathbf{O} \\
-\mathbf{s}(\sigma_{j+1}) & \mathbf{s}(\sigma_{j+1}) & \mathbf{O} \\
\hline
\mathbf{O} & \mathbf{p}(\sigma_{j+2}) & \mathbf{O} \\
\mathbf{O} & \mathbf{O} & \mathbf{p}(\sigma_{j+2}) \\
\mathbf{O} & -\mathbf{v}(\sigma_{j+2}) & \mathbf{v}(\sigma_{j+2}) \\
\mathbf{O} & -\mathbf{a}(\sigma_{j+2}) & \mathbf{a}(\sigma_{j+2}) \\
\mathbf{O} & -\mathbf{r}(\sigma_{j+2}) & \mathbf{r}(\sigma_{j+2}) \\
\mathbf{O} & -\mathbf{s}(\sigma_{j+2}) & \mathbf{s}(\sigma_{j+2}) \\
\hline
\mathbf{O} & \mathbf{O} & \mathbf{a}(\sigma_{j+3}) \\
\mathbf{O} & \mathbf{O} & \mathbf{v}(\sigma_{j+3}) \\
\mathbf{O} & \mathbf{O} & \mathbf{p}(\sigma_{j+3})
\end{array}\right) \in \mathbb{R}^{18 \times 18}$$

where

$$\mathbf{O} = \Big(0, 0, 0, 0, 0, 0\Big) \tag{2.13}$$

and

$$\mathbf{q}_{\text{way}}^{j} = \left(a_j, v_j, q_j, q_{j+1}, q_{j+1}, 0, 0, 0, 0, q_{j+2}, q_{j+2}, 0, 0, 0, 0, 0, 0, q_{j+3} \right)^{\top} \tag{2.14}$$

where the values q_j, v_j and a_j represent respectively the position, velocity and the acceleration at the considered points.

It is profitable in this context to refer to two points, first, that the start velocity v_i as well as the start acceleration a_i can be calculated from the previous iteration, and second, that the end velocity and end acceleration for each iteration is zero. In the light of this consideration we can define a frame with specific features to be shifted over the entire range of the way-points, iteratively, where initial values of velocity and acceleration at the start of the mission can be set by the user, and the final velocity and acceleration are set to be zero, i.e. "end of the mission". Thus, for a mission consisting of four way-points in the jth iteration, we obtain a vector of 18 polynomial coefficients and the considered path will be described through three resulting polynomials. Once a new way-point is available, only the first polynomial is regarded and the two others are neglected such that the algorithm may be iterated again for four way-points. The first three of them are the last three points of the previous iteration and the fourth one is the new added way-point. The iteration starts from the $(i+1)$th way-point and ends in the $(i+5)$th way-point. It means that for any new way-point added on-line to the path, a suitable intermediate path will be generated. For a 2D plane, only the polynomials (2.3) and (2.4) are considered to generate the desired path, that interpolates the given way-points in the Cartesian plane.

The generated path of the path variable σ is transformed to a time dependent trajectory by imposing the desired surge velocity profile u_0 (assuming roll and pitch equal to zero). It can be shown that σ may be obtained as the solution of the scalar differential equation

$$\dot{\sigma} = \frac{u_0(t)}{\sqrt{\left(\partial x_{\text{d}}(\sigma)/\partial \sigma \right)^2 + \left(\partial y_{\text{d}}(\sigma)/\partial \sigma \right)^2 + \left(\partial z_{\text{d}}(\sigma)/\partial \sigma \right)^2}} \tag{2.15}$$

where u_0 is the desired tangent velocity profile, which the AUV moves along the generated path $(x_{\text{d}}, y_{\text{d}}, z_{\text{d}})$. Thus, with the solution $\sigma = \sigma(t)$ we obtain a coordinate description in terms of time, hence trajectories, $x_{\text{d}} = x_{\text{d}}(t)$, $y_{\text{d}} = y_{\text{d}}(t)$ and $\psi_{\text{d}} = \psi_{\text{d}}(t)$.

For a 3D path planning, the polynomials (2.3), (2.4) and (2.5) are taken into consideration to generate the path variable $\sigma(t)$ as a function of time.

Although this approach is relatively uncomplicated to implement, numerical problems may occur in the implementation if the number of the considered way-points is relativity high. Therefore, to improve the numerical features of this approach, we introduce the B-splines technique, which leads to more robust calculation of the desired path even for a high number of interpolated way-points.

2.2 On-Line Path Planning using B-Splines

Increasing the number of interpolated way-points using piecewise polynomials may lead to a numerical problem. To avoid this problem, an efficient and numerically robust technique for the calculation of splines by utilizing so-called *B-splines* or *Basic-splines* is presented in this section. Due to their positive geometrical features, they are particularly suitable for the calculation of multidimensional curves. In many real-world industrial applications, the determination of the geometric path is often constructed by means of motion primitives, such as straight lines, arcs, etc. Regrettably, when linear and arcual motions are mixed in order to obtain complex paths, discontinuities in the acceleration profile are unavoidable.

Only in the case of zero velocity at the transition points between linear and circular motions the problem of the discontinuity can be avoided, but this is not always desired in many real-word applications. A feasible alternative approach is relying on approximating the path with an ultimately continuous function, for instance based on B-spline curves. There, the desired path (consists of primitives, such as straight lines, circles) can be sampled, and then interpolated using B-splines. Thus, the problem of the discontinuity in the acceleration is effectively avoided [43, 44, 39].

As we mentioned before, the most important advantage of using the B-splines technique is the avoidance of the numerical problems during the on-line calculation of the inverse of the matrix (2.1), that means, it is not a problematic issue to use a high number of way-points (samples of the desired path), which means in turn, that the desired path can be appropriately approximated since we are not restricted by using a maximum number of way-points in each regarded window. Moreover, the manifest benefit of the B-splines is that the resulting matrix is the same for each iteration which decisively reduces the calculation complexity.

The B-spline functions are given as a linear combination of a proper number of basis

functions [39]

$$s(\sigma) = \sum_{l=0}^{\bar{m}} p_l B_l^g(\sigma), \quad \text{defined for} \ \ \sigma_{\min} \leq \sigma \leq \sigma_{\max}, \tag{2.16}$$

where $s(\sigma)$ is the B-spline curve which interpolates the way-points and p_l is the coefficient (control point), which is calculated based on the values of the way-points, and $B_l^g(\sigma)$ is the B-spline basis function of degree g, which is determined from the values of the path variable (the independent variable σ) at the considered way-points. The number $\bar{m}$ is determined relying on the so-called knots vector which can be defined in different ways [39]. The knots vector can be set up according to the degree of the basis function g as follows:

If g is an even number then the knots vector is given through

$$\boldsymbol{\sigma}_{\text{knot}} = \left(\underbrace{\sigma_0, \ldots, \sigma_0}_{g+1}, \frac{\sigma_0 + \sigma_1}{2}, \ldots, \frac{\sigma_{k-1} + \sigma_k}{2}, \ldots, \frac{\sigma_{N-1} + \sigma_N}{2}, \underbrace{\sigma_N, \ldots, \sigma_N}_{g+1} \right) \tag{2.17}$$

with $k = 2, \ldots, N - 1$. In this case, the number $\bar{m}$ is given as summation of the degree of the B-spline function g and the number of the interpolated way-points N, that is $\bar{m} = N + g$.

For odd g, the knots vector is taken as

$$\boldsymbol{\sigma}_{\text{knot}} = \left(\underbrace{\sigma_0, \ldots, \sigma_0}_{g+1}, \sigma_1, \ldots, \sigma_{N-1}, \underbrace{\sigma_N, \ldots, \sigma_N}_{g+1} \right) \tag{2.18}$$

where for this case $\bar{m} = N + g - 1$.

Actually, one is free to choose the knots vector either according to (2.17) or (2.18), but for better interpolation results it is preferred to utilize (2.17) for odd degree and (2.18) for even degree [45].

The lth B-spline basis function of degree g can be determined iteratively using "De Boor's algorithm" as per:

For the degree 0 we have:

$$B_l^0(\sigma) = \begin{cases} 1, & \text{for} \ \ \sigma_l \leq \sigma \leq \sigma_{l+1} \\ 0, & \text{otherwise} \end{cases} \tag{2.19}$$

14

and generally, the basic function of degree g is given as

$$B_l^g(\sigma) \;=\; \frac{\sigma - \sigma_l}{\sigma_{l+g} - \sigma_l} B_l^{g-1}(\sigma) + \frac{\sigma_{l+g+1} - \sigma}{\sigma_{l+g+1} - \sigma_{l+1}} B_{l+1}^{g-1}(\sigma), \quad g > 0. \tag{2.20}$$

According to the relationships (2.19), (2.20) and (2.17) we can determine, for example, the basis function of degree $g = 1$ and $g = 2$, for 4 sampling points at time instants $(0, 1, 2, 3)$. The number of splines for $g = 1$ is $\bar{m} = 4$, and for $g = 2$ is $\bar{m} = 5$ as Figure 2.3 shows. The piecewise polynomial $B_l^g(t)$ is defined $\forall t \in [0, 3]$ and is equal to zero everywhere except for the interval $t \in [t_l, t_{l+g+1}]$ of the considered knots vector. The knots vector t_{knot} for $g = 1$ is given by $t_{\text{knot}} = (0, 0, 0.5, 1.5, 2.5, 3, 3)$ and for $g = 2$ it is $t_{\text{knot}} = (0, 0, 0, 0.5, 1.5, 2.5, 3, 3, 3)$.
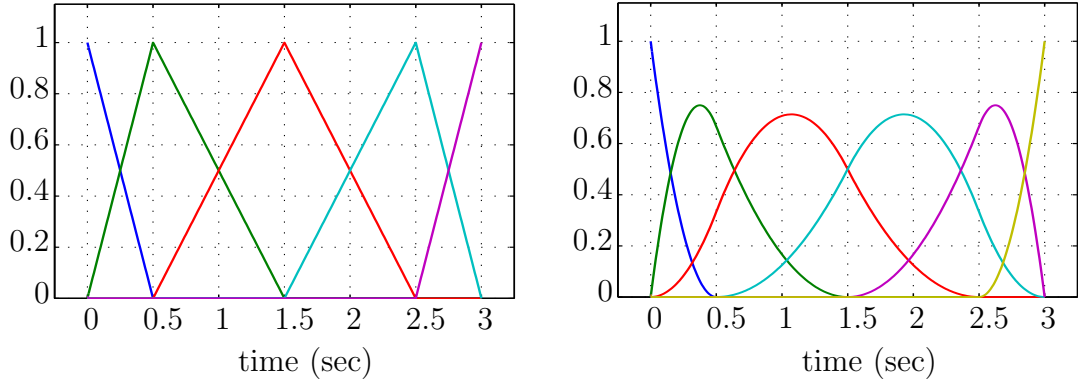
Fig. 2.3: B-spline basis functions of degree one and two

The derivative of the B-splines polynomial $s(\sigma)$ reads

$$s(\sigma)^{(1)} = \sum_{l=0}^{\bar{m}} p_l B_l^{g(1)}(\sigma), \quad \sigma_{\min} \leq \sigma \leq \sigma_{\max}. \tag{2.21}$$

The calculation of the kth derivative for the basis functions yields

$$B_l^{g(n)}(\sigma) = \frac{g!}{(g-n)!} \sum_{i=0}^{n} b_{n,i} B_{l+i}^{g-n}(\sigma) \tag{2.22}$$

with

$$b_{0,0} = 1, \quad b_{n,0} = \frac{b_{n-1,0}}{\sigma_{l+g-n+1} - \sigma_l}, \quad b_{n,i} = \frac{b_{n-1,i} - b_{n-1,i-1}}{\sigma_{l+g+i-n+1} - \sigma_{l+i}}, \quad i = 1, ..., n-1,$$

15

and $b_{n,n} = \dfrac{-b_{n-1,n-1}}{\sigma_{l+g+q} - \sigma_{l+n}}$.

The B-spline function is given as a sum of multiplications of polynomial parameters by the basis functions (B-spline) at the instant σ_k as

$$s\left(\sigma_k\right) = \sum_{l=0}^{\bar{m}} p_l B_l^g\left(\sigma_k\right) \tag{2.23}$$

and the nth derivative of B-spline polynomial at the considered point σ_k is given through

$$s^{(n)}(\sigma_k) = \sum_{l=0}^{\bar{m}} p_l B_l^{g(n)}\left(\sigma_k\right) \tag{2.24}$$

where the derivatives of the B-spline function are calculated from (2.22).

To determine the coefficients p_l for $l = 0, \ldots, \bar{m}$ of the B-spline curve with boundary conditions in velocity and acceleration, we can construct a linear system of $\bar{m} + 1$ equations for $N + 1$ way-points. At each way-point q_k this yields

$$q_k = \left(B_0^g\left(\sigma_k\right), B_1^g\left(\sigma_k\right), \ldots, B_{\bar{m}-1}^g\left(\sigma_k\right), B_m^g\left(\sigma_k\right) \right)\left(p_0, p_1, \ldots, p_{\bar{m}-1}, p_{\bar{m}} \right)^\top \tag{2.25}$$

and the velocity at the point σ_k is

$$v_k = \left(B_0^{g(1)}\left(\sigma_k\right), B_1^{g(1)}\left(\sigma_k\right), \ldots, B_{\bar{m}-1}^{g(1)}\left(\sigma_k\right), B_m^{g(1)}\left(\sigma_k\right) \right)\left(p_0, p_1, \ldots, p_{\bar{m}-1}, p_{\bar{m}} \right)^\top \tag{2.26}$$

and the acceleration is obtained through

$$a_k = \left(B_0^{g(2)}\left(\sigma_k\right), B_1^{g(2)}\left(\sigma_k\right), \ldots, B_{\bar{m}-1}^{g(2)}\left(\sigma_k\right), B_m^{g(2)}\left(\sigma_k\right) \right)\left(p_0, p_1, \ldots, p_{\bar{m}-1}, p_{\bar{m}} \right)^\top. \tag{2.27}$$

The parameter vector $\mathbf{p} = \left(p_0, p_1, \ldots, p_{\bar{m}-1}, p_{\bar{m}}\right)^\top$ is given through

$$\mathbf{p} = \mathbf{A}^{-1}\left(\sigma_0, \ldots, \sigma_N\right)\mathbf{q}. \tag{2.28}$$

Herein, we can recognize two different ways to define the matrix $\mathbf{A}(\sigma_0, \ldots, \sigma_N)$ and the vector $\mathbf{q}$ in (2.28) in order to obtain a unique solution of the parameter vector $\mathbf{p}$. Thus, if g is an even number, i.e. the matrix $\mathbf{A}(\sigma_0, \ldots, \sigma_N)$ has $\bar{m} = N + g$ columns, this matrix is square and the solution is unique only for additional g boundary conditions. For $g = 4$ for instance, we need 4 conditions (2 for each velocity and acceleration) and

in this case the matrix is given as

$$
\mathbf{A}(\sigma_0, \ldots, \sigma_N) = \begin{pmatrix}
B_0^g(\sigma_0) & B_1^g(\sigma_0) & \cdots & B_{\bar{m}}^g(\sigma_0) \\
B_0^{g^{(1)}}(\sigma_0) & B_1^{g^{(1)}}(\sigma_0) & \cdots & B_{\bar{m}}^{g^{(1)}}(\sigma_0) \\
B_0^{g^{(2)}}(\sigma_0) & B_1^{g^{(2)}}(\sigma_0) & \cdots & B_{\bar{m}}^{g^{(2)}}(\sigma_0) \\
B_0^g(\sigma_1) & B_1^g(\sigma_1) & \cdots & B_{\bar{m}}^g(\sigma_1) \\
\vdots & \vdots & & \vdots \\
B_0^g(\sigma_{N-1}) & B_1^g(\sigma_{N-1}) & \cdots & B_{\bar{m}}^g(\sigma_{N-1}) \\
B_0^{g^{(2)}}(\sigma_N) & B_1^{g^{(2)}}(\sigma_N) & \cdots & B_{\bar{m}}^{g^{(2)}}(\sigma_N) \\
B_0^{g^{(1)}}(\sigma_N) & B_1^{g^{(1)}}(\sigma_N) & \cdots & B_{\bar{m}}^{g^{(1)}}(\sigma_N) \\
B_0^g(\sigma_N) & B_1^g(\sigma_N) & \cdots & B_{\bar{m}}^g(\sigma_N)
\end{pmatrix}
\tag{2.29}
$$

and the vector $\mathbf{q} = (q_0, v_0, a_0, q_1, \ldots, q_{N-1}, a_N, v_N, q_N)^\top$.

On the other side, if g is an odd number, just $g-1$ additional boundary conditions are required, since $\bar{m} = N + g - 1$. For $g = 3$ for example, two conditions for the velocity or the acceleration are necessary for obtaining a unique solution. For two boundary conditions in the velocity for instance this yields

$$
\mathbf{A}(\sigma_0, \ldots, \sigma_N) = \begin{pmatrix}
B_0^g(\sigma_0) & B_1^g(\sigma_0) & \cdots & B_{\bar{m}}^g(\sigma_0) \\
B_0^{g^{(1)}}(\sigma_0) & B_1^{g^{(1)}}(\sigma_0) & \cdots & B_{\bar{m}}^{g^{(1)}}(\sigma_0) \\
B_0^g(\sigma_1) & B_1^g(\sigma_1) & \cdots & B_{\bar{m}}^g(\sigma_1) \\
\vdots & \vdots & & \vdots \\
B_0^g(\sigma_{N-1}) & B_1^g(\sigma_{N-1}) & \cdots & B_{\bar{m}}^g(\sigma_{N-1}) \\
B_0^{g^{(1)}}(\sigma_N) & B_1^{g^{(1)}}(\sigma_N) & \cdots & B_{\bar{m}}^{g^{(1)}}(\sigma_N) \\
B_0^g(\sigma_N) & B_1^g(\sigma_N) & \cdots & B_{\bar{m}}^g(\sigma_N)
\end{pmatrix}
\tag{2.30}
$$

17

with the vector $\mathbf{q} = (q_0, v_0, q_1, \ldots, q_{N-1}, v_N, q_N)^\top$.

Hence, the construction of the matrix $\mathbf{A}$ is relying on the way we define the knots vector and the degree of the basis functions we use. Let us consider that, the B-spline interpolation of degree $g = 3$ (C^2 continuity in each segment) takes place for two points, that means $N = 1$. Here, we can choose the knots vector according to (2.17) or (2.18) to make the matrix $\mathbf{A}$ as simple as possible (that enhances the numerical features of on-line path generation). We use the relation (2.18) despite of g is odd which leads to good results in the experiment.

We return to the algorithm of the on-line path generation, which is presented in Figure 2.2. For four way-points at each window, the curve which interpolates the considered way-points is calculated using the B-splines. To determine this curve at the jth iteration (window), we define a matrix $\mathbf{A}$ and a related vector $\mathbf{q}_{\text{way}}^j$ as

$$
\mathbf{A}(\sigma_j, \ldots, \sigma_{j+3}) =
\left(
\begin{array}{ccc}
\mathbf{p}_{1,j}(\sigma_j) & \mathbf{O} & \mathbf{O} \\
\mathbf{v}_{1,j}(\sigma_j) & \mathbf{O} & \mathbf{O} \\
\mathbf{a}_{1,j}(\sigma_j) & \mathbf{O} & \mathbf{O} \\
\hline
\mathbf{p}_{1,j}(\sigma_{j+1}) & \mathbf{O} & \mathbf{O} \\
\mathbf{O} & \mathbf{p}_{2,j}(\sigma_{j+1}) & \mathbf{O} \\
-\mathbf{v}_{1,j}(\sigma_{j+1}) & \mathbf{v}_{2,j}(\sigma_{j+1}) & \mathbf{O} \\
-\mathbf{a}_{1,j}(\sigma_{j+1}) & \mathbf{a}_{2,j}(\sigma_{j+1}) & \mathbf{O} \\
\mathbf{O} & \mathbf{r}_{2,j}(\sigma_{j+1}) & \mathbf{O} \\
\hline
\mathbf{O} & \mathbf{p}_{2,j}(\sigma_{j+2}) & \mathbf{O} \\
\mathbf{O} & \mathbf{O} & \mathbf{p}_{3,j}(\sigma_{j+2}) \\
\mathbf{O} & -\mathbf{v}_{2,j}(\sigma_{j+2}) & \mathbf{v}_{3,j}(\sigma_{j+2}) \\
\mathbf{O} & -\mathbf{a}_{2,j}(\sigma_{j+2}) & \mathbf{a}_{3,j}(\sigma_{j+2}) \\
\mathbf{O} & \mathbf{O} & \mathbf{r}_{3,j}(\sigma_{j+2}) \\
\hline
\mathbf{O} & \mathbf{O} & \mathbf{p}_{3,j}(\sigma_{j+3}) \\
\mathbf{O} & \mathbf{O} & \mathbf{v}_{3,j}(\sigma_{j+3})
\end{array}
\right), \quad
\mathbf{q}_{\text{way}}^j =
\left(
\begin{array}{c}
q_j \\
v_j \\
a_j \\
\hline
q_{j+1} \\
q_{j+1} \\
0 \\
0 \\
0 \\
\hline
q_{j+2} \\
q_{j+2} \\
0 \\
0 \\
0 \\
\hline
q_{j+3} \\
0
\end{array}
\right)
$$

where, $q_j, \ldots, q_{j+3}$ are the values of the considered way-points to be interpolated at the jth iteration (window), v_j and a_j are the initial velocity and acceleration of the jth iteration. Moreover, $\mathbf{O} = (0,0,0,0,0)$ and $\mathbf{p}_{1,j}, \mathbf{p}_{2,j}, \mathbf{p}_{3,j}$ are the first, the second and

the third B-spline functions of the jth iteration respectively. They are defined as

$$\mathbf{p}_{i,j}\left(\sigma_j\right) = \left(B_{i,0}^3(\sigma_j), B_{i,1}^3(\sigma_j), B_{i,2}^3(\sigma_j), B_{i,3}^3(\sigma_i), B_{i,4}^3(\sigma_j)\right), \quad i = 1, 2, 3, \tag{2.31}$$

where the components of the vector $\mathbf{p}_{i,j}\left(\sigma_j\right)$ are determined according to (2.19) and (2.20). $\mathbf{v}_{1,j}, \mathbf{v}_{2,j}, \mathbf{v}_{3,j}$ are the first derivative functions of $\mathbf{p}_{1,j}, \mathbf{p}_{2,j}, \mathbf{p}_{3,j}$ with respect to the path variable σ respectively and given through

$$\mathbf{v}_{i,j}\left(\sigma_j\right) = \left(B_{i,0}^{3(1)}(\sigma_j), B_{i,1}^{3(1)}(\sigma_j), B_{i,2}^{3(1)}(\sigma_j), B_{i,3}^{3(1)}(\sigma_j), B_{i,4}^{3(1)}(\sigma_j)\right), \quad i = 1, 2, 3. \tag{2.32}$$

Following the same consideration, we can define the second and the third derivative of $\mathbf{p}_{1,j}, \mathbf{p}_{2,j}, \mathbf{p}_{3,j}$ as

$$\mathbf{a}_{i,j}\left(\sigma_j\right) = \left(B_{i,0}^{3(2)}(\sigma_j), B_{i,1}^{3(2)}(\sigma_j), B_{i,2}^{3(2)}(\sigma_j), B_{i,3}^{3(2)}(\sigma_i), B_{i,4}^{3(2)}(\sigma_j)\right), \quad i = 1, 2, 3, \tag{2.33}$$

and

$$\mathbf{r}_{i,j}\left(\sigma_j\right) = \left(B_{i,0}^{3(3)}(\sigma_j), B_{i,1}^{3(3)}(\sigma_j), B_{i,2}^{3(3)}(\sigma_j), B_{i,3}^{3(3)}(\sigma_j), B_{i,4}^{3(3)}(\sigma_j)\right), \quad i = 1, 2, 3, \tag{2.34}$$

where the components of the vectors $\mathbf{v}_{i,j}\left(\sigma_j\right), \mathbf{a}_{i,j}\left(\sigma_j\right)$ and $\mathbf{r}_{i,j}\left(\sigma_j\right)$ are calculated using the relation (2.24).

Thus, we can determine the coefficient vectors for the three polynomials by solving the following linear system at each iteration (window)

$$\mathbf{p}_j = \mathbf{A}^{-1}\left(\sigma_j, \dots, \sigma_{j+3}\right) \mathbf{q}_{\text{way}}^j \tag{2.35}$$

where

$$\mathbf{p}_j = \left(\underbrace{p_0^j, p_1^j, p_2^j, p_3^j, p_4^j}_{\text{coefficients of polynomial 1}}, \underbrace{p_0^{j+1}, p_1^{j+1}, p_2^{j+1}, p_3^{j+1}, p_4^{j+1}}_{\text{coefficients of polynomial 2}}, \underbrace{p_0^{j+2}, p_1^{j+2}, p_2^{j+2}, p_3^{j+2}, p_4^{j+2}}_{\text{coefficients of polynomial 3}}\right)^\top \tag{2.36}$$

Remark 2.2.1 By using this algorithm we may generate on-line a C^2 continuous path. If a continuous jerk is required then it is necessary to set $g = 4$, while setting $g = 5$ guarantees also the continuity of the snap. Moreover, the matrix $\mathbf{A}\left(\sigma_j, \dots, \sigma_{j+3}\right)$ must be adapted to guarantee the required degree of continuity and also the uniqueness of

the solution $\mathbf{p}_j$ of (2.35). In our algorithm the matrix $\mathbf{A}\left(\sigma_j, \ldots, \sigma_{j+3}\right)$ is complemented by using the jerk vector $\mathbf{r}_{i,j}$ in order to obtain a unique solution of (2.35).

Remark 2.2.2 The significant convenience of using the B-splines in this algorithm is, that the resulting matrix $\mathbf{A}\left(\sigma_j, \ldots, \sigma_{j+3}\right)$ is constant for all iterations, which means low computational cost. This comes by virtue of the B-spline functions, since they are calculated in equivalently distributed instances of the path variable $\sigma = 0, 1, \ldots$.

Remark 2.2.3 Since this algorithm provides numerically robust results even if the number of the interpolated way-points is large, it is possible to utilize it to approximate desired paths if we use an adequate number of sampling points of the considered paths. That means we can regenerate the desired path on-line which is needed to avoid obstacles or to follow a certain primitives in the 3D space.

The path primitives (lines and circles) can be sampled and then regenerated on-line using this B-spline interpolation algorithm as Figure 2.4 demonstrates. As illustrated
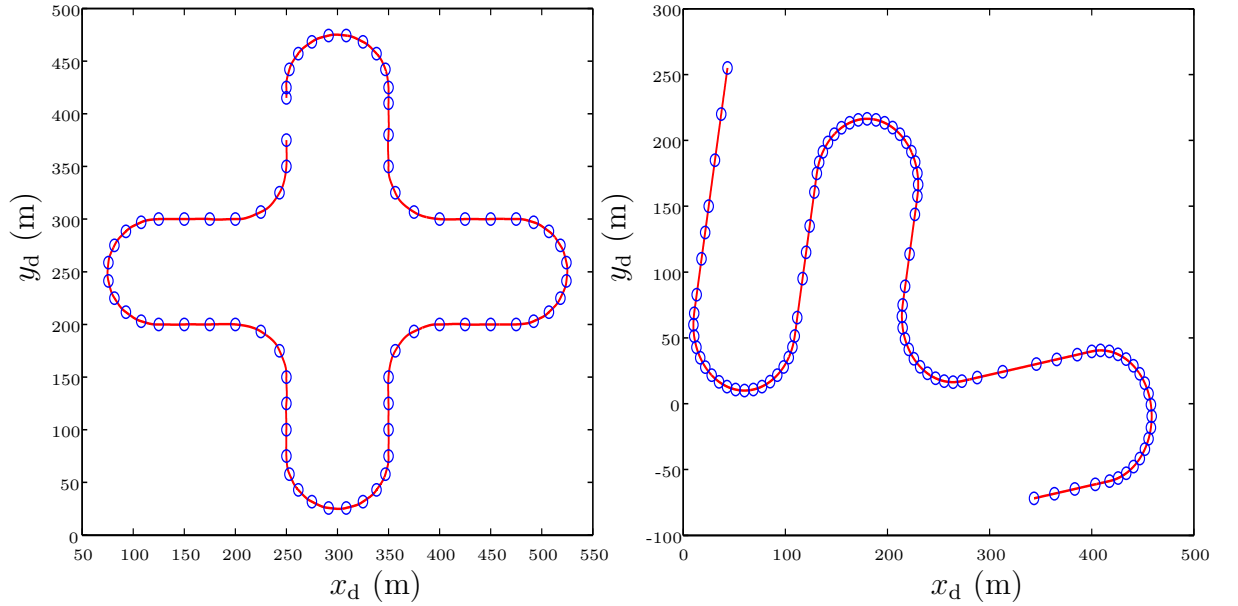
Fig. 2.4: Path primitive generation by interpolation of way-points

in Figure 2.5, the way-points are given in 3D space on-line. The path is generated via interpolation of the way-points on each axis. For perfect regeneration of the primitives, a

20
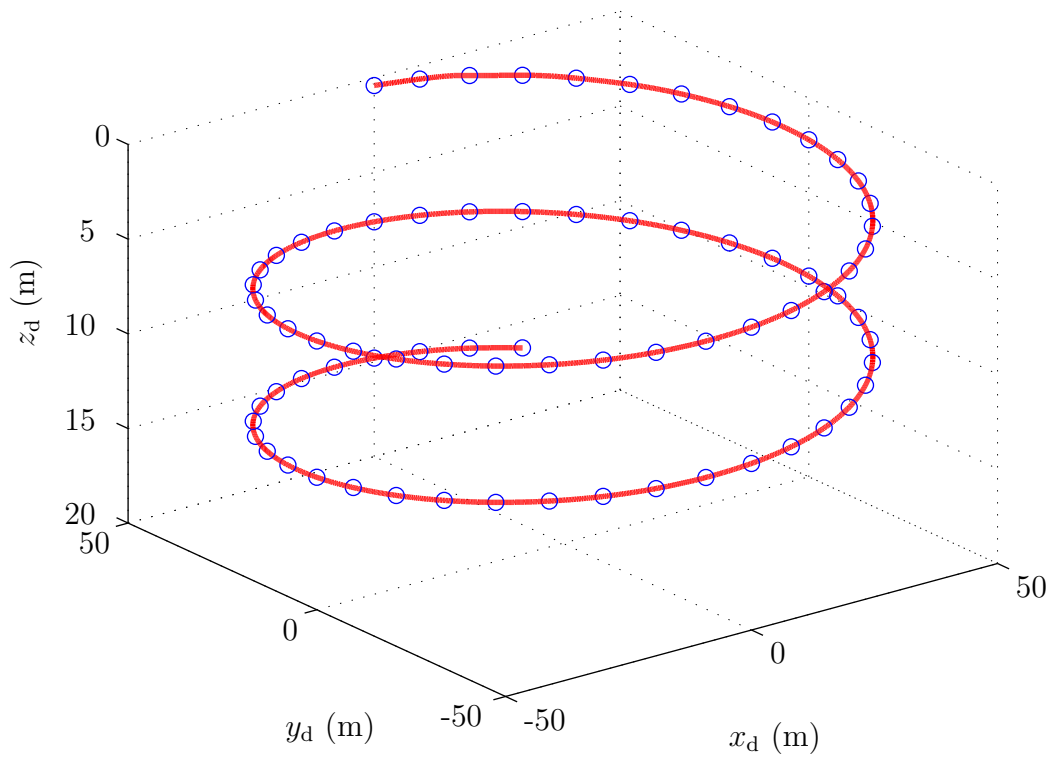
Fig. 2.5: 3D path

large (appropriate) number of way-points is necessary to attain more information about the path, consequently a good approximation. That is what Figure 2.6 indicates.
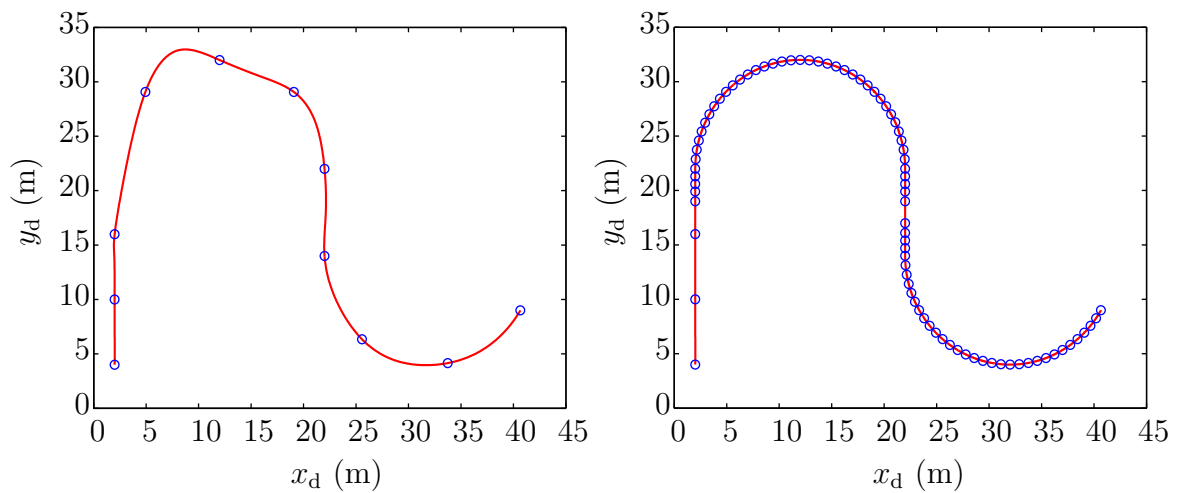
Fig. 2.6: Effect of the number of way-points

CHAPTER 3

Modeling of Marine Vessels

The investigation of the mathematical model of the AUVs can be divided into two parts: Kinematics, which deals with the geometrical aspects of the motion, and dynamics which studies the moments and the forces causing the motion. We will present the model of the AUV in vectorial form, due to the fact that this representation makes it easier to design MIMO controllers and observers for marine vessels [41, 46].

3.1 Kinematics

3.1.1 Coordinate Frames

Figure 3.1 depicts the relation of the body-fixed frame $X_0Y_0Z_0$, attached to the vehicle, with the earth-fixed frame XYZ. The origin of the body-fixed frame is chosen to coincide with the center of gravity of the moving vehicle. This definition of coordinate frames is a convenient approach for analyzing the motion of marine vessels in 6 DOF (degree of freedom). The body-fixed axes are defined as follows [47]:

- X_0: Longitudinal axis (directed from aft to fore)

- Y_0: Transverse axis (directed to starboard)

- Z_0: Normal axis (directed from top to bottom)

The position and orientation of the vessel are described in the earth-fixed frame XYZ. The linear and angular velocities of the vehicle are expressed in the body-fixed coordinate system $X_0Y_0Z_0$.
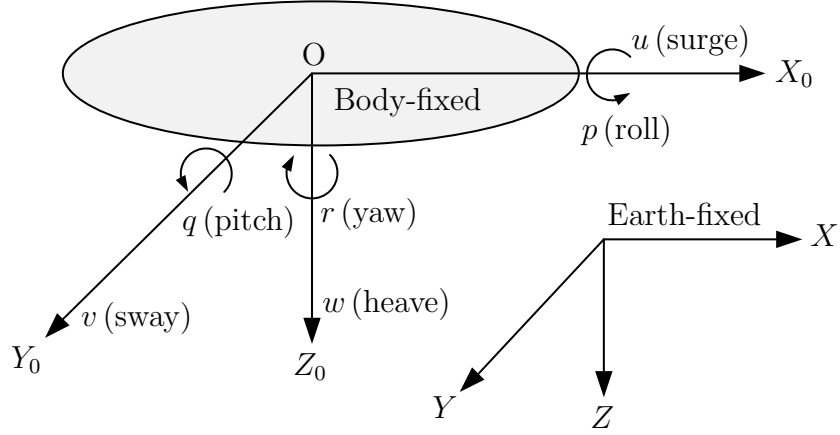
Fig. 3.1: Body-fixed and earth-fixed reference frames

The geometry of the motion is analyzed in terms of Euler angles. Using the same notation as in [48], we define the vectors:

- $\boldsymbol{\eta}_1 = (x, y, z)^\top$: Position of the origin of the frame $X_0 Y_0 Z_0$ with respect to the inertial reference frame XYZ

- $\boldsymbol{\eta}_2 = (\phi, \theta, \psi)^\top$: Angles of roll, pitch and yaw which describe the orientation of the frame $X_0 Y_0 Z_0$ with respect to the frame XYZ

- $\mathbf{v}_1 = (u, v, w)^\top$: Linear velocities (surge, sway and heave) of the origin O in the body-fixed frame $X_0 Y_0 Z_0$

- $\mathbf{v}_2 = (p, q, r)^\top$: Angular velocities (roll, pitch and yaw) of the origin O in the body-fixed frame $X_0 Y_0 Z_0$

- $\boldsymbol{\tau}_1 = (X, Y, Z)^\top$: X, Y and Z are the forces along X_0, Y_0 and Z_0, respectively

- $\boldsymbol{\tau}_2 = (K, M, N)^\top$: K, M and N are the torques about X_0, Y_0 and Z_0, respectively

In compact vectorial form, we write

$$\boldsymbol{\eta} = \left(\boldsymbol{\eta}_1^\top, \boldsymbol{\eta}_2^\top\right)^\top, \mathbf{v} = \left(\mathbf{v}_1^\top, \mathbf{v}_2^\top\right)^\top \text{ and } \boldsymbol{\tau} = \left(\boldsymbol{\tau}_1^\top, \boldsymbol{\tau}_2^\top\right)^\top. \tag{3.1}$$

The entries of the above motioned vectors are summarized in Table 3.1 according to the notation of *the Society of Naval Architectures and Marine Engineers* [48] for marine vehicles.

23

DOF		forces & torques	linear & angular velocities	position & Euler angles
1	motion in the x-direction (surge)	X	u	x
2	motion in the y-direction (sway)	Y	v	y
3	motion in the z-direction (heave)	Z	w	z
4	motion about the x-axis (roll)	K	p	ϕ
5	motion about the y-axis(pitch)	M	q	θ
6	motion about the z-axis(yaw)	N	r	ψ

Table 3.1: Notation for marine vessels

3.1.2 Euler Angles and Rotation

To determine the relation between the translation velocities $\dot{\boldsymbol{\eta}}_1 = (\dot{x}, \dot{y}, \dot{z})^\top$ in the earth-fixed frame and the velocities $\mathbf{v}_1 = (u, v, w)^\top$ in the body-fixed frame the linear velocity transformation matrix $\mathbf{J}_1(\boldsymbol{\eta}_2)$ is introduced which consists of a sequences of three rotation. Those rotations transform the body-fixed to the earth-fixed coordinates. The transformation matrix $\mathbf{J}_1(\boldsymbol{\eta}_2)$ is obtained by multiplication of three rotation matrices, over yaw (ψ), pitch (θ) and roll (ϕ) angles. The rotation matrix between body-fixed and earth-fixed frame is given as

$$\mathbf{J}_1\left(\boldsymbol{\eta}_2\right) = \begin{pmatrix} c_\psi c_\theta & -s_\psi c_\phi + s_\phi s_\theta c_\psi & s_\psi s_\phi + s_\theta c_\psi c_\phi \\ s_\phi c_\theta & c_\psi c_\phi + s_\phi s_\theta s_\psi & -c_\psi s_\phi + s_\theta s_\psi c_\phi \\ -s_\theta & s_\phi c_\theta & c_\phi c_\theta \end{pmatrix} \tag{3.2}$$

with $c_\phi = \cos\left(\phi\right), c_\theta = \cos\left(\theta\right), c_\psi = \cos\left(\psi\right), s_\phi = \sin\left(\phi\right), s_\theta = \sin\left(\theta\right)$ and $s_\psi = \sin\left(\psi\right)$. The angular velocity transformation matrix is given by [49]

$$\mathbf{J}_2\left(\boldsymbol{\eta}_2\right) = \begin{pmatrix} 1 & s_\phi s_\theta/c_\theta & c_\phi s_\theta/c_\theta \\ 0 & c_\phi & -s_\phi \\ 0 & s_\phi/c_\theta & c_\phi/c_\theta \end{pmatrix} \tag{3.3}$$

and relates the body-fixed angular velocity $\mathbf{v}_2 = (p, q, r)^\top$ with roll, pitch, and yaw rates $\dot{\boldsymbol{\eta}}_2 = \left(\dot{\phi}, \dot{\theta}, \dot{\psi}\right)^\top$ in earth-fixed frame under the assumption $\theta \neq \pm\pi/2$. This is fulfilled in most of the AUVs applications because of physical constraints. However, in some applications the AUV needs to be operated near to this critical angle. Then it is

24

possible to get rid of this singularity problem by using the quaternion representation or by defining two Euler angle representations with different singularities and switching between these two representations [41, 47].

Finally, the kinematic equation can be expressed in the form

$$\dot{\boldsymbol{\eta}} = \mathbf{J}\left(\boldsymbol{\eta}_2\right)\mathbf{v} \iff \begin{pmatrix} \dot{\boldsymbol{\eta}}_1 \\ \dot{\boldsymbol{\eta}}_2 \end{pmatrix} = \begin{pmatrix} \mathbf{J}_1(\boldsymbol{\eta}_2) & \mathbf{0} \\ \mathbf{0} & \mathbf{J}_2(\boldsymbol{\eta}_2) \end{pmatrix} \begin{pmatrix} \mathbf{v}_1 \\ \mathbf{v}_2 \end{pmatrix}. \tag{3.4}$$

3.2 Dynamics

The dynamics of an AUV, typically, is described by a rigid-body movement in viscous media [46, 47]. The 6 DOF nonlinear dynamic model is

$$\mathbf{M}\dot{\mathbf{v}} = -\left(\mathbf{C}\left(\mathbf{v}\right) + \mathbf{D}\left(\mathbf{v}\right)\right)\mathbf{v} - \mathbf{g}\left(\boldsymbol{\eta}\right) + \boldsymbol{\tau} + \boldsymbol{\tau}_{\mathrm{d}}. \tag{3.5}$$

this dynamics is deduced from the Newton-Euler equation of a rigid-body in fluid, with

$\mathbf{M}$: Inertia matrix (including added mass)
$\mathbf{C}\left(\mathbf{v}\right)$: Matrix of Coriolis and centripetal terms (including added mass)
$\mathbf{D}\left(\mathbf{v}\right)$: Damping matrix
$\mathbf{g}\left(\boldsymbol{\eta}\right)$: Vector of gravitational forces and moments
$\boldsymbol{\tau}$: Vector of control inputs
$\boldsymbol{\tau}_{\mathrm{d}}$: Vector of disturbances.

The inertia matrix, hydrodynamic damping, Coriolis and centripetal matrices, and gravitation restoring force, control input and disturbance vectors are illustrated in the following sections.

3.2.1 Inertia Matrix

The inertia matrix consists of two matrices $\mathbf{M}_{\mathrm{RB}}$ and $\mathbf{M}_{\mathrm{A}}$, i.e. $\mathbf{M} = \mathbf{M}_{\mathrm{RB}} + \mathbf{M}_{\mathrm{A}}$ where $\mathbf{M}_{\mathrm{RB}}$ is the rigid-body inertia matrix and $\mathbf{M}_{\mathrm{A}}$ is the added mass inertia matrix. The rigid-body inertia matrix is given through [41, 49]

$$
\mathbf{M}_{\mathrm{RB}} = \begin{pmatrix} \mathbf{M}_{\mathrm{RB1}} & \mathbf{M}_{\mathrm{RB2}} \\ \mathbf{M}_{\mathrm{RB3}} & \mathbf{M}_{\mathrm{RB4}} \end{pmatrix} = \begin{pmatrix} m & 0 & 0 & 0 & mz_{\mathrm{G}} & -my_{\mathrm{G}} \\ 0 & m & 0 & -mz_{\mathrm{G}} & 0 & mx_{\mathrm{G}} \\ 0 & 0 & m & my_{\mathrm{G}} & -mx_{\mathrm{G}} & 0 \\ 0 & -mz_{\mathrm{G}} & my_{\mathrm{G}} & I_{xx} & I_{xy} & -I_{xz} \\ mz_{\mathrm{G}} & 0 & -mx_{\mathrm{G}} & -I_{yx} & I_{yy} & -I_{yz} \\ -my_{\mathrm{G}} & mx_{\mathrm{G}} & 0 & -I_{zx} & -I_{zy} & I_{zz} \end{pmatrix}
$$
$$(3.6)$$

where $\mathbf{M}_{\mathrm{RB}i} \in \mathbb{R}^{3\times3}$ for $i = 1, 2, 3, 4$. Furthermore, m is the mass of the vehicle and I_{xx}, I_{yy}, I_{zz} are the moments of inertia about X_0-, Y_0- and Z_0-axis, respectively. $I_{xy} = I_{yx}$ is the product of inertia about X_0-axis, Y_0-axis, $I_{xz} = I_{zx}$ is the product of inertia about X_0-axis and Z_0-axis and $I_{yz} = I_{zy}$ is the product of inertia about Y_0-axis and Z_0-axis. Moreover, the center of gravity is $c_{\mathrm{G}} = (x_{\mathrm{G}}, y_{\mathrm{G}}, z_{\mathrm{G}})$.

Remark 3.2.1 The matrix $\mathbf{M}_{\mathrm{RB}}$ can be simplified by choosing the origin of the body-fixed coordinate system according to the following criteria: The origin O of the AUV coincides with the center of gravity that gives $c_{\mathrm{G}} = (x_{\mathrm{G}}, y_{\mathrm{G}}, z_{\mathrm{G}}) = (0, 0, 0)$, i.e. $\mathbf{M}_{\mathrm{RB2}} = \mathbf{M}_{\mathrm{RB3}} = \mathbf{0}$. Further, by allowing the body-fixed frame axes of the vehicle to coincide with the principle axes of inertia or the longitudinal, literal and normal symmetry axes of the AUV. This implies that $I_{xz} = I_{zx} = I_{yz} = I_{zy} = I_{yz} = I_{zy} = 0$ which means that the matrix $\mathbf{M}_{\mathrm{RB4}}$ is diagonal [47].

Hence, under these assumptions motivated above, the rigid-body inertia matrix reads

$$
\mathbf{M}_{\mathrm{RB}} = \begin{pmatrix} \mathbf{M}_{\mathrm{RB1}} & \mathbf{M}_{\mathrm{RB2}} \\ \mathbf{M}_{\mathrm{RB3}} & \mathbf{M}_{\mathrm{RB4}} \end{pmatrix} = \begin{pmatrix} m & 0 & 0 & 0 & 0 & 0 \\ 0 & m & 0 & 0 & 0 & 0 \\ 0 & 0 & m & 0 & 0 & 0 \\ 0 & 0 & 0 & I_{xx} & 0 & 0 \\ 0 & 0 & 0 & 0 & I_{yy} & 0 \\ 0 & 0 & 0 & 0 & 0 & I_{zz} \end{pmatrix}.
$$
$$(3.7)$$

When an AUV accelerates in a fluid (water), the surrounding water is also accelerated. That means, an additional force is required to accelerate some volume of the fluid around the AUV. This extra force relates to the acceleration of the AUV and its so-called added

mass by Newton's second law. For an AUV which accelerates in all six DOF, this yields

$$\mathbf{F}_A = \mathbf{M}_A \mathbf{A}_A \tag{3.8}$$

where

$$\mathbf{F}_A = (X_A, Y_A, Z_A, K_A, M_A, N_A)^\top \tag{3.9}$$

is part of the total external forces and moments acting on the generalized axes of the AUV. $\mathbf{A}_A$ is the generalized acceleration vector of the AUV and given by

$$\mathbf{A}_A = (\dot{u}, \dot{v}, \dot{w}, \dot{p}, \dot{q}, \dot{r})^\top . \tag{3.10}$$

It is important to understand the added mass as a virtual mass only. It is a convenient way of describing the extra force required to move a body through the water [47, 48, 50, 51]. The added mass matrix for an AUV in six DOF is given by

$$\mathbf{M}_A = \begin{pmatrix} \mathbf{M}_{A1} & \mathbf{M}_{A2} \\ \mathbf{M}_{A3} & \mathbf{M}_{A4} \end{pmatrix} = - \begin{pmatrix} X_{\dot{u}} & X_{\dot{v}} & X_{\dot{w}} & X_{\dot{p}} & X_{\dot{q}} & X_{\dot{r}} \\ Y_{\dot{u}} & Y_{\dot{v}} & Y_{\dot{w}} & Y_{\dot{p}} & Y_{\dot{q}} & Y_{\dot{r}} \\ Z_{\dot{u}} & Z_{\dot{v}} & Z_{\dot{w}} & Z_{\dot{p}} & Z_{\dot{q}} & Z_{\dot{r}} \\ K_{\dot{u}} & K_{\dot{v}} & K_{\dot{w}} & K_{\dot{p}} & K_{\dot{q}} & K_{\dot{r}} \\ M_{\dot{u}} & M_{\dot{v}} & M_{\dot{w}} & M_{\dot{p}} & M_{\dot{q}} & M_{\dot{r}} \\ N_{\dot{u}} & N_{\dot{v}} & N_{\dot{w}} & N_{\dot{p}} & N_{\dot{q}} & N_{\dot{r}} \end{pmatrix} \tag{3.11}$$

where $\mathbf{M}_{Aj} \in \mathbb{R}^{3\times 3}$ for $j = 1, 2, 3, 4$.

The components of the matrix $\mathbf{M}_A$ are called added mass derivatives and they are functions only of the AUV shape and the density of the fluid (water). We use the convention of *the Society of Naval Architects and Marine Engineers* [48] to describe the matrix $\mathbf{M}_A$, for example, the part of hydrodynamic added mass force X_A along the X_0-axis due to an acceleration $\dot{w}$ in the Z_0-direction, given as

$$X_{\dot{w}}\dot{w} \quad \text{where} \quad X_{\dot{w}} = \frac{\partial X_A}{\partial \dot{w}}. \tag{3.12}$$

The added mass derivatives are determined in detail in [41] and [51].

Remark 3.2.2 In underwater vehicle applications, practically, the AUVs move at low speed. Additionally, if the vessel also has three planes of symmetry then the off-diagonal elements of matrix (3.11) may be neglected [47].

Hence, matrix $\mathbf{M}_{\mathrm{A}}$ is simplified to

$$
\mathbf{M}_{\mathrm{A}} = \begin{pmatrix} \mathbf{M}_{\mathrm{A}1} & \mathbf{M}_{\mathrm{A}2} \\ \mathbf{M}_{\mathrm{A}3} & \mathbf{M}_{\mathrm{A}4} \end{pmatrix} = - \begin{pmatrix} X_{\dot{u}} & 0 & 0 & 0 & 0 & 0 \\ 0 & Y_{\dot{v}} & 0 & 0 & 0 & 0 \\ 0 & 0 & Z_{\dot{w}} & 0 & 0 & 0 \\ 0 & 0 & 0 & K_{\dot{p}} & 0 & 0 \\ 0 & 0 & 0 & 0 & M_{\dot{q}} & 0 \\ 0 & 0 & 0 & 0 & 0 & N_{\dot{r}} \end{pmatrix}. \tag{3.13}
$$

By noting Remarks 3.2.1 and 3.2.2, the mass inertia matrix (including added mass) can be written as

$$
\mathbf{M} = \begin{pmatrix} \mathbf{M}_1 & \mathbf{0} \\ \mathbf{0} & \mathbf{M}_2 \end{pmatrix} = \begin{pmatrix} m - X_{\dot{u}} & 0 & 0 & 0 & 0 & 0 \\ 0 & m - Y_{\dot{v}} & 0 & 0 & 0 & 0 \\ 0 & 0 & m - Z_{\dot{w}} & 0 & 0 & 0 \\ 0 & 0 & 0 & I_{xx} - K_{\dot{p}} & 0 & 0 \\ 0 & 0 & 0 & 0 & I_{yy} - M_{\dot{q}} & 0 \\ 0 & 0 & 0 & 0 & 0 & I_{zz} - N_{\dot{r}} \end{pmatrix} \tag{3.14}
$$

with $\mathbf{M}_1, \mathbf{M}_2 \in \mathbb{R}^{3\times 3}$.

3.2.2 Coriolis and Centripetal Matrix

The Coriolis and centripetal matrix is the sum of the rigid-body Coriolis and centripetal matrix $\mathbf{C}_{\mathrm{RB}}(\mathbf{v})$ and the added mass Coriolis and centripetal matrix $\mathbf{C}_{\mathrm{A}}(\mathbf{v})$, i.e.

$$
\mathbf{C}(\mathbf{v}) = \mathbf{C}_{\mathrm{RB}}(\mathbf{v}) + \mathbf{C}_{\mathrm{A}}(\mathbf{v}) \tag{3.15}
$$

where

$$
\mathbf{C}_{\mathrm{RB}}(\mathbf{v}) = \begin{pmatrix} \mathbf{C}_{\mathrm{RB}1}(\mathbf{v}) & \mathbf{C}_{\mathrm{RB}2}(\mathbf{v}) \\ \mathbf{C}_{\mathrm{RB}3}(\mathbf{v}) & \mathbf{C}_{\mathrm{RB}4}(\mathbf{v}) \end{pmatrix}, \quad \mathbf{C}_{\mathrm{RB}i}(\mathbf{v}) \in \mathbb{R}^{3\times 3}, \quad i = 1, 2, 3, 4 \tag{3.16}
$$

and

$$
\mathbf{C}_{\mathrm{A}}(\mathbf{v}) = \begin{pmatrix} \mathbf{C}_{\mathrm{A}1}(\mathbf{v}) & \mathbf{C}_{\mathrm{A}2}(\mathbf{v}) \\ \mathbf{C}_{\mathrm{A}3}(\mathbf{v}) & \mathbf{C}_{\mathrm{A}4}(\mathbf{v}) \end{pmatrix}, \quad \mathbf{C}_{\mathrm{A}j}(\mathbf{v}) \in \mathbb{R}^{3\times 3}, \quad j = 1, 2, 3, 4 \tag{3.17}
$$

where

$$\mathbf{C}_{\mathrm{RB1}}\left(\mathbf{v}\right) = \begin{pmatrix} 0 & 0 & 0 \\ 0 & 0 & 0 \\ 0 & 0 & 0 \end{pmatrix}, \quad \mathbf{C}_{\mathrm{RB2}}\left(\mathbf{v}\right) = \begin{pmatrix} m(y_{\mathrm{G}}q + z_{\mathrm{G}}r) & -m(x_{\mathrm{G}}q - w) & -m(x_{\mathrm{G}}r + v) \\ -m(y_{\mathrm{G}}p + w) & m(z_{\mathrm{G}}r + x_{\mathrm{G}}p) & -m(y_{\mathrm{G}}r - u) \\ -m(z_{\mathrm{G}}p - v) & -m(z_{\mathrm{G}}q + u) & m(x_{\mathrm{G}}p + y_{\mathrm{G}}q) \end{pmatrix}$$
$$(3.18)$$

$$\mathbf{C}_{\mathrm{RB3}}\left(\mathbf{v}\right) = \begin{pmatrix} -m(y_{\mathrm{G}}q + z_{\mathrm{G}}r) & m(y_{\mathrm{G}}p + w) & m(z_{\mathrm{G}}p - v) \\ m(x_{\mathrm{G}}q - w) & -m(z_{\mathrm{G}}r + x_{\mathrm{G}}p) & m(z_{\mathrm{G}}q + u) \\ m(x_{\mathrm{G}}r + v) & m(y_{\mathrm{G}}r - u) & -m(x_{\mathrm{G}}p + y_{\mathrm{G}}q) \end{pmatrix}, \qquad (3.19)$$

$$\mathbf{C}_{\mathrm{RB4}}\left(\mathbf{v}\right) = \begin{pmatrix} 0 & -I_{yz}q - I_{xz}p + I_{zz}r & I_{yz}r + I_{xy}p - I_{yy}q \\ I_{yz}q + I_{xz}p - I_{zz}r & 0 & -I_{xz}r - I_{xy}q + I_{xx}p \\ -I_{yz}r - I_{xy}p + I_{yy}q & I_{xz}r + I_{xy}q - I_{xx}p & 0 \end{pmatrix}. \quad (3.20)$$

According to Remark 3.2.1, matrices $\mathbf{C}_{\mathrm{RB2}}, \mathbf{C}_{\mathrm{RB3}}$ and $\mathbf{C}_{\mathrm{RB4}}$ can be simplified as

$$\mathbf{C}_{\mathrm{RB2}}\left(\mathbf{v}\right) = \mathbf{C}_{\mathrm{RB3}}\left(\mathbf{v}\right) = \begin{pmatrix} 0 & mw & -mv \\ -mw & 0 & mu \\ mv & -mu & 0 \end{pmatrix} \qquad (3.21)$$

and

$$\mathbf{C}_{\mathrm{RB4}}\left(\mathbf{v}\right) = \begin{pmatrix} 0 & I_{zz}r & -I_{yy}q \\ -I_{zz}r & 0 & I_{xx}p \\ I_{yy}q & -I_{xx}p & 0 \end{pmatrix}. \qquad (3.22)$$

Hence, the hydrodynamic Coriolis and centripetal matrix is given by

$$\mathbf{C}_{\mathrm{A}}\left(\mathbf{v}\right) = \begin{pmatrix} \mathbf{C}_{\mathrm{A1}}\left(\mathbf{v}\right) & \mathbf{C}_{\mathrm{A2}}\left(\mathbf{v}\right) \\ \mathbf{C}_{\mathrm{A3}}\left(\mathbf{v}\right) & \mathbf{C}_{\mathrm{A4}}\left(\mathbf{v}\right) \end{pmatrix} = \begin{pmatrix} 0 & 0 & 0 & 0 & -h_3 & h_2 \\ 0 & 0 & 0 & h_3 & 0 & -h_1 \\ 0 & 0 & 0 & -h_2 & h_1 & 0 \\ 0 & -h_3 & h_2 & 0 & -l_3 & l_2 \\ h_3 & 0 & -h_1 & l_3 & 0 & -l_1 \\ -h_2 & h_1 & 0 & -l_2 & l_1 & 0 \end{pmatrix} \qquad (3.23)$$

with

$$h_1 = X_{\dot{u}}u + X_{\dot{v}}v + X_{\dot{w}}w + X_{\dot{p}}p + X_{\dot{q}}q + X_{\dot{r}}r,$$

$$h_2 = X_{\dot{v}}u + Y_{\dot{v}}v + Y_{\dot{w}}w + Y_{\dot{p}}p + Y_{\dot{q}}q + Y_{\dot{r}}r,$$

$$h_3 = X_{\dot{w}}u + Y_{\dot{w}}v + Z_{\dot{w}}w + Z_{\dot{p}}p + Z_{\dot{q}}q + Z_{\dot{r}}r,$$

29

$$l_1 = X_{\dot{p}}u + Y_{\dot{p}}v + Z_{\dot{p}}w + K_{\dot{p}}p + K_{\dot{q}}q + K_{\dot{r}}r,$$

$$l_2 = X_{\dot{q}}u + Y_{\dot{q}}v + Z_{\dot{q}}w + K_{\dot{q}}p + M_{\dot{q}}q + M_{\dot{r}}r,$$

$$l_3 = X_{\dot{r}}u + Y_{\dot{r}}v + Z_{\dot{r}}w + K_{\dot{r}}p + M_{\dot{r}}q + N_{\dot{r}}r.$$

According to Remark 3.2.2, matrix $\mathbf{C}_\mathrm{A}\left(\mathbf{v}\right)$ can be reduced to

$$\mathbf{C}_\mathrm{A}\left(\mathbf{v}\right) = \begin{pmatrix} \mathbf{C}_{\mathrm{A}1}\left(\mathbf{v}\right) & \mathbf{C}_{\mathrm{A}2}\left(\mathbf{v}\right) \\ \mathbf{C}_{\mathrm{A}3}\left(\mathbf{v}\right) & \mathbf{C}_{\mathrm{A}4}\left(\mathbf{v}\right) \end{pmatrix} = \begin{pmatrix} 0 & 0 & 0 & 0 & -Z_{\dot{w}}w & Y_{\dot{v}}v \\ 0 & 0 & 0 & Z_{\dot{w}}w & 0 & -X_{\dot{u}}u \\ 0 & 0 & 0 & -Y_{\dot{v}}v & X_{\dot{u}}u & 0 \\ 0 & -Z_{\dot{w}}w & Y_{\dot{v}}v & 0 & -N_{\dot{r}}r & M_{\dot{q}}q \\ Z_{\dot{w}}w & 0 & -X_{\dot{u}}u & N_{\dot{r}}r & 0 & -K_{\dot{p}}p \\ -Y_{\dot{v}}v & X_{\dot{u}}u & 0 & -M_{\dot{q}}q & K_{\dot{p}}p & 0 \end{pmatrix}, \tag{3.24}$$

therefore, the total Coriolis matrix is given as

$$\mathbf{C}\left(\mathbf{v}_1\right) = \begin{pmatrix} \mathbf{0} & \mathbf{C}_1\left(\mathbf{v}_1\right) \\ \mathbf{C}_1\left(\mathbf{v}_1\right) & \mathbf{C}_2\left(\mathbf{v}_1\right) \end{pmatrix} \tag{3.25}$$

where

$$\mathbf{C}_1\left(\mathbf{v}_1\right) = \mathbf{C}_{\mathrm{RB}1}\left(\mathbf{v}_1\right) + \mathbf{C}_{\mathrm{A}1}\left(\mathbf{v}_1\right) = \begin{pmatrix} 0 & \left(m - Z_{\dot{w}}\right)w & -\left(m - Y_{\dot{v}}\right)v \\ -\left(m - Z_{\dot{w}}\right)w & 0 & \left(m - X_{\dot{u}}\right)u \\ -\left(m - Y_{\dot{v}}\right)v & -\left(m - X_{\dot{u}}\right)u & 0 \end{pmatrix}$$

$$\mathbf{C}_2\left(\mathbf{v}_1\right) = \mathbf{C}_{\mathrm{RB}4}\left(\mathbf{v}_1\right) + \mathbf{C}_{\mathrm{A}4}\left(\mathbf{v}_1\right) = \begin{pmatrix} 0 & \left(I_{zz} - N_{\dot{r}}\right)r & -\left(I_{yy} - M_{\dot{q}}\right)q \\ -\left(I_{zz} - N_{\dot{r}}\right)r & 0 & \left(I_{xx} - K_{\dot{p}}\right)p \\ \left(I_{yy} - M_{\dot{q}}\right)q & -\left(I_{xx} - K_{\dot{p}}\right)p & 0 \end{pmatrix} \tag{3.26}$$

with

$$m_1 = m - X_{\dot{u}}, \quad m_2 = m - Y_{\dot{v}}, \quad m_3 = m - Z_{\dot{w}},$$
$$m_4 = I_{xx} - K_{\dot{p}}, \quad m_5 = I_{yy} - M_{\dot{q}}, \quad m_6 = I_{zz} - N_{\dot{r}}. \tag{3.27}$$

It should be noticed that $m_1, m_2, m_3, m_4, m_5, m_6 > 0$ since the hydrodynamic derivatives $X_{\dot{u}}, Y_{\dot{v}}, Z_{\dot{w}}, K_{\dot{p}}, M_{\dot{q}}, N_{\dot{r}} < 0$ and $I_{xx}, I_{yy}, I_{zz} > 0$ [41].

Hence, the matrices $\mathbf{M}_1, \mathbf{M}_2, \mathbf{C}_1(\mathbf{v}_1)$ and $\mathbf{C}_2(\mathbf{v}_1)$ can be written as

$$\mathbf{M}_1 = \begin{pmatrix} m_1 & 0 & 0 \\ 0 & m_2 & 0 \\ 0 & 0 & m_3 \end{pmatrix}, \quad \mathbf{M}_2 = \begin{pmatrix} m_4 & 0 & 0 \\ 0 & m_5 & 0 \\ 0 & 0 & m_6 \end{pmatrix}, \tag{3.28}$$

$$\mathbf{C}_1(\mathbf{v}_1) = \begin{pmatrix} 0 & m_3 w & -m_2 v \\ -m_3 w & 0 & m_1 u \\ m_2 v & -m_1 u & 0 \end{pmatrix}, \quad \mathbf{C}_2(\mathbf{v}_1) = \begin{pmatrix} 0 & m_6 r & -m_5 q \\ -m_6 r & 0 & m_4 p \\ m_5 q & -m_4 p & 0 \end{pmatrix}. \tag{3.29}$$

3.2.3 Hydrodynamic Damping Matrix

The hydrodynamic damping in the AUVs basically consists of potential, skin friction, wave drift damping and the damping due to vortex shedding and contains the drag and lift forces. The total damping matrix $\mathbf{D}(\mathbf{v})$ of an AUV which is moving in ideal fluid can be expressed as a sum of the linear damping matrix $\mathbf{D}_l$ (describing the effect of the linear skin friction) and the nonlinear damping matrix $\mathbf{D}_n(\mathbf{v})$ [41, 52].

Remark 3.2.3 In an AUV which is performing low speed, shows a non-coupled motion and has three planes of symmetry, the lift forces are negligible compared to the drag forces. The damping terms of second order and higher can be also neglected [41, 46, 47].

Therefore, according to Remark 3.2.3, the linear damping matrix $\mathbf{D}_l$ is given by

$$\mathbf{D}_l = - \begin{pmatrix} X_u & 0 & 0 & 0 & 0 & 0 \\ 0 & Y_v & 0 & 0 & 0 & 0 \\ 0 & 0 & Z_w & 0 & 0 & 0 \\ 0 & 0 & 0 & K_p & 0 & 0 \\ 0 & 0 & 0 & 0 & M_q & 0 \\ 0 & 0 & 0 & 0 & 0 & N_r \end{pmatrix} \tag{3.30}$$

where X_u is the surge drag force derivative with respect to u, etc.. Again according to Remark 3.2.3 the nonlinear damping matrix $\mathbf{D}_n(\mathbf{v})$ takes the following form

$$
\mathbf{D}_\mathrm{n}\left(\mathbf{v}\right) = - \begin{pmatrix} X_{u|u|}\left|u\right| & 0 & 0 & 0 & 0 & 0 \\ 0 & Y_{v|v|}\left|v\right| & 0 & 0 & 0 & 0 \\ 0 & 0 & Z_{w|w|}\left|w\right| & 0 & 0 & 0 \\ 0 & 0 & 0 & K_{p|p|}\left|p\right| & 0 & 0 \\ 0 & 0 & 0 & 0 & M_{q|q|}\left|q\right| & 0 \\ 0 & 0 & 0 & 0 & 0 & N_{r|r|}\left|r\right| \end{pmatrix} \tag{3.31}
$$

where $X_{u|u|}$ is the surge drag force derivative with respect to $u\left|u\right|$ (u is the surge velocity of the AUV).

For example, the surge drag force X_D can be modeled as

$$
X_\mathrm{D} = -\left(\frac{1}{2}\rho\,C_\mathrm{d}A_\mathrm{c}\right)u\left|u\right| = X_{u|u|}u\left|u\right| \tag{3.32}
$$

where A_c is the projected cross-sectional area, C_d is the drag-coefficient based on the representative area and ρ is the water density [53]. The drag force derivative in surge direction with respect to $u\left|u\right|$ is given by

$$
X_{u|u|} = \frac{\partial X_\mathrm{D}}{\partial\left(u\left|u\right|\right)} = -\frac{1}{2}\rho\,C_\mathrm{d}A_\mathrm{c}. \tag{3.33}
$$

The total damping matrix of the AUV has a diagonal form and is given as

$$
\mathbf{D}\left(\mathbf{v}\right) = \mathbf{D}_\mathrm{l} + \mathbf{D}_\mathrm{n}\left(\mathbf{v}\right) = \begin{pmatrix} \mathbf{D}_1\left(\mathbf{v}\right) & \mathbf{0} \\ \mathbf{0} & \mathbf{D}_2\left(\mathbf{v}\right) \end{pmatrix} \tag{3.34}
$$

where

$$
\begin{aligned}
\mathbf{D}_1\left(\mathbf{v}\right) &= -\begin{pmatrix} X_u + X_{u|u|}\left|u\right| & 0 & 0 \\ 0 & Y_v + Y_{v|v|}\left|v\right| & 0 \\ 0 & 0 & Z_w + Z_{w|w|}\left|w\right| \end{pmatrix} \\
\mathbf{D}_2\left(\mathbf{v}\right) &= -\begin{pmatrix} K_p + K_{p|p|}\left|p\right| & 0 & 0 \\ 0 & M_q + M_{q|q|}\left|q\right| & 0 \\ 0 & 0 & N_r + N_{r|r|}\left|r\right| \end{pmatrix}
\end{aligned} \tag{3.35}
$$

with $X_u, Y_v, Z_w, K_p, M_q, N_r, X_{u|u|}, Y_{v|v|}, Z_{w|w|}, K_{p|p|}, M_{q|q|}, N_{r|r|} < 0$.

Now, by defining

$$d_1 = -X_u, \quad d_2 = -Y_v, \quad d_3 = -Z_w, \quad d_4 = -K_p, \quad d_5 = -M_q, \quad d_6 = -N_r,$$
$$d_u = -X_{u|u|}, \quad d_v = -Y_{v|v|}, \quad d_w = -Z_{w|w|}, d_p = -K_{p|p|}, \quad d_q = -M_{q|q|}, \quad d_r = -N_{r|r|}$$

the matrices $\mathbf{D}_1(\mathbf{v})$ and $\mathbf{D}_2(\mathbf{v})$ in (3.35) can be rewritten in new parameters as

$$\mathbf{D}_1(\mathbf{v}) = \begin{pmatrix} d_1 + d_u\,|u| & 0 & 0 \\ 0 & d_2 + d_v\,|v| & 0 \\ 0 & 0 & d_3 + d_w\,|w| \end{pmatrix}, \tag{3.36}$$

$$\mathbf{D}_2(\mathbf{v}) = \begin{pmatrix} d_4 + d_p\,|p| & 0 & 0 \\ 0 & d_5 + d_q\,|q| & 0 \\ 0 & 0 & d_6 + d_r\,|r| \end{pmatrix} \tag{3.37}$$

with $d_1, d_2, d_3, d_4, d_5, d_6, d_u, d_v, d_w, d_p, d_q, d_r > 0$.

3.2.4 Restoring Forces and Moments

The restoring forces acting on the AUV have two parts: The first one is the gravitational force $\mathbf{f}_G \in \mathbb{R}^3$ which is acting on the center of gravity of the underwater vehicle $c_G = (x_G, y_G, z_G)$, while the second is the buoyant force $\mathbf{f}_B \in \mathbb{R}^3$ that is acting on the center of buoyancy $c_B = (x_B, y_B, z_B)$. The gravitational and buoyant forces may produce moments about c_G and c_B respectively.

The gravitational weight W of the underwater vehicle is given in the earth-fixed coordinates as $W = mg_{ac}$, where m is the mass of the vessel and g_{ac} is the acceleration of gravity. On the other hand, the buoyancy force is defined as $B = \rho g_{ac}\nabla$ where ρ is the density of water and ∇ is the volume of the water displaced by the vessel. To describe the restoring forces $\mathbf{f}_G$ and $\mathbf{f}_B$ acting on the vehicle in the body-fixed frame, the forces W and B can be transformed into forces in the body-fixed frame using transformation matrix (3.2). We obtain

$$\mathbf{f}_G(\boldsymbol{\eta}_2) = \mathbf{J}_1^{-1}(\boldsymbol{\eta}_2)(0,0,W)^\top, \quad \mathbf{f}_B(\boldsymbol{\eta}_2) = \mathbf{J}_1^{-1}(\boldsymbol{\eta}_2)(0,0,-B)^\top \tag{3.38}$$

by noting that the z-axis is taken to be positive downwards. According to [46, 47], the

restoring force and moment vector in the body-fixed frame is

$$\mathbf{g}\left(\boldsymbol{\eta}_2\right) = - \begin{pmatrix} \mathbf{f}_G\left(\boldsymbol{\eta}_2\right) + \mathbf{f}_B\left(\boldsymbol{\eta}_2\right) \\ c_G \times \mathbf{f}_G\left(\boldsymbol{\eta}_2\right) + c_B \times \mathbf{f}_B\left(\boldsymbol{\eta}_2\right) \end{pmatrix} \tag{3.39}$$

and substituting the relationships (3.38) into (3.39) yields

$$\mathbf{g}\left(\boldsymbol{\eta}_2\right) = \left(\mathbf{g}_1^\top\left(\boldsymbol{\eta}_2\right), \mathbf{g}_2^\top\left(\boldsymbol{\eta}_2\right)\right)^\top \tag{3.40}$$

where

$$
\begin{aligned}
\mathbf{g}_1\left(\boldsymbol{\eta}_2\right) &= \begin{pmatrix} (W-B)\,s_\theta \\ -(W-B)\,c_\theta s_\phi \\ -(W-B)\,c_\theta c_\phi \end{pmatrix}, \\
\mathbf{g}_2\left(\boldsymbol{\eta}_2\right) &= \begin{pmatrix} -\left(y_G W - y_B B\right) c_\theta c\phi + \left(z_G W - z_B B\right) c_\theta s_\phi \\ \left(z_G W - z_B B\right) s_\theta + \left(x_G W - x_B B\right) c_\theta c_\phi \\ -\left(x_G W - x_B B\right) c\theta s_\phi - \left(y_G W - y_B B\right) s_\theta \end{pmatrix}.
\end{aligned}
\tag{3.41}
$$

Remark 3.2.4 A neutrally buoyant underwater vehicle will satisfy $B = W$.

The distance between the center of gravity c_G and the center of buoyancy c_B in the body-fixed frame can be represented as

$$\overline{BG} = \left(\overline{BG}_x, \overline{BG}_y, \overline{BG}_z\right)^\top = \left(x_G - x_B, y_G - y_B, z_G - z_B\right)^\top. \tag{3.42}$$

Therefore, using (3.42) and observing Remark 3.2.4, relation (3.41) can be simplified to

$$\mathbf{g}_1\left(\boldsymbol{\eta}_2\right) = \begin{pmatrix} 0 \\ 0 \\ 0 \end{pmatrix}, \quad \mathbf{g}_2\left(\boldsymbol{\eta}_2\right) = \begin{pmatrix} -\overline{BG}_y W c_\theta c\phi + \overline{BG}_z W c_\theta s_\phi \\ \overline{BG}_z W s_\theta + \overline{BG}_x W c_\theta c_\phi \\ -\overline{BG}_x W c\theta s_\phi - \overline{BG}_y W s_\theta \end{pmatrix}. \tag{3.43}$$

Remark 3.2.5 In many underwater vehicles the center of gravity c_G and the center of buoyancy c_B are located vertically on the fixed-body Z_0-axis with $x_G = x_B$ and $y_G = y_B$.

According to Remark 3.2.5, the restoring forces and moments (3.43) can be simplified

to

$$\mathbf{g}_1\left(\boldsymbol{\eta}_2\right) = \begin{pmatrix} 0 \\ 0 \\ 0 \end{pmatrix}, \quad \mathbf{g}_2\left(\boldsymbol{\eta}_2\right) = \begin{pmatrix} \alpha_{\mathrm{g}} s_\phi c_\theta \\ \alpha_{\mathrm{g}} s_\theta \\ 0 \end{pmatrix} \tag{3.44}$$

where $\alpha_{\mathrm{g}} = \overline{BG}_z W > 0$ if the distance $\overline{BG}_z$ is positive. Actually, this is positive because in underwater vehicles the center of buoyancy locates above the center of gravity. It generates a stabilizing moment about the pitch and roll axis, otherwise, the submarine turns upside down, therefore, they are also known as restoring forces. On the contrary, in ships, the center of gravity is above the center of buoyancy, which helps to stabilize the ship statically [54, 47].

3.2.5 Control Input and Disturbance Vector

Forces and torques generated by the propellers allow the underwater vehicle to move along the desired path in the 3D underwater space. If the propellers can produce forces and torques along and about all of the body-fixed axes, then we are talking about a fully-actuated system. Actually, in many AUV applications there are no actuators in the sway and heave directions. In such case the AUV is so-called underactuated.

We have seen, according to the notation of *the Society of Naval Architectures and Marine Engineers* [48] that the control input vector is

$$\boldsymbol{\tau} = (X, Y, Z, K, M, N)^\top. \tag{3.45}$$

This notation could be confused with the notation of the variables throughout of this thesis. To avoid this confusion for the rest of this thesis we will use the notation

$$\boldsymbol{\tau} = \left(\boldsymbol{\tau}_1^\top, \boldsymbol{\tau}_2^\top\right)^\top, \quad \boldsymbol{\tau}_1 = (\tau_u, \tau_v, \tau_w)^\top, \quad \boldsymbol{\tau}_2 = (\tau_p, \tau_q, \tau_r)^\top \tag{3.46}$$

where $\tau_u, \tau_v, \tau_w, \tau_p, \tau_q$ and τ_r are the control force and torques in surge, sway, heave, roll, pitch and yaw, respectively. For the underactuated case the controls in sway and heave are missing, that means $\tau_v = \tau_w = 0$.

The environmental disturbances (currents for instance) acting on the generalized axes

of the AUV are

$$\boldsymbol{\tau}_{\mathrm{d}} = \left(\boldsymbol{\tau}_{1\mathrm{d}}^{\top}, \boldsymbol{\tau}_{2\mathrm{d}}^{\top}\right)^{\top}, \quad \boldsymbol{\tau}_{1\mathrm{d}} = \left(\tau_{ud}\left(t\right), \tau_{vd}\left(t\right), \tau_{wd}\left(t\right)\right)^{\top}, \quad \boldsymbol{\tau}_{2\mathrm{d}} = \left(\tau_{pd}\left(t\right), \tau_{qd}\left(t\right), \tau_{rd}\left(t\right)\right)^{\top}$$
(3.47)

where $\tau_{ud}\left(t\right), \tau_{vd}\left(t\right), \tau_{wd}\left(t\right), \tau_{pd}\left(t\right), \tau_{qd}\left(t\right)$ and $\tau_{rd}\left(t\right)$ are the disturbance forces and torques acting on surge, sway, heave, roll, pitch and yaw directions of the vehicle, respectively.

In line with reality we assume that the disturbances are bounded as follows:

$$\begin{aligned}
|\tau_{ud}\left(t\right)| \leq \tau_{ud}^{\mathrm{max}} < \infty, \quad |\tau_{vd}\left(t\right)| \leq \tau_{vd}^{\mathrm{max}} < \infty, \quad |\tau_{wd}\left(t\right)| \leq \tau_{wd}^{\mathrm{max}} < \infty \\
|\tau_{pd}\left(t\right)| \leq \tau_{pd}^{\mathrm{max}} < \infty, \quad |\tau_{qd}\left(t\right)| \leq \tau_{qd}^{\mathrm{max}} < \infty, \quad |\tau_{rd}\left(t\right)| \leq \tau_{rd}^{\mathrm{max}} < \infty.
\end{aligned}$$
(3.48)

Summing up, the kinematics (3.4) and the dynamics (3.5) of the underwater vehicle can be represented in vectorial form as per

$$\begin{aligned}
\dot{\boldsymbol{\eta}}_1 &= \mathbf{J}_1(\boldsymbol{\eta}_2)\mathbf{v}_1 \\
\dot{\boldsymbol{\eta}}_2 &= \mathbf{J}_2(\boldsymbol{\eta}_2)\mathbf{v}_2 \\
\mathbf{M}_1\dot{\mathbf{v}}_1 &= -\mathbf{C}_1\left(\mathbf{v}_1\right)\mathbf{v}_2 - \mathbf{D}_1\left(\mathbf{v}_1\right)\mathbf{v}_1 + \boldsymbol{\tau}_1 + \boldsymbol{\tau}_{1\mathrm{d}} \\
\mathbf{M}_2\dot{\mathbf{v}}_2 &= -\mathbf{C}_1\left(\mathbf{v}_1\right)\mathbf{v}_1 - \mathbf{C}_2\left(\mathbf{v}_2\right)\mathbf{v}_2 - \mathbf{D}_2\left(\mathbf{v}_2\right)\mathbf{v}_2 - \mathbf{g}_2\left(\boldsymbol{\eta}_2\right) + \boldsymbol{\tau}_2 + \boldsymbol{\tau}_{2\mathrm{d}}.
\end{aligned}$$
(3.49)

This representation of the system in (3.49) is convenient for designing a controller based on the backstepping technique, as we will see later.

CHAPTER 4

Previous Approaches for the Fully-Actuated AUV

In the first section of this chapter we discuss a flexible on-line trajectory planning algorithm for fully-actuated autonomous underwater vehicles relying on the path generation using polynomial splines of degree 5, which is presented in Section (2.1). For dynamically allocated way-points and surge velocities, an on-line algorithm computes polynomials that smoothly link the paths between these way-points. In the next section, we devise a tracking controller that compensates for the nonlinearities of the rigid-body dynamics in order to render it linear in closed-loop. In the third section, we employ an extended state observer that helps improving the tracking performance and attenuating large disturbances.

4.1   Path and Trajectory Planning

4.1.1   Vertical Maneuver

We assume that the initial and final positions as well as the initial and final orientations (zero roll) are given for two way-points (x_0, y_0, z_0) and (x_0, y_0, z_f). To get a smooth transition, a polynomial of degree 5 is adopted to satisfy six boundary conditions (in position, velocity, and acceleration). Therefore, a stationary rest to rest transition from $z(t_0) = z_0$ and $z(t_f) = z_f$ with zero boundary values for velocity and acceleration determines the six coefficients of the polynomial

$$z_{\mathrm{d}}(t) = \alpha_5(t - t_0)^5 + \alpha_4(t - t_0)^4 + \alpha_3(t - t_0)^3 + \alpha_2(t - t_0)^2 + \alpha_1(t - t_0) + \alpha_0 \quad (4.1)$$

For unknown final time t_{f} the coefficients may be obtained by introducing a maximum value of the heave velocity for the vertical motion $w_{\max}$, reached at time $(t_{\mathrm{f}} - t_0)/2$. In

this case, see [55], we have $t_{\mathrm{f}} = \frac{15\,h_z}{8\,w_{\max}}$ and with $T_z = t_{\mathrm{f}} - t_0$, $h_z = z_{\mathrm{f}} - z_0$ the coefficients are given as

$$\alpha_5 = \frac{12h_z}{2T_z^5}, \quad \alpha_4 = \frac{-30h_z}{2T_z^4}, \quad \alpha_3 = \frac{20h_z}{2T_z^3}, \quad \alpha_2 = \alpha_1 = 0, \quad \alpha_0 = z_0. \tag{4.2}$$

Subject to the same assumptions, the trajectories for the angles $\theta(t)$ and $\psi(t)$ may be determined similarly. For example, the transition between the yaw angles ψ_0 and ψ_{f} may be planned with the polynomial

$$\psi_{\mathrm{d}}(t) = \beta_5(t - t_0)^5 + \beta_4(t - t_0)^4 + \beta_3(t - t_0)^3 + \beta_2(t - t_0)^2 + \beta_1(t - t_0) + \beta_0 \tag{4.3}$$

where the coefficients are

$$\beta_5 = \frac{12h_\psi}{2T_z^5}, \ \beta_4 = \frac{-30h_\psi}{2T_z^4}, \ \beta_3 = \frac{20h_\psi}{2T_z^3}, \ \beta_2 = \beta_1 = 0, \ \beta_0 = \psi_0 \tag{4.4}$$

with $h_\psi = \psi_{\mathrm{f}} - \psi_0$.

This way we may design the desired trajectories $z_{\mathrm{d}}(t)$, $\psi_{\mathrm{d}}(t)$, and $\phi_{\mathrm{d}}(t)$ just involving the initial and final values of position and orientation, and the maximum value of w if needed. At the end of this maneuver the AUV is located at the stationary point $(x_0, y_0, z_{\mathrm{f}})$ with orientation $(0, \theta_{\mathrm{f}}, \psi_{\mathrm{f}})$, as desired.

4.1.2 2D- and 3D-Maneuver

Based on the kinematics (4.6) to (4.11) and under the assumption of zero roll, $\phi \equiv 0$, trajectories may be designed for a path, which passes through a certain set of Cartesian way-points (x_k, y_k, z_k), with $k = 0, 1, \ldots, N - 1$, where N is the number of way-points. To this end, by introducing a path variable σ we get the parameterized path $(x_{\mathrm{d}}(\sigma), y_{\mathrm{d}}(\sigma), z_{\mathrm{d}}(\sigma))$ using a polynomial of degree 5 to interpolate the pre-defined way-points [55], and subsequently may determine σ as a function of time in order to match the desired surge velocity profile in the path planning procedure [41].

For a 2D-maneuver, polynomials (2.3) and (2.4) are considered to generate the desired path that passes through the given way-points in the Cartesian plane. Such a path is transformed to a time dependent trajectory by imposing the desired surge velocity profile $u_0(t)$ (assuming sway and heave equal to zero). It can be shown that σ may be

obtained as the solution of the scalar differential equation

$$\dot{\sigma} = \frac{u_0(t)}{\cos \psi_{\mathrm{d}}(\sigma) x_{\mathrm{d}}'(\sigma) + \sin \psi_{\mathrm{d}}(\sigma) y_{\mathrm{d}}'(\sigma)} \tag{4.5}$$

with $\sigma(0) = 0$, $(\cdot)' = \frac{\partial}{\partial \sigma}(\cdot)$ and $\psi_{\mathrm{d}}(\sigma) = \arctan\left(\frac{y_{\mathrm{d}}'(\sigma)}{x_{\mathrm{d}}'(\sigma)}\right)$. Finally, with the solution $\sigma = \sigma(t)$ we obtain a coordinate description in terms of time, hence trajectories, $x_{\mathrm{d}} = x_{\mathrm{d}}(t)$, $y_{\mathrm{d}} = y_{\mathrm{d}}(t)$ and $\psi_{\mathrm{d}} = \psi_{\mathrm{d}}(t)$.

For a 3D-maneuver, polynomials (2.3), (2.4), (2.5) and the kinematics (4.6) – (4.11) are required (supposing roll is zero). By means of the desired profile of the longitudinal velocity $u_0(t)$, the time-dependent path variable $\sigma = \sigma(t)$ is obtained as the solution of the scalar differential equation. Thus, (u, v, w) are the translation velocities in body-fixed frame coordinates and (p, q, r) the respective angular velocities related to X_0, Y_0, Z_0. For zero velocities in sway and heave ($v \equiv 0$ and $w \equiv 0$) and with $\theta \neq \pm\pi/2 + h\pi, h = 0, \ldots$, u is the longitudinal velocity and under the assumptions $v = 0$ and $w = 0$, p, q and r are the angular velocities about the body-fixed axises. Under the assumption that the roll is zero $\phi \equiv 0$ the kinematics of the moving vehicle, that is $\dot{\boldsymbol{\eta}} = \mathbf{J}(\boldsymbol{\eta})\mathbf{v}$ from (3.4), may be expressed in the following six differential equations [56]

$$\dot{x} = u\cos(\theta)\cos(\psi) \tag{4.6}$$
$$\dot{y} = u\cos(\theta)\sin(\psi) \tag{4.7}$$
$$\dot{z} = -u\sin(\theta) \tag{4.8}$$
$$\dot{\phi} = p + q\sin(\phi)\tan(\theta) + r\cos(\phi)\tan(\theta) \tag{4.9}$$
$$\dot{\theta} = q\cos(\phi) - r\sin(\phi) \tag{4.10}$$
$$\dot{\psi} = q\frac{\sin(\phi)}{\cos(\theta)} + r\frac{\cos(\phi)}{\cos(\theta)}. \tag{4.11}$$

By means of the desired profile of the longitudinal velocity $u_0(t)$, the time-dependent path variable $\sigma = \sigma(t)$ is obtained as the solution of the scalar differential equation

$$\dot{\sigma} = \frac{u_0(t)}{\sqrt{(x_{\mathrm{d}}'(\sigma))^2 + (y_{\mathrm{d}}'(\sigma))^2 + (z_{\mathrm{d}}'(\sigma))^2}}. \tag{4.12}$$

In view of

$$\theta_d(\sigma) = \arctan\left(\frac{-z_d'(\sigma)}{\sqrt{(x_d'(\sigma))^2 + (y_d'(\sigma))^2}}\right), \quad \psi_d(\sigma) = \arctan\left(\frac{y_d'(\sigma)}{x_d'(\sigma)}\right) \qquad (4.13)$$

we may eventually obtain the desired trajectories $x_d = x_d(t)$, $y_d = y_d(t)$, $z_d = z_d(t)$, $\theta_d = \theta_d(t)$, and $\psi_d = \psi_d(t)$.

For a 3D-maneuver we apply the algorithm introduced in Section 2.1 with polynomials of degree 5.

4.2 Tracking Controller Design

For the fully-actuated system, the control design idea is based on the compensation of all the nonlinear terms of the vehicle dynamics and designing a suitable continuous or (discrete) PD- or PID-controller to force the error dynamics to converge asymptotically to zero. Whenever the system is not perturbed, it is well-known that a conventional PD-controller may do the task. For the more realistic perturbed case, we advocate the use of a GESO approach (Generalized Extended State Observer [57], [58], [59]) for the on-line estimation and attenuation of the disturbance-induced adverse effects in order to improve the performance and stability of the closed-loop system. In this section we restrict ourselves to design a discrete controller (*SALMON* project [42]), which stabilizes the closed-loop system about the given reference trajectories. Therefore, we have extended the algorithm of the continuous computed torque and the GESO algorithm to cover the discrete case. These generated trajectories are imposed on the AUV dynamics invoking a discrete computed torque controller. To this end, based on the forward Euler discretization [41] a discrete 6 degrees of freedom nonlinear model is obtained from (3.49). With a slight abuse of denotation from the continuous model, we may then express the discrete equations of motion as follows

$$\boldsymbol{\eta}(k+1) = \boldsymbol{\eta}(k) + T\mathbf{J}(\boldsymbol{\eta}(k))\mathbf{v}(k) \qquad (4.14)$$

$$\mathbf{v}(k+1) = \mathbf{v}(k) - T\mathbf{M}^{-1}\Big(\mathbf{C}(\mathbf{v}(k)) + \mathbf{D}(\nu(k))\Big)\mathbf{v}(k) - T\mathbf{M}^{-1}\mathbf{g}(\boldsymbol{\eta}(k))$$
$$+ T\mathbf{M}^{-1}(\boldsymbol{\tau}(k) + \mathbf{d}(k)) \qquad (4.15)$$

where T denotes the sampling time and $\mathbf{d}(k)$ refers to the disturbance (additional input forces and torques). After substituting (4.15) in the shifted version of (4.14) we obtain

$$
\begin{aligned}
\boldsymbol{\eta}(k+2) = \boldsymbol{\eta}(k+1) + T\big(\boldsymbol{\eta}(k+1)\big)\Big(\mathbf{v}(k) - T\mathbf{M}^{-1}\mathbf{g}(\boldsymbol{\eta}(k)) \\
- T\mathbf{M}^{-1}\big(\mathbf{C}(\mathbf{v}(k)) + \mathbf{D}(\mathbf{v}(k))\big)\mathbf{v}(k) + T\mathbf{M}^{-1}\big(\boldsymbol{\tau}(k) + \mathbf{d}(k)\big)\Big).
\end{aligned}
\tag{4.16}
$$

Now, we devise the nominal controller (disturbance-free case, $\mathbf{d}(k) \equiv \mathbf{0}$) such that with a new input $\boldsymbol{\gamma}(k)$ the dynamics in closed-loop shows double integrating behavior

$$
\frac{1}{T^2}\big(\boldsymbol{\eta}(k+2) - 2\boldsymbol{\eta}(k+1) + \boldsymbol{\eta}(k)\big) = \boldsymbol{\gamma}(k).
\tag{4.17}
$$

By comparison of (4.17) with (4.16), this means that the compensator is chosen as

$$
\begin{aligned}
\boldsymbol{\tau}(k) = \mathbf{g}(\boldsymbol{\eta}(k)) + \Big(\mathbf{C}(\mathbf{v}(k)) + \mathbf{D}(\mathbf{v}(k)) - \frac{1}{T}\mathbf{M}\Big)\mathbf{v}(k) \\
+ \mathbf{M}\mathbf{J}^{-1}\big(\boldsymbol{\eta}(k+1)\big)\Big(\boldsymbol{\gamma}(k) + \frac{1}{T}\mathbf{J}(\boldsymbol{\eta}(k))\mathbf{v}(k)\Big)
\end{aligned}
\tag{4.18}
$$

where the new input $\boldsymbol{\gamma}(k)$ may be selected as a nominal discrete PD-controller with a feed-forward term, say $\boldsymbol{\gamma}(k) = \bar{\boldsymbol{\gamma}}(k)$, which is sufficient in the nominal case. Hence with $\mathbf{K}_\mathrm{P}, \mathbf{K}_\mathrm{D} \in \mathbb{R}^{6\times 6}$ as gain matrices the nominal PD-controller reads

$$
\begin{aligned}
\bar{\boldsymbol{\gamma}}(k) = \frac{1}{T^2}\big(\boldsymbol{\eta}_\mathrm{d}(k+2) - 2\boldsymbol{\eta}_\mathrm{d}(k+1) + \boldsymbol{\eta}_\mathrm{d}(k)\big) - \mathbf{K}_\mathrm{P}(\boldsymbol{\eta}(k) - \boldsymbol{\eta}_\mathrm{d}(k)) \\
- \frac{\mathbf{K}_\mathrm{D}}{T}\big(\boldsymbol{\eta}(k+1) - \boldsymbol{\eta}(k) - \boldsymbol{\eta}_\mathrm{d}(k+1) + \boldsymbol{\eta}_\mathrm{d}(k)\big).
\end{aligned}
\tag{4.19}
$$

Note that in this equation as well as in (4.18) expression $\boldsymbol{\eta}(k+1)$ may be expressed in variables at instant k using equation (4.14).

In order to assess the values of the gains, we may substitute $\bar{\boldsymbol{\gamma}}(k)$ in (4.17) which then yields the dynamics in terms of the error $\mathbf{e}(k) = \boldsymbol{\eta}(k) - \boldsymbol{\eta}_\mathrm{d}(k)$, i.e.

$$
\mathbf{e}(k+2) + (T\mathbf{K}_\mathrm{D} - 2\mathbf{I})\mathbf{e}(k+1) + (\mathbf{I} + T^2\mathbf{K}_\mathrm{P} - T\mathbf{K}_\mathrm{D})\mathbf{e}(k) = 0
\tag{4.20}
$$

with $\mathbf{I} \in \mathbb{R}^{6\times 6}$ the identity matrix. Choosing diagonal gains for suppressing the error coupling, equation (4.20) may be rewritten as six single equations

$$
e_i(k+2) + (TK_{\mathrm{D},i} - 2)e_i(k+1) + (1 + T^2 K_{\mathrm{P},i} - TK_{\mathrm{D},i})e_i(k) = 0, \quad i = 1,\ldots,6
\tag{4.21}
$$

The error dynamics are asymptotically stable whenever the zeros of all $i = 1, \ldots, 6$ polynomials

$$\lambda^2 + (TK_{\mathrm{D},i} - 2)\lambda + (1 + T^2 K_{\mathrm{P},i} - TK_{\mathrm{D},i}) = 0 \tag{4.22}$$

lie within the unit circle of the complex plane. Let those zeros be λ_1 and λ_2. Then $K_{\mathrm{D},i}$ and $K_{\mathrm{P},i}$ is given by

$$K_{\mathrm{D},i} = \frac{1}{T}(2 - \lambda_1 - \lambda_2) \tag{4.23}$$

$$K_{\mathrm{P},i} = \frac{1}{T^2}(\lambda_1\lambda_2 - \lambda_1 - \lambda_2 + 1) \tag{4.24}$$

Hence, for a deadbeat controller: $K_{\mathrm{D},i} = \frac{2}{T}$ and $K_{\mathrm{P},i} = \frac{1}{T^2}$.

4.3 Disturbance Rejection

In general, disturbance $\mathbf{d}(k)$ will not be constant or piecewise constant. In case of a measurable disturbance, using the extended nominal control law

$$\boldsymbol{\gamma}(k) = \bar{\boldsymbol{\gamma}}(k) - \mathbf{J}(\boldsymbol{\eta}(k+1))\mathbf{M}^{-1}\mathbf{d}(k) \tag{4.25}$$

together with the compensator (4.18) leads to the nominal error dynamics (4.20). However, disturbances are not measurable in a realistic setup. Therefore, the controller shall further be extended to reject dynamic disturbances by means of an additional discrete observer to estimate the disturbances. To this end, enhance (4.17) with the disturbance to obtain the disturbed discrete linear system

$$\mathbf{x}(k+1) = \mathbf{A}\,\mathbf{x}(k) + \mathbf{B}\,\boldsymbol{\gamma}(k) + \mathbf{G}(\mathbf{x}(k))\,\mathbf{d}(k) \tag{4.26}$$

where the state is defined as $\mathbf{x}(k) := \begin{pmatrix} \boldsymbol{\eta}(k) \\ \boldsymbol{\eta}(k+1) \end{pmatrix} \in \mathbb{R}^{12}$ and

$$\mathbf{A} = \begin{pmatrix} \mathbf{0} & \mathbf{I} \\ -\mathbf{I} & 2\mathbf{I} \end{pmatrix}, \quad \mathbf{B} = \begin{pmatrix} \mathbf{0} \\ T^2\mathbf{I} \end{pmatrix}, \quad \mathbf{G}(\mathbf{x}(k)) = \begin{pmatrix} \mathbf{0} \\ T^2\mathbf{J}(\mathbf{x}_2(k))\mathbf{M}^{-1} \end{pmatrix}$$

with dimensions $\mathbf{A} \in \mathbb{R}^{12\times 12}$ and both $\mathbf{B}, \mathbf{G} \in \mathbb{R}^{12\times 6}$. In view of (4.26) and by noting that $\mathbf{G}(\mathbf{x}(k))$ is bounded due to $\mathbf{J}(\mathbf{x}_2(k))$ is bounded. This justifies the use of $\bar{\mathbf{d}}(k) =$

$\mathbf{G}(\mathbf{x}(k))\,\mathbf{d}(k)$ and let $\hat{\bar{\mathbf{d}}}(k)$ denote its asymptotic estimate. Then using the pseudo inverse and the disturbance estimate leads to the control law

$$\boldsymbol{\gamma}(k) := \bar{\boldsymbol{\gamma}}(k) - \frac{1}{T^2}\big(\mathbf{0} \ \ \mathbf{I}\big)\hat{\bar{\mathbf{d}}}(k)\,. \tag{4.27}$$

For estimating the disturbance we devise a discrete version of a Generalized Extended State Observer (GESO) that we adopt from the design procedure for continuous time systems [57, 60, 59]. Along these lines, we treat the quantity $\bar{\mathbf{d}}(k)$ in (4.26) as an extended system state in order to incorporate time derivatives of signal $\bar{\mathbf{d}}(t)$ up to order ℓ in an extended system using a discrete Euler approximation [61]. Therefore, for the unknown disturbance $\mathbf{q}_1(k) = \bar{\mathbf{d}}(k)$ we have the dynamics

$$\mathbf{q}_1(k+1) = \mathbf{q}_1(k) + T\,\mathbf{q}_2(k)$$
$$\mathbf{q}_2(k+1) = \mathbf{q}_2(k) + T\,\mathbf{q}_3(k)$$
$$\vdots = \vdots$$
$$\mathbf{q}_{\ell-1}(k+1) = \mathbf{q}_{\ell-1}(k) + T\,\mathbf{q}_\ell(k)$$
$$\mathbf{q}_\ell(k+1) = \bar{\mathbf{d}}(k)^{(\ell)}.$$

These variables together with (4.26) define the extended state

$$\boldsymbol{\kappa}^\top(k) = \Big(\mathbf{x}_1^\top(k), \mathbf{x}_2^\top(k), \mathbf{q}_1^\top(k), \dots, \mathbf{q}_\ell^\top(k)\Big) \in \mathbb{R}^{6(\ell+2)}$$

of the extended system

$$\boldsymbol{\kappa}(k+1) = \mathbf{A}_{\mathrm{e}}\boldsymbol{\kappa}(k) + \mathbf{B}_\gamma\boldsymbol{\gamma}(k) + \mathbf{B}_{\mathrm{d}}\,\bar{\mathbf{d}}(k)^{(\ell)}$$
$$\mathbf{y}(k) = \mathbf{C}_{\mathrm{e}}\boldsymbol{\kappa}(k) \tag{4.28}$$

with

$$\mathbf{A}_{\mathrm{e}} = \begin{pmatrix} \mathbf{0} & \mathbf{I} & \mathbf{0} & \mathbf{0} & \mathbf{0} & \cdots & \mathbf{0} \\ -\mathbf{I} & 2\mathbf{I} & T^2\mathbf{I} & \mathbf{0} & \mathbf{0} & \cdots & \mathbf{0} \\ \mathbf{0} & \mathbf{0} & \mathbf{I} & T\mathbf{I} & \mathbf{0} & \cdots & \mathbf{0} \\ \vdots & \ddots & \ddots & \ddots & \ddots & \ddots & \vdots \\ \mathbf{0} & \cdots & \cdots & \cdots & \mathbf{I} & T\mathbf{I} & \mathbf{0} \\ \mathbf{0} & \cdots & \cdots & \cdots & \cdots & \mathbf{I} & T\mathbf{I} \\ \mathbf{0} & \cdots & \cdots & \cdots & \cdots & \cdots & \mathbf{0} \end{pmatrix}, \quad \mathbf{B}_\gamma = \begin{pmatrix} \mathbf{0} \\ T^2\mathbf{I} \\ \mathbf{0} \\ \vdots \\ \mathbf{0} \end{pmatrix}, \quad \mathbf{B}_{\mathrm{d}} = \begin{pmatrix} \mathbf{0} \\ \mathbf{0} \\ \vdots \\ \mathbf{0} \\ \mathbf{I} \end{pmatrix},$$

and $\mathbf{C}_e = \begin{pmatrix} \mathbf{I} & \mathbf{0} & \cdots & \mathbf{0} \end{pmatrix}$ of appropriate size; $\mathbf{I}$ and $\mathbf{0}$ are 6×6 identity and zero matrices, respectively. Clearly, the pair $(\mathbf{C}_e, \mathbf{A}_e)$ is observable and $\mathbf{y}(k) = \boldsymbol{\eta}(k)$ the measured output.

As a consequence, the state $\boldsymbol{\kappa}(k)$ of the extended state space representation (4.28), thus also the unknown disturbance, may be estimated with an observer of the form

$$\hat{\boldsymbol{\kappa}}(k+1) = \mathbf{A}_e \, \hat{\boldsymbol{\kappa}}(k) + \mathbf{B}_\gamma \, \boldsymbol{\gamma}(k) + \mathbf{L} \left(\mathbf{y}(k) - \mathbf{C}_e \hat{\boldsymbol{\kappa}}(k) \right) \qquad (4.29)$$

where the observer state $\hat{\boldsymbol{\kappa}}(k)$ denotes the estimate of state $\boldsymbol{\kappa}(k)$ and $\mathbf{L} \in \mathbb{R}^{6(\ell+2) \times 6}$ is the observer gain. From (4.28) and (4.29) it is obvious that the estimation error dynamics reads

$$\tilde{\boldsymbol{\kappa}}(k+1) = (\mathbf{A}_e - \mathbf{L}\,\mathbf{C}_e)\,\tilde{\boldsymbol{\kappa}}(k) + \mathbf{B}_d\,\bar{\mathbf{d}}(k)^{(\ell)}$$

with estimation error $\tilde{\boldsymbol{\kappa}}(k) = \boldsymbol{\kappa}(k) - \hat{\boldsymbol{\kappa}}(k)$. Therefore, given that $\bar{\mathbf{d}}(k)^{(\ell)}$ is bounded, $\mathbf{L}$ serves for placing the eigenvalues of $\mathbf{A}_e - \mathbf{L}\,\mathbf{C}_e$ in the unit circle of the complex plane, e.g. by using Ackermann's formula. Choosing the eigenvalues in the vicinity of the origin, the resulting observer forces the estimation error $\tilde{\boldsymbol{\kappa}}(k)$ to asymptotically converge to a small neighborhood of the origin of the error space. Finally, in control law (4.27) we may employ the disturbance estimate $\hat{\bar{\mathbf{d}}}(k) = \left(\hat{\kappa}_{13}(k), \ldots, \hat{\kappa}_{18}(k) \right)$ for an asymptotic disturbance compensation.

Remark 4.3.1 The simulation results of this chapter are summarized in the appendix (Chapter 9).

CHAPTER 5

Controller Design for Underactuated AUVs

In this chapter we consider that the AUV is underactuated, i.e. there are no actuators in sway and heave direction. Before we start with designing a path following controller, which forces the AUV to follow the reference path designed in Chapter 2, we introduce some basic concepts. These pave the comprehension of the motivation behind the design of path following controller based on the backstepping approach.

First we review some classical adaptive control approaches for linear (or linearized) plants, then we shed light on the advantage of using the dynamic (adaptive) feedback control against the conventional (static) one. For nonlinear plants, the adaptive backstepping control technique will be introduced in detail. To avoid the shifting, which may occur during the estimation of the control and plant parameter, we will employ the projection operator. In the following section we focus on the AUV dynamics and transform it into error dynamics for both position and orientation of the AUV. In the last section of this chapter, relying on the robust adaptive backstepping technique we design a path following controller, which forces the AUV to follow the reference path and to compel it to move along this path according to a predefined velocity profile.

5.1 Adaptive Control Approaches

A lot of dynamic plants to be controlled have constant or slowly-varying uncertain parameters. For those plants there are various examples like fire-fighting aircraft, power systems and underwater vehicles. To control such systems, often, the conventional controllers can not achieve the desired performance and can not stabilize suchlike systems. Therefore, adaptive controllers are applied to control systems with uncertainties which provide techniques for automatic adjustment of the controller (estimate uncertain plant

parameters) in real-time, in order to fulfill the aimed requirements when the parameters of the dynamic system are unknown and/or changing in time [62].

The design of the adaptive controller relies mainly on the plant dynamics to be controlled. For linear or linearized nonlinear plant models, many techniques are developed to control those plants under uncertainties in their parameters, among them, are:

- Gain Scheduling Control,

- Self-Tuning Regulator (STR) and

- Model Reference Adaptive Control (MRAC).

Gain Scheduling was developed, originally, for trajectory control of aircrafts. The nonlinear plant is linearized at certain operating points which cover the whole desired operation range. At each point, a linear feedback controller with constant gains is designed to achieve the control requirements at the considered point. The global controller of the nonlinear plant over the regarded range is then an interpolation or a scheduling of the linear controllers at the chosen operating points. The main disadvantage of this technique is that a rapid changing in the controller gain, may lead to instability in the closed-loop system. In addition to its simplicity, for many applications in which the gains are changing slowly, this technique is a convenient control approach. The Gain Scheduling Control is not an actual adaptive control, but it is a kind of open-loop adaptive control, where the controller gain is adapted depending on auxiliary measurements and off-line look-up tables [62, 63, 64, 65].

An on-line adaptation approach (Self-Tuning Regulator (STR)) is introduced in [62, 63]. This Regulator consists of a controller, designed based on pole placement, PID, LQR (Linear Quadratic Regulator), . . . , and an estimator, which could be designed with many techniques, the most common one is the least squares method.

In STRs, the parameters of the controller are designed based on the estimation of the plant parameters, by replacing the real values of the plant parameters with the estimated parameters, which is known as the *certainty equivalent principle*. This controller is able to tune its own parameters, therefore is called self-tuning. Beside the flexibility with designing the controller and the estimator, the applicability of this controller to control of minimum and non-minimum phase systems is actually an obvious advantage. On the downside, the analyzing of the (STR) is not simple.

In [64, 65] the so-called Model Reference Adaptive Control (MRAC) is introduced. The

MRAC consists of an adaptation law, a controller and a reference model. The idea of the MRAC, indeed, is based on the canceling of the zeros of the plant transfer function and replacing them with those of the reference model by using a feedback controller. This implies that the plant must be minimum phase (stable zeros) because the cancellation of unstable zeros leads to unbounded signals. The MRAC system can be constructed in two different ways, the MRAC-series high-gain scheme and the MRAC-parallel scheme. The most used one is the parallel structure because it has more benefits in comparison with the MRAC-series high-gain which despite its simplicity has some problems such as oscillation and saturation due to high-gain. In the MRAC-parallel scheme one can distinguish two loops: A regulator loop, which involves the unknown plant (but the structure is known) and the ordinary controller, and an adaptation loop that adjusts the parameters of the controller using a certain adaptation mechanism. The goal of the adaptation loop is to estimate the controller parameters such that the error between the output of the plant and the output of the reference model is zero.

A combination of robust control techniques, which deal with the unmodeled uncertainties and/or disturbances, and adaptive control techniques, which handle the structural uncertainties, gives a new field of work: *robust adaptive control* [65]. In this kind of combination, the robust controller would be enhanced by using an adaptive controller which increases the operation range of the closed loop system. On the other side, the robust controller may enhance the performance of the adaptive one as well [62]. An example for this combination is the Adaptive Sliding Mode Control (ASMC) [66] which can deal with a wide range of perturbed linear or nonlinear plants with uncertainties. The above mentioned approach of adaptive control, can be extended to cover many classes of nonlinear systems.

Remark 5.1.1 In the approach of Self-Tuning Regulation (STR) and the Model Reference Control (MRAC) the plant parameters can be estimated and then the controller parameters are computed. Such a scheme is called usually indirect (explicit) adaptive control, because, one must translate the estimated parameters of the plant into controller tuning parameters. In other approaches it is possible to eliminate this intermediate step of the computation by reparameterizing the plant dynamics using the controller parameters which are also unknown and to be adjusted. Therefore, this kind of adaptation is called a direct (implicit) adaptive control.

Remark 5.1.2 There are related techniques which deal with linear and nonlinear plants such as the Extremum Seeking method, which is presented in [67].

Remark 5.1.3 It is worth noticing, that the important difference between the STR and MRAC techniques lies in regarding the parameter estimation. The parameter estimation of the plant in STR can be understood, actually, as the procedure of finding (estimation) a set of parameters that matches the available input-output data from a plant. But on the other hand, this is unlike the parameter adaptation in MRAC systems, where the parameters in MRAC are adjusted so that the tracking errors converge to zero.

5.2 Static and Dynamic Feedback

To illustrate the idea of adaptation as a dynamic feedback and the difference between static and dynamic controller design we consider the following nonlinear dynamics[1] [68]

$$\dot{x} = u + \theta \, \phi(x) \tag{5.1}$$

where θ an unknown constant parameter and $\phi(x)$ is a known basis function. We distinguish between a static feedback controller and dynamic (adaptive) one:
Let a static feedback be

$$u = -c \, x - k \, x \, \phi^2(x) \tag{5.2}$$

to investigate the stability of the system (5.2) we define Lyapunov function $V = \frac{1}{2}x^2$. By placing (5.2) into system (5.1) and utilizing the completion of squares we can determine the derivative of the Lyapunov function as

$$
\begin{aligned}
\dot{V} = x \, \dot{x} &= x \left(-c \, x - k \, x \, \phi^2(x) + \theta \, \phi(x) \right) \\
&= -c \, x^2 - k \left(x \phi(x) - \frac{\theta}{2k} \right)^2 + \frac{\theta^2}{4k} \leq -c \, x^2 + \frac{\theta^2}{4k}
\end{aligned}
\tag{5.3}
$$

which means that $x(t)$ converges to the interval

$$|x| \leq \frac{|\theta|}{2\sqrt{k \, c}} \quad . \tag{5.4}$$

This interval can be reduced by increasing the gains k and c, but $x(t)$ will not converge to zero if θ is a nonzero constant. Excessive increase of these gains enlarges the system bandwidth, which is undesirable. Our task is therefore to achieve $\lim_{t \to \infty} x(t) = 0$

---

[1]The notation in this example is not to be confused with the notation of the variables throughout the remainder of this thesis

without increasing k and c. In fact, we will first accomplish this task with $k = 0$ and then use $k > 0$ to improve the transients. To achieve regulation of $x(t)$, we design a dynamic feedback controller with adaptation. If θ was known, the control

$$u = -\theta \, \phi(x) - c \, x, \qquad c > 0 \tag{5.5}$$

would yield the derivative of $V(x) = \frac{1}{2}x^2$ negative definite: $\dot{V} = -c \, x^2$.

Of course, the control law (5.5) can not be implemented, since θ is unknown. Let $\hat{\theta}$ be an estimation of the unknown parameter θ. Now we apply the certainty equivalence principle which amounts to replacing the unknown parameter θ with its estimate $\hat{\theta}$ in the control law. We get

$$u = -\hat{\theta}\phi(x) - c \, x. \tag{5.6}$$

Replacing the control law (5.6) into the system (5.1), we get the closed-loop system

$$\dot{x} = -c \, x + \tilde{\theta} \, \phi(x) \tag{5.7}$$

with $\tilde{\theta} = \theta - \hat{\theta}$ the parameter error. Then we get the derivative of the corresponding Lyapunov function $V(x) = \frac{1}{2}x^2$ as

$$\dot{V} = -c \, x^2 + \tilde{\theta} \, x \, \phi(x). \tag{5.8}$$

One can notice that this choice of the Lyapunov function candidate would not help guaranteeing the stability of the closed-loop system since the term $\tilde{\theta} \, x \, \phi(x)$ in (5.8) is indefinite. To get around this problem, one can extend the Lyapunov function candidate as

$$V_1(x, \tilde{\theta}) = \frac{1}{2}x^2 + \frac{1}{2\gamma}\tilde{\theta}^2 \tag{5.9}$$

where $\gamma > 0$ is a gain. The time derivative of the extended Lyapunov function

$$\dot{V}_1 = x\dot{x} + \frac{1}{\gamma}\tilde{\theta}\dot{\tilde{\theta}} = -c \, x^2 + \tilde{\theta} \, x \, \phi(x) + \frac{1}{\gamma}\tilde{\theta}\dot{\tilde{\theta}} = -c \, x^2 + \tilde{\theta}\left[x \, \phi(x) + \frac{1}{\gamma}\dot{\tilde{\theta}}\right]. \tag{5.10}$$

By defining the new estimator dynamics

$$\dot{\hat{\theta}} = -\dot{\tilde{\theta}} = \gamma \, x \, \phi(x) \tag{5.11}$$

and inserting it in (5.10) guarantees that

$$\dot{V}_1 \leq -c\, x^2 \leq 0. \tag{5.12}$$

Plant
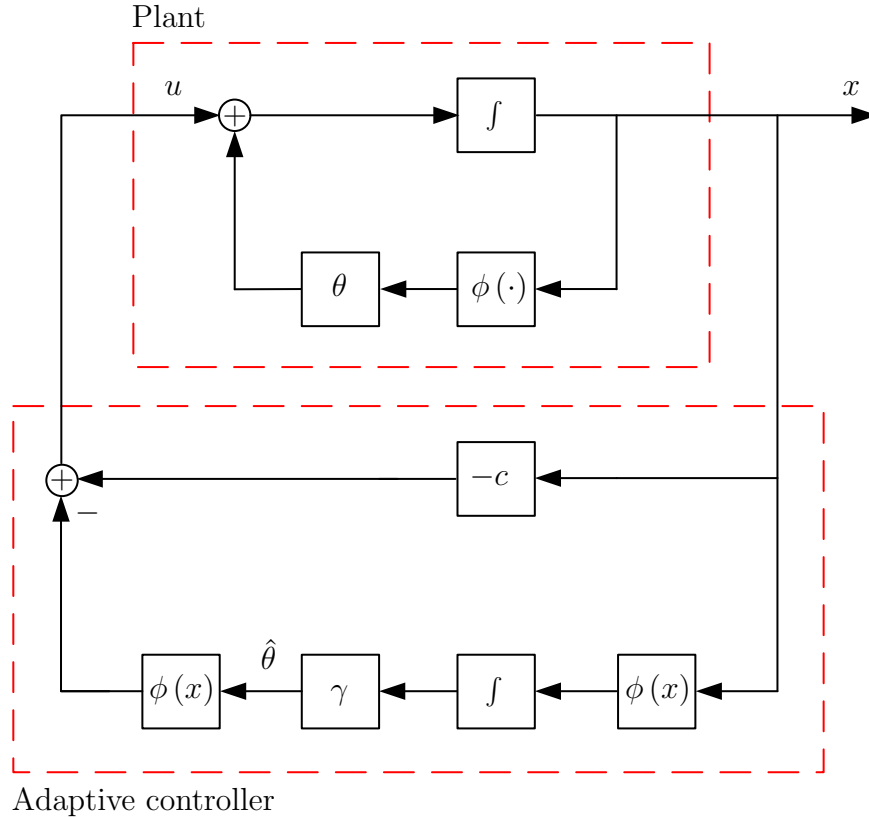
Fig. 5.1: The closed-loop adaptive system (5.13)

The resulting adaptive system consists of the system (5.1), the control law (5.6) and the update law (5.11). We can write the closed-loop system and its update law as

$$\begin{aligned}
\dot{x} &= -c\, x^2 + \tilde{\theta}\phi\,(x) \\
\dot{\tilde{\theta}} &= -\gamma\, x\, \phi(x).
\end{aligned} \tag{5.13}$$

The structure of the closed-loop system is illustrated in Figure 5.1. Since $\dot{V}_1 \leq 0$, the equilibrium $x = 0, \tilde{\phi} = 0$ of (5.13) is globally stable. In addition, the desired regulation property $\lim_{t \to \infty} x\,(t) = 0$ follows from Krasovskii's theorem [68].

From this example, we have seen that the adaptive controller is more effective than conventional feedback in presence of parameter uncertainties. The adaptive controller

is adjusted automatically in real-time, based on the system signals, in order to achieve or maintain a desired performance, when the parameters of the plant are unknown and/or changing in time.

5.3 Adaptive Backstepping Control

In this section we will introduce the approach for designing a robust adaptive controller and the backstepping approach. Finally, we will see how to combine those two approaches to design a robust and adaptive backstepping controller.

5.3.1 Robust Adaptive Control

In order to introduce the idea of designing the desired controller, let us start with an example, in which we will design a robust adaptive controller for a scalar system.

Consider a nonlinear model

$$\dot{\chi} = g_0 \, u_c + \bar{\Upsilon} \hbar \left(\chi \right) + \bar{\bar{\Xi}} \left(\chi, t \right) \tag{5.14}$$

where g_0 is an unknown constant positive parameter, $\bar{\Upsilon}$ is an unknown constant parameter, $\hbar$ is a known smooth function, $\bar{\bar{\Xi}}$ is an unknown function, and u_c is the control input. We assume that the nominal system (without $\Xi \left(\chi, t \right)$) has an equilibrium point at $\chi = 0$, which suggests that $\hbar \left(\chi \right) = 0$.

The system (5.14) has two types of uncertainty: The parametric uncertainty caused by the unknown parameter $\bar{\Upsilon}$ and the nonlinear uncertainty that appears due to $\bar{\bar{\Xi}} \left(\chi, t \right)$. The latter could arise because of unmodeled dynamics, measurement noise or external disturbance. To design the controller one needs at least the bounds for nonlinear uncertainty. Therefore, we assume that $\bar{\bar{\Xi}} \left(\chi, t \right)$ is bounded, i.e.

$$\left| \bar{\bar{\Xi}} \left(\chi, t \right) \right| \leq \bar{\Delta}, \quad \forall \chi \in \mathbb{R}, \forall t \in \mathbb{R}^+ \tag{5.15}$$

where $\bar{\Delta}$ is a known positive constant. The dynamics (5.14) can be rewritten as

$$\dot{\chi} = g_0 \left(u_c + \frac{\bar{\Upsilon}}{g_0} \hbar \left(\chi \right) + \frac{\bar{\bar{\Xi}} \left(\chi, t \right)}{g_0} \right) \tag{5.16}$$

51

or

$$\dot{\chi} = g_0 \left(u_{\mathrm{c}} + \Upsilon \hbar \left(\chi \right) + \Xi \left(\chi, t \right) \right) \tag{5.17}$$

with $\Upsilon = \dfrac{\bar{\Upsilon}}{g_0}$ and $\Xi \left(\chi, t \right) = \dfrac{\bar{\Xi} \left(\chi, t \right)}{g_0}$.

To design a stabilizing control law u_{c} for the system (5.17) we consider the Lyapunov function candidate

$$V = \frac{1}{2g_0} \chi^2 + \frac{1}{2c_1} \tilde{\Upsilon}^2 + \frac{1}{2c_2} \tilde{\Delta}^2 \tag{5.18}$$

where $\tilde{\Upsilon} = \hat{\Upsilon} - \Upsilon$ and $\tilde{\Delta} = \hat{\Delta} - \Delta$ are the estimation errors, $\hat{\Upsilon}$ and $\hat{\Delta}$ are the estimates of Υ and Δ, respectively, and c_1, c_2 are positive constants, where $\Delta = \bar{\Delta}/g_0$. The time derivative of the Lyapunov function is:

$$\dot{V} = \frac{1}{g_0} \chi \dot{\chi} + \frac{1}{c_1} \tilde{\Upsilon} \dot{\tilde{\Upsilon}} + \frac{1}{c_2} \tilde{\Delta} \dot{\tilde{\Delta}}. \tag{5.19}$$

As a control law, we consider

$$u_{\mathrm{c}} = - \left(k_{\mathrm{c}} \chi + \hat{\Upsilon} \hbar \left(\chi \right) + \varrho \left(\chi, \hat{\Delta} \right) \right) \tag{5.20}$$

where $k_{\mathrm{c}} > 0$ is a design constant and the control constituent $\varrho \left(\chi, \hat{\Delta} \right)$ deals with the uncertainty $\Xi \left(\chi, t \right)$. Now, placing (5.20) and (5.17) into (5.19), we obtain

$$
\begin{aligned}
\dot{V} \leq & \chi \left(-k_{\mathrm{c}} \chi - \tilde{\Upsilon} \hbar \left(\chi \right) - \varrho \left(\chi, \hat{\Delta} \right) + \Xi \left(\chi, t \right) \right) + \frac{1}{c_1} \tilde{\Upsilon} \dot{\hat{\Upsilon}} + \frac{1}{c_2} \tilde{\Delta} \dot{\hat{\Delta}} \\
\leq & - k_{\mathrm{c}} \chi^2 + \tilde{\Upsilon} \left(\frac{1}{c_1} \dot{\hat{\Upsilon}} - \hbar \left(\chi \right) \chi \right) + \frac{1}{c_2} \tilde{\Delta} \dot{\hat{\Delta}} - \varrho \left(\chi, \hat{\Delta} \right) \chi + \chi \Xi \left(\chi, t \right) \\
\leq & - k_{\mathrm{c}} \chi^2 + \tilde{\Upsilon} \left(\frac{1}{c_1} \dot{\hat{\Upsilon}} - \hbar \left(\chi \right) \chi \right) + \frac{1}{c_2} \tilde{\Delta} \dot{\hat{\Delta}} - \varrho \left(\chi, \hat{\Delta} \right) \chi + |\chi| \left| \Xi \left(\chi, t \right) \right| \\
\leq & - k_{\mathrm{c}} \chi^2 + \tilde{\Upsilon} \left(\frac{1}{c_1} \dot{\hat{\Upsilon}} - \hbar \left(\chi \right) \chi \right) + \frac{1}{c_2} \tilde{\Delta} \dot{\hat{\Delta}} - \varrho \left(\chi, \hat{\Delta} \right) \chi + \chi \mathrm{sgn} \left(\chi \right) \Delta
\end{aligned} \tag{5.21}
$$

where the function $\mathrm{sgn} \left(\cdot \right)$ is the sign function defined as

$$\mathrm{sgn} \left(\chi \right) = \begin{cases} 1 & \text{if } \chi \geq 0 \\ -1 & \text{if } \chi < 0. \end{cases} \tag{5.22}$$

Let the control component $\varrho \left(\chi, \hat{\Delta} \right)$ be defined as

$$\varrho \left(\chi, \hat{\Delta} \right) = \hat{\Delta} \, \mathrm{sgn} \left(\chi \right). \tag{5.23}$$

Now, by placing (5.23) into the last inequality of (5.21) we get

$$
\begin{aligned}
\dot{V} \leq & - k_{\mathrm{c}}\chi^2 + \tilde{\Upsilon}\left(\frac{1}{c_1}\dot{\hat{\Upsilon}} - \hbar\left(\chi\right)\chi\right) + \frac{1}{c_2}\tilde{\Delta}\dot{\hat{\Delta}} - \chi\mathrm{sgn}\left(\chi\right)\hat{\Delta} + \chi\mathrm{sgn}\left(\chi\right)\Delta \\
\leq & - k_{\mathrm{c}}\chi^2 + \tilde{\Upsilon}\left(\frac{1}{c_1}\dot{\hat{\Upsilon}} - \hbar\left(\chi\right)\chi\right) + \tilde{\Delta}\left(\frac{1}{c_2}\dot{\hat{\Delta}} - \chi\mathrm{sgn}\left(\chi\right)\right).
\end{aligned}
\tag{5.24}
$$

To make the time derivative of the Lyapunov function negative semidefinite, $\dot{V} \leq 0$, we choose the adaptation laws as

$$
\begin{aligned}
\dot{\hat{\Upsilon}} &= c_1\hbar\left(\chi\right)\chi \\
\dot{\hat{\Delta}} &= c_2\chi\mathrm{sgn}\left(\chi\right)
\end{aligned}
\tag{5.25}
$$

by means of which we get

$$
\dot{V} \leq - k_{\mathrm{c}}\chi^2 \leq 0,
\tag{5.26}
$$

which implies that Υ, Δ and χ are uniformly bounded. Moreover using LaSalle's invariance principle [69] the origin is asymptotically stable and $\chi\left(t\right)$ goes to zero, as t goes to infinity. We insert (5.23) in (5.20) and obtain

$$
u_{\mathrm{c}} = - \left(k_{\mathrm{c}}\chi + \hat{\Upsilon}\hbar\left(\chi\right) + \hat{\Delta}\,\mathrm{sgn}\left(\chi\right)\right).
\tag{5.27}
$$

In the control law (5.27), the chattering problem may emerge due to the sign function because in real-world implementation the measurements of χ can be perturbed [70]. For the backstepping procedure, to design the controller for the entire system, we need to derivate the intermediate control law (it may be the control (5.27)). This will lead to a singularity. Therefore, to avoid those two problems we approximate the sign function by tanh (hyperbolic tangent) function [71, 72], which means

$$
\mathrm{sgn}\left(\chi\right) \rightarrow \tanh\left(\frac{\chi}{\varepsilon_\chi}\right), \quad \varepsilon_\chi > 0.
\tag{5.28}
$$

In doing so, we obtain a new control component ϱ and a new adaptation law by replacing $\mathrm{sgn}\left(\chi\right)$ function with $\tanh\left(\frac{\chi}{\varepsilon_\chi}\right)$ function in (5.23) as well in (5.25).

Now, in light of this modification in the controller, we analyze the stability of the closed loop system. Thus, the component of the controller, which compensates the unmodeled

uncertainties will be given as

$$\varrho\left(\chi,\hat{\Delta}\right) = \hat{\Delta}\tanh\left(\frac{\chi}{\varepsilon_\chi}\right). \tag{5.29}$$

Finally, by placing (5.29) in the last inequality of (5.21) we get

$$\begin{aligned}\dot{V} \leq &-k_\mathrm{c}\chi^2 + \tilde{\Upsilon}\left(\frac{1}{c_1}\dot{\hat{\Upsilon}} - \hbar\left(\chi\right)\chi\right) + \frac{1}{c_2}\tilde{\Delta}\dot{\hat{\Delta}} - \chi\tanh\left(\frac{\chi}{\varepsilon_\chi}\right)\hat{\Delta} + \chi\mathrm{sgn}\left(\chi\right)\Delta \\ \leq &-k_\mathrm{c}\chi^2 + \tilde{\Upsilon}\left(\frac{1}{c_1}\dot{\hat{\Upsilon}} - \hbar\left(\chi\right)\chi\right) + \tilde{\Delta}\left(\frac{1}{c_2}\dot{\hat{\Delta}} - \chi\tanh\left(\frac{\chi}{\varepsilon_\chi}\right)\right) \\ &+ \Delta\left(|\chi| - \chi\tanh\left(\frac{\chi}{\varepsilon_\chi}\right)\right)\end{aligned} \tag{5.30}$$

where $|\chi| = \mathrm{sgn}\left(\chi\right)\chi$.

To render $\dot{V}$ negative, the adaptation laws in (5.30) can be chosen as

$$\dot{\hat{\Upsilon}} = c_1\hbar\left(\chi\right)\chi \text{ and } \dot{\hat{\Delta}} = c_2\chi\tanh\left(\frac{\chi}{\varepsilon_\chi}\right). \tag{5.31}$$

Note that we may use the inequality (it will be proved in 5.3.1)

$$0 \leq |\chi| - \chi\tanh\left(\frac{\chi}{\varepsilon_\chi}\right) \leq k_\chi\varepsilon_\chi, \ \ k_\chi \simeq 0.2785, \varepsilon_\chi > 0. \tag{5.32}$$

Then the time derivative of the Lyapunov function in (5.30) is given as

$$\dot{V} \leq 0.2785\,\Delta\,\varepsilon_\chi \tag{5.33}$$

where the positive constant ε_χ can be chosen arbitrary small.

Remark 5.3.1 By utilizing the tanh function we avoid the chattering as well as the singularity problem. On the other side, the value of $\chi\left(t\right)$ will never converge to zero, but to an arbitrary neighborhood around the zero.

Now, we introduce a proof of the inequality (5.32).

Proof 5.3.1 Based on the Lemma 3.3 in [73]we have that:

For any $\varepsilon_\chi > 0$ there exists a smooth function g_χ such that $g_\chi(0) = 0$ and

$$|\bar{\chi}| \le \bar{\chi} g_\chi(\bar{\chi}) + \varepsilon_\chi, \quad \forall \bar{\chi} \in \mathbb{R}. \tag{5.34}$$

Let the smooth function in (5.34) be

$$g_\chi(\bar{\chi}) = \tanh\left(\frac{k_\chi \bar{\chi}}{\varepsilon_\chi}\right), \quad k_\chi > 0 \tag{5.35}$$

then

$$|k_\chi \bar{\chi}| - k_\chi \bar{\chi} \tanh\left(\frac{k_\chi \bar{\chi}}{\varepsilon_\chi}\right) \le k_\chi \varepsilon_\chi \tag{5.36}$$

where $|k_\chi \bar{\chi}| \le k_\chi |\bar{\chi}|$. Letting $k_\chi \bar{\chi} = \chi \in \mathbb{R}$ we obtain

$$|\chi| - \chi \tanh\left(\frac{\chi}{\varepsilon_\chi}\right) \le k_\chi \varepsilon_\chi. \tag{5.37}$$

The inequality (5.37) holds for a certain interval of values of k_χ. To determine this interval of k_χ we can show that

$$0 \le |\chi| - \chi \tanh\left(\frac{\chi}{\varepsilon_\chi}\right). \tag{5.38}$$

This is true due to

$$\chi \tanh\left(\frac{\chi}{\varepsilon_\chi}\right) \ge 0, \text{ and } \tanh\left(\frac{\chi}{\varepsilon_\chi}\right) \in (-1, +1), \quad \forall \chi \in \mathbb{R} \tag{5.39}$$

which shows inequality (5.38). Then, to proof that

$$|\chi| - \chi \tanh\left(\frac{\chi}{\varepsilon_\chi}\right) \le k_\chi \varepsilon_\chi \tag{5.40}$$

we define

$$f(\chi) = \left|\frac{\chi}{\varepsilon_\chi}\right| - \frac{\chi}{\varepsilon_\chi} \tanh\left(\frac{\chi}{\varepsilon_\chi}\right) \le k_\chi. \tag{5.41}$$

It must be shown that this function has a maximum. Owing to $f(\chi) = f(-\chi)$ function $f(\chi)$ is an even function. Therefore, it is sufficient to investigate the maximum of $f(\chi)$

just for $\chi > 0$. Thus, by defining a new variable $\omega = \dfrac{\chi}{\varepsilon_\chi}$, we get

$$f(\omega) = \omega - \omega \tanh(\omega) \tag{5.42}$$

and the derivative of $f(\omega)$ with respect to ω

$$\begin{aligned}
\frac{\mathrm{d}f(\omega)}{\mathrm{d}\omega} &= 1 - \tanh(\omega) - \omega\left(1 - \tanh^2(\omega)\right) \\
&= (1 - \tanh(\omega))(1 - \omega(1 + \tanh(\omega)))
\end{aligned} \tag{5.43}$$

Letting $\dfrac{\mathrm{d}f(\omega)}{\mathrm{d}\omega} = 0$ in (5.43), we obtain either

$$\tanh(\omega) = 1 \Rightarrow \omega \to +\infty \tag{5.44}$$

which means $f(\chi)$ tends to zero in this case, or

$$\omega + \omega \tanh(\omega) = 1. \tag{5.45}$$

To find the solution of (5.45), first recall that, $\tanh(\omega) = \dfrac{e^\omega - e^{-\omega}}{e^\omega + e^{-\omega}}$ and (5.45) will result in

$$(2\omega - 1)e^{(2\omega - 1)} = e^{-1}. \tag{5.46}$$

The equation (5.46) belongs to the class of function with the following general form [74]

$$y e^y = \alpha \tag{5.47}$$

where y is so-called *Lambert* function and the solution of this class of functions is given as

$$y = \text{Lambert\_}W(\alpha). \tag{5.48}$$

Applying that on the equation (5.46) we obtain

$$2\omega - 1 = \text{Lambert\_}W\left(e^{-1}\right) \Rightarrow \omega = \frac{1}{2}\text{Lambert\_}W\left(e^{-1}\right) + \frac{1}{2} \tag{5.49}$$

which yields

$$\chi = \left(\frac{1}{2}\text{Lambert\_}W\left(e^{-1}\right) + \frac{1}{2}\right)\varepsilon_\chi. \tag{5.50}$$

Inserting (5.50) into (5.41), we obtain the value of the Extremum of $f(\chi)$ at this point.

Remark 5.3.2 The Lambert function may be calculated through

$$\text{Lambert\_}W(\alpha) = \sum_{n=1}^{\infty} \frac{(-n)^{(n-1)}}{n!} \bar{\alpha}^n. \tag{5.51}$$

The series (5.51) converges for $-e^{-1} \leq \alpha \leq e^{-1}$, see [74]. Therefore, the solution of (5.45) exists and converges, since $\alpha = e^{-1}$, with sufficiently large value of n in (5.51). Let $n = 200$ for instance, then we get $\text{Lambert\_}W(e^{-1}) = 0.2784645428$. Now we can calculate the solution of (5.45): $\omega \simeq 0.6392$. Thus, we have $\chi \simeq 0.6392\,\varepsilon_\chi$.

It can be shown that the second derivative of the function $f(\chi)$ wrt. χ evaluated at

$$\chi = 0.6392\,\varepsilon_\chi \tag{5.52}$$

is less than zero $\left(\text{actually it equals} -0.8712468223/\epsilon_\chi^2 < 0\right)$ which implies a maximum at the considered point.

By evaluating the function $f(\chi)$ at $\chi = 0.6392\,\varepsilon_\chi$ and by noticing (5.41) we obtain

$$f(\chi) = 0.2784645428 \simeq 0.2785 \leq k_\chi. \tag{5.53}$$

This means that $k_\chi \simeq 0.2785$ is the smallest value for which the inequality (5.32) is satisfied. Then

$$0 \leq |\chi| - \chi \tanh\left(\frac{\chi}{\varepsilon_\chi}\right) \leq 0.2785\,\varepsilon_\chi, \quad \varepsilon_\chi > 0. \tag{5.54}$$

This completes the proof of (5.32).

5.3.2 Backstepping Control

For a special class of nonlinear dynamical systems (triangular-like structure) a so-called backstepping controller is designed to stabilize a system of subsystems. The controllers of the subsystems are designed using some control techniques and then, recursively, the final external control for the entire system is attained [68].

In this subsection we will state the idea of the backstepping approach by introducing the so-called strict-feedback backstepping control. To this end, we will start with presenting

the simplest case: The integrator backstepping. Then we extend it to a more general form which is the strict-feedback backstepping.

5.3.2.1 Integrator Backstepping

To illustrate the idea of the integrator backstepping we consider the following nonlinear system [69]

$$\dot{\varkappa} = f(\varkappa) + g(\varkappa)\zeta \tag{5.55}$$

$$\dot{\zeta} = u_\varkappa \tag{5.56}$$

$$y_\varkappa = \varkappa \tag{5.57}$$

where $\varkappa, \zeta, y_\varkappa \in \mathbb{R}$ and $u_\varkappa \in \mathbb{R}$, and the functions $f(\varkappa), g(\varkappa)$ are known. Now, we design a state feedback controller $u_\varkappa$ to force the output to converge to zero as t goes to infinity. The controller will stabilize the equilibrium point of the system $(5.55) - (5.56)$

$$(\varkappa_R, \zeta_R) = \left(0, -\frac{f(0)}{g(0)}\right), \quad g(0) \neq 0. \tag{5.58}$$

The structure of this system suggests that the system can be seen as connection of two components or subsystems in cascade manner, as shown in Figure 5.2.
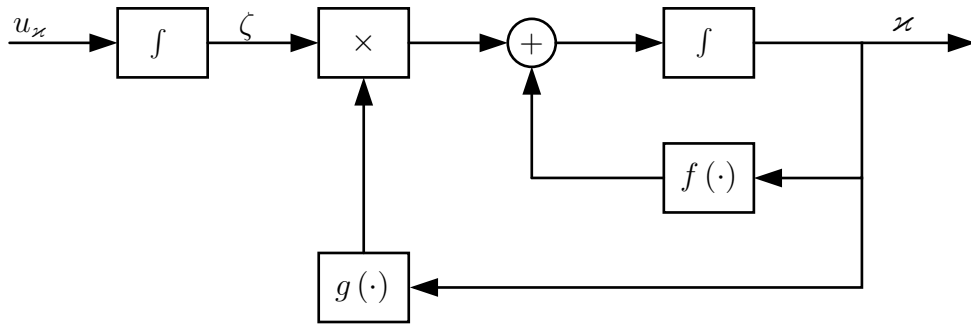
Fig. 5.2: The block diagram of the system $(5.55) - (5.56)$

The controller design is processed recursively in two steps: Suppose we can find a smooth stabilizing function $\alpha_\varkappa(\varkappa)$ which stabilizes the subsystem (5.55) at the origin $\varkappa = 0$. Now, in the first step, we choose the state ζ as a virtual control input of the subsystem

(5.55). This yields

$$\zeta = \alpha_\varkappa + (\zeta - \alpha_\varkappa)$$
$$= \alpha_\varkappa + \bar{\zeta} \tag{5.59}$$

where $\bar{\zeta} = \zeta - \alpha_\varkappa$ is a new state variable. Hence, by replacing the virtual control (5.59) into the first subsystem (5.55) we obtain

$$\dot{\varkappa} = f(\varkappa) + g(\varkappa)\alpha_\varkappa(\varkappa) + g(\varkappa)\bar{\zeta}. \tag{5.60}$$

Moreover, we suppose that a smooth and positive definite Lyapunov function $V(\varkappa)$ exists. Then by using the stabilizing function $\alpha_\varkappa$ we obtain the following inequality

$$\dot{V}(\varkappa) = \frac{\partial V}{\partial \varkappa}\Big[f(\varkappa) + g(\varkappa)\alpha_\varkappa(\varkappa)\Big] \leq -W(\varkappa), \quad \forall \varkappa \in \mathbb{R} \tag{5.61}$$

where $W(\varkappa)$ is a positive definite term. Furthermore, by differentiating (5.59) and using (5.60) the new input

$$\nu_\varkappa = u_\varkappa - \dot{\alpha}_\varkappa \tag{5.62}$$

we obtain the new system in the new coordinates

$$\dot{\varkappa} = f(\varkappa) + g(\varkappa)\alpha_\varkappa(\varkappa) + g(\varkappa)\bar{\zeta}$$
$$\dot{\bar{\zeta}} = \nu_\varkappa. \tag{5.63}$$

This is depicted in Figure 5.4. In view of Figures 5.3 and 5.4, the function $\alpha_\varkappa(\varkappa)$ is *backstepping* through the integrator. We can observe clearly that the first subsystem in (5.63) has an asymptotically stable origin when its input is identically zero, i.e. $\bar{\zeta} = 0$. Now, the task is to design a stabilizing controller $\nu_\varkappa$ to stabilize the state variable $\bar{\zeta}$ at the origin. When we find this controller, then the overall system can be stabilized. To achieve this we use the Lyapunov function candidate

$$V_\varkappa(\varkappa, \zeta) = V(\varkappa) + \frac{1}{2}\bar{\zeta}^2. \tag{5.64}$$

Its derivative is given as

$$\dot{V}_\varkappa = \frac{\partial V}{\partial \varkappa}[f(\varkappa) + g(\varkappa)\alpha_\varkappa(\varkappa)] + \frac{\partial V}{\partial \varkappa}g(\varkappa)\bar{\zeta} + \nu_\varkappa\bar{\zeta}$$
$$= -W(\varkappa) + \frac{\partial V}{\partial \varkappa}g(\varkappa)\bar{\zeta} + \nu_\varkappa\bar{\zeta} \tag{5.65}$$

which by choosing the control law

$$\nu_\varkappa = -\frac{\partial V}{\partial \varkappa} g(\varkappa) - k_\zeta \bar{\zeta}, \quad k_\zeta > 0 \tag{5.66}$$

yields

$$\dot{V}_\varkappa \leq -W(\varkappa) - k_\zeta \bar{\zeta}^2. \tag{5.67}$$

Thus, the origin $\left(\varkappa = 0, \bar{\zeta} = 0\right)$ is asymptotically stable. Also equivalently, the equilibrium

$$(\varkappa_R, \zeta_R) = \left(0, -\frac{f(0)}{g(0)}\right) \tag{5.68}$$

is asymptotically stable regarding the original coordinate system $(\varkappa, \zeta)$.
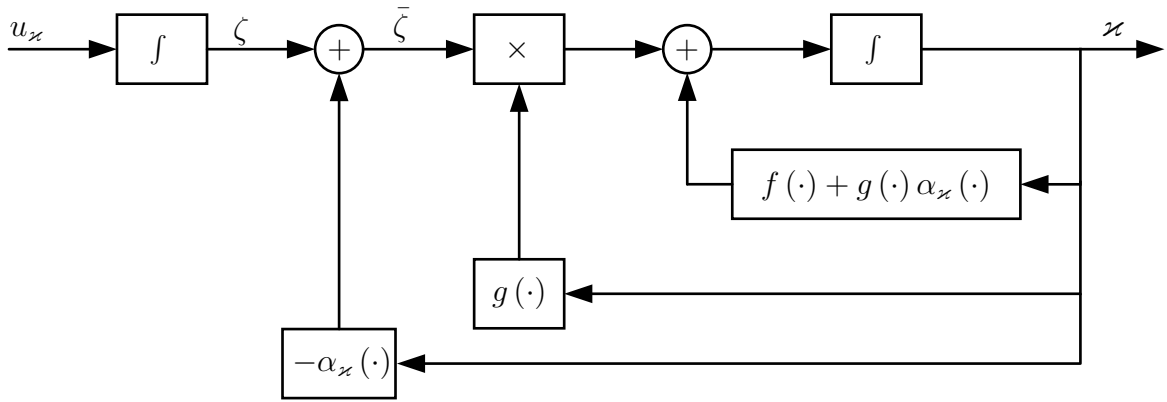
Fig. 5.3: Introducing $\alpha_\varkappa$ the stabilizing function of the subsystem (5.55)
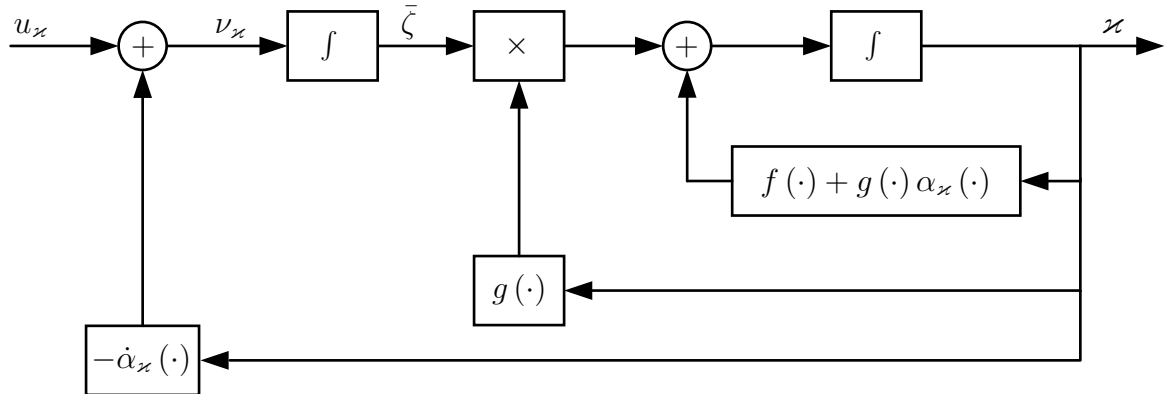
Fig. 5.4: Backstepping of $-\alpha_\varkappa(\cdot)$ through the integrator

60

Inserting (5.66) into (5.62) we obtain the feedback control law for the system (5.55) − (5.56) as

$$u_\varkappa = \frac{\partial \alpha_\varkappa}{\partial \varkappa} \left[f(\varkappa) + g(\varkappa) \zeta \right] - \frac{\partial V}{\partial \varkappa} g(\varkappa) - k_\zeta \left[\zeta - \alpha_\varkappa(\varkappa) \right]. \tag{5.69}$$

Remark 5.3.3 If the backstepping controller is performed for the nonlinear system (5.55) − (5.56), and if the Lyapunov function for the subsystem (5.55) is chosen as

$$V = \frac{1}{2}\varkappa^2 \tag{5.70}$$

then the stabilizing function is the feedback linearizing controller [75]

$$\alpha_\varkappa = -\frac{1}{g(\varkappa)}\left(f(\varkappa) + k_\varkappa \varkappa \right). \tag{5.71}$$

The dynamics in the closed loop in $\left(\varkappa, \bar{\zeta}\right)$ coordinates reads

$$\begin{pmatrix} \dot{\varkappa} \\ \dot{\bar{\zeta}} \end{pmatrix} = \underbrace{\begin{pmatrix} -k_\varkappa & 0 \\ 0 & -k_\zeta \end{pmatrix}}_{\text{diagonal matrix}} \begin{pmatrix} \varkappa \\ \bar{\zeta} \end{pmatrix} + \underbrace{\begin{pmatrix} 0 & g(\varkappa) \\ -g(\varkappa) & 0 \end{pmatrix}}_{\text{skew-symmetrical matrix}} \begin{pmatrix} \varkappa \\ \bar{\zeta} \end{pmatrix} \tag{5.72}$$

or

$$\dot{\boldsymbol{\zeta}} = -\mathbf{K}_\zeta \boldsymbol{\zeta} + \mathbf{S}(\boldsymbol{\zeta})\boldsymbol{\zeta} \tag{5.73}$$

with $\boldsymbol{\zeta} = \left(\varkappa, \bar{\zeta}\right)^\top$, $\mathbf{K}_\zeta = \mathrm{diag}\left(k_\varkappa, k_\zeta\right)$ positive definite, and

$$\mathbf{S}(\boldsymbol{\zeta}) = -\left(\mathbf{S}(\boldsymbol{\zeta})\right)^\top = \begin{pmatrix} 0 & g(\varkappa) \\ -g(\varkappa) & 0 \end{pmatrix}. \tag{5.74}$$

To investigate the stability of the equilibrium $\boldsymbol{\zeta} = \mathbf{0}$ of the autonomous system (5.73) we define the Lyapunov function

$$\begin{aligned} V_\zeta &= \frac{1}{2}\boldsymbol{\zeta}^\top \boldsymbol{\zeta} \\ \Rightarrow \dot{V}_\zeta &= \boldsymbol{\zeta}^\top \left[-\mathbf{K}_\zeta \boldsymbol{\zeta} + \mathbf{S}(\boldsymbol{\zeta})\boldsymbol{\zeta} \right] \\ &= -\boldsymbol{\zeta}^\top \mathbf{K}_\zeta \boldsymbol{\zeta}. \end{aligned} \tag{5.75}$$

Thus, according to Lyapunov's direct method the equilibrium $\boldsymbol{\zeta} = \mathbf{0}$ in the transformed

coordinates, or equivalently the equilibrium

$$(\varkappa_R, \zeta_R) = \left(0, -\frac{f(0)}{g(0)}\right) \tag{5.76}$$

in the origin coordinates, is a globally asymptotically stable equilibrium point (GAS). Moreover, we can show that this equilibrium point is globally exponentially stable (GES), see Theorem 5 in Appendix A of [75].

5.3.2.2 Strict-Feedback Backstepping

Now, we extend the above discussed integrator backstepping technique to cover a class of nonlinear systems which are given in so-called strict-feedback form. The strict-feedback form differs from the so-called pure-feedback form, where in the first form the control inputs of the subsystems appear explicit in the right-hand side of the differential equations, while they emerge implicit in the second form. Since our considered system has the strict-feedback structure, we limit ourselves to the class of strict-feedback form.

Let the triangular-like system be given in the strict-feedback form

$$\begin{aligned}
\dot{\varkappa}_1 &= f_1(\varkappa_1) + g_1(\varkappa_1)\varkappa_2 \\
\dot{\varkappa}_2 &= f_2(\varkappa_1, \varkappa_2) + g_2(\varkappa_1, \varkappa_2)\varkappa_3 \\
&\quad\vdots \qquad \vdots \qquad\qquad \vdots \\
\dot{\varkappa}_{n-1} &= f_{n-1}(\varkappa_1, ..., \varkappa_{n-1}) + g_n(\varkappa_1, ..., \varkappa_{n-1})u_n
\end{aligned} \tag{5.77}$$

where, $\varkappa_1, \ldots, \varkappa_{n-1} \in \mathbb{R}$ are the states of the system, $u_n \in \mathbb{R}$ is the input, and the output is $y_1 = \varkappa_1$. We assume that the functions $f_1, g_1, \ldots, f_{n-1}, g_{n-1}$ are nonlinear known functions. The equilibrium of this system can be determined recursively. For instance in case $n = 4$ the equilibrium point is

$$(\varkappa_{1R}, \varkappa_{2R}, \varkappa_{3R}) = \left(0, -\frac{f_1(0)}{g_1(0)}, -\frac{f_2\left(0, -\frac{f_1(0)}{g_1(0)}\right)}{g_2\left(0, -\frac{f_1(0)}{g_1(0)}\right)}\right). \tag{5.78}$$

Let us consider a nonlinear system in strict-feedback for two subsystems ($n = 3$), namely

$$\dot{\varkappa}_1 = f_1(\varkappa_1) + g_1(\varkappa_1)\varkappa_2 \tag{5.79}$$

$$\dot{\varkappa}_2 = f_2(\varkappa_1, \varkappa_2) + g_2(\varkappa_1, \varkappa_2)u_2, \tag{5.80}$$

the equilibrium of this system is

$$(\varkappa_{1R}, \varkappa_{2R}) = \left(0, -\frac{f_1(0)}{g_1(0)}\right) \tag{5.81}$$

and the output of the system is the state $\varkappa_1$. This nonlinear dynamics is illustrated in Figure 5.5. The idea of designing the controller for the system $(5.79 - 5.80)$ is to find a virtual stabilizing control law for the subsystem (5.79) at the origin $\varkappa_1 = 0$ regarding a Lyapunov function V_{1s}. Now, to find the controller, we define the following Lyapunov function for the whole system $(5.79 - 5.80)$ as

$$V_s = V_{1s} + \frac{1}{2}\Big[\varkappa_2 - \alpha_s(\varkappa_1)\Big]^2 \tag{5.82}$$

$$\Rightarrow \dot{V}_s = \frac{\partial V_{1s}}{\partial \varkappa_1}\left(f_1(\varkappa_1) + g_1(\varkappa_1)\varkappa_2\right) + (\varkappa_2 - \alpha_s)\left(\dot{\varkappa}_2 - \dot{\alpha}_s\right) \tag{5.83}$$

where $\alpha_s(\varkappa_1)$ stabilizes the subsystem (5.79) at the origin $\varkappa_1 = 0$.
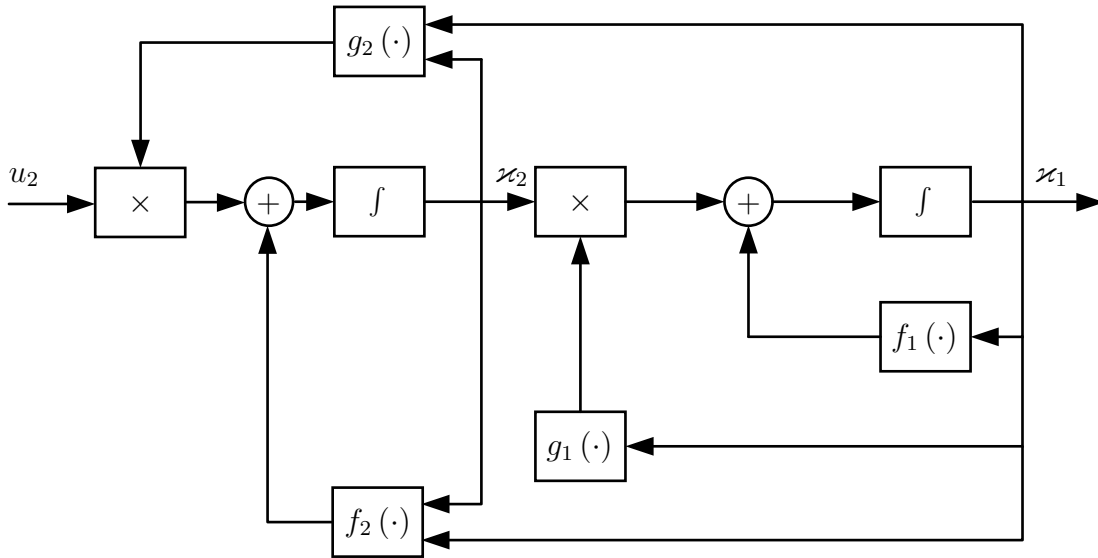
Fig. 5.5: System in strict-feedback form $(5.79 - 5.80)$

The control law is given as

$$u_2 = \frac{1}{g_2\left(\varkappa_1, \varkappa_2\right)}\left[-f_2\left(\varkappa_1, \varkappa_2\right) + \frac{\partial \alpha_s\left(\varkappa_1\right)}{\partial \varkappa_1}\left(f_1\left(\varkappa_1\right) + g_1\left(\varkappa_1\right)\varkappa_2\right)\right.$$
$$\left. -c_s\left(\varkappa_2 - \alpha_s\left(\varkappa_1\right)\right) - \frac{\partial V_{1s}}{\partial \varkappa_1}g_1\left(\varkappa_1\right)\right], \quad c_s > 0.$$

(5.84)

For more details about the complete derivation of (5.84) see previous work [42].

5.3.3   Robust and Adaptive Backstepping

We now combine the backstepping technique presented above with the robust adaptive control approach introduced in Section 5.3.1 to illustrate the design idea of the robust adaptive backstepping control. To this end, we define the following system

$$\dot{\chi}_1 = f_1\left(\chi_1\right) + g_1\left(\chi_1\right)\chi_2 \tag{5.85}$$
$$\dot{\chi}_2 = g_0\left(u_{\mathrm{c}} + \Upsilon \hbar\left(\chi_1, \chi_2\right) + \Xi\left(\chi_1, \chi_2, t\right)\right) \tag{5.86}$$

where the functions $f_1\left(\chi_1\right)$ and $g_1\left(\chi_1\right)$, and the constant g_0 are known. The output of this system is $y_\chi = \chi_1$. According to the backstepping approach we design a virtual controller $\chi_2 = \alpha\left(\chi_1\right)$ to stabilize the equilibrium $\chi_1 = 0$ of the subsystem (5.85). For the system $(5.85 - 5.86)$ we consider the Lyapunov function candidate

$$V = \frac{1}{2}\chi_1^2 + \frac{1}{2}\left(\chi_2 - \alpha\left(\chi_1\right)\right)^2 + \frac{1}{2c_1}\tilde{\Upsilon}^2 + \frac{1}{2c_2}\tilde{\Delta}^2. \tag{5.87}$$

The time derivative of (5.87) is

$$\dot{V} = \chi_1\dot{\chi}_1 + \left(\chi_2 - \alpha\left(\chi_1\right)\right)\left(\dot{\chi}_2 - \dot{\alpha}\left(\chi_1\right)\right) + \frac{1}{c_1}\tilde{\Upsilon}\dot{\tilde{\Upsilon}} + \frac{1}{c_2}\tilde{\Delta}\dot{\tilde{\Delta}}. \tag{5.88}$$

According to the backstepping approach, we choose first a virtual stabilizing function $\alpha\left(\chi_1\right)$ for the subsystem (5.85). Now, using $\chi_2 = \alpha\left(\chi_1\right) + \left(\chi_2 - \alpha\left(\chi_1\right)\right)$, and placing (5.85) into (5.88) we obtain

$$\dot{V} = \chi_1\left(f_1\left(\chi_1\right) + g_1\left(\chi_1\right)\alpha\left(\chi_1\right) + \left(\chi_2 - \alpha\left(\chi_1\right)\right)g_1\left(\chi_1\right)\right) + \frac{1}{c_1}\tilde{\Upsilon}\dot{\tilde{\Upsilon}} + \frac{1}{c_2}\tilde{\Delta}\dot{\tilde{\Delta}}$$
$$+ \left(\chi_2 - \alpha\left(\chi_1\right)\right)\left(g_0\left(u_{\mathrm{c}} + \Upsilon \hbar\left(\chi\right) + \Xi\left(\chi, t\right)\right) - \dot{\alpha}\left(\chi_1\right)\right).$$

(5.89)

Let us define a smooth stabilizing function

$$\alpha\left(\chi_1\right) = \frac{-1}{g_1\left(\chi_1\right)}\left(f_1\left(\chi_1\right) + k_\chi^1\chi_1\right) \tag{5.90}$$

where the function $g_1\left(\chi_1\right) \neq 0$ and constant $k_\chi^1 > 0$. Then (5.89) can be written as

$$\dot{V} = -k_\chi^1\chi_1^2 + \left[\chi_2 - \alpha\left(\chi_1\right)\right]\left[\chi_1 g_1\left(\chi_1\right) + g_0\Upsilon\hbar\left(\chi_1,\chi_2\right) + g_0\Xi\left(\chi_1,\chi_2,t\right) + g_0 u_c - \dot{\alpha}\left(\chi_1\right)\right]$$
$$+ \frac{1}{c_1}\tilde{\Upsilon}\dot{\tilde{\Upsilon}} + \frac{1}{c_2}\tilde{\Delta}\dot{\tilde{\Delta}}. \tag{5.91}$$

We suggest a control law as per

$$u_c = \frac{1}{g_0}\left[-k_\chi^2\left(\chi_2 - \alpha\left(\chi_1\right)\right) + \dot{\alpha}\left(\chi_1\right) - \chi_1 g_1\left(\chi_1\right) - \varrho\left(\chi_1,\chi_2,\hat{\Delta}\right)\right] - \hat{\Upsilon}\hbar\left(\chi_1,\chi_2\right) \tag{5.92}$$

where k_χ^2 is a positive constant, $\hat{\Upsilon}$ is an estimate of the modeled uncertainty in the system, and $\varrho\left(\chi_1,\chi_2,\hat{\Delta}\right)$ is the control component that deals with the unmodeled uncertainties or the disturbance. It is assumed that this disturbance is bounded by an upper bound Δ, constant but unknown, its estimated value is $\hat{\Delta}$. The function $g_1\left(\chi_1\right)$ is a known function and $\hbar\left(\chi_1,\chi_2\right)$ is a known basis function. By inserting the suggested control law (5.92) in (5.91) we obtain

$$\dot{V} = -k_\chi^1\chi_1^2 + \left(\chi_2 - \alpha\left(\chi_1\right)\right)\left[-g_0\tilde{\Upsilon}\hbar\left(\chi_1,\chi_2\right) + g_0\Xi\left(\chi_1,\chi_2,t\right) - k_\chi^2\left(\chi_2 - \alpha\left(\chi_1\right)\right)\right.$$
$$\left. - \varrho\left(\chi_1,\chi_2,\hat{\Delta}\right)\right] + \frac{1}{c_1}\tilde{\Upsilon}\dot{\tilde{\Upsilon}} + \frac{1}{c_2}\tilde{\Delta}\dot{\tilde{\Delta}} \tag{5.93}$$

where $\tilde{\Upsilon} = \hat{\Upsilon} - \Upsilon$. Now, noticing that $\dot{\tilde{\Upsilon}} = \dot{\hat{\Upsilon}}$ and $\dot{\tilde{\Delta}} = \dot{\hat{\Delta}}$, and making the assumption that the disturbance is bounded, i.e. $\left|\Xi\left(\chi_1,\chi_2,t\right)\right| \leq \Delta$ and by observing that

$$\left|\chi_2 - \alpha\left(\chi_1\right)\right| = \left(\chi_2 - \alpha\left(\chi_1\right)\right)\operatorname{sgn}\left(\chi_2 - \alpha\left(\chi_1\right)\right) \tag{5.94}$$

we can rewrite equation (5.93) as

$$\dot{V} \leq -k_\chi^1\chi_1^2 - k_\chi^2\left(\chi_2 - \alpha\left(\chi_1\right)\right)^2 + \tilde{\Upsilon}\left[\frac{\dot{\hat{\Upsilon}}}{c_1} - g_0\left(\chi_2 - \alpha\left(\chi_1\right)\right)\hbar\left(\chi_1,\chi_2\right)\right]$$
$$+ \left(\chi_2 - \alpha\left(\chi_1\right)\right)\left(g_0\operatorname{sgn}\left(\chi_2 - \alpha\left(\chi_1\right)\right)\Delta - \varrho\left(\chi_1,\chi_2,\hat{\Delta}\right)\right) + \frac{1}{c_2}\tilde{\Delta}\dot{\hat{\Delta}}. \tag{5.95}$$

Now, by choosing the control component ϱ as

$$\varrho\left(\chi_1, \chi_2, \hat{\Delta}\right) = g_0 \operatorname{sgn}\left(\chi_2 - \alpha\left(\chi_1\right)\right) \hat{\Delta}, \tag{5.96}$$

the adaptation law for the modeled uncertainties becomes

$$\dot{\hat{\Upsilon}} = c_1 g_0 \left(\chi_2 - \alpha\left(\chi_1\right)\right) \hbar\left(\chi_1, \chi_2\right). \tag{5.97}$$

Placing (5.96) and (5.97) into (5.95) yields

$$\dot{V} \leq -k_\chi^1 \chi_1^2 - k_\chi^2 \left(\chi_2 - \alpha\left(\chi_1\right)\right)^2 + \tilde{\Delta}\left[\frac{\dot{\hat{\Delta}}}{c_2} - \left(\chi_2 - \alpha\left(\chi_1\right)\right) g_0 \operatorname{sgn}\left(\chi_2 - \alpha\left(\chi_1\right)\right)\right]. \tag{5.98}$$

Thus, we can choose the adaptation law for the unmodeled uncertainties or the disturbance in the form

$$\dot{\hat{\Delta}} = c_2 \left(\chi_2 - \alpha\left(\chi_1\right)\right) g_0 \operatorname{sgn}\left(\chi_2 - \alpha\left(\chi_1\right)\right). \tag{5.99}$$

Now, by inserting (5.99) in (5.98) we obtain that

$$\dot{V} \leq -k_\chi^1 \chi_1^2 - k_\chi^2 \left(\chi_2 - \alpha\left(\chi_1\right)\right)^2 \leq 0 \tag{5.100}$$

which implies that $\chi_1, \chi_2 - \alpha\left(\chi_1\right), \tilde{\Upsilon}$ and $\tilde{\Delta}$ are bounded, moreover, χ_1 and $\chi_2 - \alpha\left(\chi_1\right)$ converge to zero. In other words, the system $(5.85 - 5.86)$ converges to its equilibrium

$$\left(\chi_{1R}, \chi_{2R}\right) = \left(0, -\frac{f_1\left(0\right)}{g_1\left(0\right)}\right) \tag{5.101}$$

despite of the presence of modeled and unmodeled uncertainties in the considered system. Also here, to avoid the chattering phenomena in the control law due to the sgn function, it can be approximated by the tanh function as in (5.28). This modification leads to the new control component

$$\varrho\left(\chi_1, \chi_2, \hat{\Delta}\right) = g_0 \tanh\left(\frac{\chi_2 - \alpha\left(\chi_1\right)}{\varepsilon_\chi}\right) \hat{\Delta} \tag{5.102}$$

and to a new adaptation law for the unmodeled uncertainties:

$$\dot{\hat{\Delta}} = c_2 g_0 \left(\chi_2 - \alpha\left(\chi_1\right)\right) \tanh\left(\frac{\chi_2 - \alpha\left(\chi_1\right)}{\varepsilon_\chi}\right). \tag{5.103}$$

66

Finally, the time derivative of the Lyapunov function becomes

$$\dot{V} \leq -k_\chi^1 \chi_1^2 - k_\chi^2 \left(\chi_2 - \alpha \left(\chi_1 \right) \right)^2 + 0.2785 \, g_0 \, \Delta \, \varepsilon_\chi \leq 0.2785 \, g_0 \, \Delta \, \varepsilon_\chi, \quad \varepsilon_\chi > 0. \quad (5.104)$$

This means that in the system with the modified controller, χ_1 and $\chi_2 - \alpha \left(\chi_1 \right)$ will not necessarily converge to the zero, but to an arbitrary small neighborhood of it which can be adjusted by the design constant ε_χ.

5.4 Projection Operator

Projection-based adaptation laws are used often to prevent parameter drift in adaptation schemes [76] and to ensure robustness properties in the adaptive law [77]. In this section, a Lipschitz-continuous version of the projection operator will be introduced. This concept is essential for enabling the adaptive laws to achieve robustness with respect to parametric and nonparametric uncertainties which might exist in the system dynamics. It will be shown that the projection operator tolerates fast adaptation, enforces uniform boundedness of the adaptive parameters and maintains closed-loop stability of the corresponding error dynamics and of the original system.

Before introducing the projection operator, we begin with essential definitions of convex sets and convex functions. We recall some definitions and theorems from [78, 79].

Definition 5.4.1 A set $E \subset \mathbb{R}^k$ is *convex* if

$$\lambda \boldsymbol{\varphi}_1 + (1 - \lambda)\boldsymbol{\varphi}_2 \in E \quad (5.105)$$

whenever $\boldsymbol{\varphi}_1 \in E, \boldsymbol{\varphi}_2 \in E$, and $0 \leq \lambda \leq 1$.

Remark 5.4.1 A convex set has the property that for any two points of the convex set E all the points on the connecting line between those two points also belong to E.

Definition 5.4.2 A function $f : \mathbb{R}^k \to \mathbb{R}$ is *convex* if

$$f \left(\lambda \boldsymbol{\varphi}_1 + (1 - \lambda) \boldsymbol{\varphi}_2 \right) \leq \lambda f \left(\boldsymbol{\varphi}_1 \right) + (1 - \lambda) f \left(\boldsymbol{\varphi}_2 \right), \quad \forall \, 0 \leq \lambda \leq 1. \quad (5.106)$$

Inequality (5.106) is illustrated in Figure 5.6. It shows that the graph of a convex function must be located below the straight line which connects the two corresponding function values
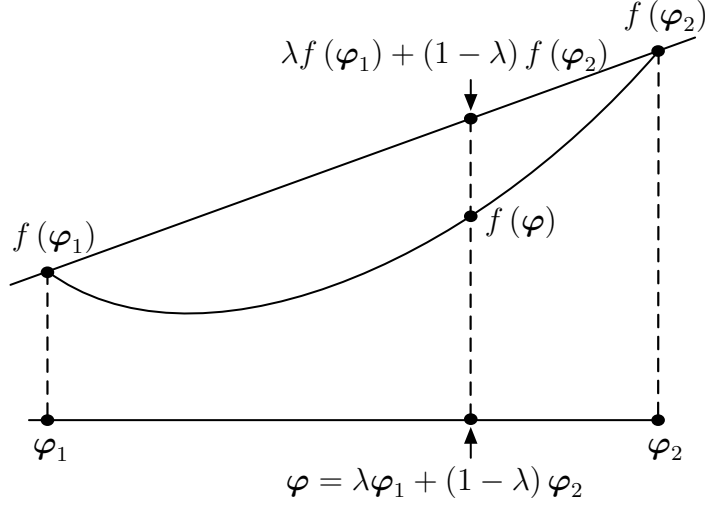
Fig. 5.6: Convex function

Lemma 5.4.1 Let $f\left(\boldsymbol{\varphi}\right):\mathbb{R}^k\to\mathbb{R}$ be a convex function. Then for any constant $\beta>0$ the set $E_\beta=\left\{\boldsymbol{\varpi}\in\mathbb{R}^k\,|f\left(\boldsymbol{\varpi}\right)\le\beta\right\}$ is convex. The set E_β is called the sublevel set.

Proof 5.4.1 Let $\boldsymbol{\varpi}_1,\boldsymbol{\varpi}_2\in E_\beta$, then $f\left(\boldsymbol{\varpi}_1\right)\le\beta$ and $f\left(\boldsymbol{\varpi}_2\right)\le\beta$. Since $f\left(\boldsymbol{\varpi}_1\right)\le\beta$ is convex then for any $0\le\lambda\le1$

$$f(\underbrace{\lambda\boldsymbol{\varpi}_1+(1-\lambda)\,\boldsymbol{\varpi}_2}_{\boldsymbol{\varpi}})\le\lambda\underbrace{f(\boldsymbol{\varpi}_1)}_{\le\,\beta}+(1-\lambda)\underbrace{f(\boldsymbol{\varpi}_2)}_{\le\,\beta}\le\lambda\beta+(1-\lambda)\beta=\beta \qquad (5.107)$$

Since $f\left(\lambda\boldsymbol{\varpi}_1+(1-\lambda)\,\boldsymbol{\varpi}_2\right)\le\beta$, then $\lambda\boldsymbol{\varpi}_1+(1-\lambda)\,\boldsymbol{\varpi}_2\in E_\beta$ as $\boldsymbol{\varpi}_1,\boldsymbol{\varpi}_2\in E_\beta$, then E_β is convex.

Lemma 5.4.2 Let $f\left(\boldsymbol{\varphi}\right):\mathbb{R}^k\to\mathbb{R}$ be a continuously differentiable convex function. Choose a constant β and consider the convex set $E_\beta=\left\{\boldsymbol{\varpi}\in\mathbb{R}^k|f\left(\boldsymbol{\varpi}\right)\le\beta\right\}\subset\mathbb{R}^k$. Let $\boldsymbol{\varpi},\boldsymbol{\varpi}^*\in E_\beta$ and $f(\boldsymbol{\varpi}^*)<\beta$ and $f(\boldsymbol{\varpi})=\beta$ (i.e. $\boldsymbol{\varpi}^*$ is not on the boundary of E_β, while $\boldsymbol{\varpi}$ is on the boundary of E_β). Then the following inequality is true

$$(\boldsymbol{\varpi}^*-\boldsymbol{\varpi})^\top\nabla f\left(\boldsymbol{\varpi}\right)\le0 \qquad (5.108)$$

where $\nabla f(\boldsymbol{\varpi})=\left(\frac{\partial f(\boldsymbol{\varpi})}{\partial\varpi_1}\ldots\frac{\partial f(\boldsymbol{\varpi})}{\partial\varpi_k}\right)^\top\in\mathbb{R}^k$ is the gradient of $f(\boldsymbol{\varpi})$ evaluated at $\boldsymbol{\varpi}$.

Figure 5.7 illustrates the relation (5.108). Here we note that the gradient evaluated at the boundary of a convex set always points away from the set.

$$E_\beta = \{\varpi : f(\varpi) = \beta\}$$
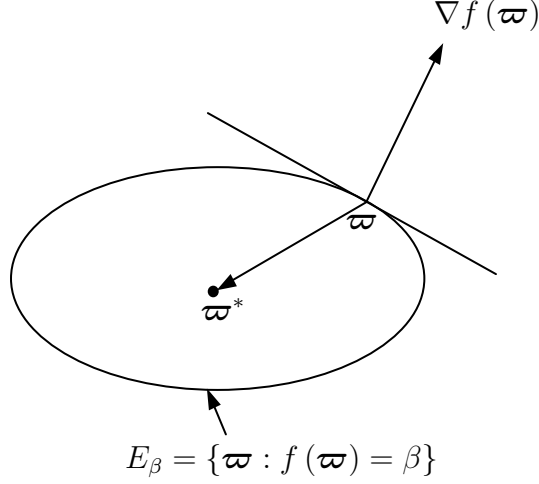
Fig. 5.7: Gradient vector on the boundary of a convex set

Proof 5.4.2 Since $f(\varphi)$ is a convex function, then

$$f(\lambda\varpi^* + (1-\lambda)\varpi) \le \lambda f(\varpi^*) + (1-\lambda)f(\varpi), \quad \forall 0 \le \lambda \le 1 \tag{5.109}$$

which can be rewritten as

$$f(\varpi + \lambda(\varpi^* - \varpi)) \le f(\varpi) + \lambda(f(\varpi^*) - f(\varpi)). \tag{5.110}$$

Then for any nonzero $0 < \lambda \le 1$ the above inequality can be written as

$$\frac{f(\varpi + \lambda(\varpi^* - \varpi)) - f(\varpi)}{\lambda} \le f(\varpi^*) - f(\varpi) \le \beta - \beta = 0. \tag{5.111}$$

It is necessary to notice that the expression $f(\varpi + \lambda(\varpi^* - \varpi))$ in the relation (5.111) is a scalar function of vector argument ϖ. On the other side, one can see this expression as a scalar function $F(\lambda)$ of the scalar argument λ. In this case, the considered function can be defined with a Taylor polynomial of degree 2 about the point $\lambda = 0$, as follows

$$F(\lambda) = F(0) + F'(0)\lambda + O(\lambda^2) \tag{5.112}$$

where $O(\lambda^2)$ is the remainder of the Taylor series. Notice that $F(0) = f(\varpi)$ and $F'(\lambda) = (\varpi^* - \varpi)^\top \nabla f(\varpi + \lambda(\varpi^* - \varpi))$ where ∇f denotes the differentiation of f

with respect to its whole vector argument $\boldsymbol{\varpi} + \lambda(\boldsymbol{\varpi}^* - \boldsymbol{\varpi})$, that is, the gradient. While $(\boldsymbol{\varpi}^* - \boldsymbol{\varpi})^\top$ is the derivative of the expression with respect to λ. Then it is not hard to see that, $F'(0) = (\boldsymbol{\varpi}^* - \boldsymbol{\varpi})^\top \nabla f(\boldsymbol{\varpi})$, replacing the values of $F(0)$ and $F'(0)$ in equation (5.112). We get therefore the considered expression as

$$f(\boldsymbol{\varpi} + \lambda(\boldsymbol{\varpi}^* - \boldsymbol{\varpi})) = f(\boldsymbol{\varpi}) + (\boldsymbol{\varpi}^* - \boldsymbol{\varpi})^\top \nabla f(\boldsymbol{\varpi})\lambda + O(\lambda^2), \tag{5.113}$$

and by substituting equation (5.113) into (5.111) we get

$$\frac{f(\boldsymbol{\varpi}) + (\boldsymbol{\varpi}^* - \boldsymbol{\varpi})^\top \nabla f(\boldsymbol{\varpi})\lambda + O(\lambda^2) - f(\boldsymbol{\varpi})}{\lambda} \leq 0$$
$$\Rightarrow (\boldsymbol{\varpi}^* - \boldsymbol{\varpi})^\top \nabla f(\boldsymbol{\varpi}) + O(\lambda^2) \leq 0. \tag{5.114}$$

Taking the limit

$$\lim_{\lambda \to 0} O(\lambda^2) = 0$$

implies $(\boldsymbol{\varpi}^* - \boldsymbol{\varpi})^\top \nabla f(\boldsymbol{\varpi}) \leq 0$ which completes the proof.

Definition 5.4.3 [79] Consider a convex set given by

$$E_\beta = \left\{ \boldsymbol{\varpi} \in \mathbb{R}^k | f(\boldsymbol{\varpi}) \leq \beta \right\}, \quad 0 \leq \beta \leq 1 \tag{5.115}$$

and a smooth convex function $f : \mathbb{R}^k \to \mathbb{R}$ defined as follows

$$f(\boldsymbol{\varpi}) = \frac{\|\boldsymbol{\varpi}\|^2 - \varpi_M^2}{\varepsilon^2 + 2\varepsilon\varpi_M} \tag{5.116}$$

where ϖ_M is the norm bound of the parameter vector $\boldsymbol{\varpi}$, and ε denotes the convergence tolerance.

Let $\boldsymbol{\varpi}^* \in E_0$ be the true value of $\boldsymbol{\varpi}$. A projection operator for two vectors $\boldsymbol{\varpi}, \mathbf{s} \in \mathbb{R}^k$ is introduced as

$$\text{Proj}(\boldsymbol{\varpi}, \mathbf{s}) = \begin{cases} \mathbf{s} - \underbrace{\frac{\nabla f(\boldsymbol{\varpi})}{\|\nabla f(\boldsymbol{\varpi})\|}}_{\text{unit vector}} \underbrace{\left\langle \frac{(\nabla f(\boldsymbol{\varpi}))^\top}{\|\nabla f(\boldsymbol{\varpi})\|}, \mathbf{s} \right\rangle}_{\text{projection}} \underbrace{f(\boldsymbol{\varpi})}_{\text{scaling}} & \text{if } f(\boldsymbol{\varpi}) > 0 \wedge \mathbf{s}^\top \nabla f(\boldsymbol{\varpi}) > 0 \\ \\ \mathbf{s} & \text{otherwise} \end{cases}$$
$$\tag{5.117}$$

or

$$\text{Proj}\,(\boldsymbol{\varpi},\mathbf{s}) = \begin{cases} \mathbf{s} - \dfrac{\nabla f\,(\boldsymbol{\varpi})\,(\nabla f\,(\boldsymbol{\varpi}))^{\top}}{\|\nabla f\,(\boldsymbol{\varpi})\|^{2}}\mathbf{s}f\,(\boldsymbol{\varpi}) & \text{if } f\,(\boldsymbol{\varpi}) > 0 \wedge \mathbf{s}^{\top}\nabla f\,(\boldsymbol{\varpi}) > 0 \\[3mm] \mathbf{s} & \text{otherwise} \end{cases}$$

(5.118)

where $\nabla f(\boldsymbol{\varpi}) = \left(\frac{\partial f(\boldsymbol{\varpi})}{\partial \varpi_1} \ldots \frac{\partial f(\boldsymbol{\varpi})}{\partial \varpi_k}\right)^{\top} \in \mathbb{R}^k$ is the gradient of $f\,(\boldsymbol{\varpi})$ evaluated at $\boldsymbol{\varpi}$.

Figure 5.8 shows the projection operator in $\mathbb{R}^2$. The projection operator $\text{Proj}(\boldsymbol{\varpi},\mathbf{s})$ as
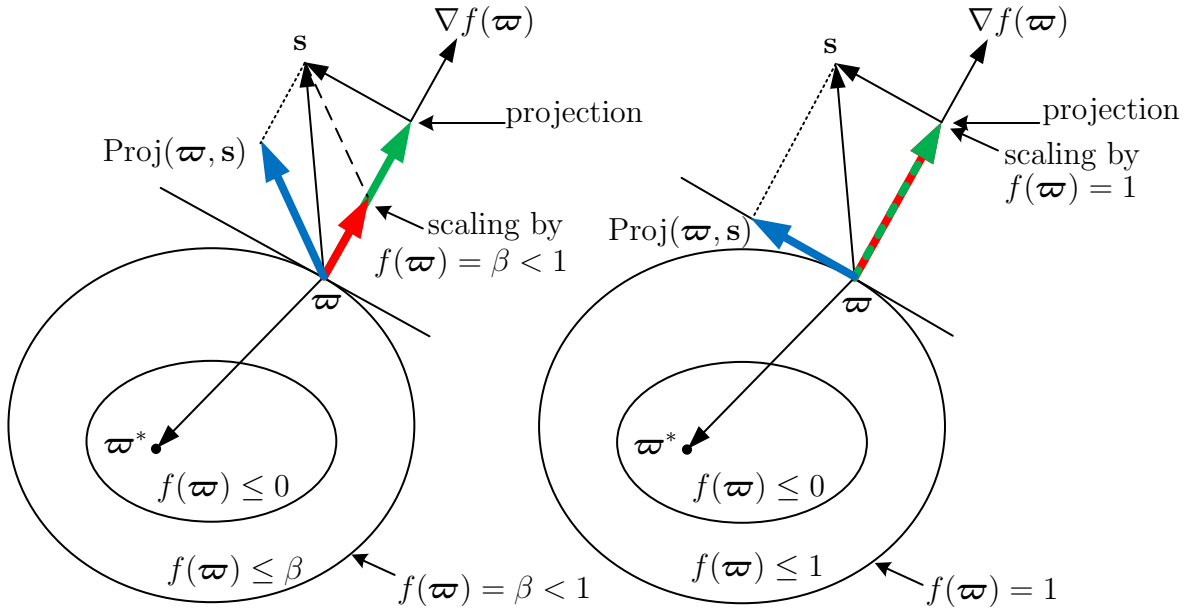
Fig. 5.8: Projection operator in $\mathbb{R}^2$

defined in (5.117) does not alter $\mathbf{s}$ if $\boldsymbol{\varpi}$ belongs to the set $E_0 = \left\{\boldsymbol{\varpi} \in \mathbb{R}^k | f(\boldsymbol{\varpi}) \leq 0\right\}$. For the set $\left\{\boldsymbol{\varpi} \in \mathbb{R}^k | 0 \leq f(\boldsymbol{\varpi}) \leq 1\right\}$ if $\mathbf{s}^{\top}\nabla f\,(\boldsymbol{\varpi}) > 0$, then the projection operator $\text{Proj}(\boldsymbol{\varpi},\mathbf{s})$ subtracts the vector normal to the boundary of the set $\left\{\boldsymbol{\varpi} \in \mathbb{R}^k | f(\boldsymbol{\varpi}) = \beta\right\}$ so that we get a smooth transformation from the original vector field $\mathbf{s}$ to an inward or tangent vector field for $\beta = 1$.

Lemma 5.4.3 Let $f : \mathbb{R}^k \to \mathbb{R}$ be a convex differentiable function. Using the definition of the projection operator (5.118) and considering the $k-$dimensional dynamics

$$\dot{\boldsymbol{\varpi}} = \text{Proj}\,(\boldsymbol{\varpi},\mathbf{s})$$

(5.119)

where $\boldsymbol{\varpi}, \mathbf{s} \in \mathbb{R}^k$. Starting from any initial point $\boldsymbol{\varpi}(0) = \boldsymbol{\varpi}_0$ within the set

$$E_0 = \left\{ \boldsymbol{\varpi} \in \mathbb{R}^k | f(\boldsymbol{\varpi}) \leq 0 \right\} \tag{5.120}$$

the solution $\boldsymbol{\varpi}(t)$ of the dynamics (5.119) for an initial point $\boldsymbol{\varpi}(0) = \boldsymbol{\varpi}_0$ will remain within the set

$$E_1 = \left\{ \boldsymbol{\varpi} \in \mathbb{R}^k | f(\boldsymbol{\varpi}) \leq 1 \right\} \tag{5.121}$$

for all $t \geq 0$.

Proof 5.4.3 [76, 78] To prove this lemma, we need to show that the following relation holds:

$$\underbrace{f(\boldsymbol{\varpi}(0)) \leq 0}_{\boldsymbol{\varpi}(0) \in E_0} \Rightarrow \underbrace{f(\boldsymbol{\varpi}(t)) \leq 1}_{\boldsymbol{\varpi}(t) \in E_1}, \quad \forall t \geq 0. \tag{5.122}$$

Taking the time derivative of $f(\boldsymbol{\varpi}(t))$ along the trajectories of the system dynamics (5.119) and using the definition of the projection operator (5.118) we obtain

$$\dot{f}(\boldsymbol{\varpi}) = (\nabla f(\boldsymbol{\varpi}))^\top \mathrm{Proj}(\boldsymbol{\varpi}, \mathbf{s}) \tag{5.123}$$

$$= \begin{cases} (\nabla f(\boldsymbol{\varpi}))^\top \mathbf{s} \, (1 - f(\boldsymbol{\varpi})) & \text{if } f(\boldsymbol{\varpi}) > 0 \ \wedge \mathbf{s}^\top \nabla f(\boldsymbol{\varpi}) > 0 \\ (\nabla f(\boldsymbol{\varpi}))^\top \mathbf{s} & \text{if } f(\boldsymbol{\varpi}) \leq 0 \ \vee \mathbf{s}^\top \nabla f(\boldsymbol{\varpi}) \leq 0 \end{cases} \tag{5.124}$$

which means that

$$\begin{aligned} \dot{f}(\boldsymbol{\varpi}) &> 0, \text{ if } \ 0 < f(\boldsymbol{\varpi}) < 1 \wedge \mathbf{s}^\top \nabla f(\boldsymbol{\varpi}) > 0 \\ \dot{f}(\boldsymbol{\varpi}) &= 0, \text{ if } \quad f(\boldsymbol{\varpi}) = 1 \wedge \mathbf{s}^\top \nabla f(\boldsymbol{\varpi}) > 0 \\ \dot{f}(\boldsymbol{\varpi}) &\leq 0, \text{ if } \quad f(\boldsymbol{\varpi}) \leq 0 \vee \mathbf{s}^\top \nabla f(\boldsymbol{\varpi}) \leq 0. \end{aligned} \tag{5.125}$$

The first and the second relation in (5.125) imply that if $f(\boldsymbol{\varpi}(0)) > 0$ then $f(\boldsymbol{\varpi}(t))$ monotonically increases in time for all $t \geq 0$, but it will never exceed the value 1. Also, the third condition in (5.125) makes clear that if $f(\boldsymbol{\varpi}(0)) \leq 0$ then $f(\boldsymbol{\varpi}(t))$ is monotonically decreasing for all $t \geq 0$. Therefore, irrespective of initial values (as long as they are negative), $f(\boldsymbol{\varpi}(t)) \leq 1$ for all $t \geq 0$, which completes the proof of the lemma.

Property 5.4.1 Given the vectors $\boldsymbol{\varpi}, \mathbf{s} \in \mathbb{R}^k$, then the next inequality is true

$$(\boldsymbol{\varpi} - \boldsymbol{\varpi}^*)^\top (\mathrm{Proj}(\boldsymbol{\varpi}, \mathbf{s}) - \mathbf{s}) \leq 0 \tag{5.126}$$

where $\boldsymbol{\varpi}^*$ is the true value of the parameter $\boldsymbol{\varpi}$.

Proof 5.4.4 To prove this property, we note that

$$(\boldsymbol{\varpi} - \boldsymbol{\varpi}^*)^\top (\mathrm{Proj}(\boldsymbol{\varpi}, \mathbf{s}) - \mathbf{s}) = (\boldsymbol{\varpi}^* - \boldsymbol{\varpi})^\top (\mathbf{s} - \mathrm{Proj}(\boldsymbol{\varpi}, \mathbf{s})). \tag{5.127}$$

Now, by placing the relation of the projection operator (5.118) into (5.126) we obtain

$$(\boldsymbol{\varpi}^* - \boldsymbol{\varpi})^\top (\mathbf{s} - \mathrm{Proj}(\boldsymbol{\varpi}, \mathbf{s})) = \begin{cases} \dfrac{(\boldsymbol{\varpi}^* - \boldsymbol{\varpi})^\top \nabla f (\nabla f)^\top \mathbf{s}\, f}{\|\nabla f\|^2} & \text{if } f > 0 \wedge \mathbf{s}^\top \nabla f > 0 \\ 0 & \text{otherwise.} \end{cases} \tag{5.128}$$

We used a shortened nomenclature for f in this equation.

In (5.128) it should be noticed that for $(\nabla f)^\top \mathbf{s} \geq 0, f \geq 0$, and according to Lemma 5.4.2 the expression $(\boldsymbol{\varpi}^* - \boldsymbol{\varpi})^\top \nabla f \leq 0$, implies $(\boldsymbol{\varpi}^* - \boldsymbol{\varpi})^\top (\mathbf{s} - \mathrm{Proj}(\boldsymbol{\varpi}, \mathbf{s})) \leq 0$. Noticing relation (5.127) we can write

$$(\boldsymbol{\varpi} - \boldsymbol{\varpi}^*)^\top (\mathrm{Proj}(\boldsymbol{\varpi}, \mathbf{s}) - \mathbf{s}) \leq 0 \tag{5.129}$$

which completes the proof.

Remark 5.4.2 For the scalar case, namely for two scalar values $s, \varpi \in \mathbb{R}$, according to the above definition (5.117, 5.118), the projection operator can be defined for the scalar quantities as follows

$$\mathrm{Proj}(\varpi, s) = \begin{cases} s - s f(\varpi) & \text{if } f(\varpi) > 0 \wedge \dfrac{\partial f(\varpi)}{\partial \varpi} \varpi > 0 \\ s & \text{otherwise} \end{cases} \tag{5.130}$$

Figure 5.9 illustrates the scalar projection. Only those points s for which the condition

$$f(\varpi) > 0 \wedge \frac{\partial f(\varpi)}{\partial \varpi} \varpi > 0 \tag{5.131}$$

is satisfied, will be projected. They are the points on the segments ab and cd. The points s on segment bc are not projected because $f(\varpi) > 0$ is not satisfied in (5.131).
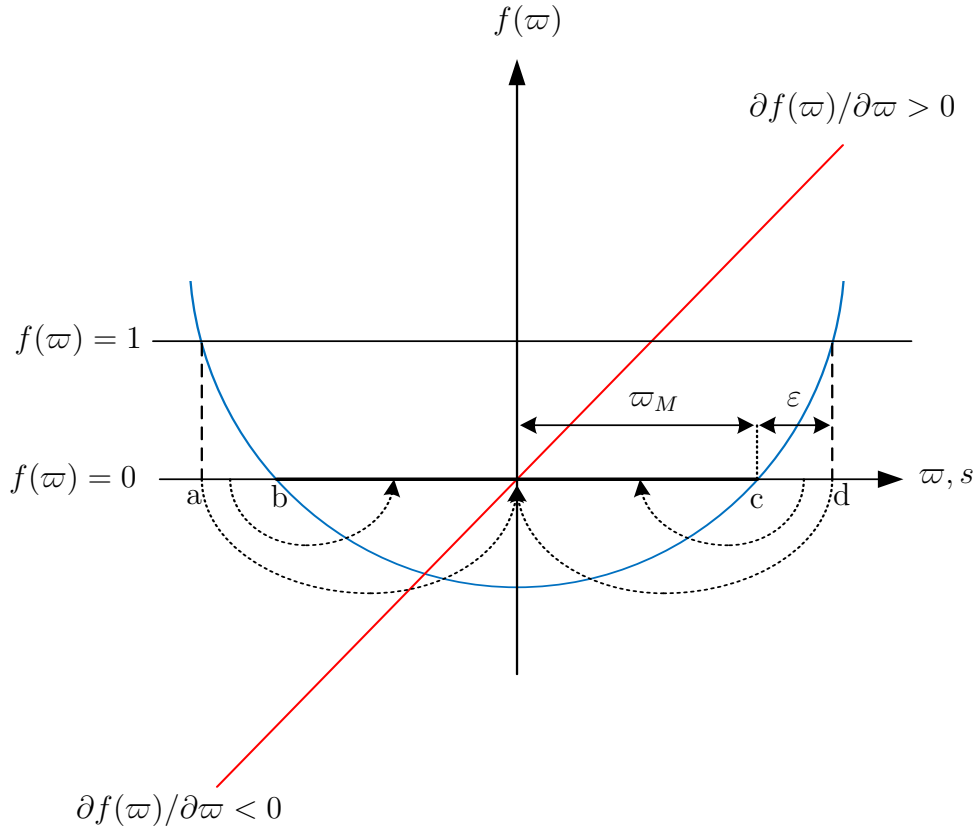
Fig. 5.9: Projection of scalar values

5.5   Coordinate Transformation for the AUV

By following the results of the work [22], we recall that the system of the AUV given in (3.49) is a second-order nonholonomic system because the constraints (the non-actuated dynamics) are not integrable. The difficulty in such a class of systems is that they cannot be stabilized by a smooth static-state feedback control, but by using an adaptive one [80]. The controller design is based on the adaptive backstepping approach. Before that we design a path following controller for the underactuated AUV system (3.49), we transform the path following problem into a stabilization one [81]. Thus, through this transformation, the AUV model can be transformed into an error triangular-like form which allows to use the backstepping method to develop an adaptive feedback control. The proposed controller stabilizes the reference trajectory exponentially [21].

To achieve this transformation, let us describe the control objective in light of Figure
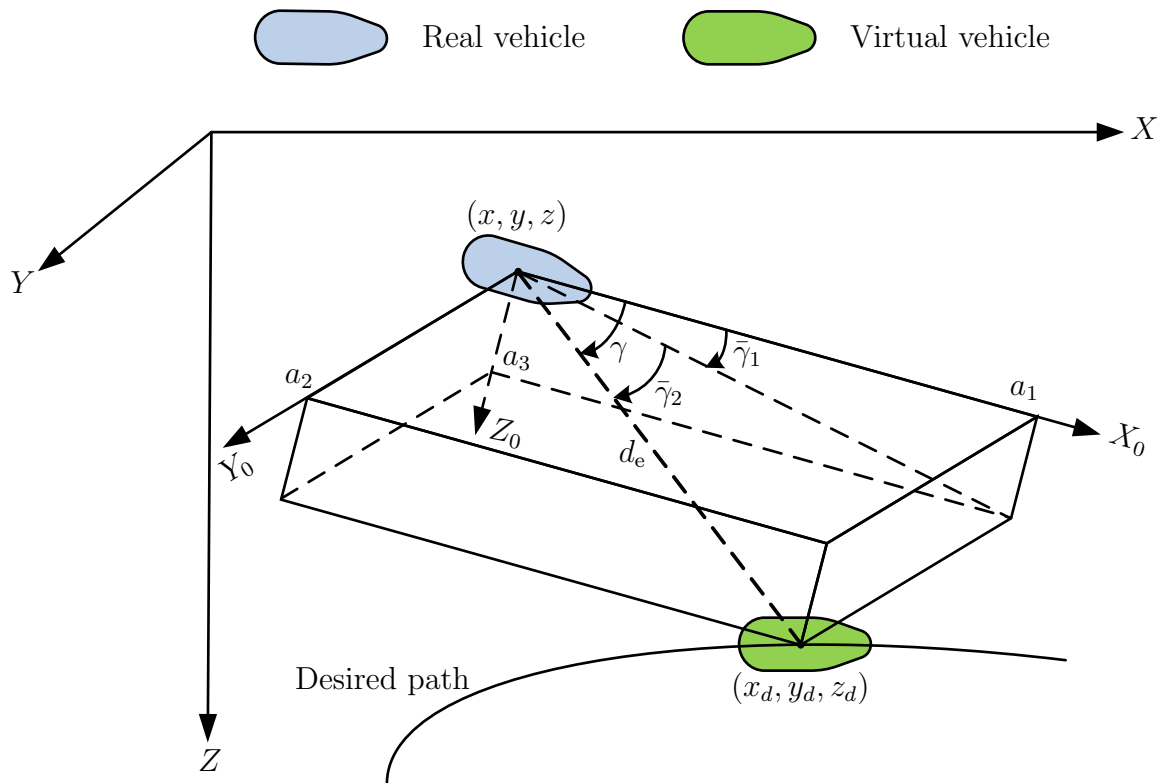
Fig. 5.10: Real and virtual vehicles

5.10. The controller must force the real vehicle to follow the virtual one, this means, that the real vehicle must track both the position and the orientation of the virtual vehicle which moves along the reference path with a desired speed profile $u_0(t)$. The control objective can be imagined in the following way: The virtual vehicle, which moves along the reference path with the velocity $u_0(t)$, pulls the real one with a cord of length d_e where the angle between this cord and the surge axis of the real vehicle is γ.

The controller must minimize the distance d_e and also the angle γ. In this approach, minimizing means, to force d_e to be close to zero (but not zero which would cause a singularity in d_e as we will see later), and to compel γ to go to zero by means of the designed controller. Therefore, when the control objective is fulfilled, the real vehicle will move very close to the virtual one along the desired path and with the desired velocity $u_0(t)$.

Let the center of the real vehicle be the point (x, y, z) which locates at the origin of the body-fixed coordinates attached to the real vehicle, and the center of the virtual vessel be (x_d, y_d, z_d) which is a point of the desired path. Thus, we define the path following

errors in the earth-fixed frame XYZ as

$$x_{\mathrm{e}} = x_{\mathrm{d}} - x, \quad y_{\mathrm{e}} = y_{\mathrm{d}} - y, \quad z_{\mathrm{e}} = z_{\mathrm{d}} - z. \tag{5.132}$$

Then the distance d_{e} in the earth-fixed frame XYZ is given as

$$d_{\mathrm{e}} = \sqrt{x_{\mathrm{e}}^2 + y_{\mathrm{e}}^2 + z_{\mathrm{e}}^2}. \tag{5.133}$$

Let a_1, a_2 and a_3 be the errors on surge, sway and heave directions respectively as Figure 5.10 shows. Then by rotating the body-fixed frame around X, Y and Z, the angles roll, pitch and yaw respectively, we can define the errors a_1, a_2 and a_3 by means of $x_{\mathrm{e}}, y_{\mathrm{e}}$ and z_{e} as

$$(a_1, a_2, a_3)^\top = \mathbf{J}_1^\top (\boldsymbol{\eta}_2) (x_{\mathrm{e}}, y_{\mathrm{e}}, z_{\mathrm{e}})^\top. \tag{5.134}$$

By placing the rotation matrix (3.2) in (5.134) we obtain

$$
\begin{aligned}
a_1 &= x_{\mathrm{e}} \cos(\psi)\cos(\theta) + y_{\mathrm{e}}\sin(\psi)\cos(\theta) - z_{\mathrm{e}}\sin(\theta) \\
a_2 &= x_{\mathrm{e}}\left(-\sin(\psi)\cos(\phi) + \sin(\phi)\sin(\theta)\cos(\psi)\right) + \\
&\quad y_{\mathrm{e}}\left(\cos(\psi)\cos(\phi) + \sin(\phi)\sin(\theta)\sin(\psi)\right) + z_{\mathrm{e}}\sin(\phi)\cos(\theta) \\
a_3 &= x_{\mathrm{e}}\left(\sin(\psi)\sin(\phi) + \sin(\theta)\cos(\psi)\cos(\phi)\right) + \\
&\quad y_{\mathrm{e}}\left(-\cos(\psi)\sin(\phi) + \sin(\theta)\sin(\psi)\cos(\phi)\right) + z_{\mathrm{e}}\cos(\phi)\cos(\theta).
\end{aligned}
\tag{5.135}
$$

Now, let the desired orientation of the virtual vessel be $\phi_{\mathrm{d}} = 0$ for roll, θ_{d} for the pitch and ψ_{d} for the yaw angles. Then from Figure 5.10 we draw

$$\lim_{(d_{\mathrm{e}}, \gamma) \to 0} (\theta, \psi) = (\theta_{\mathrm{d}}, \psi_{\mathrm{d}}) \tag{5.136}$$

where θ and ψ are the pitch and yaw angles of the real vessel. We can obviously recognize that the angles $\bar{\gamma}_1$ and $\bar{\gamma}_2$ are not defined for $d_{\mathrm{e}} = 0$, therefore, we will design the controller to force d_{e} to be a some small positive constant d_{e}^*.

In other words, the pulled (real) vessel will trace the puller (virtual) vessel under the same environment conditions, but in a time delay d_{e}/u_0, which can be made arbitrary small. This goes along with what we see in Figure 5.11.

The control objective, in addition to minimizing the distance d_{e} is to render the angles $\bar{\gamma}_1$ and $\bar{\gamma}_2$ arbitrary small which means from Figure 5.10 that the angle γ goes to an
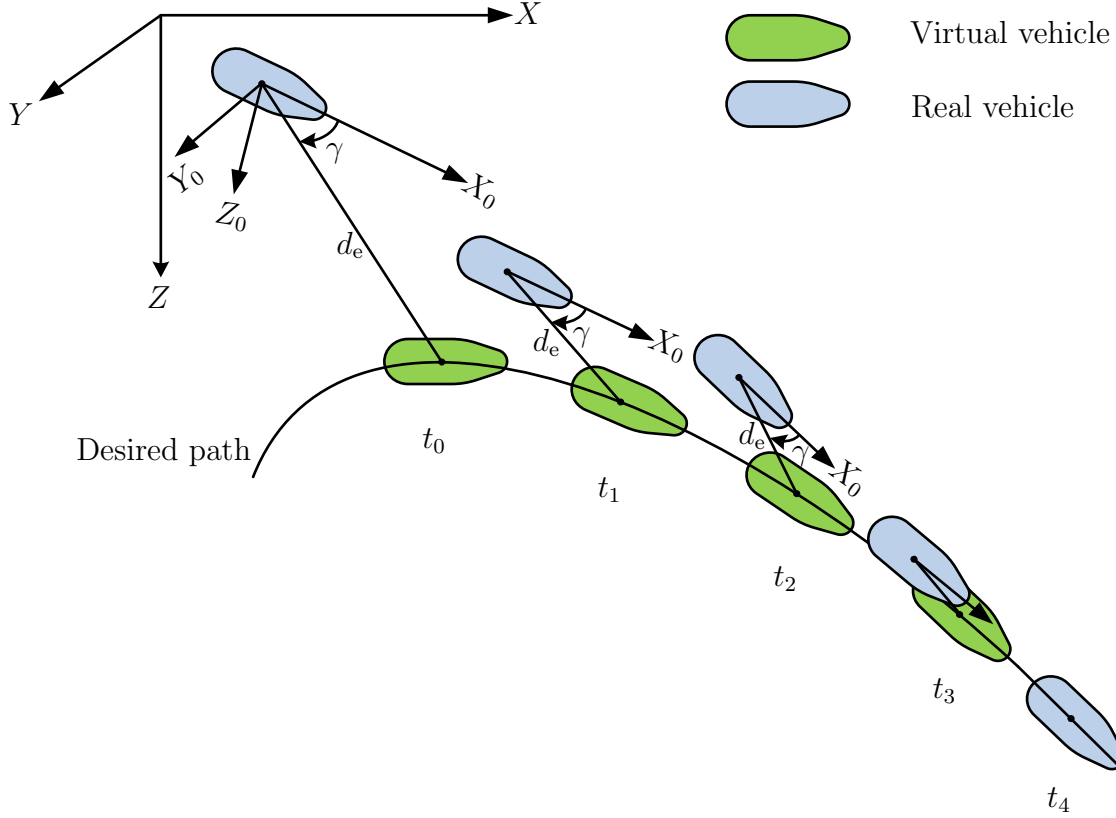
Fig. 5.11: Tracking algorithm

arbitrary small constant where, $\cos(\gamma) = \cos(\bar{\gamma}_1)\cos(\bar{\gamma}_2)$.

Practically, the controller will make the angles $\bar{\gamma}_1$ and $\bar{\gamma}_2$ zero, but because of modeled and unmodeled system uncertainties and also to avoid chattering in the control law the "tanh" function will be used instead of the "sign" function in the control law. Therefore, we can just force the orientation angles to be very close to zero, but not zero (as we saw in Remark 5.3.1). To design the controller we may introduce the error dynamics. To achieve this, we differentiate both sides of (5.133) with respect to time t. We get

$$\dot{d}_{\mathrm{e}} = \frac{\partial d_{\mathrm{e}}}{\partial x_{\mathrm{e}}} \dot{x}_{\mathrm{e}} + \frac{\partial d_{\mathrm{e}}}{\partial y_{\mathrm{e}}} \dot{y}_{\mathrm{e}} + \frac{\partial d_{\mathrm{e}}}{\partial z_{\mathrm{e}}} \dot{z}_{\mathrm{e}} = \frac{1}{d_{\mathrm{e}}} (x_{\mathrm{e}}, y_{\mathrm{e}}, z_{\mathrm{e}})^{\top} (\dot{x}_{\mathrm{d}} - \dot{x}, \dot{y}_{\mathrm{d}} - \dot{y}, \dot{z}_{\mathrm{d}} - \dot{z})$$

$$= \frac{1}{d_{\mathrm{e}}} \left(x_{\mathrm{e}} \frac{\partial x_{\mathrm{d}}(\sigma)}{\partial \sigma} + y_{\mathrm{e}} \frac{\partial y_{\mathrm{d}}(\sigma)}{\partial \sigma} + z_{\mathrm{e}} \frac{\partial z_{\mathrm{d}}(\sigma)}{\partial \sigma} \right) \dot{\sigma} - \frac{1}{d_{\mathrm{e}}} (a_1, a_2, a_3) \mathbf{J}_2^{\top}(\boldsymbol{\eta_2}) \mathbf{J}_2(\boldsymbol{\eta_2}) (u, v, w)^{\top}$$

$$(5.137)$$

where $\sigma(t)$ is the path variable of the desired path $(x_{\mathrm{d}}(\sigma), y_{\mathrm{d}}(\sigma), z_{\mathrm{d}}(\sigma))$. The path variable $\sigma(t)$ can be calculated analytically based on the reference path and desired

velocity of the virtual vessel through integration of the following relationship

$$\dot{\sigma}(t) = \frac{u_0}{\sqrt{(\partial x_{\mathrm{d}}(\sigma)/\partial\sigma)^2 + (\partial y_{\mathrm{d}}(\sigma)/\partial\sigma)^2 + (\partial z_{\mathrm{d}}(\sigma)/\partial\sigma)^2}}. \tag{5.138}$$

Now, if the real vehicle does not point to the virtual one this necessitates the desired velocity to be decreased with a correction factor a_1/d_{e}. In other words, since the real vessel does not point to the virtual one, the virtual vehicle must wait for the real one (decreasing the desired velocity u_0). That means, the term a_1/d_{e} is utilized as correction term of the desired velocity along the desired path, where $a_1/d_{\mathrm{e}} \to 1$ if the real vehicle is pointing to the virtual one. This generally yields

$$\dot{\sigma}(t) = \frac{a_1}{d_{\mathrm{e}}} \frac{u_0(t, d_{\mathrm{e}})}{\sqrt{(\partial x_{\mathrm{d}}(\sigma)/\partial\sigma)^2 + (\partial y_{\mathrm{d}}(\sigma)/\partial\sigma)^2 + (\partial z_{\mathrm{d}}(\sigma)/\partial\sigma)^2}}. \tag{5.139}$$

Since matrix $\mathbf{J}_2(\boldsymbol{\eta})$ is orthogonal and using the kinematics (3.4) and (5.137) we obtain

$$\dot{d}_{\mathrm{e}} = \frac{1}{d_{\mathrm{e}}}\left(x_{\mathrm{e}}\frac{\partial x_{\mathrm{d}}(\sigma)}{\partial\sigma} + y_{\mathrm{e}}\frac{\partial y_{\mathrm{d}}(\sigma)}{\partial\sigma} + z_{\mathrm{e}}\frac{\partial z_{\mathrm{d}}(\sigma)}{\partial\sigma}\right)\dot{\sigma} - \frac{a_1}{d_{\mathrm{e}}}u - \frac{a_2}{d_{\mathrm{e}}}v - \frac{a_3}{d_{\mathrm{e}}}w. \tag{5.140}$$

The error dynamics of d_{e} described in (5.140) is not defined for $d_{\mathrm{e}} = 0$. The error dynamics describes the first control objective for the kinematics of the system with regard to the Euclidean distance between real and virtual vessel, the second objective is the orientation.

Now, we define the dynamics which describes the orientation of the vessel in 3D underwater space. The orientation of the vehicle is described by the angle γ, see Figure 5.10. It is clear that

$$\cos(\gamma) = \frac{a_1}{d_{\mathrm{e}}} \tag{5.141}$$

which in turn means

$$\gamma \to 0 \iff \frac{a_1}{d_{\mathrm{e}}} \to 1. \tag{5.142}$$

From the first equation of (5.135), by adding and subtracting the term $a_{\mathrm{e}}\cos(\theta)$ where $a_{\mathrm{e}} = \sqrt{x_{\mathrm{e}}^2 + y_{\mathrm{e}}^2}$, we get

$$a_1 = x_{\mathrm{e}}\cos(\theta)\cos(\psi) + y_{\mathrm{e}}\cos(\theta)\sin(\psi) - z_{\mathrm{e}}\sin(\theta) + a_{\mathrm{e}}\cos(\theta) - a_{\mathrm{e}}\cos(\theta). \tag{5.143}$$

Dividing both sides of (5.143) by d_{e} we obtain

$$\frac{a_1}{d_\mathrm{e}} = \frac{a_\mathrm{e}}{d_\mathrm{e}} \cos{(\theta)} - \frac{z_\mathrm{e}}{d_\mathrm{e}} \sin{(\theta)} + \frac{a_\mathrm{e}}{d_\mathrm{e}} \cos{(\theta)} \left[\frac{x_\mathrm{e}}{a_\mathrm{e}} \cos{(\psi)} + \frac{y_\mathrm{e}}{a_\mathrm{e}} \sin{(\psi)} - 1 \right]. \qquad (5.144)$$

Since $d_\mathrm{e} > 0$ and $a_\mathrm{e} \neq 0$ (will be proved later) the relation (5.144) is defined and reveals no singularities.

To this end, let us define

$$\cos{(\psi_\mathrm{a})} = \frac{x_\mathrm{e}}{a_\mathrm{e}} \leq 1 \qquad (5.145)$$

where ψ_a is an auxiliary quantity. By using $y_\mathrm{e}^2 = a_\mathrm{e}^2 - x_\mathrm{e}^2$, we can write

$$\sin{(\psi_\mathrm{a})} = \frac{y_\mathrm{e}}{a_\mathrm{e}} \leq 1. \qquad (5.146)$$

In the same manner, let us define

$$\cos{(\theta_\mathrm{a})} = \frac{a_\mathrm{e}}{d_\mathrm{e}} \leq 1 \qquad (5.147)$$

where again, θ_a is an auxiliary quantity. Thus, because of $z_\mathrm{e}^2 = d_\mathrm{e}^2 - a_\mathrm{e}^2$, we obtain

$$\sin{(\theta_\mathrm{a})} = \frac{z_\mathrm{e}}{d_\mathrm{e}} \leq 1. \qquad (5.148)$$

Now, by replacing the relations $(5.145) - (5.148)$ into (5.144), we have

$$\frac{a_1}{d_\mathrm{e}} = \underbrace{\cos{(\theta_\mathrm{a})} \cos{(\theta)} - \sin{(\theta_\mathrm{a})} \sin{(\theta)}}_{\cos(\gamma_1)} + \frac{a_\mathrm{e}}{d_\mathrm{e}} \cos{(\theta)} \left[\underbrace{\cos{(\psi_\mathrm{a})} \cos{(\psi)} + \sin{(\psi_\mathrm{a})} \sin{(\psi)}}_{\cos(\gamma_2)} - 1 \right].$$
$$(5.149)$$

This equation is equivalent to

$$\frac{a_1}{d_\mathrm{e}} = \cos{(\gamma_1)} + \frac{a_\mathrm{e}}{d_\mathrm{e}} \cos{(\theta)} \left[\cos{(\gamma_2)} - 1 \right] \qquad (5.150)$$

where

$$\gamma_1 = \theta + \theta_\mathrm{a}, \quad \gamma_2 = \psi - \psi_\mathrm{a}. \qquad (5.151)$$

Thus, we can consider that the control objective related to the orientation of the vehicle is given by relationship (5.150). In this equation it is obvious that for $-\pi/2 < \theta < \pi/2$ (it is satisfied due to physical considerations) we have

$$\frac{a_\mathrm{e}}{d_\mathrm{e}} \cos{(\theta)} \neq 1 \qquad (5.152)$$

and from (5.150) that

$$\lim_{t \to \infty} \gamma_1 = 0, \quad \lim_{t \to \infty} \gamma_2 = 0 \tag{5.153}$$

then

$$\lim_{t \to \infty} \frac{a_1}{d_e} = 1. \tag{5.154}$$

So we may transfer the control objective to stabilizing the angles γ_1 and γ_2 at the origin (or arbitrary close to it). We have seen that

$$\cos(\gamma_1) = \frac{a_e}{d_e} \cos(\theta) - \frac{z_e}{d_e} \sin(\theta) \tag{5.155}$$

which implies that

$$\sin(\gamma_1) = \frac{z_e}{d_e} \cos(\theta) + \frac{a_e}{d_e} \sin(\theta). \tag{5.156}$$

Now, differentiating both sides of (5.156) with respect to time yields

$$\dot{\gamma}_1 \cos(\gamma_1) = \left(\frac{a_e}{d_e} \cos(\theta) - \frac{z_e}{d_e} \sin(\theta) \right) \dot{\theta} + \frac{\dot{z}_e d_e}{d_e^2} \cos(\theta) + \frac{\dot{a}_e d_e}{d_e^2} \sin(\theta)$$
$$- \frac{\dot{d}_e}{d_e} \left(\frac{z_e}{d_e} \cos(\theta) + \frac{a_e}{d_e} \sin(\theta) \right) \tag{5.157}$$

such that the dynamics of γ_1 is given through

$$\dot{\gamma}_1 = \dot{\theta} + \frac{\dot{z}_e \cos(\theta) + \dot{a}_e \sin(\theta)}{d_e \cos(\gamma_1)} - \frac{\dot{d}_e}{d_e} \frac{\sin(\gamma_1)}{\cos(\gamma_1)}. \tag{5.158}$$

Also, we obtained that

$$\cos(\gamma_2) = \frac{x_e}{a_e} \cos(\psi) + \frac{y_e}{a_e} \sin(\psi) \tag{5.159}$$

so that

$$\sin(\gamma_2) = -\frac{y_e}{a_e} \cos(\psi) + \frac{x_e}{a_e} \sin(\psi). \tag{5.160}$$

By differentiating both sides of (5.160) with respect to time we obtain

$$\dot{\gamma}_2 \cos(\gamma_2) = \left(\frac{x_e}{a_e} \cos(\psi) + \frac{y_e}{a_e} \sin(\psi) \right) \dot{\psi} - \frac{\dot{a}_e}{a_e} \left(-\frac{y_e}{a_e} \cos(\psi) + \frac{x_e}{a_e} \sin(\psi) \right)$$
$$+ \frac{\dot{x}_e \sin(\psi) - \dot{y}_e \cos(\psi)}{a_e}. \tag{5.161}$$

The dynamics of γ_2 is then given as

$$\dot{\gamma}_2 = \dot{\psi} + \frac{\dot{x}_{\mathrm{e}} \sin\left(\psi\right) - \dot{y}_{\mathrm{e}} \cos\left(\psi\right)}{a_{\mathrm{e}} \cos\left(\gamma_2\right)} - \frac{\dot{a}_{\mathrm{e}} \sin\left(\gamma_2\right)}{a_{\mathrm{e}} \cos\left(\gamma_2\right)}. \tag{5.162}$$

It is convenient to notice that the dynamics of γ_1 and γ_2 in (5.158) and in (5.162) respectively are defined on $\mathbb{R}$ for $a_{\mathrm{e}} \neq 0, d_{\mathrm{e}} \neq 0, \cos\left(\gamma_1\right) \neq 0$ and $\cos\left(\gamma_2\right) \neq 0$. Those conditions can be guaranteed by suitable choice of the initial conditions for the position and the orientation of the real vehicle. On the other side, we will show that the singularity which might appear in (5.158) and in (5.162) if $a_{\mathrm{e}} = 0$ is completely avoided by using the designed controller.

To show that $a_{\mathrm{e}} > 0$ let us consider $\sin\left(\theta_{\mathrm{a}}\right) = z_{\mathrm{e}}/d_{\mathrm{e}}$, or equivalently $\left|\sin\left(\theta_{\mathrm{a}}\right)\right| < 1$ as long as $\theta_{\mathrm{a}} < \pi/2$. This gives $z_{\mathrm{e}}^2 < d_{\mathrm{e}}^2 \Rightarrow d_{\mathrm{e}}^2 - z_{\mathrm{e}}^2 = a_{\mathrm{e}}^2 > 0 \Rightarrow a_{\mathrm{e}} > 0$ where generally

$$a_e = \sqrt{x_e^2 + y_e^2} \geq 0, \tag{5.163}$$

which implies $a_{\mathrm{e}}\left(t\right) > 0 \ \forall t > t_0$.

Now define the orientation error vector as

$$\boldsymbol{\eta}_\gamma = \left(\phi, \gamma_1, \gamma_2\right)^\top. \tag{5.164}$$

Based on this definition we can transform the kinematics of the system into ϕ, γ_1, γ_2 coordinates.

From relationships (5.158) and (5.162), we may write

$$\dot{\boldsymbol{\eta}}_\gamma = \begin{pmatrix} \dot{\phi} \\ \dot{\theta} + \dfrac{\dot{z}_{\mathrm{e}} \cos\left(\theta\right) + \dot{a}_{\mathrm{e}} \sin\left(\theta\right)}{d_{\mathrm{e}} \cos\left(\gamma_1\right)} - \dfrac{\dot{d}_{\mathrm{e}} \sin\left(\gamma_1\right)}{d_{\mathrm{e}} \cos\left(\gamma_1\right)} \\ \dot{\psi} + \dfrac{\dot{x}_{\mathrm{e}} \sin\left(\psi\right) - \dot{y}_{\mathrm{e}} \cos\left(\psi\right)}{a_{\mathrm{e}} \cos\left(\gamma_2\right)} - \dfrac{\dot{a}_{\mathrm{e}} \sin\left(\gamma_2\right)}{a_{\mathrm{e}} \cos\left(\gamma_2\right)} \end{pmatrix}. \tag{5.165}$$

Noticing the kinematics (3.4) of the system, we see that

$$\dot{\boldsymbol{\eta}}_\gamma = \mathbf{J}_2\left(\boldsymbol{\eta}_2\right) \mathbf{v}_2 + \mathbf{f}_\gamma\left(\cdot\right) \tag{5.166}$$

81

where

$$\mathbf{f}_\gamma(\cdot) = \begin{pmatrix} 0 \\ \dfrac{\dot{z}_e \cos(\theta) + \dot{a}_e \sin(\theta)}{d_e \cos(\gamma_1)} - \dfrac{\dot{d}_e \sin(\gamma_1)}{d_e \cos(\gamma_1)} \\ \dfrac{\dot{x}_e \sin(\psi) - \dot{y}_e \cos(\psi)}{a_e \cos(\gamma_2)} - \dfrac{\dot{a}_e \sin(\gamma_2)}{a_e \cos(\gamma_2)} \end{pmatrix}. \tag{5.167}$$

Hence, according to this coordinates transformation the kinematics of the AUV system, described in the first two equations in (3.49), can be transformed in the error coordinates

$$\dot{d}_e = \frac{1}{d_e}\left(x_e \frac{\partial x_d(\sigma)}{\partial \sigma} + y_e \frac{\partial y_d(\sigma)}{\partial \sigma} + z_e \frac{\partial z_d(\sigma)}{\partial \sigma}\right)\dot{\sigma} - \frac{a_1}{d_e}u - \frac{a_2}{d_e}v - \frac{a_3}{d_e}w$$

$$\dot{\boldsymbol{\eta}}_\gamma = \mathbf{J}_2(\boldsymbol{\eta}_2)\mathbf{v}_2 + \mathbf{f}_\gamma(\cdot). \tag{5.168}$$

Then the whole system which describes the system (kinematics and dynamics) of the AUV in the new coordinates reads

$$\dot{d}_e = \frac{1}{d_e}\left(x_e \frac{\partial x_d(\sigma)}{\partial \sigma} + y_e \frac{\partial y_d(\sigma)}{\partial \sigma} + z_e \frac{\partial z_d(\sigma)}{\partial \sigma}\right)\dot{\sigma} - \frac{a_1}{d_e}u - \frac{a_2}{d_e}v - \frac{a_3}{d_e}w$$

$$\dot{\boldsymbol{\eta}}_\gamma = \mathbf{J}_2(\boldsymbol{\eta}_2)\mathbf{v}_2 + \mathbf{f}_\gamma(\cdot)$$

$$\mathbf{M}_1\dot{\mathbf{v}}_1 = -\mathbf{C}_1(\mathbf{v}_1)\mathbf{v}_2 - \mathbf{D}_1(\mathbf{v}_1)\mathbf{v}_1 + \boldsymbol{\tau}_1 + \boldsymbol{\tau}_{1d}$$

$$\mathbf{M}_2\dot{\mathbf{v}}_2 = -\mathbf{C}_1(\mathbf{v}_1)\mathbf{v}_1 - \mathbf{C}_2(\mathbf{v}_2)\mathbf{v}_2 - \mathbf{D}_2(\mathbf{v}_2)\mathbf{v}_2 - \mathbf{g}_2(\boldsymbol{\eta}_2) + \boldsymbol{\tau}_2 + \boldsymbol{\tau}_{2d}. \tag{5.169}$$

This triangular-like form is suitable to implement the backstepping technique to design the controller, which fulfills the path following objectives.

Le us consider that the virtual vehicle is moving along the desired path according to a speed function

$$u_0(t, d_e) = u_0^*\left(1 - u_1^* e^{-u_2^*(t-t_0)}\right)e^{-u_3^* d_e} \tag{5.170}$$

where u_0^*, u_2^* and u_3^* are positive constants, and $0 < u_1^* < 1$. The advantage of choosing the speed profile as in (5.170) is that if d_e is large, that means, the speed of the virtual vessel is decreasing, which implies that the virtual vehicle is waiting for the real one. On the other side, if d_e is small, we get

$$\lim_{t\to\infty} u_0(t, d_e) \simeq u_0^* \tag{5.171}$$

which means that the virtual vehicle moves with a velocity close to u_0^* and the real

vehicle follows it, but after an arbitrary small delay time $d_{\mathrm{e}}/u_0\,(t, d_{\mathrm{e}})$.

5.6 Robust and Adaptive Backstepping Controller for an Underactuated AUV

Based on the robust adaptive backstepping control approach, which is introduced in the Section 5.3.3, we design a path following controller for the underactuated model of the AUV, described in the error dynamics coordinates (5.169).

The structure of the system (5.169) allows to design the control inputs in two steps: In the first one, we design a force controller $\boldsymbol{\tau}_1$ to compel the error d_{e} to converge to an arbitrary small constant, then in the second step we design the torque control $\boldsymbol{\tau}_2$, which forces the real vehicle to rotate and point always to the virtual vessel.

5.6.1 Force Control

To design the force input $\boldsymbol{\tau}_1$, which steers the real vehicle to move arbitrary close to the virtual one, we consider the following subsystem of (5.169)

$$\dot{d}_{\mathrm{e}} = \frac{1}{d_{\mathrm{e}}}\left(x_{\mathrm{e}}\frac{\partial x_{\mathrm{d}}(\sigma)}{\partial \sigma} + y_{\mathrm{e}}\frac{\partial y_{\mathrm{d}}(\sigma)}{\partial \sigma} + z_{\mathrm{e}}\frac{\partial z_{\mathrm{d}}(\sigma)}{\partial \sigma}\right)\dot{\sigma} - \frac{a_1}{d_{\mathrm{e}}}u - \frac{a_2}{d_{\mathrm{e}}}v - \frac{a_3}{d_{\mathrm{e}}}w \qquad (5.172)$$

$$\mathbf{M}_1\dot{\mathbf{v}}_1 = -\mathbf{C}_1\left(\mathbf{v}_1\right)\mathbf{v}_2 - \mathbf{D}_1\left(\mathbf{v}_1\right)\mathbf{v}_1 + \boldsymbol{\tau}_1 + \boldsymbol{\tau}_{1\mathrm{d}}. \qquad (5.173)$$

Hence, by following the control design procedure, which we introduced in the Section 5.3.3, we design $\boldsymbol{\tau}_1$ in two steps. Firstly, we design a virtual stabilizing intermediate controller u_{d} for (5.172) under the assumption that the velocities v and w are bounded. Secondly, we design $\boldsymbol{\tau}_1$ in (5.173) which is responsible to force u to converge to u_{d}.

For this purpose, we define $\tilde{d}_{\mathrm{e}} = d_{\mathrm{e}} - \delta$, where δ is some arbitrary small positive design constant. Let the virtual controller for the first subsystem (5.172) be

$$u_{\mathrm{d}} = k_1\tilde{d}_{\mathrm{e}} - \frac{1}{a_1}\left(a_2 v + a_3 w\right) + \frac{1}{a_1}\left(x_{\mathrm{e}}\frac{\partial x_{\mathrm{d}}(\sigma)}{\partial \sigma} + y_{\mathrm{e}}\frac{\partial y_{\mathrm{d}}(\sigma)}{\partial \sigma} + z_{\mathrm{e}}\frac{\partial z_{\mathrm{d}}(\sigma)}{\partial \sigma}\right)\dot{\sigma} \qquad (5.174)$$

where k_1 is a positive design parameter. Thereafter, by placing the virtual control

(5.174) into the dynamics (5.172), we obtain

$$\dot{\tilde{d}}_{\mathrm{e}} = -k_1 \frac{a_1}{d_{\mathrm{e}}} \tilde{d}_{\mathrm{e}} - \frac{a_1}{d_{\mathrm{e}}} \tilde{u} \tag{5.175}$$

where

$$\tilde{u} = u - u_{\mathrm{d}}. \tag{5.176}$$

In (5.175), a_1 the projection of d_{e} on the surge axis X_0, can be guaranteed to be positive through an adequate choice of the initial conditions (as we will see in Section 6.5) and of course by means of the torque controller $\boldsymbol{\tau}_2$ as well. On the other hand, the controller $\boldsymbol{\tau}_1$ is concerned with letting $\tilde{u}$ be zero (or very close to zero), which implies that the equilibrium point $d_{\mathrm{e}} = \delta$ in (5.175) is asymptotically stable.

Therefore, to design the control $\boldsymbol{\tau}_1$, we differentiate both sides of (5.176). Then we obtain the error dynamics of the velocity as

$$\dot{\tilde{u}} = \dot{u} - \dot{u}_{\mathrm{d}}. \tag{5.177}$$

The dynamics of the surge velocity u can be obtained from the dynamics of the underwater vehicle model in (3.5). We have

$$
\begin{aligned}
\dot{u} &= -\frac{m_3}{m_1} wq + \frac{m_2}{m_1} vr - \frac{1}{m_1} \left(d_1 + d_u \left| u \right| \right) u + \frac{1}{m_1} \tau_u + \frac{1}{m_1} \tau_{ud} \left(t \right) \\
\dot{v} &= \frac{m_3}{m_2} wp - \frac{m_1}{m_2} ur - \frac{1}{m_2} \left(d_2 + d_v \left| v \right| \right) v + \frac{1}{m_2} \tau_{vd} \left(t \right) \\
\dot{w} &= -\frac{m_2}{m_3} vp + \frac{m_1}{m_3} up - \frac{1}{m_3} \left(d_3 + d_w \left| w \right| \right) w + \frac{1}{m_3} \tau_{wd} \left(t \right).
\end{aligned}
\tag{5.178}
$$

Now, under the assumption of smoothness of the intermediate control u_{d} in $x_{\mathrm{e}}, y_{\mathrm{e}}, z_{\mathrm{e}}, \sigma$, u_0, $\boldsymbol{\eta}_2$, v and w in (5.174), we determine analytically the derivative of u_{d}, that is

$$\dot{u}_{\mathrm{d}} = \frac{\partial u_{\mathrm{d}}}{\partial x_{\mathrm{e}}} \dot{x}_{\mathrm{e}} + \frac{\partial u_{\mathrm{d}}}{\partial y_{\mathrm{e}}} \dot{y}_{\mathrm{e}} + \frac{\partial u_{\mathrm{d}}}{\partial z_{\mathrm{e}}} \dot{z}_{\mathrm{e}} + \frac{\partial u_{\mathrm{d}}}{\partial u_0} \dot{u}_0 + \frac{\partial u_{\mathrm{d}}}{\partial \sigma} \dot{\sigma} + \frac{\partial u_{\mathrm{d}}}{\partial \boldsymbol{\eta}_2} \dot{\boldsymbol{\eta}}_2 + \frac{\partial u_{\mathrm{d}}}{\partial v} \dot{v} + \frac{\partial u_{\mathrm{d}}}{\partial w} \dot{w}. \tag{5.179}$$

This approach is just applicable in the case of off-line planning of the desired path [82], meaning that, the reference trajectories $x_{\mathrm{d}} \left(\sigma \right), y_{\mathrm{d}} \left(\sigma \right)$ and $z_{\mathrm{d}} \left(\sigma \right)$ must be predefined (off-line), which is not admissible in an on-line tracking control approach.

Therefore, in the on-line path planning procedure it is impossible to determine $\frac{\partial u_{\mathrm{d}}}{\partial \sigma} \dot{\sigma}$ in (5.179), unless the path is predefined (off-line). To extend this technique to cover the

on-line path planning case, we calculate this term on-line as follows

$$\frac{\partial u_{\mathrm{d}}}{\partial \sigma}\dot{\sigma} = \frac{\partial u_{\mathrm{d}}}{\partial x'_{\mathrm{d}}}\dot{x}'_{\mathrm{d}} + \frac{\partial u_{\mathrm{d}}}{\partial y'_{\mathrm{d}}}\dot{y}'_{\mathrm{d}} + \frac{\partial u_{\mathrm{d}}}{\partial z'_{\mathrm{d}}}\dot{z}'_{\mathrm{d}} \tag{5.180}$$

where

$$\begin{aligned}
x'_{\mathrm{d}} &= \frac{\partial x_{\mathrm{d}}\left(\sigma\right)}{\partial \sigma}, \quad \dot{x}'_{\mathrm{d}} = \frac{\partial 2x_{\mathrm{d}}\left(\sigma\right)}{\partial \sigma^2}\dot{\sigma}, \quad y'_{\mathrm{d}} = \frac{\partial y_{\mathrm{d}}\left(\sigma\right)}{\partial \sigma}, \quad \dot{y}'_{\mathrm{d}} = \frac{\partial 2y_{\mathrm{d}}\left(\sigma\right)}{\partial \sigma^2}\dot{\sigma}, \\
z'_{\mathrm{d}} &= \frac{\partial z_{\mathrm{d}}\left(\sigma\right)}{\partial \sigma}, \quad \dot{z}'_{\mathrm{d}} = \frac{\partial 2z_{\mathrm{d}}\left(\sigma\right)}{\partial \sigma^2}\dot{\sigma}.
\end{aligned} \tag{5.181}$$

The terms in (5.181) exist and can be calculated, just under the assumption of continuity of the first and the second derivative of the reference trajectories $x_{\mathrm{d}}, y_{\mathrm{d}}$ and z_{d} regarding to the path variable σ. We can now determine the error dynamics of the intermediate control u_{d} by replacing the relations (5.179) and (5.178) into (5.177). Then we obtain

$$\begin{aligned}
\dot{\tilde{u}} =& -\frac{1}{m_1}\left(d_1 + d_u\left|u\right|\right)\tilde{u} + \frac{m_2}{m_1}vr - \frac{m_3}{m_1}wq - \frac{1}{m_1}\left(d_1 + d_u\left|u\right|\right)u_{\mathrm{d}} + \frac{1}{m_1}\tau_u \\
&+ \frac{1}{m_1}\tau_{ud}\left(t\right) - \frac{\partial u_{\mathrm{d}}}{\partial x_{\mathrm{e}}}\dot{x}_{\mathrm{e}} - \frac{\partial u_{\mathrm{d}}}{\partial y_{\mathrm{e}}}\dot{y}_{\mathrm{e}} - \frac{\partial u_{\mathrm{d}}}{\partial z_{\mathrm{e}}}\dot{z}_{\mathrm{e}} - \frac{\partial u_{\mathrm{d}}}{\partial u_0}\dot{u}_0 - \left[\frac{\partial u_{\mathrm{d}}}{\partial x'_{\mathrm{d}}}\frac{\partial 2x_{\mathrm{d}}\left(\sigma\right)}{\partial \sigma^2} + \frac{\partial u_{\mathrm{d}}}{\partial y'_{\mathrm{d}}}\frac{\partial 2y_{\mathrm{d}}\left(\sigma\right)}{\partial \sigma^2}\right. \\
&\left. + \frac{\partial u_{\mathrm{d}}}{\partial z'_{\mathrm{d}}}\frac{\partial 2z_{\mathrm{d}}\left(\sigma\right)}{\partial \sigma^2}\right]\dot{\sigma} - \frac{\partial u_{\mathrm{d}}}{\partial \boldsymbol{\eta}_2}\dot{\boldsymbol{\eta}}_2 - \frac{\partial u_{\mathrm{d}}}{\partial v}\left[\frac{m_3}{m_2}wp - \frac{m_1}{m_2}ur - \frac{1}{m_2}\left(d_2 + d_v\left|v\right|\right)v\right. \\
&\left. + \frac{1}{m_2}\tau_{vd}\left(t\right)\right] - \frac{\partial u_{\mathrm{d}}}{\partial w}\left[\frac{m_1}{m_3}up - \frac{m_2}{m_3}vp - \frac{1}{m_3}\left(d_3 + d_w\left|w\right|\right)w + \frac{1}{m_3}\tau_{wd}\left(t\right)\right]
\end{aligned} \tag{5.182}$$

where $\dot{x}_{\mathrm{e}} = \dot{x}_{\mathrm{d}} - \dot{x}, \dot{y}_{\mathrm{e}} = \dot{y}_{\mathrm{d}} - \dot{y}$ and $\dot{z}_{\mathrm{e}} = \dot{z}_{\mathrm{d}} - \dot{z}$. Also the time derivative of the desired velocity along the desired path is given analytically as

$$\dot{u}_0 = \frac{\partial u_0}{\partial t} + \frac{\partial u_0}{\partial x_{\mathrm{e}}}\dot{x}_{\mathrm{e}} + \frac{\partial u_0}{\partial y_{\mathrm{e}}}\dot{y}_{\mathrm{e}} + \frac{\partial u_0}{\partial z_{\mathrm{e}}}\dot{z}_{\mathrm{e}}. \tag{5.183}$$

Hence, we utilize a known basis vector function

$$\begin{aligned}
\mathbf{f}_1\left(\cdot\right) =& \left(vr, -wq, -u_{\mathrm{d}}, -\left|u\right|u_{\mathrm{d}}, -\frac{\partial u_{\mathrm{d}}}{\partial x_{\mathrm{e}}}\dot{x}_{\mathrm{e}} - \frac{\partial u_{\mathrm{d}}}{\partial y_{\mathrm{e}}}\dot{y}_{\mathrm{e}} - \frac{\partial u_{\mathrm{d}}}{\partial z_{\mathrm{e}}}\dot{z}_{\mathrm{e}} - \frac{\partial u_{\mathrm{d}}}{\partial x'_{\mathrm{d}}}\frac{\partial 2x_{\mathrm{d}}\left(\sigma\right)}{\partial \sigma^2}\dot{\sigma}\right. \\
&- \frac{\partial u_{\mathrm{d}}}{\partial y'_{\mathrm{d}}}\frac{\partial 2y_{\mathrm{d}}\left(\sigma\right)}{\partial \sigma^2}\dot{\sigma} - \frac{\partial u_{\mathrm{d}}}{\partial z'_{\mathrm{d}}}\frac{\partial 2z_{\mathrm{d}}\left(\sigma\right)}{\partial \sigma^2}\dot{\sigma} - \frac{\partial u_{\mathrm{d}}}{\partial u_0}\dot{u}_0 - \frac{\partial u_{\mathrm{d}}}{\partial \boldsymbol{\eta}_2}\dot{\boldsymbol{\eta}}_2, -\frac{\partial u_{\mathrm{d}}}{\partial v}wp, \frac{\partial u_{\mathrm{d}}}{\partial v}ur, \\
&\left.\frac{\partial u_{\mathrm{d}}}{\partial v}v, \frac{\partial u_{\mathrm{d}}}{\partial v}\left|v\right|v, -\frac{\partial u_{\mathrm{d}}}{\partial w}uq, \frac{\partial u_{\mathrm{d}}}{\partial w}vp, \frac{\partial u_{\mathrm{d}}}{\partial w}w, \frac{\partial u_{\mathrm{d}}}{\partial w}\left|w\right|w\right)^\top
\end{aligned} \tag{5.184}$$

85

and a vector of unknown parameters $\boldsymbol{\theta}_1$, which represents the modeled uncertainties of the first subsystem $(5.172 - 5.173)$, constructed as

$$\boldsymbol{\theta}_1 = \left(m_2, m_3, d_1, d_u, m_1, \frac{m_1 m_3}{m_2}, \frac{m_1^2}{m_2}, \frac{m_1 d_2}{m_2}, \frac{m_1 d_v}{m_2}, \frac{m_1^2}{m_2}, \frac{m_1 m_2}{m_3}, \frac{m_1 d_3}{m_3}, \frac{m_1 d_w}{m_3} \right)^\top .$$
(5.185)

The unmodeled uncertainties and the disturbances act on the first three channels of the system. They are given regarding their upper bounds and are lumped in a vector

$$\boldsymbol{\theta}_2 = (\theta_{21}, \theta_{22}, \theta_{23})^\top = \left(\tau_{ud}^{\max}, \frac{m_1}{m_2} \tau_{vd}^{\max}, \frac{m_1}{m_3} \tau_{wd}^{\max} \right)^\top .$$
(5.186)

Thereafter, by replacing (5.184), (5.185), and (5.186) in (5.182), we get

$$\dot{\tilde{u}} = \frac{1}{m_1} \left[- (d_1 + d_u |u|) \tilde{u} + \boldsymbol{\theta}_1^\top \mathbf{f}_1 (\cdot) + \tau_u + \tau_{ud} (t) - \frac{\partial u_d}{\partial v} \frac{m_1}{m_2} \tau_{vd} (t) - \frac{\partial u_d}{\partial w} \frac{m_1}{m_3} \tau_{wd} (t) \right] .$$
(5.187)

Now, applying the *certainty equivalence principle*, the control input τ_u in (5.187) can be chosen as

$$\tau_u = -c_u \tilde{u} - \hat{\boldsymbol{\theta}}_1^\top \mathbf{f}_1 (\cdot) - \hat{\theta}_{21} \tanh \left(\frac{\tilde{u} \hat{\theta}_{21}}{\epsilon_{21}} \right) - \hat{\theta}_{22} \frac{\partial u_d}{\partial v} \tanh \left(\frac{\partial u_d}{\partial v} \frac{\tilde{u} \hat{\theta}_{22}}{\epsilon_{22}} \right)$$
$$- \hat{\theta}_{23} \frac{\partial u_d}{\partial w} \tanh \left(\frac{\partial u_d}{\partial w} \frac{\tilde{u} \hat{\theta}_{23}}{\epsilon_{23}} \right)$$
(5.188)

where c_u is a designed positive control parameter, $\hat{\boldsymbol{\theta}}_1$ is the estimate of the unknown parameter vector $\boldsymbol{\theta}_1$, and $\hat{\theta}_{21}, \hat{\theta}_{22}$ and $\hat{\theta}_{23}$ are the estimates of θ_{21}, θ_{22} and θ_{23} respectively. The estimates of the parameters in (5.188) can be determined using the update laws

$$\dot{\hat{\boldsymbol{\theta}}}_1 = \boldsymbol{\Gamma}_1 \text{Proj} \left(\mathbf{f}_1 (\cdot) \tilde{u}, \hat{\boldsymbol{\theta}}_1 \right)$$
$$\dot{\hat{\theta}}_{21} = \gamma_{21} \text{Proj} \left(|\tilde{u}|, \hat{\theta}_{21} \right), \dot{\hat{\theta}}_{22} = \gamma_{22} \text{Proj} \left(\left| \tilde{u} \frac{\partial u_d}{\partial v} \right|, \hat{\theta}_{22} \right),$$
$$\dot{\hat{\theta}}_{23} = \gamma_{23} \text{Proj} \left(\left| \tilde{u} \frac{\partial u_d}{\partial w} \right|, \hat{\theta}_{23} \right)$$
(5.189)

where $\boldsymbol{\Gamma}_1 \in \mathbb{R}^{13 \times 13}$ is a diagonal design matrix with entries $\gamma_{1i} > 0$, for $i = 1, \ldots, 13$, and, $\gamma_{21}, \gamma_{22}, \gamma_{23} > 0$ as well, and "Proj" is the projection operator which is already defined in (5.117).

5.6.2 Torque Control

The control input $\boldsymbol{\tau}_2$ is concerned with the orientation of the real vehicle and rotates the real vehicle to point permanently to the virtual one. To design the control law $\boldsymbol{\tau}_2$ we consider the second subsystem of the model (5.169)

$$\dot{\boldsymbol{\eta}}_\gamma = \mathbf{J}_2\left(\boldsymbol{\eta}_2\right)\mathbf{v}_2 + \mathbf{f}_\gamma\left(\cdot\right) \tag{5.190}$$

$$\mathbf{M}_2\dot{\mathbf{v}}_2 = -\mathbf{C}_1\left(\mathbf{v}_1\right)\mathbf{v}_1 - \mathbf{C}_2\left(\mathbf{v}_2\right)\mathbf{v}_2 - \mathbf{D}_2\left(\mathbf{v}_2\right)\mathbf{v}_2 - \mathbf{g}_2\left(\boldsymbol{\eta}_2\right) + \boldsymbol{\tau}_2 + \boldsymbol{\tau}_{2\mathrm{d}}. \tag{5.191}$$

The triangular-like structure of the system $(5.190 - 5.191)$ allows to design the control law $\boldsymbol{\tau}_2$ based on the backstepping approach where the goal is to force the vector $\boldsymbol{\eta}_\gamma = \left(\phi, \gamma_1, \gamma_2\right)^\top$ to go to zero as t goes to infinity.

To achieve that, we divide the procedure of control design into two steps. In the first one we design an intermediate controller

$$\mathbf{v}_{2\mathrm{d}} = \left(p_\mathrm{d}, q_\mathrm{d}, r_\mathrm{d}\right)^\top \tag{5.192}$$

which stabilizes $\boldsymbol{\eta}_\gamma$ at the origin while, in the second step, we design $\boldsymbol{\tau}_2$ to force $\tilde{\mathbf{v}}_2$ to converge to zero, where

$$\tilde{\mathbf{v}}_2 = \mathbf{v}_2 - \mathbf{v}_{2\mathrm{d}}. \tag{5.193}$$

For this purpose, we consider first the dynamics (5.190) and choose the intermediate control law as

$$\mathbf{v}_{2\mathrm{d}} = \left(p_\mathrm{d}, q_\mathrm{d}, r_\mathrm{d}\right)^\top = \mathbf{J}_2^\top\left(\boldsymbol{\eta}_2\right)\left[-\mathbf{f}_\gamma\left(\cdot\right) - \mathbf{K}_2\boldsymbol{\eta}_\gamma\right] \tag{5.194}$$

where $\mathbf{K}_2 = \mathrm{diag}\left(k_{21}, k_{22}, k_{23}\right)$ is a positive definite diagonal design matrix. Thus, with substitution of the controller (5.194) in (5.190) we obtain

$$\dot{\boldsymbol{\eta}}_\gamma = -\mathbf{K}_2\boldsymbol{\eta}_\gamma + \mathbf{J}_2\left(\boldsymbol{\eta}_2\right)\tilde{\mathbf{v}}_2. \tag{5.195}$$

In (5.195), the equilibrium $\boldsymbol{\eta}_\gamma = \mathbf{0}$ can be exponentially stabilized if the controller $\boldsymbol{\tau}_2$ guarantees that

$$\lim_{t\to\infty}\tilde{\mathbf{v}}_2 = 0. \tag{5.196}$$

To obtain (5.196) we differentiate both sides of (5.193) with respect to time

$$\dot{\tilde{\mathbf{v}}}_2 = \dot{\mathbf{v}}_2 - \dot{\mathbf{v}}_{2\mathrm{d}} \tag{5.197}$$

where

$$\dot{\mathbf{v}}_{2\mathrm{d}} = \frac{\partial \mathbf{v}_{2\mathrm{d}}}{\partial x_{\mathrm{e}}}\dot{x}_{\mathrm{e}} + \frac{\partial \mathbf{v}_{2\mathrm{d}}}{\partial y_{\mathrm{e}}}\dot{y}_{\mathrm{e}} + \frac{\partial \mathbf{v}_{2\mathrm{d}}}{\partial z_{\mathrm{e}}}\dot{z}_{\mathrm{e}} + \frac{\partial \mathbf{v}_{2\mathrm{d}}}{\partial x_{\mathrm{d}}'}\frac{\partial 2x_{\mathrm{d}}}{\partial \sigma^2}\dot{\sigma} + \frac{\partial \mathbf{v}_{2\mathrm{d}}}{\partial y_{\mathrm{d}}'}\frac{\partial 2y_{\mathrm{d}}}{\partial \sigma^2}\dot{\sigma} + \frac{\partial \mathbf{v}_{2\mathrm{d}}}{\partial z_{\mathrm{d}}'}\frac{\partial 2z_{\mathrm{d}}}{\partial \sigma^2}\dot{\sigma} + \frac{\partial \mathbf{v}_{2\mathrm{d}}}{\partial u_0}\dot{u}_0$$
$$+ \frac{\partial \mathbf{v}_{2\mathrm{d}}}{\partial \boldsymbol{\eta}_2}\dot{\boldsymbol{\eta}}_2. \tag{5.198}$$

Multiplying both sides of (5.197) with the matrix $\mathbf{M}_2$ and utilizing the dynamics (5.191) we obtain

$$\mathbf{M}_2\dot{\tilde{\mathbf{v}}}_2 = -\mathbf{C}_2\left(\mathbf{v}_2\right)\tilde{\mathbf{v}}_2 - \mathbf{D}_2\left(\mathbf{v}_2\right)\tilde{\mathbf{v}}_2 + \mathbf{F}\left(\cdot\right)\boldsymbol{\theta}_3 + \mathbf{G}\left(\cdot\right)\boldsymbol{\theta}_4\left(t\right) + \boldsymbol{\tau}_2 \tag{5.199}$$

where the vectors $\mathbf{F}\left(\cdot\right)\boldsymbol{\theta}_3$ and $\mathbf{G}\left(\cdot\right)\boldsymbol{\theta}_4\left(t\right)$ are determined from the relations (5.125) (5.193), (5.197) and (5.198), given through

$$\mathbf{F}\left(\cdot\right)\boldsymbol{\theta}_3 = -\mathbf{C}_1\left(\mathbf{v}_1\right)\mathbf{v}_1 - \mathbf{C}_2\left(\mathbf{v}_2\right)\mathbf{v}_{2\mathrm{d}} - \mathbf{D}_2\left(\mathbf{v}_2\right)\mathbf{v}_{2\mathrm{d}} - \mathbf{g}_2\left(\boldsymbol{\eta}_2\right) - \mathbf{M}_2\left[\frac{\partial \mathbf{v}_{2\mathrm{d}}}{\partial x_{\mathrm{e}}}\dot{x}_{\mathrm{e}} + \frac{\partial \mathbf{v}_{2\mathrm{d}}}{\partial y_{\mathrm{e}}}\dot{y}_{\mathrm{e}}\right.$$
$$+\frac{\partial \mathbf{v}_{2\mathrm{d}}}{\partial z_{\mathrm{e}}}\dot{z}_{\mathrm{e}} + \frac{\partial \mathbf{v}_{2\mathrm{d}}}{\partial x_{\mathrm{d}}'}\frac{\partial 2x_{\mathrm{d}}}{\partial \sigma^2}\dot{\sigma} + \frac{\partial \mathbf{v}_{2\mathrm{d}}}{\partial y_{\mathrm{d}}'}\frac{\partial 2y_{\mathrm{d}}}{\partial \sigma^2}\dot{\sigma} + \frac{\partial \mathbf{v}_{2\mathrm{d}}}{\partial z_{\mathrm{d}}'}\frac{\partial 2z_{\mathrm{d}}}{\partial \sigma^2}\dot{\sigma} + \frac{\partial \mathbf{v}_{2\mathrm{d}}}{\partial u_0}\dot{u}_0 + \left.\frac{\partial \mathbf{v}_{2\mathrm{d}}}{\partial \boldsymbol{\eta}_2}\dot{\boldsymbol{\eta}}_2\right]$$
$$-\mathbf{M}_2\frac{\partial \mathbf{v}_{2\mathrm{d}}}{\partial \mathbf{v}_1}\mathbf{M}_1^{-1}\left(-\mathbf{C}_1\left(\mathbf{v}_1\right)\mathbf{v}_2 - \mathbf{D}_1\left(\mathbf{v}_1\right)\mathbf{v}_1 + \boldsymbol{\tau}_1\right) \tag{5.200}$$

and

$$\mathbf{G}\left(\cdot\right)\boldsymbol{\theta}_4\left(t\right) = \boldsymbol{\tau}_{2\mathrm{d}}\left(t\right) - \mathbf{M}_2\frac{\partial \mathbf{v}_{2\mathrm{d}}}{\partial \mathbf{v}_1}\mathbf{M}_1^{-1}\boldsymbol{\tau}_{1\mathrm{d}}\left(t\right) \tag{5.201}$$

where $\mathbf{F}\left(\cdot\right)$ and $\mathbf{G}\left(\cdot\right)$ are the basis matrices, which are calculated in Sections 5.6.2.1 and 5.6.2.2, respectively.

In the dynamics (5.199), the controller $\boldsymbol{\tau}_2$ is chosen to compensate $\mathbf{F}\left(\cdot\right)\boldsymbol{\theta}_3$ and $\mathbf{G}\left(\cdot\right)\boldsymbol{\theta}_4\left(t\right)$, and to satisfy (5.196).

Since the modeled uncertainties $\boldsymbol{\theta}_3$ and unmodeled uncertainties (disturbances) $\boldsymbol{\theta}_4\left(t\right)$ are not known we estimate $\boldsymbol{\theta}_3$ and the maximum value of $\boldsymbol{\theta}_4\left(t\right)$, under the assumption that the disturbance is bounded, with $\mathbf{F}\left(\cdot\right) \in \mathbb{R}^{3\times n_3}$, $\mathbf{G}\left(\cdot\right) \in \mathbb{R}^{3\times n_4}$, $\boldsymbol{\theta}_3 \in \mathbb{R}^{n_3}$ and $\boldsymbol{\theta}_4\left(t\right) \in \mathbb{R}^{n_4}$, where n_3 and n_4 are the numbers of unknown modeled and unmodeled uncertainties, respectively.

Our task now is indeed, to design a control law $\boldsymbol{\tau}_2$ for (5.199) to fulfill the control

objective (5.196). Therefore, we choose the controller as

$$\boldsymbol{\tau}_2 = -\mathbf{K}_3 \tilde{\mathbf{v}}_2 - \left(\boldsymbol{\eta}_\gamma^\top \mathbf{J}_2 \left(\boldsymbol{\eta}_2 \right) \right)^\top - \mathbf{F} \left(\cdot \right) \hat{\boldsymbol{\theta}}_3 - \mathbf{G}_\theta \left(\cdot \right) \tag{5.202}$$

where $\mathbf{K}_3 \in \mathbb{R}^3$ is a positive definite diagonal design matrix, and the vectors $\mathbf{F} \left(\cdot \right) \hat{\boldsymbol{\theta}}_3$ and $\mathbf{G}_\theta \left(\cdot \right)$ are given in (5.203) and (5.205), respectively. Let us start with the vector $\mathbf{F} \left(\cdot \right) \hat{\boldsymbol{\theta}}_3$, it is defined as

$$\mathbf{F} \left(\cdot \right) \hat{\boldsymbol{\theta}}_3 = \begin{pmatrix} f_{11}\hat{\theta}_{31} + \cdots + f_{1n_3}\hat{\theta}_{3n_3} \\ f_{21}\hat{\theta}_{31} + \cdots + f_{2n_3}\hat{\theta}_{3n_3} \\ f_{31}\hat{\theta}_{31} + \cdots + f_{3n_3}\hat{\theta}_{3n_3} \end{pmatrix} \tag{5.203}$$

where $\hat{\theta}_{3i}$ is the estimate of the unknown vector parameter θ_{3i}, for $1 \leq i \leq n_3$, with the update law

$$\dot{\hat{\theta}}_{3i} = \gamma_{3i} \mathrm{Proj} \left(\sum_{j=1}^{3} \tilde{v}_{2j} f_{ji}, \hat{\theta}_{3i} \right), \quad 1 \leq i \leq n_3. \tag{5.204}$$

The functions f_{ji} for $1 \leq j \leq 3$ and $1 \leq i \leq n_3$ are the components of the matrix $\mathbf{F} \left(\cdot \right)$ and $\gamma_{3i} \in \mathbb{R}^+$ are design parameters.

For instance, if $n_3 = 53$ (all of the parameters of the considered AUV are unknown), the rows of the matrix $\mathbf{F} \left(\cdot \right)$ can be calculated using the relations (5.212), (5.213) and (5.214). The other component of the controller (5.202) to be determined is the vector $\mathbf{G}_\theta \left(\cdot \right)$. To reach this purpose, let us replace the unknown vector $\boldsymbol{\theta}_4 \left(t \right)$ by the estimation of the maximum value of it (as we will see in the section 5.6.2.2). Thus, the vector $\mathbf{G}_\theta \left(\cdot \right)$ may be chosen as

$$\mathbf{G}_\theta \left(\cdot \right) = \begin{pmatrix} g_{11}\hat{\theta}_{41} \tanh \left(\dfrac{\tilde{v}_{21} g_{11}\hat{\theta}_{41}}{\epsilon_{11}} \right) + \cdots + g_{1n_4}\hat{\theta}_{4n_4} \tanh \left(\dfrac{\tilde{v}_{21} g_{1n_4}\hat{\theta}_{4n_4}}{\epsilon_{1n_4}} \right) \\ g_{21}\hat{\theta}_{41} \tanh \left(\dfrac{\tilde{v}_{22} g_{21}\hat{\theta}_{41}}{\epsilon_{21}} \right) + \cdots + g_{2n_4}\hat{\theta}_{4n_4} \tanh \left(\dfrac{\tilde{v}_{22} g_{2n_4}\hat{\theta}_{4n_4}}{\epsilon_{2n_4}} \right) \\ g_{31}\hat{\theta}_{41} \tanh \left(\dfrac{\tilde{v}_{23} g_{31}\hat{\theta}_{41}}{\epsilon_{31}} \right) + \cdots + g_{3n_4}\hat{\theta}_{4n_4} \tanh \left(\dfrac{\tilde{v}_{23} g_{3n_4}\hat{\theta}_{4n_4}}{\epsilon_{3n_4}} \right) \end{pmatrix} \tag{5.205}$$

where $\hat{\theta}_{4i}$ is the estimate of the maximum value of the component $\theta_{4i} \left(t \right)$ for $1 \leq i \leq n_4$,

with the update law

$$\dot{\hat{\theta}}_{4i} = \gamma_{4i}\text{Proj}\left(\sum_{j=1}^{3}|\tilde{v}_{2j}g_{ji}|,\hat{\theta}_{4i}\right), \quad 1 \le i \le n_4. \tag{5.206}$$

The functions g_{ji} for $1 \le j \le 3$ and $1 \le i \le n_4$ are the entries of the matrix $\mathbf{G}\left(\cdot\right)$ and $\gamma_{4i} \in \mathbb{R}^+$ are the designed gains.

5.6.2.1 Parameter Vector $\boldsymbol{\theta}_3$ and Basis Matrix $\mathbf{F}\left(\cdot\right)$

We have the following expression

$$\begin{aligned}
\mathbf{F}\left(\cdot\right)\boldsymbol{\theta}_3 = &- \mathbf{C}_1\left(\mathbf{v}_1\right)\mathbf{v}_1 - \mathbf{C}_2\left(\mathbf{v}_2\right)\mathbf{v}_{2d} - \mathbf{D}_2\left(\mathbf{v}_2\right)\mathbf{v}_{2d} - \mathbf{g}_2\left(\boldsymbol{\eta}_2\right) - \mathbf{M}_2\left[\frac{\partial \mathbf{v}_{2d}}{\partial x_e}\dot{x}_e + \frac{\partial \mathbf{v}_{2d}}{\partial y_e}\dot{y}_e\right.\\
&\left.+\frac{\partial \mathbf{v}_{2d}}{\partial z_e}\dot{z}_e + \frac{\partial \mathbf{v}_{2d}}{\partial x'_d}\frac{\partial 2x_d}{\partial \sigma^2}\dot{\sigma} + \frac{\partial \mathbf{v}_{2d}}{\partial y'_d}\frac{\partial 2y_d}{\partial \sigma^2}\dot{\sigma} + \frac{\partial \mathbf{v}_{2d}}{\partial z'_d}\frac{\partial 2z_d}{\partial \sigma^2}\dot{\sigma} + \frac{\partial \mathbf{v}_{2d}}{\partial u_0}\dot{u}_0 + \frac{\partial \mathbf{v}_{2d}}{\partial \boldsymbol{\eta}_2}\dot{\boldsymbol{\eta}}_2\right]\\
&- \mathbf{M}_2\frac{\partial \mathbf{v}_{2d}}{\partial \mathbf{v}_1}\mathbf{M}_1^{-1}\left(-\mathbf{C}_1\left(\mathbf{v}_1\right)\mathbf{v}_2 - \mathbf{D}_1\left(\mathbf{v}_1\right)\mathbf{v}_1 + \boldsymbol{\tau}_1\right).
\end{aligned} \tag{5.207}$$

To find the vector $\boldsymbol{\theta}_3$ and the matrix $\mathbf{F}\left(\cdot\right)$ we assume, in the worst case, that all parameters of the vessel are unknown, that means, $\boldsymbol{\theta}_3 \in \mathbb{R}^{53}$ and $\mathbf{F}\left(\cdot\right) \in \mathbb{R}^{3\times 53}$.

Thus, to express the parameter vector and the basis matrix explicitly we define

$$\begin{aligned}
\boldsymbol{\theta}_3 = &\left(m_2, m_3, m_5, m_6, d_4, d_p, \alpha_g, m_4, \frac{m_4 m_3}{m_2}, \frac{m_4 m_2}{m_3}, \frac{m_4 m_3}{m_1}, \frac{m_4 m_1}{m_3}, \frac{m_4 m_2}{m_1}, \frac{m_4 m_1}{m_2}, \frac{m_4 d_1}{m_1},\right.\\
&\frac{m_4 d_u}{m_1}, \frac{m_4 d_2}{m_2}, \frac{m_4 d_v}{m_2}, \frac{m_4 d_3}{m_3}, \frac{m_4 d_w}{m_3}, \frac{m_4}{m_1}, m_1, d_5, \alpha_g, \frac{m_5 m_3}{m_2}, \frac{m_5 m_2}{m_3}, \frac{m_5 m_3}{m_1}, \frac{m_5 m_1}{m_3},\\
&\frac{m_5 m_2}{m_1}, \frac{m_5 m_1}{m_2}, \frac{m_5 d_1}{m_1}, \frac{m_5 d_u}{m_1}, \frac{m_5 d_2}{m_2}, \frac{m_5 d_v}{m_2}, \frac{m_5 d_3}{m_3}, \frac{m_5 d_w}{m_3}, \frac{m_5}{m_1}, d_6, d_r, \frac{m_6 m_3}{m_2}, \frac{m_6 m_2}{m_3},\\
&\left.\frac{m_6 m_3}{m_1}, \frac{m_6 m_1}{m_3}, \frac{m_6 m_2}{m_1}, \frac{m_6 m_1}{m_2}, \frac{m_6 d_1}{m_1}, \frac{m_6 d_u}{m_1}, \frac{m_6 d_2}{m_2}, \frac{m_6 d_v}{m_2}, \frac{m_6 d_3}{m_3}, \frac{m_6 d_w}{m_3}, \frac{m_6}{m_1}, d_q\right)^\top\\
= &\left(\theta_{31}, \dots, \theta_{3n_3}\right)^\top, \quad \text{where } n_3 = 53.
\end{aligned} \tag{5.208}$$

Let the Jacobian matrix be

$$\frac{\partial \mathbf{v}_{2d}}{\partial \mathbf{v}_1} = \begin{pmatrix} b_{11} & b_{12} & b_{13} \\ b_{21} & b_{22} & b_{23} \\ b_{31} & b_{32} & b_{33} \end{pmatrix} \tag{5.209}$$

and let us define the following vector

$$
\left(X_{11}, X_{12}, X_{13}\right)^{\top} = \frac{\partial \mathbf{v}_{2\mathrm{d}}}{\partial x_{\mathrm{e}}}\dot{x}_{\mathrm{e}} + \frac{\partial \mathbf{v}_{2\mathrm{d}}}{\partial y_{\mathrm{e}}}\dot{y}_{\mathrm{e}} + \frac{\partial \mathbf{v}_{2\mathrm{d}}}{\partial z_{\mathrm{e}}}\dot{z}_{\mathrm{e}} + \frac{\partial \mathbf{v}_{2\mathrm{d}}}{\partial x'_{\mathrm{d}}}\frac{\partial 2 x_{\mathrm{d}}}{\partial \sigma^2}\dot{\sigma} + \frac{\partial \mathbf{v}_{2\mathrm{d}}}{\partial y'_{\mathrm{d}}}\frac{\partial 2 y_{\mathrm{d}}}{\partial \sigma^2}\dot{\sigma}
$$
$$
+ \frac{\partial \mathbf{v}_{2\mathrm{d}}}{\partial z'_{\mathrm{d}}}\frac{\partial 2 z_{\mathrm{d}}}{\partial \sigma^2}\dot{\sigma} + \frac{\partial \mathbf{v}_{2\mathrm{d}}}{\partial u_0}\dot{u}_0 + \frac{\partial \mathbf{v}_{2\mathrm{d}}}{\partial \boldsymbol{\eta}_2}\dot{\boldsymbol{\eta}}_2 \qquad (5.210)
$$

Then, according to the definitions above and by means of some calculations, we can find the matrix $\mathbf{F}\left(\cdot\right)$, through its rows as follows

$$
\mathbf{F}\left(\cdot\right) = \left(\mathbf{F}_1\left(\cdot\right), \mathbf{F}_2\left(\cdot\right), \mathbf{F}_3\left(\cdot\right)\right)^{\top}, \text{where } \mathbf{F}_1^{\top}\left(\cdot\right), \mathbf{F}_2^{\top}\left(\cdot\right), \mathbf{F}_3^{\top}\left(\cdot\right) \in \mathbb{R}^{53}. \qquad (5.211)
$$

These rows of the matrix $\mathbf{F}\left(\cdot\right)$ are given as

$$
\mathbf{F}_1\left(\cdot\right) = \Big(vw, -vw, qr_{\mathrm{d}}, -rq_{\mathrm{d}}, -p_{\mathrm{d}}, -p_{\mathrm{d}}\left|p\right|, -\sin\left(\phi\right)\cos\left(\theta\right), -X_{11}, -pb_{12}w, pb_{13}v, qb_{11}w,
$$
$$
- qb_{13}u, -rb_{11}v, rb_{12}u, b_{11}u, ub_{11}\left|u\right|, b_{12}v, b_{12}v\left|v\right|, b_{13}w, b_{13}w\left|w\right|, -b_{11}\tau_u,
$$
$$
0,0,0,0,0,0,0,0,0,0,0,0,0,0,0,0,0,0,0,0,0,0,0,0,0,0,0,0,0,0,0\Big), \qquad (5.212)
$$
$$
\mathbf{F}_2\left(\cdot\right) = \Big(0, wu, -X_{12}, rp_{\mathrm{d}}, 0, 0, 0, -pr_{\mathrm{d}}, 0,0,0,0,0,0,0,0,0,0,0,0, -wu, -q_{\mathrm{d}},
$$
$$
- \sin\left(\theta\right), -pb_{22}w, pb_{23}v, qb_{21}w, -qb_{23}\,u, -rb_{21}v, rb_{22}u, b_{21}u, b_{21}u\left|u\right|, vb_{22},
$$
$$
b_{22}v\left|v\right|, b_{23}w, b_{23}w\left|w\right|, -b_{21}\tau_u, 0,0,0,0,0,0,0,0,0,0,0,0,0,0,0,0, -q_{\mathrm{d}}\left|q\right|\Big), \qquad (5.213)
$$
$$
\mathbf{F}_3\left(\cdot\right) = \Big(- vu, 0, -qp_{\mathrm{d}}, -X_{13}, 0,0,0, pq_{\mathrm{d}}, 0,0,0,0,0,0,0,0,0,0,0,0, vu, 0,0,0,0,0,0,0,
$$
$$
0,0,0,0,0,0,0,0,0, -r_{\mathrm{d}}, -r_{\mathrm{d}}\left|r\right|, -pb_{32}w, pb_{33}v, qb_{31}w, -qb_{33}u, -rb_{31}v, rb_{32}u,
$$
$$
b_{31}u, b_{31}u\left|u\right|, b_{32}v, b_{32}v\left|v\right|, b_{33}w, b_{33}w\left|w\right|, -b_{31}\tau_u, 0\Big) \qquad (5.214)
$$

5.6.2.2 Parameter Vector $\boldsymbol{\theta}_4\left(t\right)$ and Basis Matrix $\mathbf{G}\left(\cdot\right)$

We have already from (5.201) that

$$
\mathbf{G}\left(\cdot\right)\boldsymbol{\theta}_4\left(t\right) = \boldsymbol{\tau}_{2\mathrm{d}}\left(t\right) - \mathbf{M}_2\frac{\partial \mathbf{v}_{2\mathrm{d}}}{\partial \mathbf{v}_1}\mathbf{M}_1^{-1}\boldsymbol{\tau}_{1\mathrm{d}}\left(t\right). \qquad (5.215)
$$

Let us define the vector of unknown unmodeled uncertainties (disturbances) as

$$\boldsymbol{\theta}_4(t) = \left(\tau_{pd}(t), \frac{m_4 \tau_{ud}(t)}{m_1}, \frac{m_4 \tau_{vd}(t)}{m_2}, \frac{m_4 \tau_{wd}(t)}{m_3}, \tau_{qd}(t), \frac{m_5 \tau_{ud}(t)}{m_1}, \frac{m_5 \tau_{vd}(t)}{m_2}, \frac{m_5 \tau_{wd}(t)}{m_3}, \right.$$
$$\left. \frac{m_6 \tau_{ud}(t)}{m_1}, \frac{m_6 \tau_{vd}(t)}{m_2}, \frac{m_6 \tau_{wd}(t)}{m_3} \right)^\top.$$

$$(5.216)$$

Then, we can determine the matrix $\mathbf{G}(\cdot)$ by defining its rows as

$$\mathbf{G}(\cdot) = \left(\mathbf{G}_1(\cdot), \mathbf{G}_2(\cdot), \mathbf{G}_3(\cdot) \right)^\top, \quad \mathbf{G}_1^\top(\cdot), \mathbf{G}_2^\top(\cdot), \mathbf{G}_3^\top(\cdot) \in \mathbb{R}^{12}. \qquad (5.217)$$

These rows of the matrix $\mathbf{G}(\cdot)$ are given as

$$\mathbf{G}_1(\cdot) = \left(1, -b_{11}, -b_{12}, -b_{13}, 0, 0, 0, 0, 0, 0, 0, 0 \right) \qquad (5.218)$$

$$\mathbf{G}_2(\cdot) = \left(0, 0, 0, 0, 1, -b_{21}, -b_{22}, -b_{23}, 0, 0, 0, 0 \right) \qquad (5.219)$$

$$\mathbf{G}_3(\cdot) = \left(0, 0, 0, 0, 0, 0, 0, 0, 1, -b_{31}, -b_{32}, -b_{33} \right) \qquad (5.220)$$

CHAPTER 6

Stability-Analysis

In this chapter we present in detail, a clear and extensive stability analysis for the complete dynamics of the AUV compared to previous works like [82, 83].

The high complexity of the AUV system renders the study of stability a tough task. Therefore, it is necessary to analyze individually the stability of the subsystems, which construct the entire AUV system. To serve this purpose we divide the entire closed-loop AUV system into subsystems, then we investigate their stability individually. The AUV system is divided into four sub-dynamics as follows: The underactuated dynamics $(\tilde{d}_e, \tilde{u})$, fully-actuated dynamics $\left(\boldsymbol{\eta}_\gamma, \tilde{\mathbf{v}}_2\right)$, and finally the non-actuated dynamics (v, w).

In the last section of this chapter we will study how to initialize the position and the orientation of a real vehicle to guarantee such that the controller is able to steer the real AUV to the virtual one.

6.1   Stability of the Underactuated Dynamics

To show the stability of the dynamics $(\tilde{d}_e, \tilde{u})$, we choose Lyapunov function candidate

$$\bar{V}_1 = \frac{1}{2}m_1\tilde{u}^2 + \frac{1}{2}\tilde{d}_e^2 + \frac{1}{2}\tilde{\boldsymbol{\theta}}_1^\top \boldsymbol{\Gamma}_1^{-1}\tilde{\boldsymbol{\theta}}_1 + \frac{1}{2}\tilde{\boldsymbol{\theta}}_2^\top \boldsymbol{\Gamma}_2^{-1}\tilde{\boldsymbol{\theta}}_2. \tag{6.1}$$

Since it is not simple to show that the time derivative of $\bar{V}_1$ is negative definite [84], we divide this dynamics into $\tilde{u}$-dynamics and $\tilde{d}_e$-dynamics, and then we investigate stability individually.

6.1.1 The Intermediate Control $\tilde{u}$

To study the stability of the first subsystem $(5.172)-(5.173)$, we substitute the controller (5.188) into the dynamics (5.187) and obtain the following closed-loop system

$$
\begin{aligned}
\dot{\tilde{u}} = & -\frac{1}{m_1}\left(c_u + d_1 + d_u|u|\right)\tilde{u} + \frac{1}{m_1}\boldsymbol{\theta}_1^\top \mathbf{f}_1\left(\cdot\right) - \frac{1}{m_1}\hat{\boldsymbol{\theta}}_1^\top \mathbf{f}_1\left(\cdot\right) + \frac{1}{m_1}\tau_{ud}(t) \\
& -\frac{1}{m_1}\hat{\theta}_{21}\tanh\left(\frac{\tilde{u}\hat{\theta}_{21}}{\epsilon_{21}}\right) - \frac{\partial u_d}{\partial v}\frac{1}{m_2}\tau_{vd}\left(t\right) - \frac{1}{m_1}\hat{\theta}_{22}\frac{\partial u_d}{\partial v}\tanh\left(\frac{\partial u_d}{\partial v}\frac{\tilde{u}\hat{\theta}_{22}}{\epsilon_{22}}\right) \\
& -\frac{\partial u_d}{\partial w}\frac{1}{m_3}\tau_{wd}\left(t\right) - \frac{1}{m_1}\hat{\theta}_{23}\frac{\partial u_d}{\partial w}\tanh\left(\frac{\partial u_d}{\partial w}\frac{\tilde{u}\hat{\theta}_{23}}{\epsilon_{23}}\right).
\end{aligned}
\tag{6.2}
$$

Now, by taking into account the assumption in (3.48) and considering the dynamics (6.2) we can write

$$
\tau_{ud}(t) \leq \tau_{ud}^{\max} \quad \Leftrightarrow \quad \tau_{ud}(t) \leq \theta_{21}, \quad \theta_{21} = \tau_{ud}^{\max}
\tag{6.3}
$$

$$
\begin{aligned}
\frac{m_1}{m_2}\tau_{ud}(t) \leq \frac{m_1}{m_2}\tau_{ud}^{\max} \quad &\Leftrightarrow \quad \frac{m_1}{m_2}\tau_{ud}(t) \leq \theta_{22}, \quad \theta_{22} = \frac{m_1}{m_2}\tau_{vd}^{\max} \\
\frac{m_1}{m_3}\tau_{wd}(t) \leq \frac{m_1}{m_3}\tau_{wd}^{\max} \quad &\Leftrightarrow \quad \frac{m_1}{m_3}\tau_{wd}(t) \leq \theta_{23}, \quad \theta_{23} = \frac{m_1}{m_3}\tau_{wd}^{\max}
\end{aligned}
\tag{6.4}
$$

and

$$
\boldsymbol{\theta}_2 = \left(\theta_{21}\ \theta_{22}\ \theta_{23}\right)^\top.
\tag{6.5}
$$

Let the Lyapunov function candidate be

$$
V_1 = \frac{1}{2}m_1\tilde{u}^2 + \frac{1}{2}\tilde{\boldsymbol{\theta}}_1^\top \boldsymbol{\Gamma}_1^{-1}\tilde{\boldsymbol{\theta}}_1 + \frac{1}{2}\tilde{\boldsymbol{\theta}}_2^\top \boldsymbol{\Gamma}_2^{-1}\tilde{\boldsymbol{\theta}}_2
\tag{6.6}
$$

where

$$
\tilde{\boldsymbol{\theta}}_i = \hat{\boldsymbol{\theta}}_i - \boldsymbol{\theta}_i, \quad i = 1, 2.
\tag{6.7}
$$

The time derivative of the Lyapunov function candidate in (6.6) is

$$
\begin{aligned}
\dot{V}_1 &= m_1\tilde{u}\dot{\tilde{u}} + \tilde{\boldsymbol{\theta}}_1^\top \boldsymbol{\Gamma}_1^{-1}\dot{\tilde{\boldsymbol{\theta}}}_1 + \tilde{\boldsymbol{\theta}}_2^\top \boldsymbol{\Gamma}_2^{-1}\dot{\tilde{\boldsymbol{\theta}}}_2 \\
&= m_1\tilde{u}\dot{\tilde{u}} + \tilde{\boldsymbol{\theta}}_1^\top \boldsymbol{\Gamma}_1^{-1}\dot{\hat{\boldsymbol{\theta}}}_1 + \tilde{\boldsymbol{\theta}}_2^\top \boldsymbol{\Gamma}_2^{-1}\dot{\hat{\boldsymbol{\theta}}}_2.
\end{aligned}
\tag{6.8}
$$

Now, by placing (6.2) in (6.8) we get

$$\dot{V}_1 = -\left(c_u + d_1 + d_u |u|\right)\tilde{u}^2 - \tilde{\boldsymbol{\theta}}_1^\top \mathbf{f}_1\left(\cdot\right)\tilde{u} + \tilde{\boldsymbol{\theta}}_1^\top \boldsymbol{\Gamma}_1^{-1}\dot{\hat{\boldsymbol{\theta}}}_1 + \tilde{\boldsymbol{\theta}}_2^\top \boldsymbol{\Gamma}_2^{-1}\dot{\hat{\boldsymbol{\theta}}}_2$$
$$+ \left(\tau_{ud}(t)\tilde{u} - \hat{\theta}_{21}\tilde{u}\tanh\left(\frac{\tilde{u}\hat{\theta}_{21}}{\epsilon_{21}}\right)\right)$$
$$+ \left(-\frac{\partial u_{\mathrm{d}}}{\partial v}\tilde{u}\frac{m_1}{m_2}\tau_{vd}\left(t\right) - \tilde{u}\hat{\theta}_{22}\frac{\partial u_{\mathrm{d}}}{\partial v}\tanh\left(\frac{\partial u_{\mathrm{d}}}{\partial v}\frac{\tilde{u}\hat{\theta}_{22}}{\epsilon_{22}}\right)\right) \tag{6.9}$$
$$+ \left(-\frac{\partial u_{\mathrm{d}}}{\partial w}\tilde{u}\frac{m_1}{m_3}\tau_{wd}\left(t\right) - \hat{\theta}_{23}\tilde{u}\frac{\partial u_{\mathrm{d}}}{\partial w}\tanh\left(\frac{\partial u_{\mathrm{d}}}{\partial w}\frac{\tilde{u}\hat{\theta}_{23}}{\epsilon_{23}}\right)\right).$$

We consider the disturbance terms in (6.9)

$$\tau_{ud}(t)\tilde{u} \leq |\tau_{ud}(t)\tilde{u}| \leq |\tau_{ud}(t)|\,|\tilde{u}| \leq \theta_{21}\,|\tilde{u}| = \left(\hat{\theta}_{21} - \tilde{\theta}_{21}\right)|\tilde{u}|$$
$$\leq \hat{\theta}_{21}\,|\tilde{u}| - \tilde{\theta}_{21}\,|\tilde{u}| \leq \left|\hat{\theta}_{21}\,|\tilde{u}|\right| - \tilde{\theta}_{21}\,|\tilde{u}| = \left|\hat{\theta}_{21}\tilde{u}\right| - \tilde{\theta}_{21}\,|\tilde{u}| \tag{6.10}$$

which means that

$$\tau_{ud}\left(t\right)\tilde{u} \leq \left|\hat{\theta}_{21}\tilde{u}\right| - \tilde{\theta}_{21}\,|\tilde{u}|. \tag{6.11}$$

Also we have

$$-\frac{\partial u_{\mathrm{d}}}{\partial v}\tilde{u}\frac{m_1}{m_2}\tau_{vd}\left(t\right) \leq \left|\frac{\partial u_{\mathrm{d}}}{\partial v}\tilde{u}\frac{m_1}{m_2}\tau_{vd}\left(t\right)\right| \leq \left|\frac{m_1}{m_2}\tau_{vd}\left(t\right)\right|\left|\frac{\partial u_{\mathrm{d}}}{\partial v}\tilde{u}\right|$$
$$\leq \theta_{22}\left|\frac{\partial u_{\mathrm{d}}}{\partial v}\tilde{u}\right| = \left(\hat{\theta}_{22} - \tilde{\theta}_{22}\right)\left|\frac{\partial u_{\mathrm{d}}}{\partial v}\tilde{u}\right| \tag{6.12}$$
$$\leq \hat{\theta}_{22}\left|\frac{\partial u_{\mathrm{d}}}{\partial v}\tilde{u}\right| - \tilde{\theta}_{22}\left|\frac{\partial u_{\mathrm{d}}}{\partial v}\tilde{u}\right| \leq \left|\hat{\theta}_{22}\left|\frac{\partial u_{\mathrm{d}}}{\partial v}\tilde{u}\right|\right| - \tilde{\theta}_{22}\left|\frac{\partial u_{\mathrm{d}}}{\partial v}\tilde{u}\right|$$

which gives

$$-\frac{\partial u_{\mathrm{d}}}{\partial v}\tilde{u}\frac{m_1}{m_2}\tau_{vd}\left(t\right) \leq \left|\hat{\theta}_{22}\frac{\partial u_{\mathrm{d}}}{\partial v}\tilde{u}\right| - \tilde{\theta}_{22}\left|\frac{\partial u_{\mathrm{d}}}{\partial v}\tilde{u}\right|. \tag{6.13}$$

Also, we can write

$$-\frac{\partial u_{\mathrm{d}}}{\partial w}\tilde{u}\frac{m_1}{m_3}\tau_{wd}\left(t\right) \leq \left|\frac{\partial u_{\mathrm{d}}}{\partial w}\tilde{u}\frac{m_1}{m_3}\tau_{wd}\left(t\right)\right| \leq \left|\frac{m_1}{m_3}\tau_{wd}\left(t\right)\right|\left|\frac{\partial u_{\mathrm{d}}}{\partial w}\tilde{u}\right|$$
$$\leq \theta_{23}\left|\frac{\partial u_{\mathrm{d}}}{\partial w}\tilde{u}\right| = \left(\hat{\theta}_{23} - \tilde{\theta}_{23}\right)\left|\frac{\partial u_{\mathrm{d}}}{\partial w}\tilde{u}\right|$$
$$\leq \hat{\theta}_{23}\left|\frac{\partial u_{\mathrm{d}}}{\partial w}\tilde{u}\right| - \tilde{\theta}_{23}\left|\frac{\partial u_{\mathrm{d}}}{\partial w}\tilde{u}\right| \leq \left|\hat{\theta}_{23}\left|\frac{\partial u_{\mathrm{d}}}{\partial w}\tilde{u}\right|\right| - \tilde{\theta}_{23}\left|\frac{\partial u_{\mathrm{d}}}{\partial w}\tilde{u}\right| \tag{6.14}$$
$$\leq \left|\hat{\theta}_{23}\frac{\partial u_{\mathrm{d}}}{\partial w}\tilde{u}\right| - \tilde{\theta}_{23}\left|\frac{\partial u_{\mathrm{d}}}{\partial w}\tilde{u}\right|$$

which implies

$$-\frac{\partial u_{\mathrm{d}}}{\partial w}\tilde{u}\frac{m_1}{m_3}\tau_{w\mathrm{d}}\left(t\right)\leq\left|\hat{\theta}_{23}\frac{\partial u_{\mathrm{d}}}{\partial w}\tilde{u}\right|-\tilde{\theta}_{23}\left|\frac{\partial u_{\mathrm{d}}}{\partial w}\tilde{u}\right|. \tag{6.15}$$

Then, by inserting the inequalities (6.11),(6.13) and (6.15) into (6.9) we obtain the following inequality

$$\begin{aligned}
\dot{V}_1 \leq &- \left(c_u + d_1\right)\tilde{u}^2 + \tilde{\boldsymbol{\theta}}_1^\top\left(\boldsymbol{\Gamma}_1^{-1}\dot{\hat{\boldsymbol{\theta}}}_1 - \mathbf{f}_1\left(\cdot\right)\tilde{u}\right) + \tilde{\theta}_{21}\gamma_{21}^{-1}\dot{\hat{\theta}}_{21}\\
&+ \tilde{\theta}_{22}\gamma_{22}^{-1}\dot{\hat{\theta}}_{22} + \tilde{\theta}_{23}\gamma_{23}^{-1}\dot{\hat{\theta}}_{23} + \left|\hat{\theta}_{21}\tilde{u}\right| - \tilde{\theta}_{21}\left|\tilde{u}\right| - \hat{\theta}_{21}\tilde{u}\tanh\left(\frac{\hat{\theta}_{21}\tilde{u}}{\epsilon_{21}}\right)\\
&+ \left|\hat{\theta}_{22}\frac{\partial u_{\mathrm{d}}}{\partial v}\tilde{u}\right| - \tilde{\theta}_{22}\left|\frac{\partial u_{\mathrm{d}}}{\partial v}\tilde{u}\right| - \hat{\theta}_{22}\frac{\partial u_{\mathrm{d}}}{\partial v}\tilde{u}\tanh\left(\frac{\hat{\theta}_{22}\frac{\partial u_{\mathrm{d}}}{\partial v}\tilde{u}}{\epsilon_{22}}\right)\\
&+ \left|\hat{\theta}_{23}\frac{\partial u_{\mathrm{d}}}{\partial w}\tilde{u}\right| - \tilde{\theta}_{23}\left|\frac{\partial u_{\mathrm{d}}}{\partial w}\tilde{u}\right| - \hat{\theta}_{23}\frac{\partial u_{\mathrm{d}}}{\partial w}\tilde{u}\tanh\left(\frac{\hat{\theta}_{23}\frac{\partial u_{\mathrm{d}}}{\partial w}\tilde{u}}{\epsilon_{23}}\right).
\end{aligned} \tag{6.16}$$

Our goal is to make the derivative of V_1 negative. To this end, we choose the estimate of $\boldsymbol{\theta}_1$ such that some terms in (6.16) are compensated. For that, we use the projection operator in the update law of the vector $\boldsymbol{\theta}_1$ as follows

$$\dot{\hat{\boldsymbol{\theta}}}_1 = \boldsymbol{\Gamma}_1\mathrm{Proj}\left(\mathbf{f}_1\left(\cdot\right)\tilde{u}, \hat{\boldsymbol{\theta}}_1\right) \Rightarrow \boldsymbol{\Gamma}_1^{-1}\dot{\hat{\boldsymbol{\theta}}}_1 = \mathrm{Proj}\left(\mathbf{f}_1\left(\cdot\right)\tilde{u}, \hat{\boldsymbol{\theta}}_1\right) \tag{6.17}$$

with $\boldsymbol{\Gamma}_1 = \mathrm{diag}\left(\gamma_{1j}\right)$ a positive gain matrix, where $j = 1, \ldots, 13$.

Thus, by replacing the relation (6.17) in (6.16) we obtain

$$\begin{aligned}
\dot{V}_1 \leq &- \left(c_u + d_1\right)\tilde{u}^2 + \tilde{\boldsymbol{\theta}}_1^\top\left(\mathrm{Proj}\left(\mathbf{f}_1\left(\cdot\right)\tilde{u}, \hat{\boldsymbol{\theta}}_1\right) - \mathbf{f}_1\left(\cdot\right)\tilde{u}\right)\\
&+ \tilde{\theta}_{21}\left(\gamma_{21}^{-1}\dot{\hat{\theta}}_{21} - \left|\tilde{u}\right|\right) + \tilde{\theta}_{22}\left(\gamma_{22}^{-1}\dot{\hat{\theta}}_{22} - \left|\frac{\partial u_{\mathrm{d}}}{\partial v}\tilde{u}\right|\right) + \tilde{\theta}_{23}\left(\gamma_{23}^{-1}\dot{\hat{\theta}}_{23} - \left|\frac{\partial u_{\mathrm{d}}}{\partial w}\tilde{u}\right|\right)\\
&+ \left|\hat{\theta}_{21}\tilde{u}\right| - \hat{\theta}_{21}\tilde{u}\tanh\left(\frac{\hat{\theta}_{21}\tilde{u}}{\epsilon_{21}}\right) + \left|\hat{\theta}_{22}\frac{\partial u_{\mathrm{d}}}{\partial v}\tilde{u}\right| - \hat{\theta}_{22}\frac{\partial u_{\mathrm{d}}}{\partial v}\tilde{u}\tanh\left(\frac{\hat{\theta}_{22}\frac{\partial u_{\mathrm{d}}}{\partial v}\tilde{u}}{\epsilon_{22}}\right)\\
&+ \left|\hat{\theta}_{23}\frac{\partial u_{\mathrm{d}}}{\partial w}\tilde{u}\right| - \hat{\theta}_{23}\frac{\partial u_{\mathrm{d}}}{\partial w}\tilde{u}\tanh\left(\frac{\hat{\theta}_{23}\frac{\partial u_{\mathrm{d}}}{\partial w}\tilde{u}}{\epsilon_{23}}\right).
\end{aligned} \tag{6.18}$$

By using the definition of the projection operator (5.118) and by utilizing relation (5.32)

the inequality (6.18) can be rewritten as

$$\dot{V}_1 \leq - \left(c_u + d_1\right) \tilde{u}^2 + \tilde{\theta}_{21} \left(\mathrm{Proj}\left(|\tilde{u}|, \hat{\theta}_{21}\right) - |\tilde{u}|\right) + \tilde{\theta}_{22} \left(\mathrm{Proj}\left(\left|\frac{\partial u_{\mathrm{d}}}{\partial v} \tilde{u}\right|, \hat{\theta}_{22}\right) - \left|\frac{\partial u_{\mathrm{d}}}{\partial v} \tilde{u}\right|\right)$$
$$+ \tilde{\theta}_{23} \left(\mathrm{Proj}\left(\left|\frac{\partial u_{\mathrm{d}}}{\partial w} \tilde{u}\right|, \hat{\theta}_{21}\right) - \left|\frac{\partial u_{\mathrm{d}}}{\partial w} \tilde{u}\right|\right) + 0.2785 \sum_{i=1}^{3} \epsilon_{2i}$$

(6.19)

where ϵ_{2i} for $i = 1, 2, 3$ are some arbitrary small positive constants.

Further, we define the update laws for $\hat{\theta}_{21}, \hat{\theta}_{22}$ and $\hat{\theta}_{23}$ as follows

$$\dot{\hat{\theta}}_{21} = \gamma_{21} \mathrm{Proj}\left(|\tilde{u}|, \hat{\theta}_{21}\right), \quad \dot{\hat{\theta}}_{22} = \gamma_{22} \mathrm{Proj}\left(\left|\tilde{u}\frac{\partial u_{\mathrm{d}}}{\partial v}\right|, \hat{\theta}_{22}\right),$$
$$\dot{\hat{\theta}}_{23} = \gamma_{23} \mathrm{Proj}\left(\left|\tilde{u}\frac{\partial u_{\mathrm{d}}}{\partial w}\right|, \hat{\theta}_{23}\right).$$

(6.20)

By placing (6.20) in (6.19) we obtain

$$\dot{V}_1 \leq - \left(c_u + d_1\right) \tilde{u}^2 + 0.2785 \sum_{i=1}^{3} \epsilon_{2i}$$

(6.21)

and adding and subtracting the terms $\frac{1}{2}\sum_{i=1}^{2} \tilde{\boldsymbol{\theta}}_i^\top \boldsymbol{\Gamma}_i^{-1} \tilde{\boldsymbol{\theta}}_i$ to the right-hand side of the relation (6.21) yields

$$\dot{V}_1 \leq - \left(c_u + d_1\right) \tilde{u}^2 + 0.2785 \sum_{i=1}^{3} \epsilon_{2i} + \frac{1}{2}\sum_{i=1}^{2} \tilde{\boldsymbol{\theta}}_i^\top \boldsymbol{\Gamma}_i^{-1} \tilde{\boldsymbol{\theta}}_i - \frac{1}{2}\sum_{i=1}^{2} \tilde{\boldsymbol{\theta}}_i^\top \boldsymbol{\Gamma}_i^{-1} \tilde{\boldsymbol{\theta}}_i.$$

(6.22)

Now, defining

$$\rho_1 = 0.2785 \sum_{i=1}^{3} \epsilon_{2i} + \frac{1}{2}\sum_{i=1}^{2} \tilde{\boldsymbol{\theta}}_i^\top \boldsymbol{\Gamma}_i^{-1} \tilde{\boldsymbol{\theta}}_i$$

(6.23)

we get

$$\dot{V}_1 \leq - \left(\left(c_u + d_1\right) \tilde{u}^2 + \frac{1}{2}\sum_{i=1}^{2} \tilde{\boldsymbol{\theta}}_i^\top \boldsymbol{\Gamma}_i^{-1} \tilde{\boldsymbol{\theta}}_i\right) + \rho_1$$
$$\leq - \left(\frac{2\left(c_u + d_1\right)}{m_1}\frac{1}{2}m_1\tilde{u}^2 + \frac{1}{2}\sum_{i=1}^{2} \tilde{\boldsymbol{\theta}}_i^\top \boldsymbol{\Gamma}_i^{-1} \tilde{\boldsymbol{\theta}}_i\right) + \rho_1.$$

(6.24)

With $\sigma_u = \min\left(1, \dfrac{2\left(c_u + d_1\right)}{m_1}\right)$ we can write the inequality (6.24) as

$$\dot{V}_1 \leq - \sigma_u V_1 + \rho_1.$$

(6.25)

In the inequality (6.25) we discuss two cases for σ_u, namely: Firstly, if $\dfrac{2\left(c_u + d_1\right)}{m_1} > 1$, thus $\sigma_u = 1$. Considering (6.6) and (6.24) we can write

$$
\begin{aligned}
&\frac{2\left(c_u + d_1\right)}{m_1}\frac{1}{2}m_1\tilde{u}^2 + \frac{1}{2}\sum_{i=1}^{2}\tilde{\boldsymbol{\theta}}_i^{\top}\boldsymbol{\Gamma}_i^{-1}\tilde{\boldsymbol{\theta}}_i \geq \frac{1}{2}m_1\tilde{u}^2 + \frac{1}{2}\sum_{i=1}^{2}\tilde{\boldsymbol{\theta}}_i^{\top}\boldsymbol{\Gamma}_i^{-1}\tilde{\boldsymbol{\theta}}_i \Leftrightarrow \\
&-\left(\frac{2\left(c_u + d_1\right)}{m_1}\frac{1}{2}m_1\tilde{u}^2 + \frac{1}{2}\sum_{i=1}^{2}\tilde{\boldsymbol{\theta}}_i^{\top}\boldsymbol{\Gamma}_i^{-1}\tilde{\boldsymbol{\theta}}_i\right) \leq -\left(\frac{1}{2}m_1\tilde{u}^2 + \frac{1}{2}\sum_{i=1}^{2}\tilde{\boldsymbol{\theta}}_i^{\top}\boldsymbol{\Gamma}_i^{-1}\tilde{\boldsymbol{\theta}}_i\right) \Leftrightarrow \quad (6.26) \\
&-\left(\frac{2\left(c_u + d_1\right)}{m_1}\frac{1}{2}m_1\tilde{u}^2 + \frac{1}{2}\sum_{i=1}^{2}\tilde{\boldsymbol{\theta}}_i^{\top}\boldsymbol{\Gamma}_i^{-1}\tilde{\boldsymbol{\theta}}_i\right) + \rho_1 \leq -V_1 + \rho_1 \Leftrightarrow
\end{aligned}
$$

$$
\dot{V}_1 \leq -V_1 + \rho_1. \tag{6.27}
$$

We can obviously find that inequality (6.27) coincides with (6.25) for $\sigma_u = 1$. Secondly, if $\dfrac{2\left(c_u + d_1\right)}{m_1} < 1$, thus $\sigma_u < 1$. By noticing (6.24), we can write

$$
\dot{V}_1 \leq -\left(\frac{1}{2}m_1\sigma_u\tilde{u}^2 + \frac{1}{2}\sum_{i=1}^{2}\tilde{\boldsymbol{\theta}}_i^{\top}\boldsymbol{\Gamma}_i^{-1}\tilde{\boldsymbol{\theta}}_i\right) + \rho_1 \leq -\sigma_u\left(\frac{1}{2}m_1\tilde{u}^2 + \frac{1}{2\sigma_u}\sum_{i=1}^{2}\tilde{\boldsymbol{\theta}}_i^{\top}\boldsymbol{\Gamma}_i^{-1}\tilde{\boldsymbol{\theta}}_i\right) + \rho_1. \tag{6.28}
$$

Because of $\dfrac{1}{\sigma_u} > 1$ it is clear that

$$
V_1 < \frac{1}{2}m_1\tilde{u}^2 + \frac{1}{2\sigma_u}\sum_{i=1}^{2}\tilde{\boldsymbol{\theta}}_i^{\top}\boldsymbol{\Gamma}_i^{-1}\tilde{\boldsymbol{\theta}}_i. \tag{6.29}
$$

Thus, from (6.25), (6.28) and (6.29) we write

$$
\dot{V}_1 \leq -\sigma_u V_1 + \rho_1 \leq -\sigma_u V_1 + \rho_1^{\max} \tag{6.30}
$$

where, $\rho_1^{\max}$ is the maximum value of ρ_1 by using the comparison principle [69]. It can directly be shown that, the solution of (6.30) is given as

$$
V_1\left(t\right) \leq V_1\left(t_0\right)e^{-\sigma_u\left(t - t_0\right)} + \frac{\rho_1^{\max}}{\sigma_u}. \tag{6.31}
$$

Obviously, from (6.6) it can be shown that

$$
\left|\tilde{u}\left(t\right)\right| \leq \sqrt{\frac{2V_1\left(t\right)}{m_1}}. \tag{6.32}
$$

Then, from (6.31) and (6.32) it follows that

$$|\tilde{u}(t)| \leq \sqrt{\frac{2V_1(t_0)}{m_1} e^{-\sigma_u(t-t_0)} + \frac{2\rho_1^{\max}}{m_1\sigma_u}} \leq \sqrt{\frac{2V_1(t_0)}{m_1}} e^{-\sigma_u(t-t_0)/2} + \sqrt{\frac{2\rho_1^{\max}}{m_1\sigma_u}}$$
$$\leq \alpha_u e^{-\sigma_u(t-t_0)/2} + \rho_u \tag{6.33}$$

with

$$\alpha_u = \sqrt{\frac{2V_1(t_0)}{m_1}} \quad \text{and} \quad \rho_u = \sqrt{\frac{2\rho_1^{\max}}{m_1\sigma_u}}. \tag{6.34}$$

Finally, from (6.33) we conclude that the error of the intermediate control $\tilde{u}$ converges globally exponentially to a line segment of length $2\rho_u$ and centered at the origin.

6.1.2 The Path Following Error d_{e}

In this subsection we will demonstrate that the path following error d_{e} stays within a bounded area and never leaves it.

6.1.2.1 Lower Bound of d_{e}

We have already seen from (5.175) that the dynamics of the path following error is given as

$$\dot{d}_{\mathrm{e}} = -k_1 \frac{a_1}{d_{\mathrm{e}}}(d_{\mathrm{e}} - \delta) - \frac{a_1}{d_{\mathrm{e}}}\tilde{u}. \tag{6.35}$$

An equilibrium point of the dynamics (6.35) is $d_{\mathrm{e}} = \delta, \tilde{u} = 0$, where δ is a small positive constant.

The equation (6.35) can be rewritten as

$$\dot{\tilde{d}}_{\mathrm{e}} = -k_1 \frac{a_1}{d_{\mathrm{e}}}\tilde{d}_{\mathrm{e}} - \frac{a_1}{d_{\mathrm{e}}}\tilde{u} \tag{6.36}$$

where $\tilde{d}_{\mathrm{e}} = d_{\mathrm{e}} - \delta$. Under the assumptions $a_1 > 0$ and $\tilde{d}_{\mathrm{e}} > 0$ which are guaranteed by the controller and through a suitable choice of the initial conditions (as it will be shown later), we can write

$$\dot{\tilde{d}}_{\mathrm{e}} = \frac{a_1}{d_{\mathrm{e}}}\left(-k_1\tilde{d}_{\mathrm{e}} - \tilde{u}\right) \Leftrightarrow \frac{d_{\mathrm{e}}}{a_1}\dot{\tilde{d}}_{\mathrm{e}} + k_1\tilde{d}_{\mathrm{e}} = -\tilde{u} \tag{6.37}$$

and because of $-\tilde{u} \geq -|\tilde{u}|$, equation (6.37) implies

$$\frac{d_\text{e}}{a_1}\dot{\tilde{d}}_\text{e} + k_1\tilde{d}_\text{e} \geq -|\tilde{u}| \Rightarrow \dot{\tilde{d}}_\text{e} \geq \frac{a_1}{d_\text{e}}\left(-k_1\tilde{d}_\text{e} - |\tilde{u}|\right) \Rightarrow \dot{\tilde{d}}_\text{e} \geq \left(-k_1\tilde{d}_\text{e} - |\tilde{u}|\right). \qquad (6.38)$$

Inserting the inequality (6.33) into (6.38) we obtain

$$\dot{\tilde{d}}_\text{e} \geq -k_1\tilde{d}_\text{e} - \left(\alpha_u\, e^{-\sigma_u(t-t_0)/2} + \rho_u\right). \qquad (6.39)$$

The solution of the linear system (6.39) satisfies

$$\begin{aligned}
\tilde{d}_\text{e}(t) &\geq e^{-k_1(t-t_0)}\tilde{d}_\text{e}(t_0) - \int_{t_0}^{t} e^{-k_1(t-\tau)}\left(\alpha_u\, e^{\frac{-\sigma_u}{2}(\tau-t_0)} + \rho_u\right)d\tau \\
&\geq e^{-k_1(t-t_0)}\tilde{d}_\text{e}(t_0) - \int_{t_0}^{t} \alpha_u e^{-k_1(t-\tau)-\frac{\sigma_u}{2}(\tau-t_0)}\,d\tau - \int_{t_0}^{t}\rho_u\, e^{-k_1(t-\tau)}\,d\tau \\
&\geq e^{-k_1(t-t_0)}\tilde{d}_\text{e}(t_0) - \frac{\alpha_u}{k_1 - \sigma_u/2}\, e^{-k_1(t-\tau)-\frac{\sigma_u}{2}(\tau-t_0)}\Big|_{t_0}^{t} - \frac{\rho_u}{k_1}\, e^{-k_1(t-\tau)}\Big|_{t_0}^{t} \\
&\geq e^{-k_1(t-t_0)}\tilde{d}_\text{e}(t_0) - \frac{\alpha_u}{k_1 - \frac{\sigma_u}{2}}\left[e^{\frac{-\sigma_u}{2}(t-t_0)} - e^{-k_1(t-t_0)}\right] - \frac{\rho_u}{k_1}\left[1 - e^{-k_1(t-t_0)}\right] \\
&\geq e^{-k_1(t-t_0)}\tilde{d}_\text{e}(t_0) + \frac{\alpha_u}{\frac{\sigma_u}{2} - k_1}\, e^{-k_1(t-t_0)}\left[-1 + e^{-\left(\frac{\sigma_u}{2}-k_1\right)(t-t_0)}\right] - \frac{\rho_u}{k_1}\left[1 - e^{-k_1(t-t_0)}\right].
\end{aligned}$$
$$(6.40)$$

For (6.40) as $t \to \infty$ the error $\tilde{d}_\text{e}$ converges to $-\dfrac{\rho_u}{k_1}$, for $k_1 > 0$ and $\sigma_u > 2k_1$. This means, ultimately we get $d_\text{e} \geq \delta - \dfrac{\rho_u}{k_1} = d_\text{e}^\star$, where $d_\text{e}^\star$ is the lower bound of d_e. This bound exists if the constant δ is chosen as $\delta > \dfrac{\rho_u}{k_1}$. Thus, we can adjust this lower bound $d_\text{e}^\star$ and make it arbitrary small by choosing the designed constant δ.

6.1.2.2 Upper Bound of d_e

To investigate the upper bound of error d_e, we insert (5.150) into (6.36)

$$\dot{\tilde{d}}_\text{e} = -k_1\left(\cos(\gamma_1) + \frac{a_\text{e}}{d_\text{e}}\cos(\theta)\left(\cos(\gamma_2) - 1\right)\right)\tilde{d}_\text{e} - \cos(\gamma)\,\tilde{u}. \qquad (6.41)$$

Adding and subtracting of one in the relation (6.41) and rearranging yields

$$\begin{aligned}
\dot{\tilde{d}}_\text{e} &= -k_1\left(\left(\cos(\gamma_1) - 1\right) + 1 + \frac{a_\text{e}}{d_\text{e}}\cos(\theta)\left(\cos(\gamma_2) - 1\right)\right)\tilde{d}_\text{e} - \cos(\gamma)\,\tilde{u} \\
&= -k_1\tilde{d}_\text{e} - \cos(\gamma)\,\tilde{u} - k_1\left(\left(\cos(\gamma_1) - 1\right) + \frac{a_\text{e}}{d_\text{e}}\cos(\theta)\left(\cos(\gamma_2) - 1\right)\right)\tilde{d}_\text{e}.
\end{aligned}$$
$$(6.42)$$

Before we study the upper bound of d_e we consider the following lemma which is introduced in [83, 85, 86].

Lemma 6.1.1 Consider the nonlinear system

$$\dot{\boldsymbol{\varsigma}} = \mathbf{f}(t, \boldsymbol{\varsigma}) + \mathbf{g}(t, \boldsymbol{\varsigma}, \boldsymbol{\xi}(t)) \tag{6.43}$$

where $\boldsymbol{\varsigma} \in \mathbb{R}^n$, $\boldsymbol{\xi}(t) \in \mathbb{R}^m$ and $\mathbf{f}(t, \boldsymbol{\varsigma})$ is piecewise continuous in t and locally Lipschitz in $\boldsymbol{\varsigma}$. If there exist positive constants r_i for $i = 1, \ldots, 4$, μ_j for $j = 1, 2$, β_0 and σ_ξ, and positive constants r_0 and ϵ_ξ. Furthermore, let be given a class-k function α_0 such that the following conditions are satisfied:

Condition 1: There exists a proper function $V(t, \boldsymbol{\varsigma})$ satisfying for all $t \geq t_0 \geq 0$ and all $\boldsymbol{\xi}$ in $\mathbb{R}^m$

$$r_1 \|\boldsymbol{\varsigma}\|^2 \leq V(t, \boldsymbol{\varsigma}) \leq r_2 \|\boldsymbol{\varsigma}\|^2, \quad \frac{\partial V(t, \boldsymbol{\varsigma})}{\partial \boldsymbol{\varsigma}} \leq r_3 \|\boldsymbol{\varsigma}\|^2,$$
$$\text{and} \quad \frac{\partial V(t, \boldsymbol{\varsigma})}{\partial t} + \frac{\partial V(t, \boldsymbol{\varsigma})}{\partial \boldsymbol{\varsigma}} \mathbf{f}(t, \boldsymbol{\varsigma}) \leq -r_4 \|\boldsymbol{\varsigma}\|^2 + r_0 \quad \text{where} \quad r_0 \geq 0. \tag{6.44}$$

Condition 2: The vector function $\mathbf{g}(t, \boldsymbol{\varsigma}, \boldsymbol{\xi}(t))$ fulfills

$$\|\mathbf{g}(t, \boldsymbol{\varsigma}, \boldsymbol{\xi}(t))\| \leq (\mu_1 + \mu_2 \|\boldsymbol{\varsigma}\|) \|\boldsymbol{\xi}(t)\|. \tag{6.45}$$

Condition 3: $\boldsymbol{\xi}(t)$ globally exponentially converges to a ball centered at the origin

$$\|\boldsymbol{\xi}(t)\| \leq \alpha_0(\|\boldsymbol{\xi}(t_0)\|) e^{-\sigma_\xi(t-t_0)} + \epsilon_\xi, \quad \forall t \geq t_0 \geq 0. \tag{6.46}$$

Condition 4: The following gain condition is satisfied

$$r_4 - \mu_2 r_3 \epsilon_\xi - \frac{\mu_1 r_3 \epsilon_\xi}{\beta_0} > 0. \tag{6.47}$$

Then the solution $\boldsymbol{\varsigma}(t)$ of (6.43) globally exponentially converges to a ball centered at the origin, i.e.

$$\|\boldsymbol{\varsigma}(t)\| \leq \alpha(\|(\boldsymbol{\varsigma}(t_0), \boldsymbol{\xi}(t_0))\|) e^{-\sigma_\varsigma(t-t_0)} + \epsilon_\varsigma, \quad \forall t \geq t_0 \geq 0. \tag{6.48}$$

We give now the complete proof for this lemma in detail.

Proof of the Lemma 6.1.1

Let the Lyapunov function candidate be V. From (6.43) the time derivative is

$$\dot{V} = \frac{\partial V}{\partial t} + \frac{\partial V}{\partial \varsigma} \left(\mathbf{f}\left(t, \varsigma\right) + \mathbf{g}\left(t, \varsigma, \boldsymbol{\xi}\left(t\right)\right) \right). \tag{6.49}$$

By using the Conditions 1 to 3 we can write

$$\begin{aligned}
\dot{V} \leq & \frac{\partial V}{\partial t} + \frac{\partial V}{\partial \varsigma} \mathbf{f}\left(t, \varsigma\right) + \frac{\partial V}{\partial \varsigma} \left\| \mathbf{g}\left(t, \varsigma, \boldsymbol{\xi}\left(t\right)\right) \right\| \\
\leq & - r_4 \left\| \varsigma \right\|^2 + r_0 + r_3 \left\| \varsigma \right\| \left(\mu_1 + \mu_2 \left\| \varsigma \right\| \right) \left\| \boldsymbol{\xi}\left(t\right) \right\| \\
\leq & - r_4 \left\| \varsigma \right\|^2 + r_0 + r_3 \left\| \varsigma \right\| \left(\mu_1 + \mu_2 \left\| \varsigma \right\| \right) \left(\alpha \left(\left\| \left(\varsigma\left(t_0\right), \boldsymbol{\xi}\left(t_0\right) \right) \right\| \right) e^{-\sigma_\xi \left(t - t_0\right)} + \epsilon_\xi \right) \\
\leq & - r_4 \left\| \varsigma \right\|^2 + r_0 + r_3 \left\| \varsigma \right\| \left(\mu_1 + \mu_2 \left\| \varsigma \right\| \right) \alpha \left(\left\| \left(\varsigma\left(t_0\right), \boldsymbol{\xi}\left(t_0\right) \right) \right\| \right) e^{-\sigma_\xi \left(t - t_0\right)} \\
& + r_3 \epsilon_\xi \mu_1 \left\| \varsigma \right\| + r_3 \epsilon_\xi \mu_2 \left\| \varsigma \right\|^2.
\end{aligned} \tag{6.50}$$

Now, we consider the term $r_3 \epsilon_\xi \mu_1 \left\| \varsigma \right\|$ in the last line of relationships (6.50)

$$r_3 \epsilon_\xi \mu_1 \left\| \varsigma \right\| = r_3 \epsilon_\xi \mu_1 \left(\left\| \varsigma \right\| \right) \leq r_3 \epsilon_\xi \mu_1 \left(\beta_0 + \frac{1}{\beta_0} \left\| \varsigma \right\|^2 \right) \tag{6.51}$$

where we obtained the relationship (6.51) by applying Young's inequality for an arbitrary positive constant $\beta_0 > 0$ [68].

Now, we put (6.51) into the last inequality of the (6.50) we get

$$\begin{aligned}
\dot{V} \leq & - r_4 \left\| \varsigma \right\|^2 + r_0 + r_3 \left\| \varsigma \right\| \left(\mu_1 + \mu_2 \left\| \varsigma \right\| \right) \alpha \left(\left\| \left(\varsigma\left(t_0\right), \boldsymbol{\xi}\left(t_0\right) \right) \right\| \right) e^{-\sigma_\xi \left(t - t_0\right)} + r_3 \epsilon_\xi \mu_1 \beta_0 \\
& + \frac{r_3 \epsilon_\xi \mu_1}{\beta_0} \left\| \varsigma \right\|^2 + r_3 \epsilon_\xi \mu_2 \left\| \varsigma \right\|^2
\end{aligned} \tag{6.52}$$

or also

$$\begin{aligned}
\dot{V} \leq & - \left(r_4 - r_3 \epsilon_\xi \mu_2 - \frac{r_3 \epsilon_\xi \mu_1}{\beta_0} \right) \left\| \varsigma \right\|^2 + r_3 \left\| \varsigma \right\| \left(\mu_1 + \mu_2 \left\| \varsigma \right\| \right) \alpha \left(\left\| \left(\varsigma\left(t_0\right), \boldsymbol{\xi}\left(t_0\right) \right) \right\| \right) e^{-\sigma_\xi \left(t - t_0\right)} \\
& + r_3 \epsilon_\xi \mu_1 \beta_0 + r_0.
\end{aligned} \tag{6.53}$$

Now, using the above mentioned four conditions, we try to write the right-hand side of the inequality (6.53) as a function of V. To this end, we consider the term

$$r_3 \left\| \varsigma \right\| \left(\mu_1 + \mu_2 \left\| \varsigma \right\| \right) \alpha \left(\left\| \left(\varsigma\left(t_0\right), \boldsymbol{\xi}\left(t_0\right) \right) \right\| \right) e^{-\sigma_\xi \left(t - t_0\right)}, \tag{6.54}$$

by using $\bar{\alpha} \equiv \alpha \left(\left\| \left(\boldsymbol{\varsigma}\left(t_0\right), \boldsymbol{\xi}\left(t_0\right)\right) \right\| \right)$ to be more compact we may write (6.54) using Young's inequality again (we choose here the positive constant $\beta_0 = 1$) as per

$$
\begin{aligned}
r_3 \left\| \boldsymbol{\varsigma} \right\| \left(\mu_1 + \mu_2 \left\| \boldsymbol{\varsigma} \right\| \right) \bar{\alpha} \, e^{-\sigma_\xi (t-t_0)} &= \left(r_3 \mu_1 \left\| \boldsymbol{\varsigma} \right\| + r_3 \mu_2 \left\| \boldsymbol{\varsigma} \right\|^2 \right) \bar{\alpha} \, e^{-\sigma_\xi (t-t_0)} \\
&\leq \left(r_3 \mu_1 \left(1 + \left\| \boldsymbol{\varsigma} \right\|^2 \right) + r_3 \mu_2 \left\| \boldsymbol{\varsigma} \right\|^2 \right) \bar{\alpha} \, e^{-\sigma_\xi (t-t_0)} \quad (6.55) \\
&\leq \left(r_3 \mu_1 + r_3 \left(\mu_1 + \mu_2 \right) \left\| \boldsymbol{\varsigma} \right\|^2 \right) \bar{\alpha} \, e^{-\sigma_\xi (t-t_0)}.
\end{aligned}
$$

Noticing Condition 1, i.e. $\left\| \boldsymbol{\varsigma} \right\|^2 \leq V/r_1$, this inequality may be placed into the relationship (6.55) which yields

$$
r_3 \left\| \boldsymbol{\varsigma} \right\| \left(\mu_1 + \mu_2 \left\| \boldsymbol{\varsigma} \right\| \right) \bar{\alpha} \, e^{-\sigma_\xi (t-t_0)} \leq r_3 \mu_1 \bar{\alpha} \, e^{-\sigma_\xi (t-t_0)} + \frac{r_3}{r_1} \left(\mu_1 + \mu_2 \right) V \bar{\alpha} \, e^{-\sigma_\xi (t-t_0)}. \quad (6.56)
$$

Again, from Condition 1 we may write

$$
V \leq r_2 \left\| \boldsymbol{\varsigma} \right\|^2 \Rightarrow - \left\| \boldsymbol{\varsigma} \right\|^2 \leq - \frac{V}{r_2}. \quad (6.57)
$$

By using the two inequalities (6.56) and (6.57) in (6.53) we get the time derivative of V as follows

$$
\begin{aligned}
\dot{V} \leq &- \frac{1}{r_2} \left(r_4 - r_3 \epsilon_\xi \mu_2 - \frac{r_3 \epsilon_\xi \mu_1}{\beta_0} \right) V + \frac{r_3}{r_1} \left(\mu_1 + \mu_2 \right) V \bar{\alpha} \, e^{-\sigma_\xi (t-t_0)} \\
&+ r_3 \mu_1 \bar{\alpha} \, e^{-\sigma_\xi (t-t_0)} + r_3 \epsilon_\xi \mu_1 \beta_0 + r_0.
\end{aligned} \quad (6.58)
$$

Rearranging (6.58) yields

$$
\begin{aligned}
\dot{V} \leq &- \left[\frac{1}{r_2} \left(r_4 - r_3 \epsilon_\xi \mu_2 - \frac{r_3 \epsilon_\xi \mu_1}{\beta_0} \right) - \frac{r_3}{r_1} \left(\mu_1 + \mu_2 \right) \bar{\alpha} \, e^{-\sigma_\xi (t-t_0)} \right] V \\
&+ r_3 \mu_1 \bar{\alpha} \, e^{-\sigma_\xi (t-t_0)} + r_3 \epsilon_\xi \mu_1 \beta_0 + r_0.
\end{aligned} \quad (6.59)
$$

Define

$$
\delta_1 = \frac{1}{r_2} \left(r_4 - r_3 \epsilon_\xi \mu_2 - \frac{r_3 \epsilon_\xi \mu_1}{\beta_0} \right), \quad \delta_2 = \frac{r_3}{r_1} \left(\mu_1 + \mu_2 \right) \bar{\alpha}, \quad \delta_3 = r_3 \mu_1 \bar{\alpha},
$$
$$
\delta_4 = r_3 \epsilon_\xi \mu_1 \beta_0 + r_0 \quad (6.60)
$$

and such that we have

$$
\dot{V} \leq - \left(\delta_1 - \delta_2 \, e^{-\sigma_\xi (t-t_0)} \right) V + \delta_3 \, e^{-\sigma_\xi (t-t_0)} + \delta_4. \quad (6.61)
$$

At this point let us consider the following differential equation associated to (6.61)

$$\dot{h} = -\left(\delta_1 - \delta_2\, e^{-\sigma_\xi(t-t_0)}\right) h + \delta_3\, e^{-\sigma_\xi(t-t_0)} + \delta_4. \tag{6.62}$$

By change of variable $b = h - \dfrac{\delta_4}{\delta_1} \Rightarrow \dot{b} = \dot{h}$ differential equation (6.62) can be rewritten as

$$\dot{b} = -\left(\delta_1 - \delta_2\, e^{-\sigma_\xi(t-t_0)}\right)\left(b + \frac{\delta_4}{\delta_1}\right) + \delta_3\, e^{-\sigma_\xi(t-t_0)} + \delta_4$$

$$= -\left(\delta_1 - \delta_2\, e^{-\sigma_\xi(t-t_0)}\right) b - \left(\delta_1 - \delta_2\, e^{-\sigma_\xi(t-t_0)}\right)\frac{\delta_4}{\delta_1} + \delta_3\, e^{-\sigma_\xi(t-t_0)} + \delta_4 \quad \Leftrightarrow \tag{6.63}$$

$$\dot{b} = -\left(\delta_1 - \delta_2\, e^{-\sigma_\xi(t-t_0)}\right) b + \left(\delta_3 + \frac{\delta_2\delta_4}{\delta_1}\right) e^{-\sigma_\xi(t-t_0)}. \tag{6.64}$$

The solution of the linear differential equation (6.64) is

$$b(t) = \Phi(t,t_0)\, b(t_0) + \left(\delta_3 + \frac{\delta_2\delta_4}{\delta_1}\right) \int_{t_0}^{t} \Phi(t,\tau)\, e^{-\sigma_\xi(\tau-t_0)} \mathrm{d}\tau \tag{6.65}$$

with $\Phi(t,t_0)\, b(t_0)$, the transition matrix which here reads

$$\Phi(t,t_0) = e^{-\int_{t_0}^{t}\left(\delta_1 - \delta_2\, e^{-\sigma_\xi(\tau-t_0)}\right)\mathrm{d}\tau} = e^{-\int_{t_0}^{t}\delta_1 \mathrm{d}\tau}\, e^{\int_{t_0}^{t}\left(\delta_2\, e^{-\sigma_\xi(\tau-t_0)}\right)\mathrm{d}\tau}$$

$$= e^{-\delta_1(t-t_0)}\, e^{\frac{\delta_2}{\sigma_\xi}\left(1-e^{-\sigma_\xi(t-t_0)}\right)} \tag{6.66}$$

thus, also

$$\Phi(t,\tau) = e^{-\delta_1(t-\tau)}\, e^{\frac{\delta_2}{\sigma_\xi}\left(1-e^{-\sigma_\xi(t-\tau)}\right)}. \tag{6.67}$$

The solution is

$$b(t) = e^{-\delta_1(t-t_0)}\, e^{\frac{\delta_2}{\sigma_\xi}\left(1-e^{-\sigma_\xi(t-t_0)}\right)} b(t_0)$$

$$+ \left(\delta_3 + \frac{\delta_2\delta_4}{\delta_1}\right) \int_{t_0}^{t} \left(e^{-\delta_1(t-\tau)}\, e^{\frac{\delta_2}{\sigma_\xi}\left(1-e^{-\sigma_\xi(t-\tau)}\right)}\right) e^{-\sigma_\xi(\tau-t_0)} \mathrm{d}\tau \tag{6.68}$$

$$= e^{-\delta_1(t-t_0)}\, e^{\frac{\delta_2}{\sigma_\xi}\left(1-e^{-\sigma_\xi(t-t_0)}\right)} b(t_0) + \left(\delta_3 + \frac{\delta_2\delta_4}{\delta_1}\right) e^{-\delta_1 t + \sigma_\xi t_0}\, e^{\frac{\delta_2}{\sigma_\xi}}$$

$$\times \int_{t_0}^{t} e^{(\delta_1-\sigma_\xi)\tau}\, e^{-\frac{\delta_2}{\sigma_\xi} e^{-\sigma_\xi(t-\tau)}} \mathrm{d}\tau. \tag{6.69}$$

This implies

$$b\left(t\right) \leq e^{-\delta_1(t-t_0)}e^{\frac{\delta_2}{\sigma_\xi}\left(1-e^{-\sigma_\xi(t-t_0)}\right)}b\left(t_0\right) + \left(\delta_3 + \frac{\delta_2\delta_4}{\delta_1}\right)e^{-\delta_1 t + \sigma_\xi t_0}e^{\frac{\delta_2}{\sigma_\xi}}\int_{t_0}^t e^{(\delta_1-\sigma_\xi)\tau}\mathrm{d}\tau$$
(6.70)

and by (6.70) we have for the solution of (6.62) that

$$h\left(t\right) \leq e^{-\delta_1(t-t_0)}e^{\frac{\delta_2}{\sigma_\xi}\left(1-e^{-\sigma_\xi(t-t_0)}\right)}\left(h\left(t_0\right) - \frac{\delta_4}{\delta_1}\right) + \left(\delta_3 + \frac{\delta_2\delta_4}{\delta_1}\right)e^{-\delta_1 t + \sigma_\xi t_0}e^{\frac{\delta_2}{\sigma_\xi}}\int_{t_0}^t e^{(\delta_1-\sigma_\xi)\tau}\mathrm{d}\tau$$
$$+ \frac{\delta_4}{\delta_1}$$
$$\leq e^{-\delta_1(t-t_0)}e^{\frac{\delta_2}{\sigma_\xi}\left(1-e^{-\sigma_\xi(t-t_0)}\right)}h\left(t_0\right) + \left(\delta_3 + \frac{\delta_2\delta_4}{\delta_1}\right)e^{-\delta_1 t + \sigma_\xi t_0}e^{\frac{\delta_2}{\sigma_\xi}}\int_{t_0}^t e^{(\delta_1-\sigma_\xi)\tau}\mathrm{d}\tau + \frac{\delta_4}{\delta_1}.$$
(6.71)

Since $e^{-\sigma_\xi(t-t_0)} \leq 1$ we see that $e^{\frac{\delta_2}{\sigma_\xi}\left(1-e^{-\sigma_\xi(t-t_0)}\right)} \leq e^{\frac{\delta_2}{\sigma_\xi}}$ and the solution $h\left(t\right)$ can be written as

$$h\left(t\right) \leq e^{-\delta_1(t-t_0)}e^{\frac{\delta_2}{\sigma_\xi}}h\left(t_0\right) + \left(\delta_3 + \frac{\delta_2\delta_4}{\delta_1}\right)e^{-\delta_1 t + \sigma_\xi t_0}e^{\frac{\delta_2}{\sigma_\xi}}\int_{t_0}^t e^{(\delta_1-\sigma_\xi)\tau}\mathrm{d}\tau + \frac{\delta_4}{\delta_1}. \qquad (6.72)$$

By applying the comparison principle in [69], we have

$$V\left(t\right) \leq V\left(t_0\right)e^{\frac{\delta_2}{\sigma_\xi}}e^{-\delta_1(t-t_0)} + \left(\delta_3 + \frac{\delta_2\delta_4}{\delta_1}\right)e^{-\delta_1 t + \sigma_\xi t_0}e^{\frac{\delta_2}{\sigma_\xi}}\int_{t_0}^t e^{(\delta_1-\sigma_\xi)\tau}\mathrm{d}\tau + \frac{\delta_4}{\delta_1}. \qquad (6.73)$$

Consequently, we discuss the inequality (6.73) in two cases:

Firstly, for $\delta_1 = \sigma_\xi$ relationship (6.73) yields

$$V\left(t\right) \leq V\left(t_0\right)e^{\frac{\delta_2}{\sigma_\xi}}e^{-\delta_1(t-t_0)} + \left(\delta_3 + \frac{\delta_2\delta_4}{\delta_1}\right)e^{\frac{\delta_2}{\sigma_\xi}}e^{-\delta_1(t-t_0)}\int_{t_0}^t \mathrm{d}\tau + \frac{\delta_4}{\delta_1}$$
$$\leq V\left(t_0\right)e^{\frac{\delta_2}{\sigma_\xi}}e^{-\delta_1(t-t_0)} + \left(\delta_3 + \frac{\delta_2\delta_4}{\delta_1}\right)e^{\frac{\delta_2}{\sigma_\xi}}e^{-\delta_1(t-t_0)}\left(t - t_0\right) + \frac{\delta_4}{\delta_1}$$
(6.74)

which by adding and subtracting a positive constant c to constant δ_1 in (6.74) results in

$$V\left(t\right) \leq V\left(t_0\right)e^{\frac{\delta_2}{\sigma_\xi}}e^{-\delta_1(t-t_0)} + \left(\delta_3 + \frac{\delta_2\delta_4}{\delta_1}\right)e^{\frac{\delta_2}{\sigma_\xi}}e^{-(\delta_1-c)(t-t_0)}\left(t - t_0\right)e^{-c(t-t_0)} + \frac{\delta_4}{\delta_1}.$$
(6.75)

Now, inspecting function $(t - t_0) e^{-c(t-t_0)}$ we notice that this function has always an upper bound. Let this upper bound be a, i.e.

$$(t - t_0) e^{-c(t-t_0)} \leq a. \tag{6.76}$$

Clearly, for $\delta_1, c > 0$, we have $\delta_1 > \delta_1 - c$ and consequently

$$e^{-\delta_1(t-t_0)} \leq e^{-(\delta_1-c)(t-t_0)}. \tag{6.77}$$

Inserting inequalities (6.76) and (6.77) into (6.75) we get

$$
\begin{aligned}
V(t) &\leq V(t_0) e^{\frac{\delta_2}{\sigma_\xi}} e^{-(\delta_1-c)(t-t_0)} + \left(\delta_3 + \frac{\delta_2\delta_4}{\delta_1}\right) e^{\frac{\delta_2}{\sigma_\xi}} e^{-(\delta_1-c)(t-t_0)} a + \frac{\delta_4}{\delta_1} \\
&\leq \left[V(t_0) e^{\frac{\delta_2}{\sigma_\xi}} + \left(\delta_3 + \frac{\delta_2\delta_4}{\delta_1}\right) e^{\frac{\delta_2}{\sigma_\xi}} a\right] e^{-(\delta_1-c)(t-t_0)} + \frac{\delta_4}{\delta_1}.
\end{aligned}
\tag{6.78}
$$

Thus, considering Condition 1 and using inequality (6.78) we have

$$r_1 \|\varsigma(t)\|^2 \leq \left[r_2 \|\varsigma(t_0)\|^2 e^{\frac{\delta_2}{\sigma_\xi}} + \left(\delta_3 + \frac{\delta_2\delta_4}{\delta_1}\right) e^{\frac{\delta_2}{\sigma_\xi}} a\right] e^{-(\delta_1-c)(t-t_0)} + \frac{\delta_4}{\delta_1}. \tag{6.79}$$

It can readily seen that

$$\|\varsigma(t)\| \leq \sqrt{(r_1)^{-1} \left[r_2 \|\varsigma(t_0)\|^2 e^{\frac{\delta_2}{\sigma_\xi}} + \left(\delta_3 + \frac{\delta_2\delta_4}{\delta_1}\right) e^{\frac{\delta_2}{\sigma_\xi}} a\right]} e^{-\frac{(\delta_1-c)}{2}(t-t_0)} + \sqrt{\frac{\delta_4}{r_1\delta_1}}. \tag{6.80}$$

By comparing inequality (6.48) with (6.80) it is clear that

$$
\begin{aligned}
\alpha\left(\|(\varsigma(t_0), \boldsymbol{\xi}(t_0))\|\right) &= \sqrt{(r_1)^{-1} \left[r_2 \|\varsigma(t_0)\|^2 e^{\frac{\delta_2}{\sigma_\xi}} + \left(\delta_3 + \frac{\delta_2\delta_4}{\delta_1}\right) e^{\frac{\delta_2}{\sigma_\xi}} a\right]}, \\
\sigma_\varsigma &= \frac{\delta_1 - c}{2} \text{ and } \epsilon_\varsigma = \sqrt{\frac{\delta_4}{r_1\delta_1}}.
\end{aligned}
\tag{6.81}
$$

Secondly, we discuss the general case, but for $\delta_1 \neq \sigma_\xi$. Returning to inequality (6.73) we may write

$$
\begin{aligned}
V(t) &\leq V(t_0) e^{\frac{\delta_2}{\sigma_\xi}} e^{-\delta_1(t-t_0)} + \left(\delta_3 + \frac{\delta_2\delta_4}{\delta_1}\right) e^{-\delta_1 t + \sigma_\xi t_0} e^{\frac{\delta_2}{\sigma_\xi}} \int_{t_0}^t e^{(\delta_1 - \sigma_\xi)\tau} d\tau + \frac{\delta_4}{\delta_1} \\
&\leq V(t_0) e^{\frac{\delta_2}{\sigma_\xi}} e^{-\delta_1(t-t_0)} + \frac{1}{\delta_1 - \sigma_\xi} \left(\delta_3 + \frac{\delta_2\delta_4}{\delta_1}\right) e^{-\delta_1 t + \sigma_\xi t_0} e^{\frac{\delta_2}{\sigma_\xi}} \left[e^{(\delta_1 - \sigma_\xi)t} - e^{(\delta_1 - \sigma_\xi)t_0} \right] \\
&\quad + \frac{\delta_4}{\delta_1}
\end{aligned}
\tag{6.82}
$$

thus,

$$
V(t) \leq V(t_0) e^{\frac{\delta_2}{\sigma_\xi}} e^{-\delta_1(t-t_0)} + \frac{1}{\delta_1 - \sigma_\xi} \left(\delta_3 + \frac{\delta_2\delta_4}{\delta_1}\right) e^{\frac{\delta_2}{\sigma_\xi}} \left[e^{-\sigma_\xi(t-t_0)} - e^{-\delta_1(t-t_0)} \right] + \frac{\delta_4}{\delta_1}
\tag{6.83}
$$

and since $e^{-\delta_1(t-t_0)} > 0$ we obtain

$$
V(t) \leq V(t_0) e^{\frac{\delta_2}{\sigma_\xi}} e^{-\delta_1(t-t_0)} + \frac{1}{\delta_1 - \sigma_\xi} \left(\delta_3 + \frac{\delta_2\delta_4}{\delta_1}\right) e^{\frac{\delta_2}{\sigma_\xi}} e^{-\sigma_\xi(t-t_0)} + \frac{\delta_4}{\delta_1}.
\tag{6.84}
$$

For the worst case inequality (6.84) can be rewritten as

$$
V(t) \leq V(t_0) e^{\frac{\delta_2}{\sigma_\xi}} e^{-\delta_1(t-t_0)} + \left|\frac{1}{\delta_1 - \sigma_\xi}\right| \left(\delta_3 + \frac{\delta_2\delta_4}{\delta_1}\right) e^{\frac{\delta_2}{\sigma_\xi}} e^{-\sigma_\xi(t-t_0)} + \frac{\delta_4}{\delta_1}
\tag{6.85}
$$

with $\beta^\star = \min(\sigma_\xi, \delta_1)$ we can write

$$
V(t) \leq \left[V(t_0) e^{\frac{\delta_2}{\sigma_\xi}} + \left|\frac{1}{\delta_1 - \sigma_\xi}\right| \left(\delta_3 + \frac{\delta_2\delta_4}{\delta_1}\right) e^{\frac{\delta_2}{\sigma_\xi}} \right] e^{-\beta^\star(t-t_0)} + \frac{\delta_4}{\delta_1}.
\tag{6.86}
$$

Again from Condition 1 we then obtain

$$
r_1 \|\varsigma(t)\|^2 \leq \left[r_2 \|\varsigma(t_0)\|^2 e^{\frac{\delta_2}{\sigma_\xi}} + \left|\frac{1}{\delta_1 - \sigma_\xi}\right| \left(\delta_3 + \frac{\delta_2\delta_4}{\delta_1}\right) e^{\frac{\delta_2}{\sigma_\xi}} \right] e^{-\beta^\star(t-t_0)} + \frac{\delta_4}{\delta_1}.
\tag{6.87}
$$

Clearly,

$$
\|\varsigma(t)\| \leq \sqrt{(r_1)^{-1} \left[r_2 \|\varsigma(t_0)\|^2 e^{\frac{\delta_2}{\sigma_\xi}} + \left|\frac{1}{\delta_1 - \sigma_\xi}\right| \left(\delta_3 + \frac{\delta_2\delta_4}{\delta_1}\right) \right]} e^{-\frac{\beta^\star}{2}(t-t_0)} + \sqrt{\frac{\delta_4}{r_1\delta_1}}
\tag{6.88}
$$

and by comparing inequality (6.48) with (6.80) we get

$$\alpha\left(\|(\boldsymbol{\varsigma}\left(t_0\right),\boldsymbol{\xi}\left(t_0\right))\|\right) = \sqrt{(r_1)^{-1}\left[r_2\left\|\boldsymbol{\varsigma}\left(t_0\right)\right\|^2 e^{\frac{\delta_2}{\sigma_\xi}} + \left|\frac{1}{\delta_1 - \sigma_\xi}\right|\left(\delta_3 + \frac{\delta_2\delta_4}{\delta_1}\right)\right]} \tag{6.89}$$

where $\sigma_\varsigma = \beta^\star/2$ and $\epsilon_\varsigma = \sqrt{\delta_4/r_1\delta_1}$. This completes the proof of Lemma 6.1.1. $\square$

Now, to determine the upper bound of $\tilde{d}_e$ we apply Lemma 6.1.1 for our nonlinear system (6.42) and verify the Conditions 1 to 4. Before that we need to provide the functions $\mathbf{f}(\tilde{d}_e)$ and $\mathbf{g}(\tilde{d}_e, \boldsymbol{\xi}\left(t\right))$ which are scalars in Lemma 6.1.1, based on the relationship (6.42). By comparing the relations (6.42) and (6.43) we obtain

$$f(\tilde{d}_e) = -k_1\tilde{d}_e$$
$$g(\tilde{d}_e, \boldsymbol{\xi}) = -\cos\left(\gamma\right)\tilde{u} - k_1\left(\left(\cos\left(\gamma_1\right) - 1\right) + \frac{a_e}{d_e}\cos\left(\theta\right)\left(\cos\left(\gamma_2\right) - 1\right)\right)\tilde{d}_e \tag{6.90}$$

where $\boldsymbol{\xi} = (\gamma_1, \gamma_2, \tilde{u})^\top$. Here it is reasonable to notice in (6.90) that the variables a_e and γ also are functions of γ_1, γ_2 and $\tilde{d}_e$.

Verification of Condition 1: To verify this condition, we take function $V = \frac{1}{2}\tilde{d}_e^2$. It holds

$$r_1\left|\tilde{d}_e\right|^2 \leq V \leq r_2\left|\tilde{d}_e\right|^2, \quad \frac{\partial V}{\partial\tilde{d}_e} \leq r_3\left|\tilde{d}_e\right|^2, \quad \frac{\partial V}{\partial\tilde{d}_e}f(\tilde{d}_e) \leq -r_4\left|\tilde{d}_e\right|^2 + r_0 \tag{6.91}$$

i.e. the first condition is fulfilled for

$$r_1 = r_2 = 0.5, \quad r_3 = 1, \quad r_4 = k_1, \quad r_0 = 0. \tag{6.92}$$

Verification of Condition 2: Taking into account that the functions $f(\tilde{d}_e), g(\tilde{d}_e, \boldsymbol{\xi})$ and the variable $\tilde{d}_e$ are all scalars, from the second equation of (6.90) we get

$$\left|g(\tilde{d}_e, \boldsymbol{\xi})\right| \leq \left|-\cos\left(\gamma\right)\tilde{u}\right| + |k_1|\left(\left|\cos\left(\gamma_1\right) - 1\right| + \left|\frac{a_e}{d_e}\cos\left(\theta\right)\right|\left|\cos\left(\gamma_2\right) - 1\right|\right)\left|\tilde{d}_e\right| \tag{6.93}$$

and since $\left|\dfrac{a_e}{d_e}\cos\left(\theta\right)\right| \leq 1$ we may write

$$\left|g(\tilde{d}_e, \boldsymbol{\xi})\right| \leq \left|\cos\left(\gamma\right)\right|\left|\tilde{u}\right| + k_1\left(\left|\cos\left(\gamma_1\right) - 1\right| + \left|\cos\left(\gamma_2\right) - 1\right|\right)\left|\tilde{d}_e\right|. \tag{6.94}$$

Noticing that $|\cos(\gamma)| \le 1$, $|\cos(\gamma_1) - 1| \le \gamma_1$, for $\gamma_1 \ge 0$ and $|\cos(\gamma_2) - 1| \le \gamma_2$, for $\gamma_2 \ge 0$, inequality (6.94) leads to

$$\left| g(\tilde{d}_{\rm e}, \boldsymbol{\xi}) \right| \le |\tilde{u}| + k_1 \left(|\gamma_1| + |\gamma_2| \right) \left| \tilde{d}_{\rm e} \right|. \tag{6.95}$$

It is clear that $|\gamma_1|, |\gamma_2|, |\tilde{u}| \le \|\boldsymbol{\xi}\|$, hence

$$\begin{aligned} \left| g(\tilde{d}_{\rm e}, \boldsymbol{\xi}) \right| &\le \|\boldsymbol{\xi}\| + k_1 \left(\|\boldsymbol{\xi}\| + \|\boldsymbol{\xi}\| \right) \left| \tilde{d}_{\rm e} \right| \\ &\le \left(1 + 2k_1 \left| \tilde{d}_{\rm e} \right| \right) \|\boldsymbol{\xi}\|. \end{aligned} \tag{6.96}$$

Inspecting (6.96) we see that the third condition of Lemma 6.1.1 is fulfilled for

$$\mu_1 = 1, \quad \mu_2 = 2k_1. \tag{6.97}$$

Verification of Condition 3: Note that

$$\begin{aligned} \|\boldsymbol{\xi}\| &= \sqrt[p]{|\gamma_1|^p + |\gamma_2|^p + |\tilde{u}|^p}, \quad p \ge 0 \\ &\le |\gamma_1| + |\gamma_2| + |\tilde{u}| \end{aligned} \tag{6.98}$$

for $\boldsymbol{\eta}_\gamma = (\phi, \gamma_1, \gamma_2)^\top$ and inequality (6.98) may be written as

$$\|\boldsymbol{\xi}\| \le 2 \left\| \boldsymbol{\eta}_\gamma \right\| + |\tilde{u}|. \tag{6.99}$$

On the other hand, it is not difficult to realize from (6.33) as well as form (6.146) that this inequality can be expressed as

$$\begin{aligned} \|\boldsymbol{\xi}\| &\le 2 \left(\alpha_\eta \, e^{-\sigma_v(t-t_0)/2} + \rho_\eta \right) + \alpha_u \, e^{-\sigma_u(t-t_0)/2} + \rho_u \\ &\le 2\alpha_\eta \, e^{-\sigma_v(t-t_0)/2} + \alpha_u \, e^{-\sigma_u(t-t_0)/2} + 2\rho_\eta + \rho_u \\ &\le \bar{\alpha}_0 \, e^{-\sigma_\xi(t-t_0)} + \epsilon_\xi \end{aligned} \tag{6.100}$$

where

$$\bar{\alpha}_0 = \max\left(2\alpha_\eta, \alpha_u \right), \quad \sigma_\xi = \min\left(\sigma_v/2, \sigma_u/2 \right), \quad \epsilon_\xi = \max\left(2\rho_\eta, \rho_u \right) \tag{6.101}$$

which satisfies the third condition of Lemma 6.1.1.

This means that $\boldsymbol{\xi}(t)$ is globally exponentially converging to a ball centered at the origin, with radius ϵ_ξ. Further, we can render this radius arbitrary small.

Verification of Condition 4: To verify this condition, we place the relationships (6.92), (6.97) and (6.101) into (6.47) and we obtain

$$k_1 - 2k_1 \max\left(2\rho_\eta, \rho_u\right) - \frac{\max\left(2\rho_\eta, \rho_u\right)}{\beta_0} > 0. \tag{6.102}$$

This inequality is satisfied for $k_1, \beta_0 > 0$ if we choose $\max\left(2\rho_\eta, \rho_u\right)$ small enough. This is always guaranteed in turn by noting the relations $(6.23), (6.34)$ and (5.164).

Now, we have verified all conditions of Lemma 6.1.1 based on the dynamics (6.42). Thus, we may use the result of this lemma (6.48), which is

$$\left|\tilde{d_e}\right| \leq \alpha_d \, e^{-\sigma_d(t-t_0)} + \epsilon_d \tag{6.103}$$

where α_d, σ_d and ϵ_d are calculated from the relations (6.81) or (6.89) in Lemma 6.1.1.

Figure 6.1 illustrates the lower bound (6.40) and the upper bound (6.103) of the error d_e. The area between upper and lower bound gets smaller (narrower) with time, that means, this area can be made arbitrarily small. The error d_e goes to a small corridor as t goes to infinity.

For very small d_e the real vehicle is very close to the virtual one, which moves along the reference path with the reference velocity. This means that the real vehicle moves according to the reference velocity along the desired path. In other words, if d_e is very small, the virtual vehicle does not wait for the real one and they both move according to the reference velocity with a small delay d_e/u_0 where u_0 is the reference velocity.
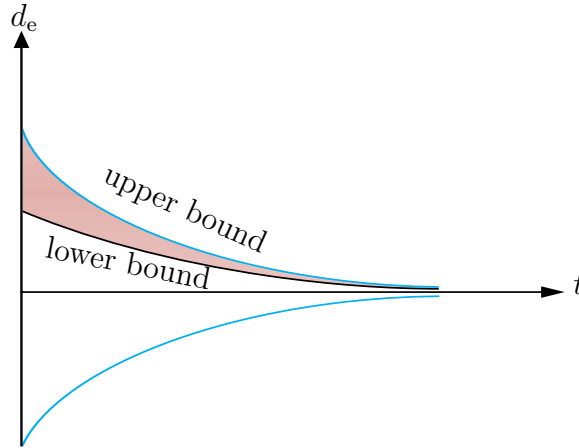
Fig. 6.1: Lower and upper bound of d_e

6.2 Stability of the Fully-Actuated Dynamics

To investigate the stability of the fully-actuated system $\left(\boldsymbol{\eta}_\gamma, \tilde{\mathbf{v}}_2\right)$, we define Lyapunov function candidate as

$$V_2 = \frac{1}{2}\boldsymbol{\eta}_\gamma^\top \boldsymbol{\eta}_\gamma + \frac{1}{2}\tilde{\mathbf{v}}_2^\top \mathbf{M}_2 \tilde{\mathbf{v}}_2 + \frac{1}{2}\tilde{\boldsymbol{\theta}}_3^\top \boldsymbol{\Gamma}_3^{-1}\tilde{\boldsymbol{\theta}}_3 + \frac{1}{2}\tilde{\boldsymbol{\theta}}_4^\top \boldsymbol{\Gamma}_4^{-1}\tilde{\boldsymbol{\theta}}_4 \tag{6.104}$$

with $\tilde{\boldsymbol{\theta}}_i = \hat{\boldsymbol{\theta}}_i - \boldsymbol{\theta}_i$ for $i = 3, 4$ where $\hat{\boldsymbol{\theta}}_i$ is the estimate of the constant value $\boldsymbol{\theta}_i$. Thus, time derivative of the suggested Lyapunov function is

$$\dot{V}_2 = \boldsymbol{\eta}_\gamma^\top \dot{\boldsymbol{\eta}}_\gamma + \tilde{\mathbf{v}}_2^\top \mathbf{M}_2 \dot{\tilde{\mathbf{v}}}_2 + \tilde{\boldsymbol{\theta}}_3^\top \boldsymbol{\Gamma}_3^{-1}\dot{\hat{\boldsymbol{\theta}}}_3 + \tilde{\boldsymbol{\theta}}_4^\top \boldsymbol{\Gamma}_4^{-1}\dot{\hat{\boldsymbol{\theta}}}_4. \tag{6.105}$$

By inserting (5.195), (5.199) and (5.202) into (6.105) we obtain

$$\dot{V}_2 = \boldsymbol{\eta}_\gamma^\top \left(-\mathbf{K}_2 \boldsymbol{\eta}_\gamma + \mathbf{J}_2\left(\boldsymbol{\eta}_2\right)\tilde{\mathbf{v}}_2\right) + \tilde{\mathbf{v}}_2^\top \left[-\mathbf{C}_2\left(\mathbf{v}_2\right)\tilde{\mathbf{v}}_2 - \left(\mathbf{K}_3 + \mathbf{D}_2\left(\mathbf{v}_2\right)\right)\tilde{\mathbf{v}}_2 - \left(\boldsymbol{\eta}_\gamma^\top \mathbf{J}_2\left(\boldsymbol{\eta}_2\right)\right)^\top \right.$$
$$\left. + \mathbf{F}\left(\cdot\right)\boldsymbol{\theta}_3 + \mathbf{G}\left(\cdot\right)\boldsymbol{\theta}_4\left(t\right) - \mathbf{F}\left(\cdot\right)\hat{\boldsymbol{\theta}}_3 - \mathbf{G}_\theta\left(\cdot\right)\right] + \tilde{\boldsymbol{\theta}}_3^\top \boldsymbol{\Gamma}_3^{-1}\dot{\hat{\boldsymbol{\theta}}}_3 + \tilde{\boldsymbol{\theta}}_4^\top \boldsymbol{\Gamma}_4^{-1}\dot{\hat{\boldsymbol{\theta}}}_4$$

where $\tilde{\mathbf{v}}_2^\top = \left(\tilde{v}_{21}, \tilde{v}_{22}, \tilde{v}_{23}\right)$ and $\mathbf{K}_2, \mathbf{K}_3$ are diagonal positive definite design matrices, $\mathbf{F}\left(\cdot\right) \in \mathbb{R}^{3\times n_3}$ with n_3 the number of the unknown parameters due to the modeled uncertainties, while $\mathbf{G}\left(\cdot\right) \in \mathbb{R}^{3\times n_4}$ with n_4 the number of parameters owing to unmodeled uncertainties and the disturbance on the system. For studying the stability of the dynamics $\left(\boldsymbol{\eta}_\gamma, \tilde{\mathbf{v}}_2\right)$, for simplicity let us choose $n_3 = n_4 = 2$. Then we generalize the result of this investigation to arbitrary values of n_3 and n_4. Following this consideration we write

$$\boldsymbol{\theta}_3^\top = \left(\theta_{31}, \theta_{32}\right), \quad \boldsymbol{\theta}_4^\top\left(t\right) = \left(\theta_{41}\left(t\right), \theta_{42}\left(t\right)\right), \quad \mathbf{F}\left(\cdot\right) = \begin{pmatrix} f_{11} & f_{12} \\ f_{21} & f_{22} \\ f_{31} & f_{32} \end{pmatrix}, \quad \mathbf{G}\left(\cdot\right) = \begin{pmatrix} g_{11} & g_{12} \\ g_{21} & g_{22} \\ g_{31} & g_{32} \end{pmatrix}.$$

Then

$$\dot{V}_2 = -\boldsymbol{\eta}_\gamma^\top \mathbf{K}_2 \boldsymbol{\eta}_\gamma + \boldsymbol{\eta}_\gamma^\top \mathbf{J}_2\left(\boldsymbol{\eta}_2\right)\tilde{\mathbf{v}}_2 - \tilde{\mathbf{v}}_2^\top \mathbf{C}_2\left(\mathbf{v}_2\right)\tilde{\mathbf{v}}_2 - \tilde{\mathbf{v}}_2^\top \left(\mathbf{K}_3 + \mathbf{D}_2\left(\mathbf{v}_2\right)\right)\tilde{\mathbf{v}}_2$$
$$- \tilde{\mathbf{v}}_2^\top \left(\boldsymbol{\eta}_\gamma^\top \mathbf{J}_2\left(\boldsymbol{\eta}_2\right)\right)^\top + \tilde{\mathbf{v}}_2^\top \left(\mathbf{F}\left(\cdot\right)\boldsymbol{\theta}_3 + \mathbf{G}\left(\cdot\right)\boldsymbol{\theta}_4\left(t\right) - \mathbf{F}\left(\cdot\right)\hat{\boldsymbol{\theta}}_3 - \mathbf{G}_\theta\left(\cdot\right)\right) \tag{6.106}$$
$$+ \tilde{\boldsymbol{\theta}}_3^\top \boldsymbol{\Gamma}_3^{-1}\dot{\hat{\boldsymbol{\theta}}}_3 + \tilde{\boldsymbol{\theta}}_4^\top \boldsymbol{\Gamma}_4^{-1}\dot{\hat{\boldsymbol{\theta}}}_4.$$

Since the term $\tilde{\mathbf{v}}_2^\top \left(\boldsymbol{\eta}_\gamma^\top \mathbf{J}_2 \left(\boldsymbol{\eta}_2 \right) \right)^\top$ is scalar we write

$$\tilde{\mathbf{v}}_2^\top \left(\boldsymbol{\eta}_\gamma^\top \mathbf{J}_2 \left(\boldsymbol{\eta}_2 \right) \right)^\top = \boldsymbol{\eta}_2^\top \mathbf{J}_2 \left(\boldsymbol{\eta}_2 \right) \tilde{\mathbf{v}}_2 \tag{6.107}$$

and from (3.29) we can determine that the matrix $\mathbf{C}_2$ is skew-symmetric. Therefore, by using this property of $\mathbf{C}_2$ and (6.107) then relationship (6.106) can be expressed as

$$\begin{aligned}
\dot{V}_2 = & - \left(\boldsymbol{\eta}_\gamma^\top \mathbf{K}_2 \boldsymbol{\eta}_\gamma + \tilde{\mathbf{v}}_2^\top \left(\mathbf{K}_3 + \mathbf{D}_2 \left(\mathbf{v}_2 \right) \right) \tilde{\mathbf{v}}_2 \right) + \tilde{\boldsymbol{\theta}}_3^\top \boldsymbol{\Gamma}_3^{-1} \dot{\hat{\boldsymbol{\theta}}}_3 - \tilde{\mathbf{v}}_2^\top \mathbf{F} \left(\cdot \right) \tilde{\boldsymbol{\theta}}_3 \\
& + \tilde{\boldsymbol{\theta}}_4^\top \boldsymbol{\Gamma}_4^{-1} \dot{\hat{\boldsymbol{\theta}}}_4 + \tilde{\mathbf{v}}_2^\top \left(\mathbf{G} \left(\cdot \right) \boldsymbol{\theta}_4 \left(t \right) - \mathbf{G}_\theta \left(\cdot \right) \right).
\end{aligned} \tag{6.108}$$

We can write from (3.36) and (3.37) that

$$\mathbf{D}_{20} \le \mathbf{D}_2 \left(\mathbf{v}_2 \right) \tag{6.109}$$

where $\mathbf{D}_{20} = \mathrm{diag} \left(d_4, d_5, d_6 \right)$. Thus, by utilizing (6.109) relation (6.108) is turned into the following inequality

$$\begin{aligned}
\dot{V}_2 \le & - \left(\boldsymbol{\eta}_\gamma^\top \mathbf{K}_2 \boldsymbol{\eta}_\gamma + \tilde{\mathbf{v}}_2^\top \left(\mathbf{K}_3 + \mathbf{D}_{20} \right) \tilde{\mathbf{v}}_2 \right) + \underbrace{\tilde{\boldsymbol{\theta}}_3^\top \boldsymbol{\Gamma}_3^{-1} \dot{\hat{\boldsymbol{\theta}}}_3 - \tilde{\mathbf{v}}_2^\top \mathbf{F} \left(\cdot \right) \tilde{\boldsymbol{\theta}}_3}_{\text{term}_1} \\
& + \underbrace{\tilde{\boldsymbol{\theta}}_4^\top \boldsymbol{\Gamma}_4^{-1} \dot{\hat{\boldsymbol{\theta}}}_4 + \tilde{\mathbf{v}}_2^\top \mathbf{G} \left(\cdot \right) \boldsymbol{\theta}_4 \left(t \right) - \tilde{\mathbf{v}}_2^\top \mathbf{G}_\theta \left(\cdot \right)}_{\text{term}_2}.
\end{aligned} \tag{6.110}$$

To find out the values of term_1 and term_2, let us assume that the unknown parameters are just two, i.e. $\boldsymbol{\theta}_3 \in \mathbb{R}^2$ and $\boldsymbol{\theta}_4 \in \mathbb{R}^2$. Then under this assumption we can determine the terms term_1 and term_2 in (6.110) as follows

$$\begin{aligned}
\text{term}_1 = & \tilde{\boldsymbol{\theta}}_3^\top \boldsymbol{\Gamma}_3^{-1} \dot{\hat{\boldsymbol{\theta}}}_3 - \tilde{\mathbf{v}}_2^\top \mathbf{F} \left(\cdot \right) \tilde{\boldsymbol{\theta}}_3 \\
= & \left(\tilde{\theta}_{31}, \tilde{\theta}_{32} \right) \begin{pmatrix} \gamma_{31}^{-1} & 0 \\ 0 & \gamma_{32}^{-1} \end{pmatrix} \begin{pmatrix} \dot{\hat{\theta}}_{31} \\ \dot{\hat{\theta}}_{32} \end{pmatrix} - \left(\tilde{v}_{21}, \tilde{v}_{22}, \tilde{v}_{23} \right) \begin{pmatrix} f_{11} & f_{12} \\ f_{21} & f_{22} \\ f_{31} & f_{32} \end{pmatrix} \begin{pmatrix} \tilde{\theta}_{31} \\ \tilde{\theta}_{32} \end{pmatrix} \\
= & \tilde{\theta}_{31} \left(\gamma_{31}^{-1} \dot{\hat{\theta}}_{31} - \sum_{j=1}^3 \tilde{v}_{2j} f_{j1} \right) + \tilde{\theta}_{32} \left(\gamma_{32}^{-1} \dot{\hat{\theta}}_{32} - \sum_{j=1}^3 \tilde{v}_{2j} f_{j2} \right)
\end{aligned} \tag{6.111}$$

which generally, for arbitrary n_3 (the number of the unknown parameters), amounts to

$$\text{term}_1 = \sum_{i=1}^{n_3} \tilde{\theta}_{3i} \left(\gamma_{3i}^{-1} \dot{\hat{\theta}}_{3i} - \sum_{j=1}^3 \tilde{v}_{2j} f_{ji} \right). \tag{6.112}$$

By choosing the adaptation law as

$$\dot{\hat{\theta}}_{3i} = \gamma_{3i} \text{Proj} \left(\sum_{j=1}^{3} \tilde{v}_{2j} f_{ji}, \hat{\theta}_{3i} \right) \qquad (6.113)$$

and inserting it into (6.112) we get

$$\text{term}_1 = \sum_{i=1}^{n_3} \tilde{\theta}_{3i} \left(\text{Proj} \left(\sum_{j=1}^{3} \tilde{v}_{2j} f_{ji}, \hat{\theta}_{3i} \right) - \sum_{j=1}^{3} \tilde{v}_{2j} f_{ji} \right). \qquad (6.114)$$

Further, according to the property (5.126) of the *projection operator*, readily we get

$$\text{term}_1 \leq 0. \qquad (6.115)$$

Now, we consider the third part of the inequality (6.110), namely, term_2.

$$\text{term}_2 = \tilde{\boldsymbol{\theta}}_4^\top \boldsymbol{\Gamma}_4^{-1} \dot{\hat{\boldsymbol{\theta}}}_4 + \tilde{\mathbf{v}}_2^\top \mathbf{G} \left(\cdot \right) \boldsymbol{\theta}_4 \left(t \right) - \tilde{\mathbf{v}}_2^\top \mathbf{G}_\theta \left(\cdot \right)$$

$$= \left(\tilde{\theta}_{41}, \tilde{\theta}_{42} \right) \begin{pmatrix} \gamma_{41}^{-1} & 0 \\ 0 & \gamma_{42}^{-1} \end{pmatrix} \begin{pmatrix} \dot{\hat{\theta}}_{41} \\ \dot{\hat{\theta}}_{42} \end{pmatrix} + \left(\tilde{v}_{21}, \tilde{v}_{22}, \tilde{v}_{23} \right) \begin{pmatrix} g_{11} & g_{12} \\ g_{21} & g_{22} \\ g_{31} & g_{32} \end{pmatrix} \begin{pmatrix} \theta_{41} \left(t \right) \\ \theta_{42} \left(t \right) \end{pmatrix} - \tilde{\mathbf{v}}_2^\top \mathbf{G}_\theta \left(\cdot \right)$$

$$= \tilde{\theta}_{41} \gamma_{41}^{-1} \dot{\hat{\theta}}_{41} + \tilde{\theta}_{42} \gamma_{42}^{-1} \dot{\hat{\theta}}_{42} + \left(\tilde{v}_{21} g_{11} + \tilde{v}_{22} g_{21} + \tilde{v}_{23} g_{31} \right) \theta_{41} \left(t \right) - \tilde{\mathbf{v}}_2^\top \mathbf{G}_\theta \left(\cdot \right)$$

$$+ \left(\tilde{v}_{21} g_{12} + \tilde{v}_{22} g_{22} + \tilde{v}_{23} g_{32} \right) \theta_{42} \left(t \right). \qquad (6.116)$$

Under the assumption that the disturbances acting on the system are bounded and by noticing (5.216) we write

$$\left| \theta_{41} \left(t \right) \right| = \left| \tau_{pd} \left(t \right) \right| \leq \tau_{pd}^{\max} = \theta_{41}, \; \left| \theta_{42} \left(t \right) \right| = \left| \frac{m_4 \tau_{ud} \left(t \right)}{m_1} \right| \leq \tau_{ud}^{\max} = \theta_{42} \qquad (6.117)$$

and from (6.116) we obtain

$$\text{term}_2 = \tilde{\theta}_{41} \gamma_{41}^{-1} \dot{\hat{\theta}}_{41} + \tilde{\theta}_{42} \gamma_{42}^{-1} \dot{\hat{\theta}}_{42} + \tilde{v}_{21} g_{11} \theta_{41} \left(t \right) + \tilde{v}_{22} g_{21} \theta_{41} \left(t \right) + \tilde{v}_{23} g_{31} \theta_{41} \left(t \right)$$

$$+ \tilde{v}_{21} g_{12} \theta_{42} \left(t \right) + \tilde{v}_{22} g_{22} \theta_{42} \left(t \right) + \tilde{v}_{23} g_{32} \theta_{42} \left(t \right) - \left(\tilde{v}_{21}, \tilde{v}_{22}, \tilde{v}_{23} \right) \mathbf{G}_\theta \left(\cdot \right)$$

$$\leq \tilde{\theta}_{41} \gamma_{41}^{-1} \dot{\hat{\theta}}_{41} + \left| \tilde{v}_{21} g_{11} \right| \left(\hat{\theta}_{41} - \tilde{\theta}_{41} \right) + \left| \tilde{v}_{22} g_{21} \right| \left(\hat{\theta}_{41} - \tilde{\theta}_{41} \right) + \left| \tilde{v}_{23} g_{31} \right| \left(\hat{\theta}_{41} - \tilde{\theta}_{41} \right)$$

$$+ \tilde{\theta}_{42} \gamma_{42}^{-1} \dot{\hat{\theta}}_{42} + \left| \tilde{v}_{21} g_{12} \right| \left(\hat{\theta}_{42} - \tilde{\theta}_{42} \right) + \left| \tilde{v}_{22} g_{22} \right| \left(\hat{\theta}_{42} - \tilde{\theta}_{42} \right) + \left| \tilde{v}_{23} g_{32} \right| \left(\hat{\theta}_{42} - \tilde{\theta}_{42} \right)$$

$$- \left(\tilde{v}_{21}, \tilde{v}_{22}, \tilde{v}_{23} \right) \mathbf{G}_\theta \left(\cdot \right)$$

$$\Rightarrow \text{term}_2 \leq \tilde{\theta}_{41}\left(\gamma_{41}^{-1}\dot{\hat{\theta}}_{41} - \sum_{i=1}^{3}|\tilde{v}_{2i}g_{i1}|\right) + \left(|v_{21}g_{11}| + |v_{22}g_{21}| + |v_{23}g_{31}|\right)\hat{\theta}_{41}$$

$$+ \tilde{\theta}_{42}\left(\gamma_{42}^{-1}\dot{\hat{\theta}}_{42}\sum_{i=1}^{3}|\tilde{v}_{2i}g_{i2}|\right) + \left(|v_{21}g_{12}| + |v_{22}g_{22}| + |v_{23}g_{32}|\right)\hat{\theta}_{42} \qquad (6.118)$$

$$- \left(\tilde{v}_{21}, \tilde{v}_{22}, \tilde{v}_{23}\right)\mathbf{G}_{\theta}\left(\cdot\right).$$

We choose the update laws for $\hat{\theta}_{41}$ and $\hat{\theta}_{42}$ as

$$\dot{\hat{\theta}}_{41} = \text{Proj}\left(\hat{\theta}_{41}, \sum_{i=1}^{3}|\tilde{v}_{2i}g_{i1}|\right), \dot{\hat{\theta}}_{42} = \text{Proj}\left(\hat{\theta}_{42}, \sum_{i=1}^{3}|\tilde{v}_{2i}g_{i2}|\right) \qquad (6.119)$$

and use the relations $|\tilde{v}_{2j}g_{ji}|\,\hat{\theta}_{4i} \leq \left||\tilde{v}_{21}g_{1i}|\,\hat{\theta}_{41}\right| = \left|\tilde{v}_{2i}g_{1i}\hat{\theta}_{4i}\right|$ for $i = 1, 2$ and $j = 1, 2, 3$ and define

$$\mathbf{G}_{\theta}\left(\cdot\right) = \begin{pmatrix} g_{11}\hat{\theta}_{41}\tanh\left(\dfrac{\tilde{v}_{21}g_{11}\hat{\theta}_{41}}{\epsilon_{11}}\right) + g_{12}\hat{\theta}_{42}\tanh\left(\dfrac{\tilde{v}_{21}g_{12}\hat{\theta}_{42}}{\epsilon_{12}}\right) \\ g_{21}\hat{\theta}_{41}\tanh\left(\dfrac{\tilde{v}_{22}g_{21}\hat{\theta}_{41}}{\epsilon_{21}}\right) + g_{22}\hat{\theta}_{42}\tanh\left(\dfrac{\tilde{v}_{22}g_{22}\hat{\theta}_{42}}{\epsilon_{22}}\right) \\ g_{31}\hat{\theta}_{41}\tanh\left(\dfrac{\tilde{v}_{23}g_{31}\hat{\theta}_{41}}{\epsilon_{31}}\right) + g_{32}\hat{\theta}_{42}\tanh\left(\dfrac{\tilde{v}_{23}g_{32}\hat{\theta}_{42}}{\epsilon_{32}}\right) \end{pmatrix} \qquad (6.120)$$

where ϵ_{ji} for $i = 1, 2$ and $j = 1, 2, 3$ are positive arbitrarily small design constants. This way we finally obtain

$$\text{term}_2 \leq \left|\tilde{v}_{21}g_{11}\hat{\theta}_{41}\right| - \tilde{v}_{21}g_{11}\hat{\theta}_{41}\tanh\left(\frac{\tilde{v}_{21}g_{11}\hat{\theta}_{41}}{\epsilon_{11}}\right) - \tilde{v}_{21}g_{12}\hat{\theta}_{42}\tanh\left(\frac{\tilde{v}_{21}g_{12}\hat{\theta}_{42}}{\epsilon_{12}}\right)$$

$$+ \left|\tilde{v}_{21}g_{12}\hat{\theta}_{42}\right| + \left|\tilde{v}_{22}g_{21}\hat{\theta}_{41}\right| - \tilde{v}_{22}g_{21}\hat{\theta}_{41}\tanh\left(\frac{\tilde{v}_{22}g_{21}\hat{\theta}_{41}}{\epsilon_{21}}\right) + \left|\tilde{v}_{22}g_{22}\hat{\theta}_{42}\right|$$

$$- \tilde{v}_{22}g_{22}\hat{\theta}_{42}\tanh\left(\frac{\tilde{v}_{22}g_{22}\hat{\theta}_{42}}{\epsilon_{22}}\right) + \left|\tilde{v}_{23}g_{31}\hat{\theta}_{41}\right| - \tilde{v}_{23}g_{31}\hat{\theta}_{41}\tanh\left(\frac{\tilde{v}_{23}g_{31}\hat{\theta}_{41}}{\epsilon_{31}}\right)$$

$$+ \left|\tilde{v}_{23}g_{32}\hat{\theta}_{42}\right| - \tilde{v}_{23}g_{32}\hat{\theta}_{42}\tanh\left(\frac{\tilde{v}_{23}g_{32}\hat{\theta}_{42}}{\epsilon_{32}}\right).$$

$$(6.121)$$

Using the property (5.32) and from (6.121) we get

$$\text{term}_2 \leq 0.2875 \sum_{j=1}^{3} \sum_{i=1}^{2} \epsilon_{ji}. \tag{6.122}$$

Generally, for n_4 unmodeled uncertainties in the system we get

$$\text{term}_2 \leq 0.2875 \sum_{j=1}^{3} \sum_{i=1}^{n_4} \epsilon_{ji} \tag{6.123}$$

and placing the relations (6.115) and (6.123) into (6.110) we obtain

$$\dot{V}_2 \leq -\boldsymbol{\eta}_\gamma^\top \mathbf{K}_2 \boldsymbol{\eta}_\gamma - \tilde{\mathbf{v}}_2^\top \left(\mathbf{K}_3 + \mathbf{D}_{20} \right) \tilde{\mathbf{v}}_2 + 0.2875 \sum_{j=1}^{3} \sum_{i=1}^{n_4} \epsilon_{ji}. \tag{6.124}$$

We see that $\boldsymbol{\eta}_\gamma$ and $\tilde{\mathbf{v}}_2$ converge to a small neighborhood about the origin.

To determine the convergence interval, we add and subtract to the right hand side of (6.124) the term $\frac{1}{2}\tilde{\boldsymbol{\theta}}_3^\top \boldsymbol{\Gamma}_3^{-1} \tilde{\boldsymbol{\theta}}_3 + \frac{1}{2}\tilde{\boldsymbol{\theta}}_4^\top \boldsymbol{\Gamma}_4^{-1} \tilde{\boldsymbol{\theta}}_4$ such that

$$\dot{V}_2 \leq -\boldsymbol{\eta}_\gamma^\top \mathbf{K}_2 \boldsymbol{\eta}_\gamma - \tilde{\mathbf{v}}_2^\top \left(\mathbf{K}_3 + \mathbf{D}_{20} \right) \tilde{\mathbf{v}}_2 - \frac{1}{2}\tilde{\boldsymbol{\theta}}_3^\top \boldsymbol{\Gamma}_3^{-1} \tilde{\boldsymbol{\theta}}_3 - \frac{1}{2}\tilde{\boldsymbol{\theta}}_4^\top \boldsymbol{\Gamma}_4^{-1} \tilde{\boldsymbol{\theta}}_4 + 0.2875 \sum_{j=1}^{3} \sum_{i=1}^{n_4} \epsilon_{ji}$$

$$+ \frac{1}{2}\tilde{\boldsymbol{\theta}}_3^\top \boldsymbol{\Gamma}_3^{-1} \tilde{\boldsymbol{\theta}}_3 + \frac{1}{2}\tilde{\boldsymbol{\theta}}_4^\top \boldsymbol{\Gamma}_4^{-1} \tilde{\boldsymbol{\theta}}_4. \tag{6.125}$$

To evaluate $\dot{V}_2$ in (6.125) we note that

$$\frac{1}{2}\boldsymbol{\eta}_\gamma^\top \boldsymbol{\eta}_\gamma \leq \frac{1}{2}\lambda_{\max}\left(\mathbf{I}_\gamma \right) \|\boldsymbol{\eta}_\gamma\|^2 = \frac{1}{2}\|\boldsymbol{\eta}_\gamma\|^2 \tag{6.126}$$

where $\mathbf{I}_\gamma \in \mathbb{R}^{3 \times 3}$ the identity matrix, and

$$\frac{1}{2}\lambda_{\min}\left(\mathbf{M}_2 \right) \|\tilde{\mathbf{v}}\|^2 \leq \frac{1}{2}\tilde{\mathbf{v}}_2 \mathbf{M}_2 \tilde{\mathbf{v}}_2 \leq \frac{1}{2}\lambda_{\max}\left(\mathbf{M}_2 \right) \|\tilde{\mathbf{v}}\|^2. \tag{6.127}$$

On the other side, we have

$$\lambda_{\min}\left(\mathbf{K}_2 \right) \|\boldsymbol{\eta}_\gamma\|^2 \leq \boldsymbol{\eta}_\gamma^\top \mathbf{K}_2 \boldsymbol{\eta}_\gamma \leq \lambda_{\max}\left(\mathbf{K}_2 \right) \|\boldsymbol{\eta}_\gamma\|^2 \tag{6.128}$$

and also

$$\lambda_{\min} \left(\mathbf{K}_3 + \mathbf{D}_{20} \right) \| \tilde{\mathbf{v}}_2 \|^2 \leq \tilde{\mathbf{v}}_2^\top \left(\mathbf{K}_3 + \mathbf{D}_{20} \right) \tilde{\mathbf{v}}_2 \leq \lambda_{\max} \left(\mathbf{K}_3 + \mathbf{D}_{20} \right) \| \tilde{\mathbf{v}}_2 \|^2. \qquad (6.129)$$

Let

$$\rho_2 = \frac{1}{2} \tilde{\boldsymbol{\theta}}_3^\top \boldsymbol{\Gamma}_3^{-1} \tilde{\boldsymbol{\theta}}_3 + \frac{1}{2} \tilde{\boldsymbol{\theta}}_4^\top \boldsymbol{\Gamma}_4^{-1} \tilde{\boldsymbol{\theta}}_4 + 0.2875 \sum_{j=1}^{3} \sum_{i=1}^{m_4} \epsilon_{ji} \qquad (6.130)$$

then by using inequalities (6.128) and (6.129) and placing them into (6.124) we get

$$\dot{V}_2 \leq -\lambda_{\min} \left(\mathbf{K}_2 \right) \| \boldsymbol{\eta}_\gamma \|^2 - \lambda_{\min} \left(\mathbf{K}_3 + \mathbf{D}_{20} \right) \| \tilde{\mathbf{v}}_2 \|^2 - \frac{1}{2} \tilde{\boldsymbol{\theta}}_3^\top \boldsymbol{\Gamma}_3^{-1} \tilde{\boldsymbol{\theta}}_3 - \frac{1}{2} \tilde{\boldsymbol{\theta}}_4^\top \boldsymbol{\Gamma}_4^{-1} \tilde{\boldsymbol{\theta}}_4 + \rho_2. \tag{6.131}$$

Now, we employ inequalities (6.126) and (6.127) such that from (6.131) we obtain

$$\dot{V}_2 \leq -\lambda_{\min} \left(\mathbf{K}_2 \right) \boldsymbol{\eta}_\gamma^\top \boldsymbol{\eta}_\gamma - \frac{\lambda_{\min} \left(\mathbf{K}_3 + \mathbf{D}_{20} \right)}{\lambda_{\max} \left(\mathbf{M}_2 \right)} \tilde{\mathbf{v}}_2^\top \mathbf{M}_2 \tilde{\mathbf{v}}_2 - \frac{1}{2} \tilde{\boldsymbol{\theta}}_3^\top \boldsymbol{\Gamma}_3^{-1} \tilde{\boldsymbol{\theta}}_3 - \frac{1}{2} \tilde{\boldsymbol{\theta}}_4^\top \boldsymbol{\Gamma}_4^{-1} \tilde{\boldsymbol{\theta}}_4 + \rho_2. \tag{6.132}$$

In this inequality, we discuss two cases depending on the values of the minimum eigenvalues of the matrices $\mathbf{K}_2$ and $\left(\mathbf{K}_3 + \mathbf{D}_{20} \right)$ and the maximum eigenvalue of the matrix $\mathbf{M}_2$, namely:

- Case 1: If

$$\lambda_{\min} \left(\mathbf{K}_2 \right) \leq \frac{\lambda_{\min} \left(\mathbf{K}_3 + \mathbf{D}_{20} \right)}{\lambda_{\max} \left(\mathbf{M}_2 \right)} \qquad (6.133)$$

then

$$\dot{V}_2 \leq -\sigma_v V_2 + \rho_2, \ \text{with} \ \sigma_v = 2\lambda_{\min} \left(\mathbf{K}_2 \right). \qquad (6.134)$$

- Case 2: If

$$\lambda_{\min} \left(\mathbf{K}_2 \right) > \frac{\lambda_{\min} \left(\mathbf{K}_3 + \mathbf{D}_{20} \right)}{\lambda_{\max} \left(\mathbf{M}_2 \right)} \qquad (6.135)$$

then

$$\dot{V}_2 \leq -\sigma_v V_2 + \rho_2 \qquad (6.136)$$

with

$$\sigma_v = 2\frac{\lambda_{\min} \left(\mathbf{K}_3 + \mathbf{D}_{20} \right)}{\lambda_{\max} \left(\mathbf{M}_2 \right)}. \qquad (6.137)$$

Thus, generally, we get the inequality

$$\dot{V}_2 \leq -\sigma_v V_2 + \rho_2 \qquad (6.138)$$

116

where

$$\sigma_v = \min\left(2\lambda_{\min}\left(\mathbf{K}_2\right), 2\frac{\lambda_{\min}\left(\mathbf{K}_3 + \mathbf{D}_{20}\right)}{\lambda_{\max}\left(\mathbf{M}_2\right)}\right). \tag{6.139}$$

To determine the convergence interval of $\boldsymbol{\eta}_\gamma$ and $\tilde{\mathbf{v}}_2$, we consider inequality (6.138)

$$\dot{V}_2 \le -\sigma_v V_2 + \rho_2^{\max} \tag{6.140}$$

where $\rho_2^{\max}$ is a constant (the upper bound of ρ_2), practically the value of

$$\lim_{t\to\infty} \rho_2 = 0.2875 \sum_{j=1}^{3} \sum_{i=1}^{n_4} \epsilon_{ji}. \tag{6.141}$$

Let us consider the following differential equation

$$\dot{V}_2 = -\sigma_v V_2 + \rho_2^{\max} \tag{6.142}$$

whose solution is

$$
\begin{aligned}
V_2\left(t\right) &= V_2\left(t_0\right) e^{-\sigma_v(t-t_0)} + \frac{\rho_2^{\max}}{\sigma_v} - \frac{\rho_2^{\max}}{\sigma_v} e^{-\sigma_v(t-t_0)} \\
&\le V_2\left(t_0\right) e^{-\sigma_v(t-t_0)} + \frac{\rho_2^{\max}}{\sigma_v}.
\end{aligned} \tag{6.143}
$$

According to the comparison principle [69], the solution of (6.140) reads

$$V_2\left(t\right) \le V_2\left(t_0\right) e^{-\sigma_v(t-t_0)} + \frac{\rho_2^{\max}}{\sigma_v}. \tag{6.144}$$

Now, to estimate the bounds of $\boldsymbol{\eta}_\gamma$ and $\tilde{\mathbf{v}}_2$, we can write from (6.104) and from (6.144)

$$
\begin{aligned}
&\frac{1}{2}\|\boldsymbol{\eta}_\gamma\|^2 \le V_2\left(t_0\right) e^{-\sigma_v(t-t_0)} + \frac{\rho_2^{\max}}{\sigma_v} \\
&\Rightarrow \|\boldsymbol{\eta}_\gamma\| \le \sqrt{2V_2\left(t_0\right) e^{-\sigma_v(t-t_0)} + \frac{2\rho_2^{\max}}{\sigma_v}} \le \sqrt{2V_2\left(t_0\right) e^{-\sigma_v(t-t_0)}} + \sqrt{\frac{2\rho_2^{\max}}{\sigma_v}}
\end{aligned} \tag{6.145}
$$

or

$$\|\boldsymbol{\eta}_\gamma\| \le \alpha_\eta\left(\cdot\right) e^{-\sigma_v(t-t_0)/2} + \rho_\eta \tag{6.146}$$

where

$$\alpha_\eta = \sqrt{2V_2\left(t_0\right)}, \quad \rho_\eta = \sqrt{\frac{2\rho_2^{\max}}{\sigma_v}}. \tag{6.147}$$

For estimation of the bounds of $\tilde{\mathbf{v}}_2$ we consider the relations (6.104), (6.127) and (6.144). This leads to

$$\frac{1}{2}\lambda_{\min}\left(\mathbf{M}_2\right)\left\|\tilde{\mathbf{v}}_2\right\|^2 \leq \frac{1}{2}\tilde{\mathbf{v}}_2\mathbf{M}_2\tilde{\mathbf{v}}_2 \leq V_1\left(t_0\right)e^{-\sigma_v(t-t_0)} + \frac{\rho_2^{\max}}{\sigma_v}, \tag{6.148}$$

hence

$$\left\|\tilde{\mathbf{v}}_2\right\|^2 \leq \frac{2V_1\left(t_0\right)}{\lambda_{\min}\left(\mathbf{M}_2\right)}e^{-\sigma_v(t-t_0)} + \frac{2\rho_2^{\max}}{\sigma_v\lambda_{\min}\left(\mathbf{M}_2\right)} \tag{6.149}$$

and

$$\left\|\tilde{\mathbf{v}}_2\right\| \leq \sqrt{\frac{2V_1\left(t_0\right)}{\lambda_{\min}\left(\mathbf{M}_2\right)}}e^{-\sigma_v(t-t_0)/2} + \sqrt{\frac{2\rho_2^{\max}}{\sigma_v\lambda_{\min}\left(\mathbf{M}_2\right)}} \tag{6.150}$$

and finally

$$\left\|\tilde{\mathbf{v}}_2\right\| \leq \alpha_v\left(\cdot\right)e^{-\sigma_v(t-t_0)/2} + \rho_v \tag{6.151}$$

where

$$\alpha_v\left(\cdot\right) = \sqrt{\frac{2V_1\left(t_0\right)}{\lambda_{\min}\left(\mathbf{M}_2\right)}}, \quad \rho_v = \sqrt{\frac{2\rho_2^{\max}}{\sigma_v\lambda_{\min}\left(\mathbf{M}_2\right)}}. \tag{6.152}$$

Thus, from (6.146) and (6.151) we may determine that $\boldsymbol{\eta}_\gamma$ and $\tilde{\mathbf{v}}_2$ converge exponentially to a ball centered at the origin.

6.3 Stability of the Non-Actuated Dynamics

To investigate the stability of the dynamics (v, w), we define the following Lyapunov function

$$V_3 = \frac{1}{2}m_2v^2 + \frac{1}{2}m_3w^2. \tag{6.153}$$

Thus, we have

$$\dot{V}_3 = m_2v\dot{v} + m_3w\dot{w}. \tag{6.154}$$

Before we evaluate $\dot{V}_3$ in (6.154), we consider the vector $\mathbf{f}_\gamma\left(\cdot\right)$ in (5.167) which can be expressed as

$$\mathbf{f}_\gamma\left(\cdot\right) = \left(0, f_1^\sigma\dot{\sigma} + f_1^u u + f_1^v v + f_1^w w, f_2^\sigma\dot{\sigma} + f_2^u u + f_2^v v + f_2^w w\right)^\top$$

where

$$f_1^\sigma = \mu_{11}\frac{\partial x_d(\sigma)}{\partial\sigma} + \mu_{12}\frac{\partial y_d(\sigma)}{\partial\sigma} + \mu_{13}\frac{\partial z_d(\sigma)}{\partial\sigma}$$

$$f_1^u = -\left[\mu_{11}\mathbf{J}_1^{11}(\boldsymbol{\eta}_2) + \mu_{12}\mathbf{J}_1^{21}(\boldsymbol{\eta}_2) + \mu_{13}\mathbf{J}_1^{31}(\boldsymbol{\eta}_2)\right]$$

$$f_1^v = -\left[\mu_{11}\mathbf{J}_1^{12}(\boldsymbol{\eta}_2) + \mu_{12}\mathbf{J}_1^{22}(\boldsymbol{\eta}_2) + \mu_{13}\mathbf{J}_1^{32}(\boldsymbol{\eta}_2)\right]$$

$$f_1^w = -\left[\mu_{11}\mathbf{J}_1^{13}(\boldsymbol{\eta}_2) + \mu_{12}\mathbf{J}_1^{23}(\boldsymbol{\eta}_2) + \mu_{13}\mathbf{J}_1^{33}(\boldsymbol{\eta}_2)\right]$$

$$f_2^\sigma = \mu_{21}\frac{\partial x_d(\sigma)}{\partial \sigma} + \mu_{22}\frac{\partial y_d(\sigma)}{\partial \sigma}, \quad f_2^u = -\left[\mu_{21}\mathbf{J}_1^{11}(\boldsymbol{\eta}_2) + \mu_{22}\mathbf{J}_1^{21}(\boldsymbol{\eta}_2)\right]$$

$$f_2^v = -\left[\mu_{21}\mathbf{J}_1^{12}(\boldsymbol{\eta}_2) + \mu_{22}\mathbf{J}_1^{22}(\boldsymbol{\eta}_2)\right], \quad f_2^w = -\left[\mu_{21}\mathbf{J}_1^{13}(\boldsymbol{\eta}_2) + \mu_{22}\mathbf{J}_1^{23}(\boldsymbol{\eta}_2)\right]$$

with $\mathbf{J}_1^{ij}(\boldsymbol{\eta}_2)$ the element of the matrix $\mathbf{J}_1(\boldsymbol{\eta}_2)$ at the ith row and jth column, and

$$\mu_{11} = \left(\frac{x_{\mathrm{e}}\sin(\theta)}{a_{\mathrm{e}}d_{\mathrm{e}}\cos(\gamma_1)} - \frac{x_{\mathrm{e}}\sin(\gamma_1)}{d_{\mathrm{e}}^2\cos(\gamma_1)}\right), \mu_{12} = \left(\frac{y_{\mathrm{e}}\sin(\theta)}{a_{\mathrm{e}}d_{\mathrm{e}}\cos(\gamma_1)} - \frac{y_{\mathrm{e}}\sin(\gamma_1)}{d_{\mathrm{e}}^2\cos(\gamma_1)}\right),$$

$$\mu_{13} = \left(\frac{\cos(\theta)}{d_{\mathrm{e}}\cos(\gamma_1)} - \frac{z_{\mathrm{e}}\sin(\gamma_1)}{d_{\mathrm{e}}^2\cos(\gamma_1)}\right), \quad \mu_{21} = \left(\frac{\sin(\psi)}{a_{\mathrm{e}}\cos(\gamma_2)} - \frac{x_{\mathrm{e}}\sin(\gamma_2)}{a_{\mathrm{e}}^2\cos(\gamma_2)}\right),$$

$$\mu_{22} = \left(-\frac{\cos(\psi)}{a_{\mathrm{e}}\cos(\gamma_2)} - \frac{y_{\mathrm{e}}\sin(\gamma_2)}{a_{\mathrm{e}}^2\cos(\gamma_2)}\right).$$

By inserting $\dot{v}$ and $\dot{w}$ in (6.154) with their values from the second and third equations in the system dynamics (5.178) we conclude that

$$
\begin{aligned}
\dot{V}_3 = & -m_2 d_v |v|v^2 + \big(m_2 m_1 u\cos(\phi)\cos(\theta)f_2^v - m_2 m_1 u\sin(\phi)f_1^v - m_2 d_2 v^2 \\
& + \Big((m_2 m_1 u\cos(\phi)\cos(\theta)f_2^w - m_3 m_1 u\cos(\theta)\sin(\phi)f_2^v - m_3 m_1 u\cos(\phi)f_1^v \\
& - m_2 m_1 u\sin(\phi)f_1^w)w + m_2 m_1 u\cos(\phi)\cos(\theta)f_2^\sigma\dot{\sigma} + m_2 m_1 u^2\cos(\phi)\cos(\theta)f_2^u \\
& + m_2 m_1 u\cos(\phi)\cos(\theta)\gamma_2 k_{23} - m_2 m_1 u\sin(\phi)f_1^\sigma\dot{\sigma} - m_2 m_1 u^2\sin(\phi)f_1^u \\
& - m_2 m_1 u\sin(\phi)\gamma_1 k_{22} - m_2 m_1 u\tilde{r} + m_2 \tau_{v\mathrm{d}}(t)\Big)v - m_3 d_w|w|w^2 \\
& + \Big(-m_3 m_1 u\cos(\theta)\sin(\phi)f_2^w - m_3 m_1 u\cos(\phi)f_1^w - m_3 d_3\Big)w^2 \\
& + \Big(-m_3 m_1 u\cos(\theta)\sin(\phi)f_2^\sigma\dot{\sigma} - m_3 m_1 u^2\cos(\theta)\sin(\phi)f_2^u \\
& - m_3 m_1 u\cos(\theta)\sin(\phi)\gamma_2 k_{23} - m_3 m_1 u\cos(\phi)f_1^\sigma\dot{\sigma} - m_3 m_1 u^2\cos(\phi)f_1^u \\
& - m_3 m_1 u\cos(\phi)\gamma_1 k_{22} + m_3 m_1 u\tilde{q} + m_3 \tau_{w\mathrm{d}}(t)\Big)w.
\end{aligned}
$$

(6.155)

With (5.194) we calculate the desired pitch and yaw velocities as

$$
\begin{aligned}
q_{\mathrm{d}} = & -\cos\left(\theta\right)\sin\left(\phi\right)f_2^\sigma\dot\sigma - \cos\left(\theta\right)\sin\left(\phi\right)f_2^u u - \cos\left(\theta\right)\sin\left(\phi\right)f_2^v v - \cos\left(\theta\right)\sin\left(\phi\right)f_2^w w \\
& -\cos\left(\theta\right)\sin\left(\phi\right)\gamma_2 k_{23} - \cos\left(\phi\right)f_1^\sigma\dot\sigma - \cos\left(\phi\right)f_1^u u - \cos\left(\phi\right)f_1^v v - \cos\left(\phi\right)f_1^w w \\
& -\cos\left(\phi\right)\gamma_1 k_{22}, \\
r_{\mathrm{d}} = & -\cos(\phi)\cos(\theta)f_2^\sigma\dot\sigma - \cos(\phi)\cos(\theta)f_2^u u - \cos(\phi)\cos(\theta)f_2^v v - \cos(\phi)\cos(\theta)f_2^w w, \\
& -\cos(\phi)\cos(\theta)\gamma_2 k_{23} + \sin(\phi)f_1^\sigma\dot\sigma + \sin(\phi)f_1^u u + \sin(\phi)f_1^v v + \sin(\phi)f_1^w w \\
& +\sin(\phi)\gamma_1 k_{22}.
\end{aligned}
\tag{6.156}
$$

Thus, if we replace the relations of q_d and r_d from (6.156) in (6.155) then we obtain

$$
\dot V_3 = -m_2 d_v|v|v^2 - m_3 d_w|w|w^2 + H_1 v^2 + H_2 + H_3 w^2 + H_4
\tag{6.157}
$$

with

$$
H_1 = m_2 m_1 u \cos(\phi)\cos(\theta)f_2^v - m_2 m_1 u \sin(\phi)f_1^v - m_2 d_2
\tag{6.158}
$$

$$
\begin{aligned}
H_2 = & \left(m_2 m_1 u \cos(\phi)\cos(\theta)f_2^w - m_3 m_1 u \cos(\theta)\sin(\phi)f_2^v - m_3 m_1 u \cos(\phi)f_1^v \right. \\
& \left. - m_2 m_1 u \sin(\phi)f_1^w \right)w + m_2 m_1 u \cos(\phi)\cos(\theta)f_2^\sigma\dot\sigma + m_2 m_1 u^2 \cos(\phi)\cos(\theta)f_2^u \\
& + m_2 m_1 u \cos(\phi)\cos(\theta)\gamma_2 k_{23} - m_2 m_1 u \sin(\phi)f_1^\sigma\dot\sigma - m_2 m_1 u^2 \sin(\phi)f_1^u \\
& - m_2 m_1 u \sin(\phi)\gamma_1 k_{22} - m_2 m_1 u\tilde r + m_2 \tau_{v\mathrm{d}}\left(t\right)
\end{aligned}
\tag{6.159}
$$

$$
H_3 = -m_3 m_1 u \cos(\theta)\sin(\phi)f_2^w - m_3 m_1 u \cos(\phi)f_1^w - m_3 d_3
\tag{6.160}
$$

$$
\begin{aligned}
H_4 = & \left(-m_3 m_1 u \cos(\theta)\sin(\phi)f_2^\sigma\dot\sigma - m_3 m_1 u^2 \cos(\theta)\sin(\phi)f_2^u \right. \\
& - m_3 m_1 u \cos(\theta)\sin(\phi)\gamma_2 k_{23} - m_3 m_1 u \cos(\phi)f_1^\sigma\dot\sigma - m_3 m_1 u^2 \cos(\phi)f_1^u \\
& \left. - m_3 m_1 u \cos(\phi)\gamma_1 k_{22}, + m_3 m_1 u\tilde q + m_3 \tau_{w\mathrm{d}}\left(t\right) \right)w.
\end{aligned}
\tag{6.161}
$$

Further, to prove stability we assume Assumption 2A in [87], that means the sway and the heave velocities are small compared to the surge velocity. On the other hand, the designed controller guarantees that the values $\gamma_1, \gamma_2, \tilde q, \tilde r, x_e, x_e, z_e, u$ are bounded. Moreover, the functions $\sin\left(\cdot\right)$ and $\cos\left(\cdot\right)$ are bounded, and the disturbances as well. This implies that the terms H_1, H_2, H_3 and H_4 are bounded. Thus, we may write

$$
|H_i| \le H_i^{\max}, \quad i = 1, \ldots, 4
\tag{6.162}
$$

120

and see that

$$
\begin{aligned}
\dot{V}_3 &\leq - m_2 d_v |v| v^2 - m_3 d_w |w| w^2 + H_1^{\max} v^2 + H_2^{\max} + H_3^{\max} w^2 + H_4^{\max} \\
&\leq \left(H_1^{\max} - m_2 d_v |v| \right) v^2 + \left(H_3^{\max} - m_3 d_w |w| \right) w^2 + H^{\max}
\end{aligned} \tag{6.163}
$$

where

$$
H^{\max} \leq H_2^{\max} + H_4^{\max}. \tag{6.164}
$$

Clearly, $\dot{V}_3$ is negative outside some closed curve, centered at the origin and conclude that the (v, w)-dynamics is bounded.

Figure 6.2 shows the time derivative of the Lyapunov function V_3. We recognize two areas: Inside the closed curve where $\dot{V}_3 > 0$ and outside of it where $\dot{V}_3 < 0$.
If we start from a point $(v_\mathrm{o}, w_\mathrm{o})$ outside the curve or from a point $(v_\mathrm{i}, w_\mathrm{i})$ within it.

Then in both cases $\dot{V}_3$ will converge to the closed curve $\dot{V}_3 = 0$, as Figure 6.2 illustrates. This implies, both of the velocities v and w are bounded which means that the non-actuated subsystem (we can not control it directly) is bounded.
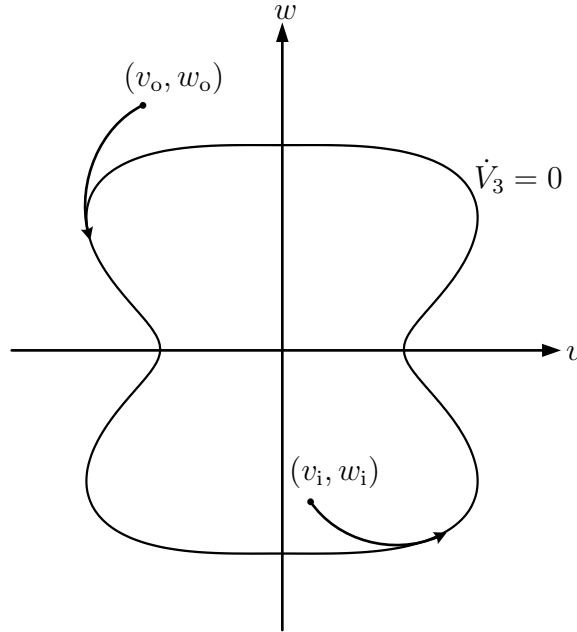
Fig. 6.2: Time derivative of Lyapunov function V_3

6.4 Stability Proof Overview

The proof concept relies on bounded-input bounded-state stability over either subsystems. As illustrated in Figure 6.3.
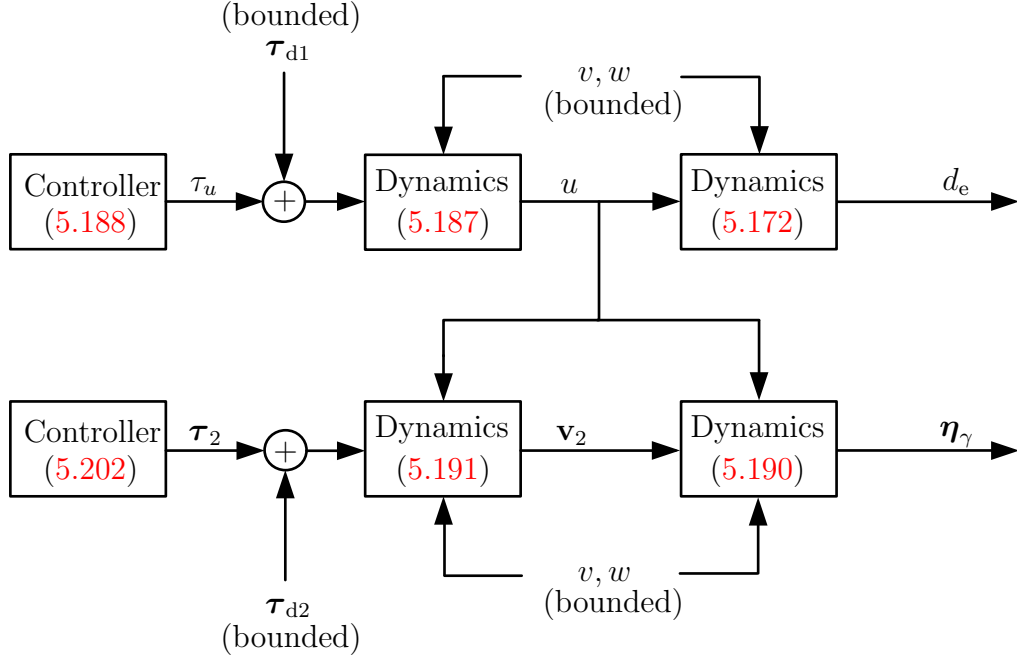
Fig. 6.3: Stability proof overview

6.5 Initial Conditions

We have seen in the Section 5.6.2 that the controller $\boldsymbol{\tau}_2$ rotates the real vehicle towards the virtual one, and forces the angle γ to go to zero. From (5.141), for γ tending to zero we see that

$$\cos(\gamma) = \frac{a_1}{d_e} \to 1 \tag{6.165}$$

where a_1 is the projection of the position error d_e on the X_0-axis (Figure 5.10). From (6.165), if $-\pi/2 < \gamma < \pi/2$, then it can be guaranteed that a_1 is positive which is already assumed for the dynamics (5.175). To determine the initial conditions that satisfy

$$-\frac{\pi}{2} < \gamma < \frac{\pi}{2} \tag{6.166}$$

considering (5.150) we may write

$$0 \leq \cos(\gamma) < 1 \Leftrightarrow 0 \leq \cos(\gamma_1) + \frac{a_e}{d_e}\cos(\theta)(\cos(\gamma_2) - 1) < \cos(\gamma_1) + \cos(\gamma_2) - 1 \tag{6.167}$$

$$\Rightarrow \cos(\gamma_1) + \cos(\gamma_2) > 1 \tag{6.168}$$

where

$$0 \leq \frac{a_e}{d_e}\cos(\theta) < 1 \quad \text{with} \quad -\frac{\pi}{2} < \theta < \frac{\pi}{2}. \tag{6.169}$$

Thus, for this choice, the condition (6.166) may be modified to

$$-\frac{\pi}{3} < \gamma_1 < \frac{\pi}{3} \quad \text{and} \quad -\frac{\pi}{3} < \gamma_2 < \frac{\pi}{3}. \tag{6.170}$$

By noting that $\boldsymbol{\eta}_\gamma = (\phi, \gamma_1, \gamma_2)^\top$ it is clear that

$$|\phi|, |\gamma_1|, |\gamma_2| \leq \|\boldsymbol{\eta}_\gamma\|. \tag{6.171}$$

If guaranteed that $\|\boldsymbol{\eta}_\gamma\| < \pi/3$ then $|\gamma_1|, |\gamma_2| < \pi/3$. From (6.146), for $t = t_0$, we get

$$\|\boldsymbol{\eta}_\gamma\| < \sqrt{2V_1(t_0)} + \sqrt{\frac{2\rho_\eta}{\sigma_v}}. \tag{6.172}$$

Using (6.104), (6.127) and (6.126) for $t = t_0$ we see that

$$2V_1(t_0) = \boldsymbol{\eta}_2^\top(t_0)\,\boldsymbol{\eta}_2(t_0) + \tilde{\mathbf{v}}_2^\top(t_0)\,\mathbf{M}_2\tilde{\mathbf{v}}_2(t_0) + \sum_{i=3}^{4}\boldsymbol{\Gamma}_i^{-1}\|\tilde{\boldsymbol{\theta}}_i(t_0)\|^2$$
$$\leq \|\boldsymbol{\eta}_2(t_0)\|^2 + \lambda_{\max}(\mathbf{M}_2)\|\tilde{\mathbf{v}}_2(t_0)\|^2 + \sum_{i=3}^{4}\boldsymbol{\Gamma}_i^{-1}\|\tilde{\boldsymbol{\theta}}_i(t_0)\|^2. \tag{6.173}$$

Placing (6.173) into (6.172) we obtain

$$\|\boldsymbol{\eta}_\gamma\| \leq \sqrt{\|\boldsymbol{\eta}_2(t_0)\|^2 + \lambda_{\max}(\mathbf{M}_2)\|\tilde{\mathbf{v}}_2(t_0)\|^2 + \sum_{i=3}^{4}\boldsymbol{\Gamma}_i^{-1}\|\tilde{\boldsymbol{\theta}}_i(t_0)\|^2} + \sqrt{\frac{2\rho_\eta}{\sigma_v}} \tag{6.174}$$

and by noting (6.171) the conditions (6.170) can be satisfied if we choose the initial conditions to fulfill the following inequality

$$\|\boldsymbol{\eta}_\gamma\| \leq \sqrt{\|\boldsymbol{\eta}_2(t_0)\|^2 + \lambda_{\max}(\mathbf{M}_2)\|\tilde{\mathbf{v}}_2(t_0)\|^2 + \sum_{i=3}^{4}\boldsymbol{\Gamma}_i^{-1}\|\tilde{\boldsymbol{\theta}}_i(t_0)\|^2} + \sqrt{\frac{2\rho_\eta}{\sigma_v}} \leq \frac{\pi}{3}. \tag{6.175}$$

Thus, to satisfy this inequality, for $t = t_0$ we have to investigate the following terms:

- The term $\|\boldsymbol{\eta}_2(t_0)\|^2 = \phi(t_0)^2 + \theta(t_0)^2 + \psi(t_0)^2$ can be rendered to be arbitrary small by choosing the start values for the orientation in a convenient way.
- In $\lambda_{\max}(\mathbf{M}_2)\|\tilde{\mathbf{v}}_2(t_0)\|^2$, the entries of $\mathbf{M}_2$ are unknown parameters to be estimated. We choose the initial conditions for the update laws "small enough", and by considering (5.194), a convenient initialization of the position and the orientation of the real vehicle can make $\lambda_{\max}(\mathbf{M}_2)\|\tilde{\mathbf{v}}_2(t_0)\|^2$ arbitrary small as well.
- The summation $\sum_{i=3}^{4} \boldsymbol{\Gamma}_i^{-1}\|\tilde{\boldsymbol{\theta}}_i(t_0)\|^2$ can be made arbitrary small if we have some knowledge about the parameters to be estimated and if we choose the gain matrices $\boldsymbol{\Gamma}_i$, for $i = 3, 4$, "large enough".
- Regarding $\sqrt{2\rho_\eta/\sigma_v}$, to make this term small we consider the relations (6.130) and (6.147). That is, by choosing the gain matrices $\boldsymbol{\Gamma}_3$ and $\boldsymbol{\Gamma}_4$ "large enough", and the ϵ_{ji} in (6.130) "small enough". One the other hand, we must choose σ_v "large enough" which is achievable from (6.139) if the term $\lambda_{\max}(\mathbf{M}_2)\|\tilde{\mathbf{v}}_2(t_0)\|^2$ is chosen to be small and the gains matrices $\mathbf{K}_2$ and $\mathbf{K}_3$ "large enough".

As we have seen from the above discussion, we may satisfy condition (6.168) just by means of a convenient reutilization of the position and the orientation of the real AUV, while the translational and rotational velocities $u(t_0), v(t_0), w(t_0), p(t_0), q(t_0)$ and $r(t_0)$ are set to zero at the start time $t = t_0$. The above discussed conditions of the orientation errors γ_1 and γ_2 are summarized in Figure 6.4.

The admissible area is the square with edge of length $2\pi/3$.
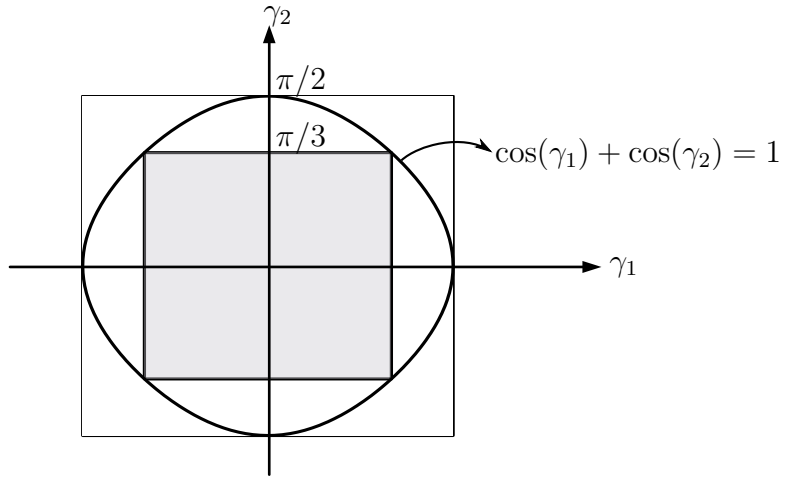
Fig. 6.4: Admissible initial conditions for γ_1 and γ_2

CHAPTER 7

Simulation Results

7.1 Underactuated System

In real-world applications the AUVs have no actuators on the sway and heave directions. In this chapter we check the effectiveness and the efficiency of the proposed robust adaptive backstepping control laws presented in Sections 5.6.1 and 5.6.2 in steering the real vehicle to follow the virtual one, which moves on some desired path. We test those controllers, firstly, for the off-line path generation, and secondly, in the case of on-line path generation.

7.1.1 Results for Off-Line Planning

For illustrating the ability of the controller to force the AUV to follow the predefined path and reject the disturbances under the parameter uncertainties of the plant, we consider the reference trajectories (depending on the path variable σ)

$$x_{\mathrm{d}} = -50\cos(\sigma), \ \ y_{\mathrm{d}} = 50\sin(\sigma), \ \ z_{\mathrm{d}} = 3\sigma. \tag{7.1}$$

Those represent the 3D path, a spiral with radius 50 (m).

The virtual vehicle moves along this path according to the reference velocity profile. We consider this profile to be given as $u_0 = u_0^*(1 - u_1^* e^{-u_2^* t})e^{-u_3^* de}$ with $u_0^* = 1.1, u_1^* = 0.5, u_2^* = 2, u_3^* = 1$. We choose $d_e^\star = 0.1$m, and the gain $k_1 = 0.4$, then the reference position error is given through $\delta = d_e^\star + \rho_u/k_1$. Through simulation we get $\delta \approx 0.104$m. For solving the ordinary differential equations we choose the solver function "ode3" fixed-step (Bogacki Shampine method) the gains $\mathbf{K}_2 = \mathrm{diag}(0.05, 0.05, 0.05)$, $\mathbf{K}_3 = \mathrm{diag}(580, 580, 580)$, $c_u = 73.09$. Let us consider that the all of the degrees of freedom of the AUV are perturbed with the signal: $\sin(t)$ (N/Nm). The adaptation gain matrices

are chosen as follows: $\mathbf{\Gamma}_3 = \text{diag}(100, 100, 100)$ and $\mathbf{\Gamma}_4 = \text{diag}(100, 100, 100)$. Figure 7.1 shows the path in XY plane. Actually, it is a circle with radius 50 (m). In Figure 7.2 the surge velocity u and its reference u_0 are shown. The figure illustrates that the sway v and heave w velocities are bounded despite of the disturbances.
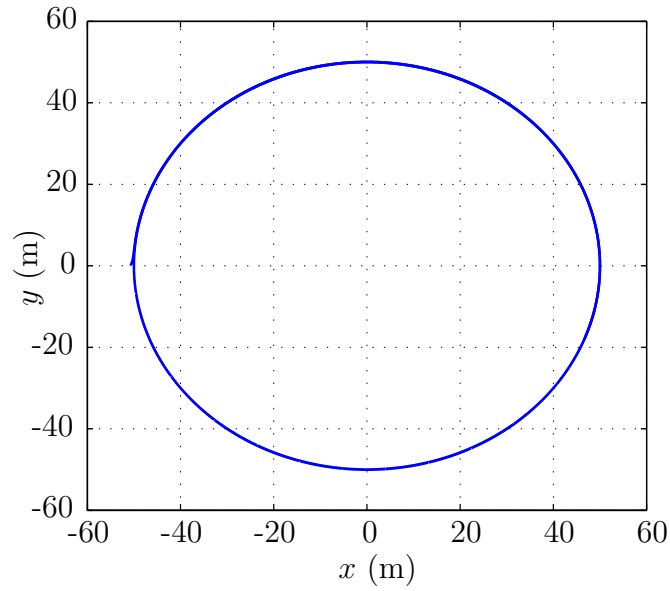
Fig. 7.1: Path in XY plane (off-line)
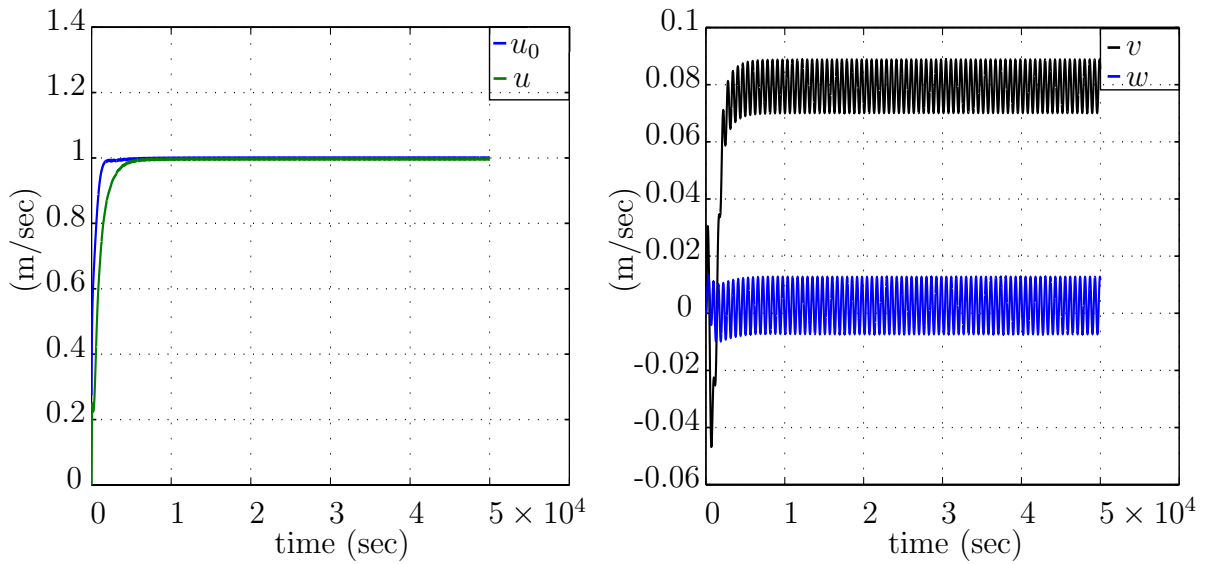
Fig. 7.2: Translation velocities (off-line)

The control inputs of the underactuated AUV are presented in Figure 7.3.
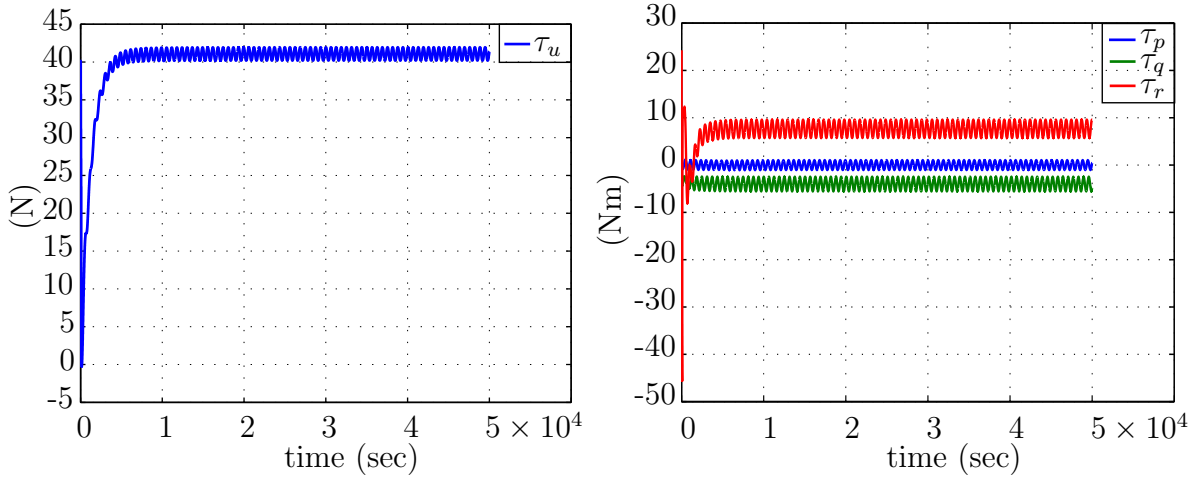
Fig. 7.3: Forces and torques (off-line)

The tracking position and orientation errors are shown in Figure 7.4.
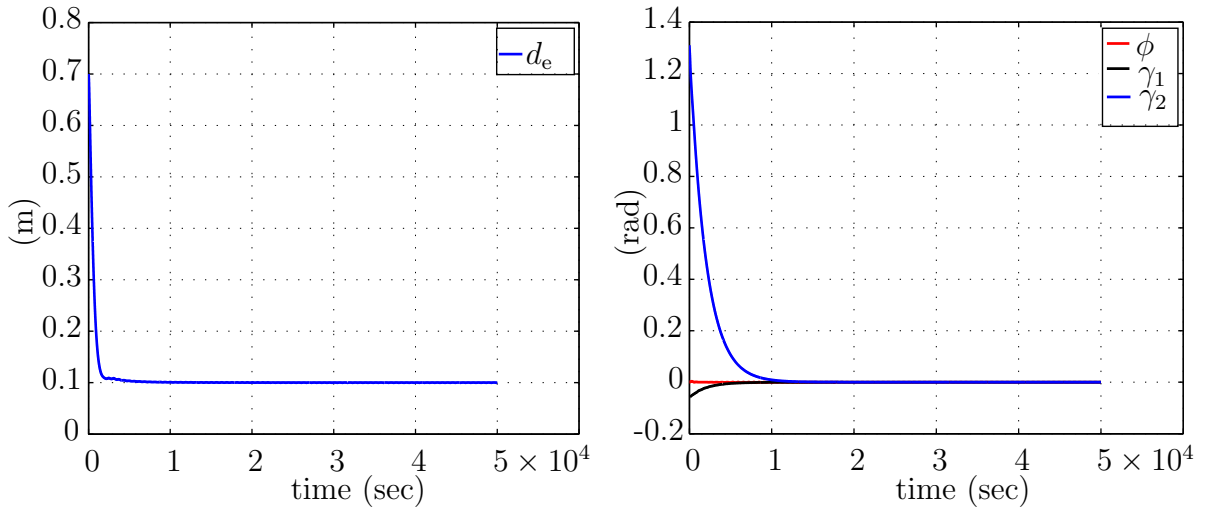
Fig. 7.4: Position and orientation errors (off-line)

Figure 7.5 indicates the reference 3D path (7.1) and the actual path presented through measured position x, y and z.
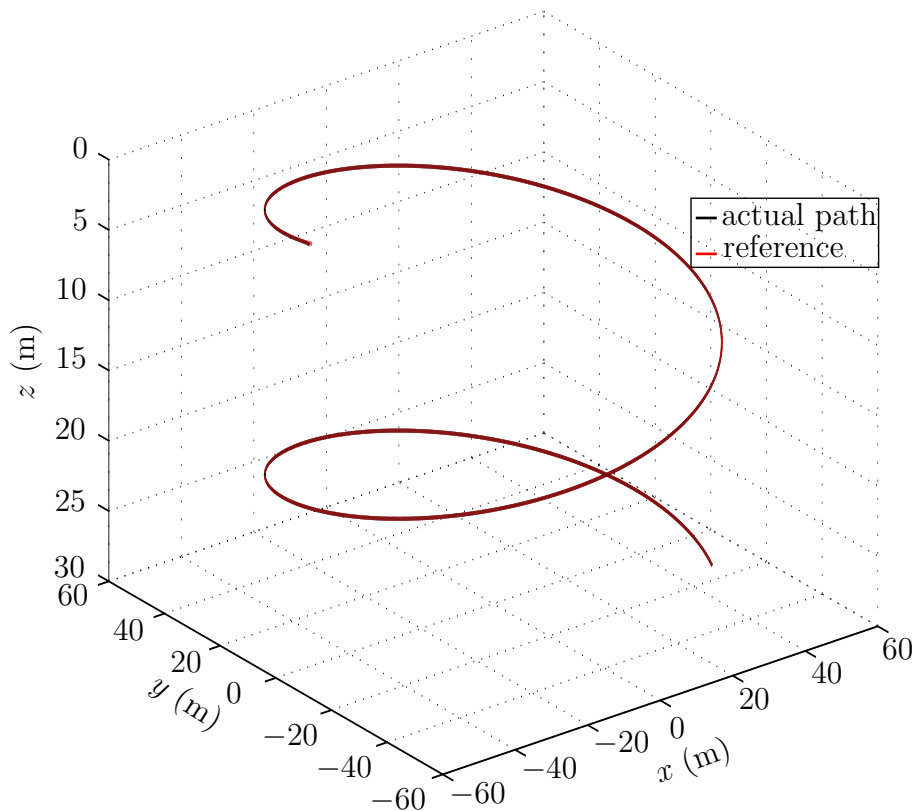
Fig. 7.5: 3D path (off-line)

The small oscillation in the reference trajectories and reference velocity occur essentially because of the oscillation in the derivative of the path variable $\dot{\sigma}$ (due to the disturbances).

7.1.2 Results for On-Line Planning

Now, let us consider that the way-points are fed to the path generator, on-line, point by point. Then according to the algorithm developed in Section in 2.2 a convenient path is generated by interpolating the way-points at each considered window.

As simulation example we consider that the spiral (7.1) is sampled at 76 points. The values of x, y and z are given in Table 7.1.

#	1	2	3	4	5	6	7	8	9	10
x	0	8.68	18.35	25	32.14	38.3	43.3	46.98	49.24	50
y	50	49.24	46.98	43.3	38.3	32.14	25	17.1	8.68	0
z	0.4	0.6	0.8	1	1.2	1.4	1.6	1.8	2	2.2
#	11	12	13	14	15	16	17	18	19	20
x	49.24	46.98	43.3	38.3	32.14	25	17.1	8.68	0	-8.68
y	-8.68	-17.1	-25	-32.14	-38.3	-43.3	-46.98	-49.24	-50	-49.24
z	2.4	2.6	2.8	3	3.2	3.4	3.6	3.8	4	4.2
#	21	22	23	24	25	26	27	28	29	30
x	-17.1	-25	-32.14	-38.3	-43.3	-46.98	-49.24	-50	-49.24	-46.98
y	-46.98	-43.3	-38.3	-32.14	-25	-17.1	-8.68	0	8.68	17.1
z	4.4	4.6	4.8	5	5.2	5.4	5.6	5.8	6	6.2
#	31	32	33	34	35	36	37	38	39	40
x	-43.3	-38.3	-32.14	-25	-17.1	-8.68	0	8.68	17.1	25
y	25	32.14	38.3	43.3	46.98	49.24	50	49.24	46.98	43.3
z	6.4	6.6	6.8	7	7.2	7.4	7.6	7.8	8	8.2
#	41	42	43	44	45	46	47	48	49	50
x	32.14	38.3	43.3	46.98	49.24	50	49.24	46.98	43.3	38.3
y	38.3	32.14	25	17.1	8.68	0	-8.68	-17.1	-25	-32.14
z	8.4	8.6	8.8	9	9.2	9.4	9.6	9.8	10	10.2
#	51	52	53	54	55	56	57	58	59	60
x	32.14	25	17.1	8.68	0	-8.68	-17.1	-25	-32.14	-38.3
y	-38.3	-43.3	-46.98	-49.24	-50	-49.24	-46.98	-43.3	-38.3	-32.14
z	10.4	10.6	10.8	11	11.2	11.4	11.6	11.8	12	12.2
#	61	62	63	64	65	66	67	68	69	70
x	-43.3	-46.98	-49.24	-50	-49.24	-46.98	-43.3	-38.3	-32.14	-25
y	-25	-17.1	-8.68	0	8.68	17.1	25	32.14	38.3	43.3
z	12.4	12.6	12.8	13	13.2	13.4	13.6	13.8	14	14.2
#	71	72	73	74	75	76				
x	-17.1	-8.68	0	8.68	17.1	25				
y	46.98	49.24	50	49.24	46.98	43.3				
z	14.4	14.6	14.8	15	15.2	15.4				

Table 7.1: Specified way-points for the underactuated system

In this example, we let the length of the horizon of the on-line path planning algorithm illustrated in Figure 2.2 be 7, i.e. in each iteration we regard 7 way-points. That helps to suppress interpolation oscillations during the on-line path generation. If we consider more points in each window then we will gain more information about the behavior of the path, but incur more computational costs. Hence, we must find a compromise between oscillation and the computational costs.

Let the reference profile of the velocity along the desired path be

$$u_0\left(t\right) = u_0^*(1 - u_1^* e^{-u_2^* t})e^{-u_3^* de} \tag{7.2}$$

with $u_0^* = 0.6344, u_1^* = 0.5, u_2^* = 2, u_3^* = 1,$. We choose $d_e^\star = 0.1$ (m), and the gain $k_1 = 0.1$. The reference position error is $\delta = d_e^\star + \rho_u/k_1 = \delta = 0.22$ (m). For solving the ordinary differential equations, we choose the solver function "ode1" fixed-step (Euler) and the gains $\mathbf{K}_2 = \text{diag}(0.1, 0.1, 0.1)$, $\mathbf{K}_3 = \text{diag}(580, 580, 580)$, $c_u = 1$. The adaptation gain matrices are chosen as follows: $\mathbf{\Gamma}_3 = \text{diag}(100, 100, 100)$ and $\mathbf{\Gamma}_4 = \text{diag}(100, 100, 100)$. Disturbance on the system shall take the following form:
On X_0 it is $\sin\left(0.5t\right)$ (N), on Y_0 it is $\sin\left(0.5t\right)$ (N), on Z_0 it is 2 (N) , and the disturbance about Z_0 is $\cos\left(0.1t\right)$ (Nm). All of those disturbance signals start at time $t = 100$ (sec). Figure 7.6 shows the actual path in XY plane.
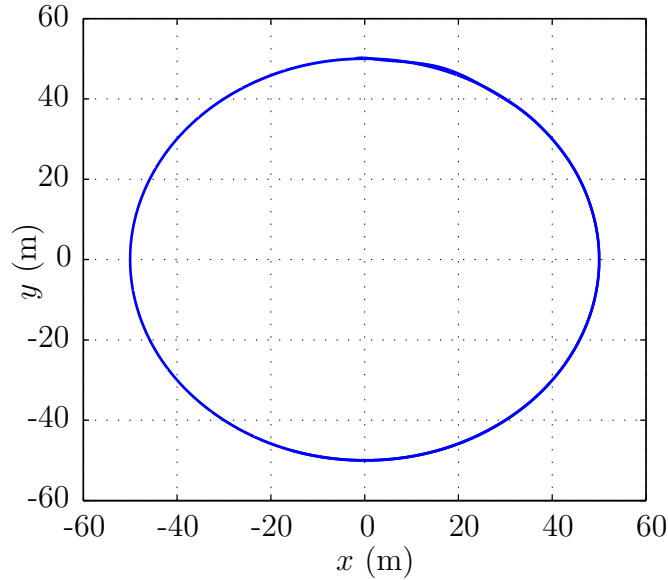
Fig. 7.6: Path in XY plane (on-line)

In Figure 7.7 the surge velocity u and its reference u_0 are illustrated. It also illustrates that the sway v and heave w velocities are bounded despite of the disturbances.
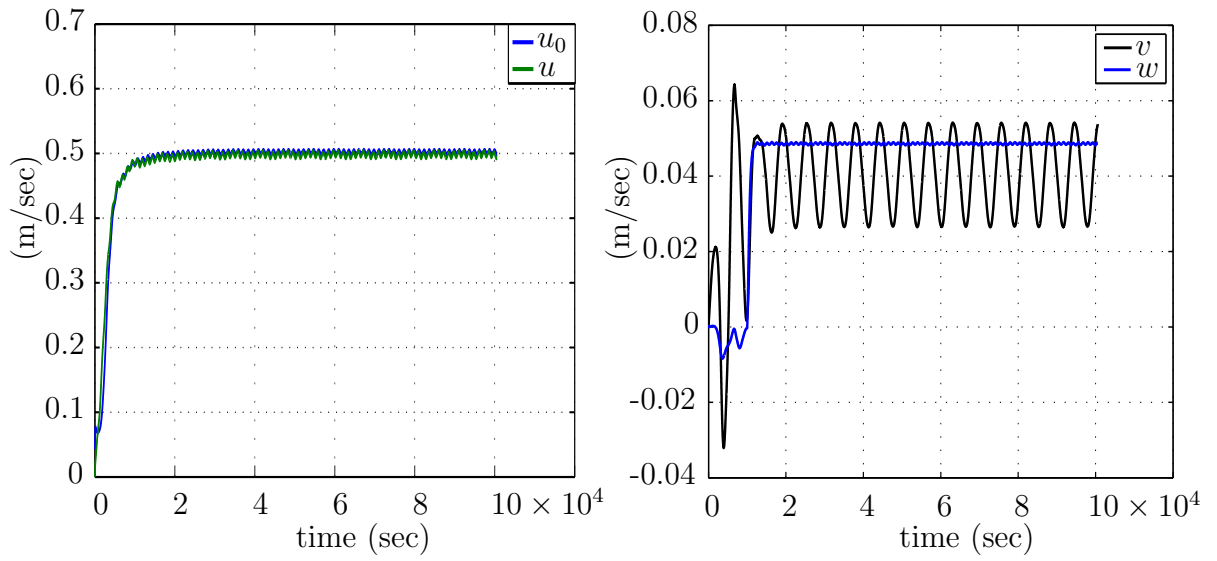
Fig. 7.7: Translational velocities (on-line)

The control inputs of the underactuated AUV are presented in Figure 7.8.
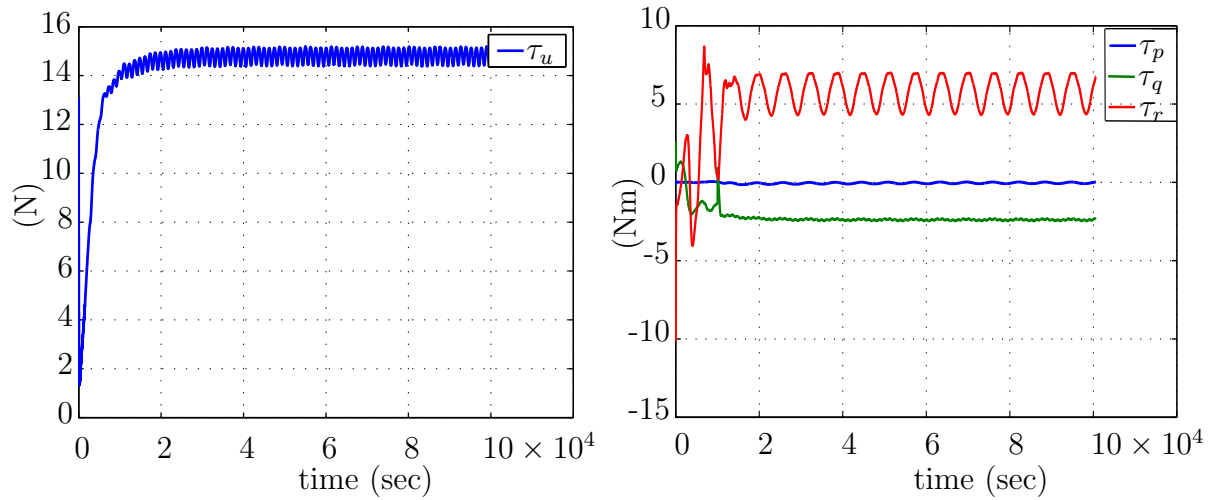
Fig. 7.8: Forces and torques (on-line)

The tracking position and orientation errors are shown in Figure 7.9.

131
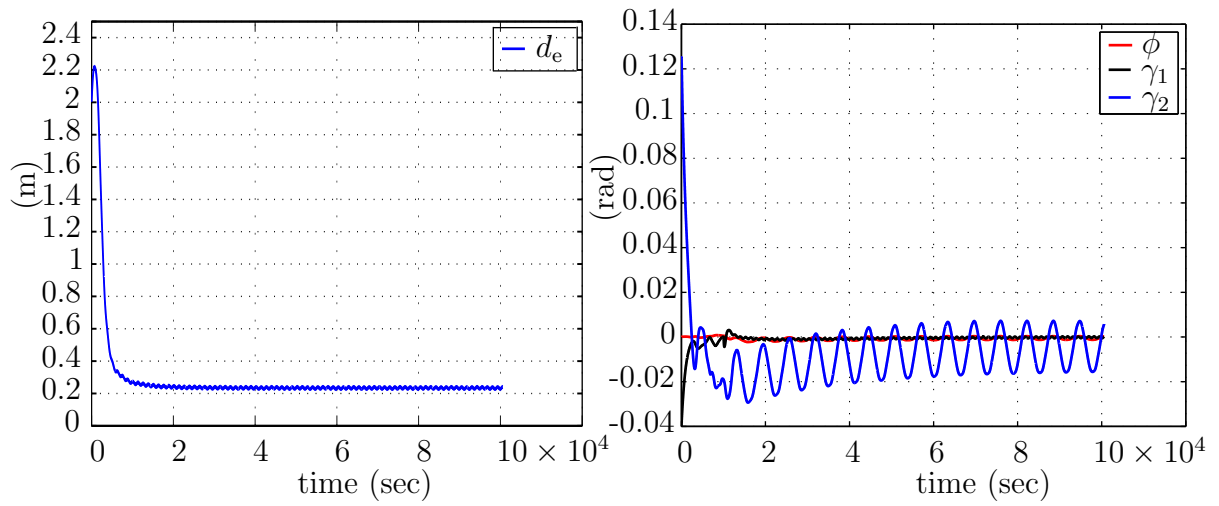
Fig. 7.9: Position and orientation errors (on-line)
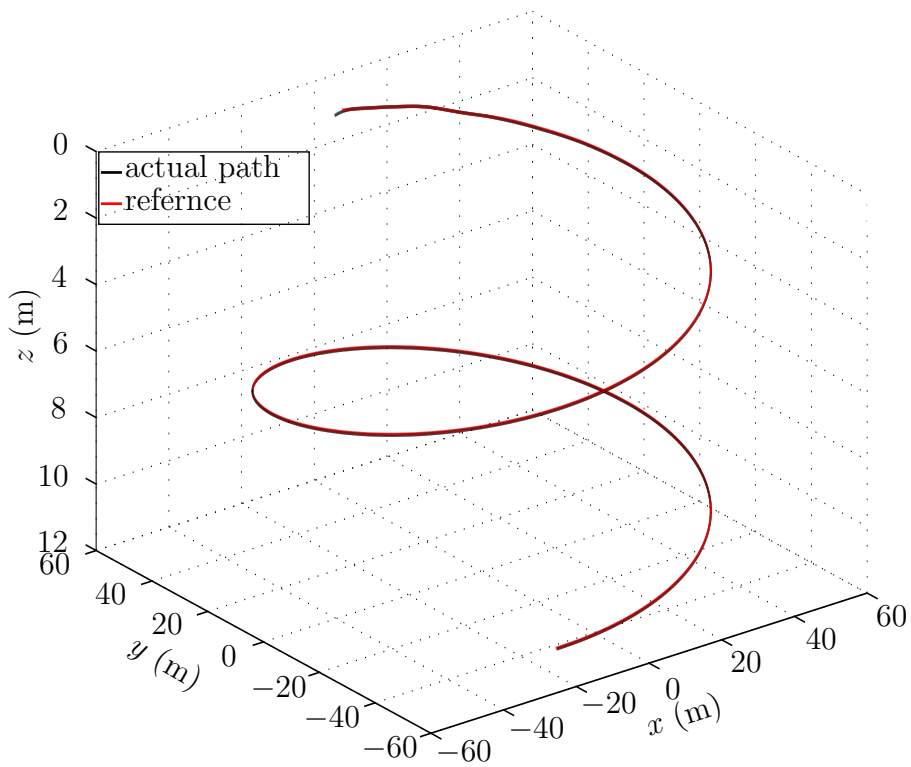
Fig. 7.10: 3D path (on-line)

132

Figure 7.10 indicates the reference and the actual 3D path.

The small oscillations in the reference trajectories and reference velocity occur essentially because of the oscillation in the derivative of the path variable $\dot{\sigma}$, firstly, due to the disturbances signals, and secondly because of the on-line path generation.

CHAPTER 8

Conclusion

8.1 Summary of the Work

In this dissertation, we have investigated a numerically robust technique, which allows to generate a reference path for dynamically allocated way-points to be followed by an autonomous underwater vehicle (AUV) in an on-line way. Based on the B-splines interpolation approach and by using a moving window over the way-points to be interpolated, an adequate reference path in the underwater 3D space is generated on-line.

Since the proposed path generation algorithm bestows low computational-cost features, it is contingent to use a sufficient number of way-points, which sample the desired motion primitives. The sampled way-points can be interpolated on-line to approximate the desired primitives that are designed such that the AUV avoids some environmental obstacles in the 3D space.

Relying on the number of the actuators steering the AUV, and on the modeled and unmodeled uncertainties in the system, two approaches are presented to force the AUV to follow the desired path/trajectories.

For the fully-actuated plant with modeled perturbations, a compensator-based PD-controller is utilized to force the AUV to track the reference trajectories. Furthermore, this controller is enhanced with a generalized extended state observer to attenuate the disturbances acting on the AUV.

For an underactuated system, in presence of parametric and unmodeled uncertainties, a robust adaptive control law is designed. The introduced path following controller is designed utilizing Lyapunov's direct method, adaptive backstepping and parameter projection techniques. This controller steers the AUV to an arbitrarily small neighborhood centered at the reference 3D path, under a suitable choice of the initial conditions for both of position and orientation of the considered AUV. Under assumption of stability of the non-controlled subsystem (sway and heave dynamics), it has been proven that

position and orientation errors are globally exponentially convergent to a ball centered at the origin.

For the aforementioned introduced control approaches, an extensive and complete proof of the stability is presented in detail.

Some elementary simulations give a first illustration of the practicability of the approach. However, these have not been in focus of the underlying work.

8.2   Perspectives and Open Problems

Potential future investigations related to this work may contribute to the following prospects:

- Implementation and realization of the proposed on-line path generator and also the path following controller on a real-world AUV.

- Defining and solving the on-line path planning in sense of an optimization problem to minimize oscillations.
  Also the control following problem may be defined as optimization problem regarding the control inputs, to minimize the consumption of the on-board power.

- Elevation of the admissible area of the initial conditions, such that the AUV can start its mission for a wide range and flexible initial conditions.
  Another prospect that can be investigated in this field is the "self-tuning" of the initial conditions such that the AUV resumes the mission without external interference (initialization) if the mission is interrupted for some reason far away at sea.

- Enhancement of the presented path planning, and control algorithm to deal with dynamic obstacle avoidance, and to cover the issue of multiple AUVs coordinated missions.

- Extension of the proposed path planning and control approaches presented in this work for the space and hovering vehicles.

CHAPTER 9

Appendix

In this Appendix, we recall the results of previous approaches for the fully-actuated AUV which is presented in Chapter 4.

9.1 Fully-Actuated System

Here we assumed that the AUV is fully-actuated, that is, the six degrees of freedom are actuated. The tracking controller is designed with the computed torque technique (exact input-state feedback linearizion).

In the simulations, we assume 11 way-points associated with their related longitudinal velocities as listed in Table 9.1. Using the afore-presented algorithm (in Section 2.1), these way-points determine the path depicted in Figure 9.1. Between the first and the second way-point the vertical trajectory planning is considered, i.e. $z_0 = 0$ and $z_f = 20$. Note that in the algorithm it is assumed that four way-points are known, that means, $\psi_f = \arctan\left(\frac{y_d'(0)}{x_d'(0)}\right) = 0.9409\,(\text{rad})$ and initial value $\boldsymbol{\psi}_0 = 0\,(\text{rad})$. When assuming a maximum velocity of $w_{\max} = 0.4\,(\text{m/sec})$ we obtain $t_f = \frac{15(\mathbf{z}_f - \mathbf{z}_0)}{8w_{\max}} = 93.75$ (sec). These generate the coefficients for the trajectories $z_d(t)$ and $\psi_d(t)$ using the relations (4.1), (4.2), (4.3) and (4.4), where $x_d(t)$, $y_d(t)$, $\phi_d(t)$, and $\theta_d(t)$ are all zero. The second phase of the motion planning starts at way-point two which is a stationary point. The 3D planning algorithm determines the intermediate paths, see Figure 9.1, based on the

#	1	2	3	4	5	6	7	8	9	10	11
x	0	0	40	80	120	160	200	240	280	320	360
y	0	0	60	80	60	80	80	80	80	80	80
z	0	20	20	20	20	20	20	30	40	50	40
u	0	0	1	1	1	1	1	1	1	1	0

Table 9.1: Specified way-points for the fully-actuated system

desired way-point velocity data in such a way that $u_0(t)$ is obtained as the low-pass filtered linear interpolation of σ.
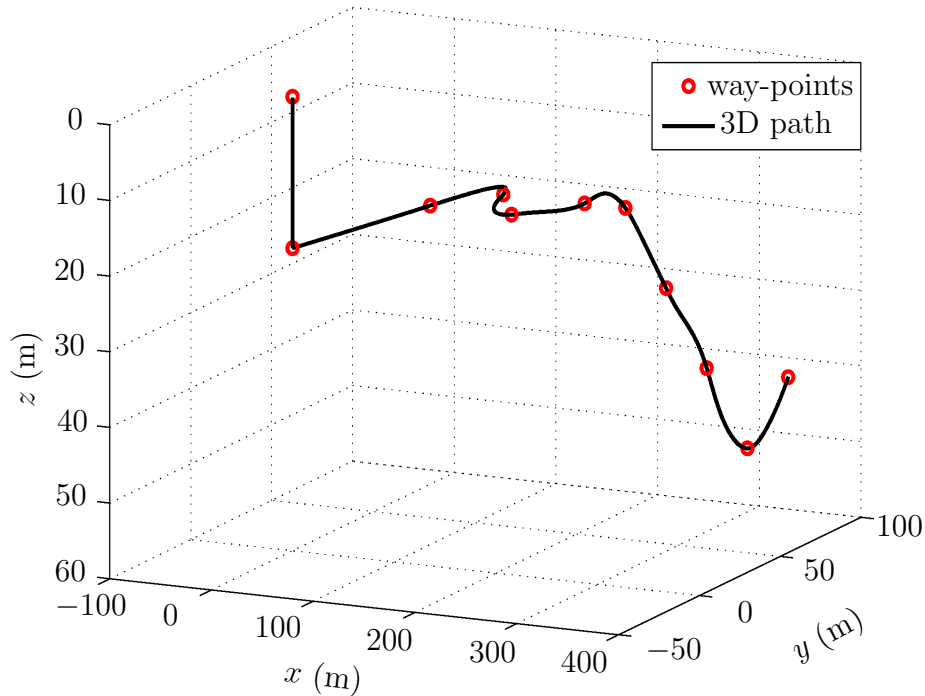
Fig. 9.1: Way-points and path in 3D space

The controller was simulated referring to real-world data of an AUV that is available locally at the Institute of Automation and Systems Technology, Technische Universität Ilmenau. For brevity, we omit the matrices $\mathbf{M}$, $\mathbf{C}$, and $\mathbf{D}$ here. The mass of the AUV is $m = 132.535\,(\mathrm{kg})$, length $l = 2.30\,(\mathrm{m})$ and radius $r = 0.15\,(\mathrm{m})$, to give a rough idea of its dimensions. So as to investigate a realistic setting, we chose the sampling time as $T = 0.1\,(\mathrm{sec})$. The discrete PD-controller is designed for eigenvalues $\lambda_1 = \lambda_2 = 0.95$, hence, with (4.23) and (4.24) we have $\mathbf{K}_{\mathrm{D},i} = 1$ and $\mathbf{K}_{\mathrm{P},i} = 0.25$ for $i = 1, \ldots, 6$.

In the simulation, we show two closed-loop scenarios: the nominal case (no disturbance) and the perturbed case.

9.1.1 Nominal Case

Figure 9.2 illustrates the tracking performance for position and orientation, respectively.
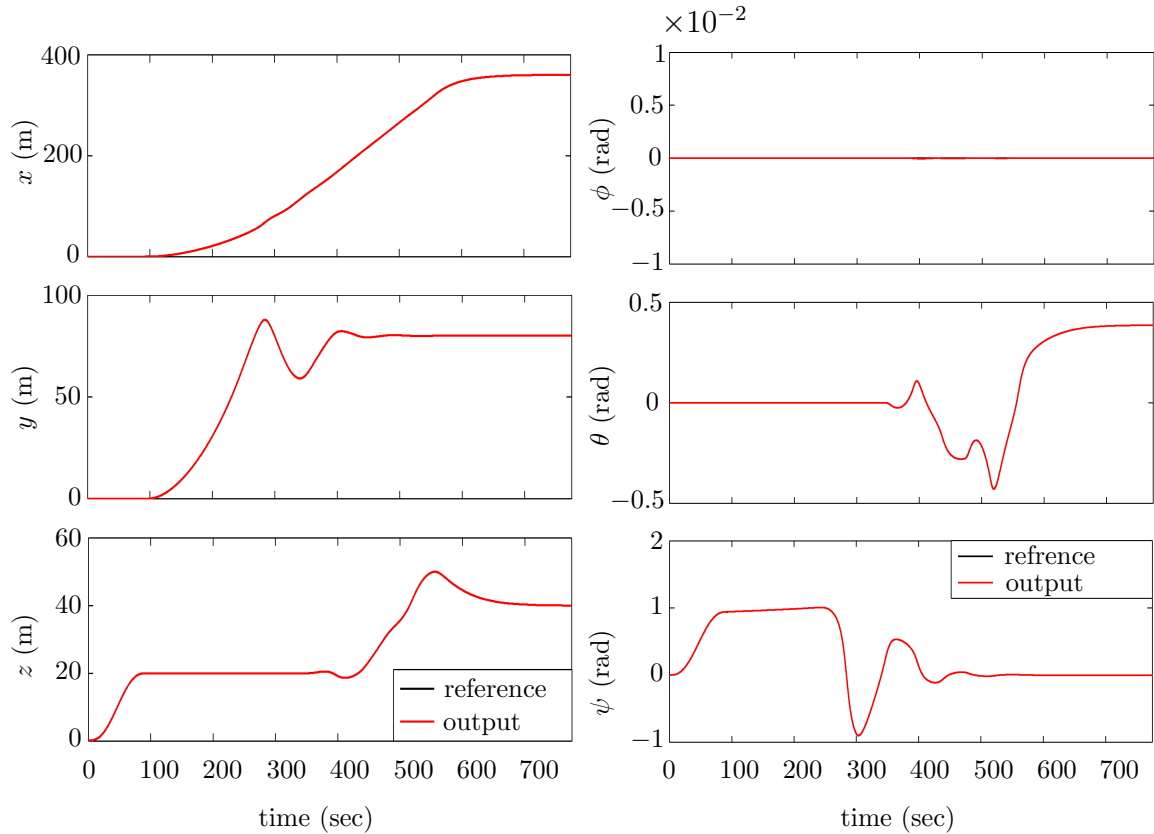
Fig. 9.2: Position and orientation

The reference and resulting translational and angular velocities are shown in Figure 9.3.

The figure shows that the reference trajectories generated by the path planner may be tracked with an acceptable control effort, see Figure 9.4. Because of utilizing a polynomial of degree 5, numerical problems appear. That is reflected in the control inputs as small peaks, Figure 9.4.

For the vertical motion, i.e. from 0 (sec) to 100 (sec) all control inputs are zero except for the force in heave direction. This force borrows its behavior actually from the profile

of the reference velocity on Z_0 direction. The maximum velocity on Z_0 is reached at time $t = 50$ (sec).
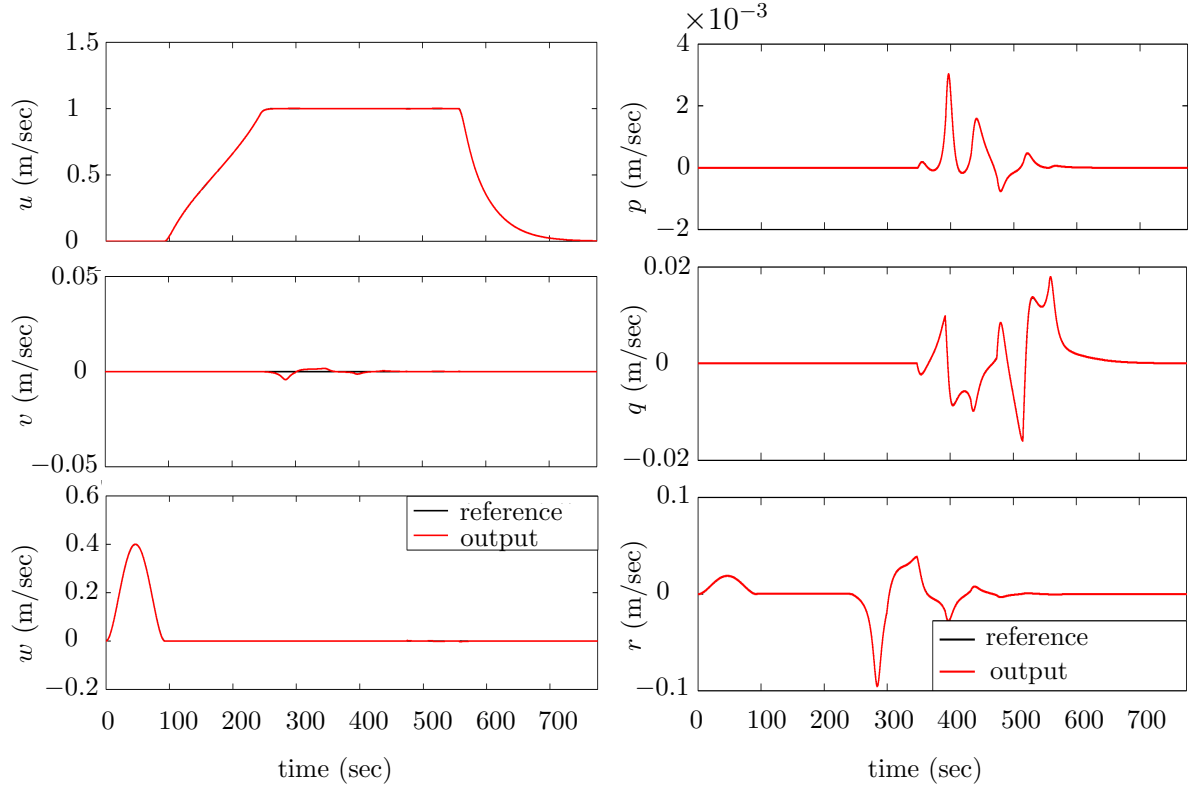
Fig. 9.3: Translational and angular velocities

9.1.2 Perturbed Case

We assume a sinusoidal disturbance acting on the first and the sixth channel of the control input $\boldsymbol{\tau}$, that is $d_1(t) = 10\sin(2\pi\,0.01)\,(\text{N})$ and $d_6(t) = 10\sin(2\pi\,0.01)\,(\text{Nm})$, which both are bounded as are its derivatives. The disturbance acts beginning from time $t = 300$ (sec). The GESO is designed for $\ell = 4$.

The eigenvalues of the estimation error dynamics, $\mathbf{A}_e - \mathbf{L}\,\mathbf{C}_e$, are chosen all real with absolute value less than 0.1 such that the observation error dynamics decays faster than the controlled loop dynamics.

Comparing the resulting tracking performance with and without GESO when subject
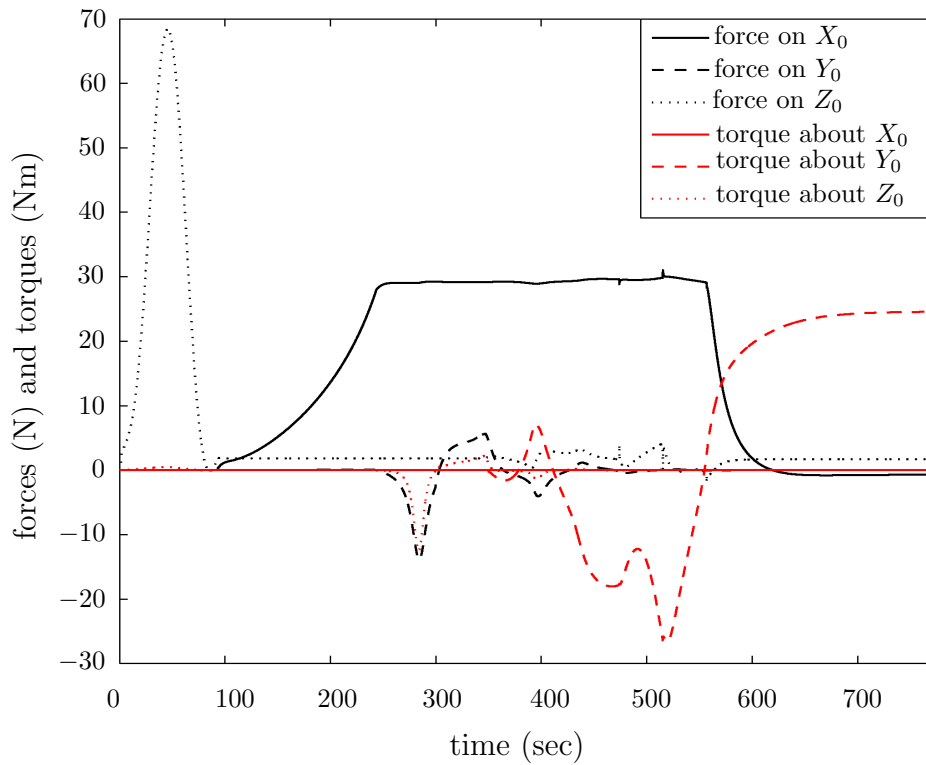
Fig. 9.4: Forces and torques for nominal case

to these disturbances is shown in Figures 9.5 and 9.6. In those two figures, we can recognize the effect of the disturbance upon the performance of the controller and the benefits of using the GESO. Figure 9.7 illustrates the input control actions.
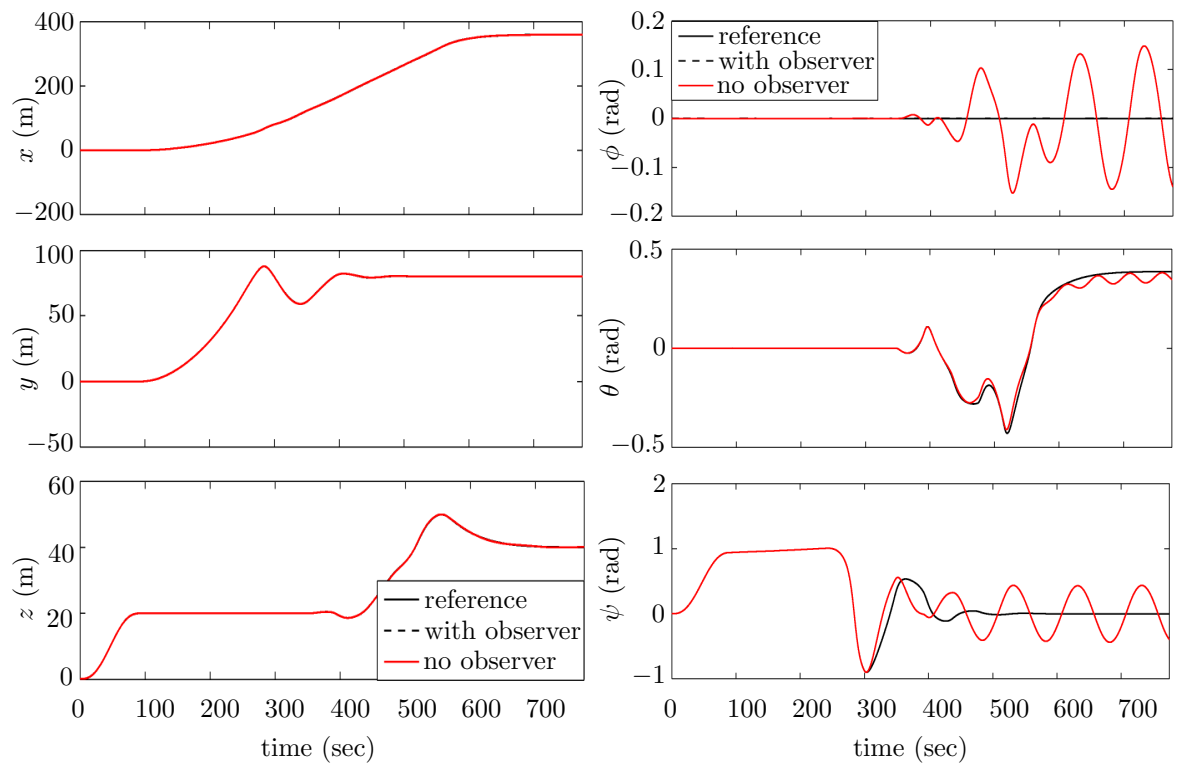
Fig. 9.5: Position and orientation under disturbance
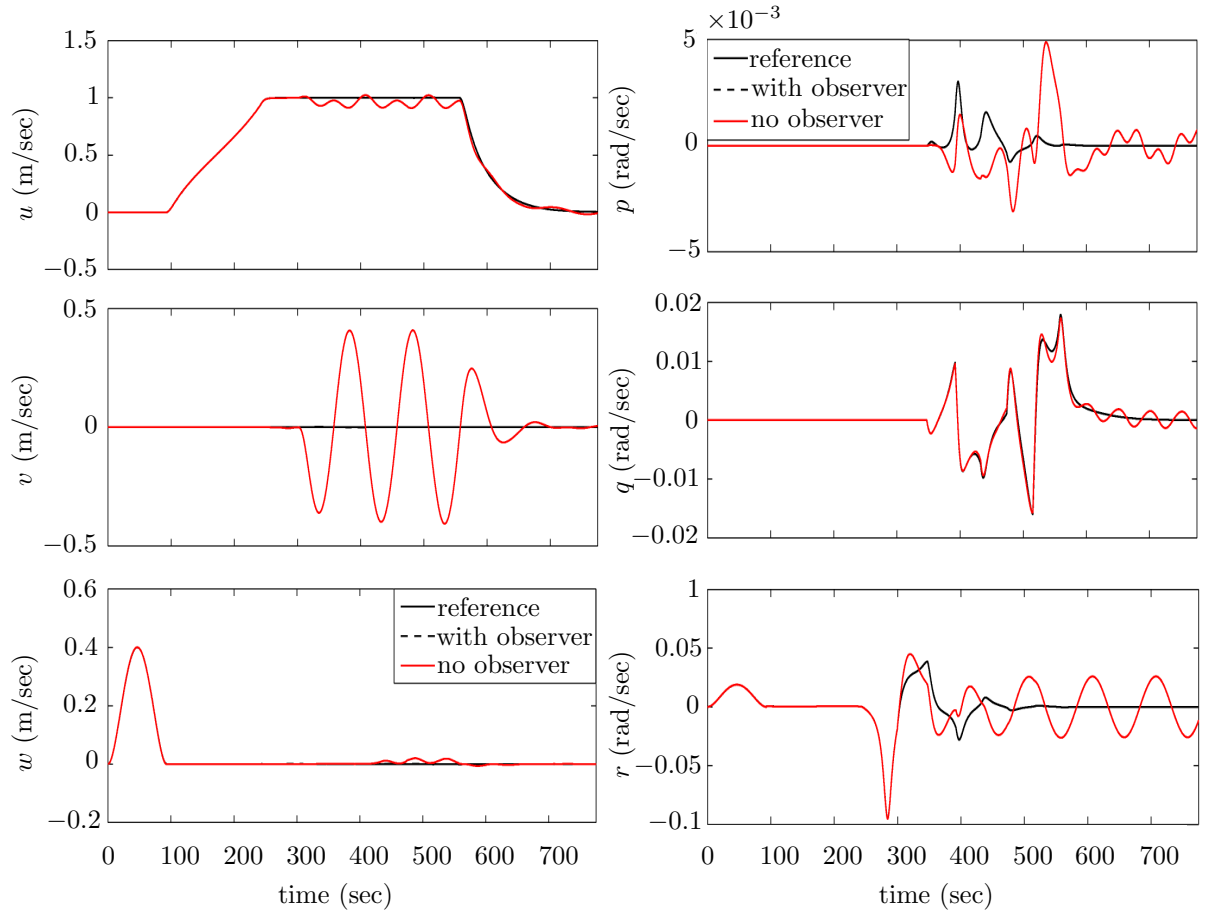
Fig. 9.6: Translational and angular velocities under disturbances

It turns out that the tracking performance is remarkably improved when using the GESO while maintaining the control effort at approximately the same level, see Figure 9.7.

Note that for reducing the peaking-phenomenon after initializing, which may arise for high gain observers, we use a "clutch" function for smoothing the transient peaking responses in the observer variables [88].

In our case, we employ

$$s_c(t) = \begin{cases} 1 & \text{for } t > \varepsilon_c \\ \sin^{q_c}\left(\frac{\pi t}{2\varepsilon_c}\right) & \text{for } t \leq \varepsilon_c \end{cases} \text{, for } q_c = 10 \text{ and } \varepsilon_c = 6$$
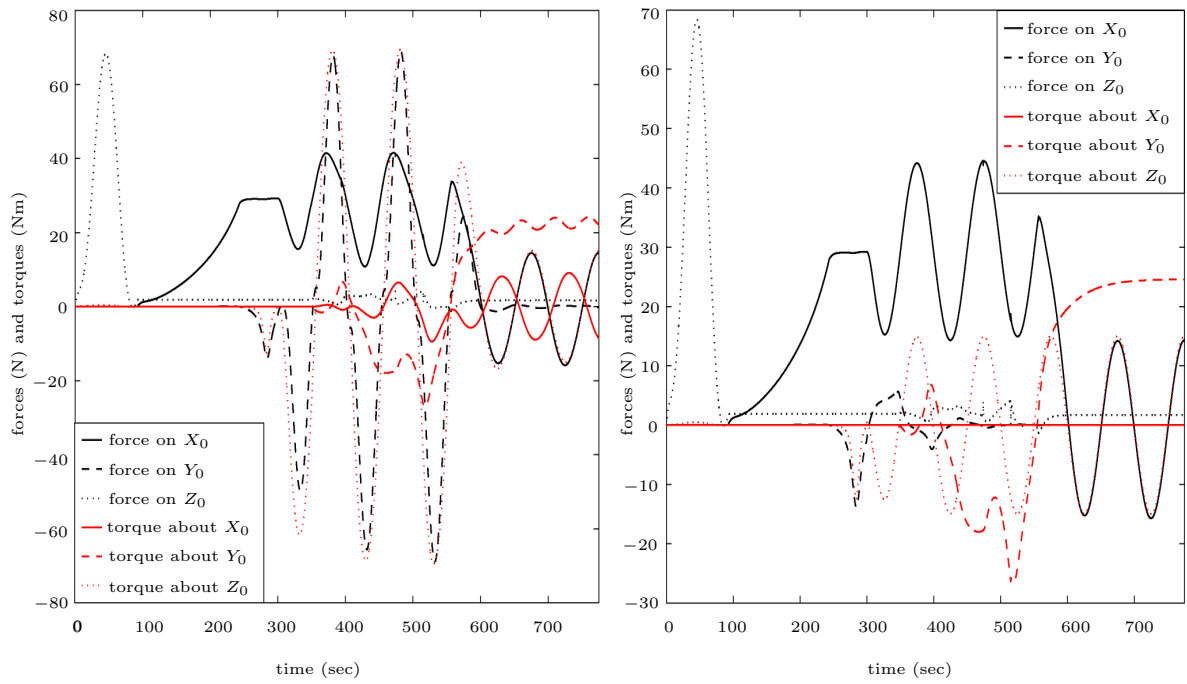
Fig. 9.7: Forces and torques with (right)/ without observer (left)

Bibliography

[1] K. P. Valavanis, D. Gracanin, M. Matijasevic, R. Kolluru, and G. A. Demetriou, "Control architectures for autonomous underwater vehicles," in *IEEE Control Systems*, vol. 17, no. 6, pp. 48–64, 1997. 1

[2] P. J. Craven, R. Sutton, and R. S. Burns, "Control strategies for unmanned underwater vehicles," in *Journal of Navigation*, vol. 51, no. 1, pp. 79–105, 1998. 1

[3] Y. Nakamura and S. Savant, "Nonlinear tracking control of autonomous underwater vehicles," in *the IEEE International Conference on Robotics and Automation*, pp. A4–A9, 1992. 1

[4] S. Arinaga, S. Nakajima, H. Okabe, A. Ono, and Y. Kanayama, "A motion planning method for an auv," in *the Symposium on Autonomous Underwater Vehicle Technology*, pp. 477–484, 1996. 1

[5] D. Fu-guang, J. Peng, B. Xin-qian, and W. Hong-jian, "Auv local path planning based on virtual potential field," in *IEEE International Conference Mechatronics and Automation*, pp. 1711–1716, 2005. 1

[6] M. Breivik and T. Fossen, "Guidance-based path following for autonomous underwater vehicles," in *MTS/IEEE OCEANS*, pp. 2807–2814, 2005. 1, 3

[7] R. Skjetne, T. Fossen, and P. V. Kokotović, "Robust output maneuvering for a class of nonlinear systems," in *Automatica*, vol. 40, no. 3, pp. 373–383, 2004. 1, 3

[8] A. P. Aguiar, D. B. Dačić, J. P. Hespanha, and P. Kokotović, "Path-following or reference-tracking? an answer relaxing the limits to performance," in *the 5th IFAC/EURON Symposium on Intelligent Autonomous Vehicles*, 2004. 1

[9] E. Besada-Portas, L. de la Torre, M. Jesus, and B. de Andrés-Toro, "Evolutionary trajectory planner for multiple uavs in realistic scenarios," in *IEEE Transactions on Robotics*, vol. 26, no. 4, pp. 619–634, 2010. 1

[10] S. Mittal and K. Deb, "Three-dimensional offline path planning for uavs using multiobjective evolutionary algorithms," in *IEEE Congress on Evolutionary Computation*, pp. 3195–3202, 2007. 1

[11] I. Nikolos, N. Tsourveloudis, and K. Valavanis, "Evolutionary algorithm based path planning for multiple uav cooperation," in *Advances in Unmanned Aerial Vehicles*, pp. 309–340, 2007. 2

[12] J. M. de la Cruz, E. Besada-Portas, L. Torre-Cubillo, B. Andres-Toro, and J. A. Lopez-Orozco, "Evolutionary path planner for uavs in realistic environments," in *the 10th annual conference on Genetic and evolutionary computation*, pp. 1477–1484, 2008. 2

[13] C. Liu, S. Fan, B. Li, S. Chen, Y. Xu, and W. Xu, "Path planning for autonomous underwater vehicle docking in stationary obstacle environment," in *IEEE OCEANS*, pp. 1–5, 2016. 2

[14] J.-D. Boissonnat, A. Cérézo, and J. Leblond, "Shortest paths of bounded curvature in the plane," in *Journal of Intelligent and Robotic Systems*, vol. 11, no. 1-2, pp. 5–20, 1994. 2

[15] L. E. Dubins, "On curves of minimal length with a constraint on average curvature, and with prescribed initial and terminal positions and tangents," in *American Journal of Mathematics*, vol. 79, no. 3, pp. 497–516, 1957. 2

[16] B. Fornberg and J. Zuev, "The runge phenomenon and spatially variable shape parameters in rbf interpolation," in *Computers & Mathematics with Applications*, vol. 54, no. 3, pp. 379–398, 2007. 2

[17] J. C. Mason and D. C. Handscomb, *Chebyshev polynomials*. Chapman & Hall/CRC Press, Boca Raton, 2002. 2

[18] A. M. Lekkas, *Guidance and path-planning systems for autonomous vehicles*. PhD thesis, Norges teknisk-naturvitenskapelige universitet, Norway, 2014. 2

[19] F. N. Fritsch and R. E. Carlson, "Monotone piecewise cubic interpolation," in *SIAM Journal on Numerical Analysis*, vol. 17, no. 2, pp. 238–246, 1980. 2

[20] C. Manni, "On shape preserving c2 hermite interpolation," in *BIT Numerical Mathematics*, vol. 41, no. 1, pp. 127–148, 2001. 2

[21] K. Y. Pettersen and H. Nijmeijer, "Underactuated ship tracking control: theory and experiments," in *International Journal of Control*, vol. 74, no. 14, pp. 1435–1446, 2001. 2, 74

[22] K. Wichlund, O. Sordalen, and O. Egeland, "Control properties of underactuated vehicles," in *the IEEE International Conference on Robotics and Automation*, vol. 2, pp. 2009–2014, 1995. 2, 74

[23] K. Y. Pettersen and O. Egeland, "Exponential stabilization of an underactuated surface vessel," in *Journal of Modelling, Identification and Control*, vol. 18, no. 3, pp. 239–248, 1997. 2

[24] M. Reyhanoglu, "Control and stabilization of an underactuated surface vessel," in *the 35th IEEE Conference on Decision and Control*, vol. 3, pp. 2371–2376, 1996. 2

[25] K. Y. Pettersen and H. Nijmeijer, "Global practical stabilization and tracking for an underactuated ship-a combined averaging and backstepping approach," in *Journal of Modelling, Identification and Control*, vol. 20, no. 4, pp. 189–199, 1999. 2

[26] J.-M. Godhavn, "Nonlinear tracking of underactuated surface vessels," in *the 35th IEEE Conference on Decision and Control*, vol. 1, pp. 975–980, 1996. 2

[27] S. P. Berge, K. Ohtsu, and T. Fossen, "Nonlinear control of ships minimizing the position tracking errors," in *Journal of Modelling, Identification and Control*, vol. 20, no. 3, pp. 177–187, 1999. 2

[28] K. Pettersen and H. Nijmeijer, "Tracking control of an underactuated surface vessel," in *the 37th IEEE Conference on Decision and Control*, vol. 4, pp. 4561–4566, 1998. 2

[29] I. Kaminer, A. Pascoal, E. Hallberg, and C. Silvestre, "Trajectory tracking for autonomous vehicles: An integrated approach to guidance and control," in *Journal of Guidance, Control, and Dynamics*, vol. 21, no. 1, pp. 29–38, 1998. 2

[30] A. Wahl and E. Gilles, "Model predictive versus linear quadratic control for the tracking problem of automatic river navigation," in *IEEE European Control Conference*, pp. 1137–1142, 1999. 3

[31] P. Encarnação and A. Pascoal, "3d path following for autonomous underwater vehicle," in *the 39 th IEEE Conference on Decision and Control*, 2000. 3

[32] A. P. Aguiar, J. P. Hespanha, *et al.*, "Trajectory-tracking and path-following of underactuated autonomous vehicles with parametric modeling uncertainty," in *IEEE Transactions on Automatic Control*, vol. 52, no. 8, pp. 1362–1379, 2007. 3

[33] H. Li, P. Xie, and W. Yan, "Receding horizon formation tracking control of constrained underactuated autonomous underwater vehicles," in *IEEE Transactions on Industrial Electronics*, 2016. 3

[34] W. Caharija, K. Y. Pettersen, J. T. Gravdahl, and E. Børhaug, "Path following of underactuated autonomous underwater vehicles in the presence of ocean currents," in *51st IEEE Conference on Decision and Control*, pp. 528–535, 2012. 3

[35] X. Xiang, L. Lapierre, C. Liu, and B. Jouvencel, "Path tracking: combined path following and trajectory tracking for autonomous underwater vehicles," in *IEEE/RSJ International Conference on Intelligent Robots and Systems*, pp. 3558–3563, 2011. 3

[36] P. Encarnação and A. Pascoal, "Combined trajectory tracking and path following: an application to the coordinated control of autonomous marine craft," in *the 40th IEEE Conference on Decision and Control*, vol. 1, pp. 964–969, 2001. 3

[37] R. Hindman and J. Hauser, "Maneuver modified trajectory tracking," in *the IEEE International Symposium on Mathematical Theory of Networks and Systems*, pp. 1473–1479, 1996. 3

[38] L. Piegl and W. Tiller, *The NURBS Book, second edition.* Springer, New York, 1997. 7

[39] L. Biagiotti and C. Melchiorri, *Trajectory planning for automatic machines and robots.* Springer, Berlin Heidelberg, 2008. 7, 13, 14

[40] E. V. Shikin and A. I. Plis, *Handbook on Splines for the User.* CRC Press, Boca Raton, 1995. 7

[41] T. Fossen, *Marine control systems: guidance, navigation and control of ships, rigs and underwater vehicles.* Marine Cybernetics AS, Norway, 2002. 8, 22, 25, 27, 30, 31, 38, 40

[42] R. Al Azrak, K. Treichel, and J. Reger, "Discrete-time auv tracking controller design based on disturbance rejection and dynamic trajectory planning," in *MTS/IEEE OCEANS*, pp. 1–8, 2013. 8, 40, 64

[43] G. Rordriguez and S. Seatzu, "Numerical solution of the finite moment problem in a reproducing kernel hilbert space," in *Journal of Computational and Applied Mathematics*, vol. 33, no. 3, pp. 233–244, 1990. 13

[44] R. Bennell and J. Mason, "Continuous approximation methods for the regularization and smoothing of integral transforms," in *Journal of Mathematics*, vol. 19, no. 1, 1989. 13

[45] H. Park, "Choosing nodes and knots in closed b-spline curve interpolation to point data," in *Computer-Aided Design*, vol. 33, no. 13, pp. 967–974, 2001. 14

[46] T. Fossen, *Nonlinear modelling and control of underwater vehicles.* PhD thesis, Norwegian University of Science and Technology, 1991. 22, 25, 31, 33

[47] T. Fossen, *Guidance and control of ocean vehicles.* John Wiley & Sons, Chichester, 1994. 22, 25, 26, 27, 31, 33, 35

[48] E. SNAM, "Nomenclature for treating the motion of a submerged body through a fluid," in *Technical and Research Bulletin*, pp. 5–15, 1950. 23, 27, 35

[49] T. Fossen, *Guidance and control of ocean vehicles.* John Wiley & Sons, Chichester, 1994. 24, 25

[50] D. Perrault, N. Bose, S. O'Young, and C. D. Williams, "Sensitivity of auv added mass coefficients to variations in hull and control plane geometry," *in Ocean Engineering*, vol. 30, no. 5, pp. 645–671, 2003. 27

[51] F. H. Imlay, "The complete expressions for added mass of a rigid body moving in an ideal fluid," tech. rep., David Taylor Model Basin (DTMB), Washington DC, 1961. 27

[52] W. Wang and C. M. Clark, "Modeling and simulation of the videoray pro iii underwater vehicle," in *IEEE OCEANS-Asia Pacific*, pp. 1–7, 2007. 31

[53] O. M. O. M. Faltinsen, *Sea loads on ships and offshore structures.* Cambridge University Press, New York, 1990. 32

[54] G. Griffiths, *Technology and applications of autonomous underwater vehicles*, vol. 2. CRC Press, Boca Raton, 2002. 35

[55] L. Biagiotti and C. Melchiorri, *Trajectory planning for automatic machines and robots.* Springer, Berlin Heidelberg, 2008. 38

[56] H. Yuan and Z. Qu, "Optimal real-time collision-free motion planning for autonomous underwater vehicles in a 3d underwater space," in *IET Control Theory & Applications*, vol. 3, no. 6, pp. 712–721, 2009. 39

[57] J. Han, "From pid to active disturbance rejection control," in *IEEE Transactions on Industrial Electronics*, vol. 56, no. 3, pp. 900–906, 2009. 40, 43

[58] Z. Gao, "Active disturbance rejection control: a paradigm shift in feedback control system design," in *IEEE American Control Conference*, pp. 2399–2405, 2006. 40

[59] A. Radke and Z. Gao, "A survey of state and disturbance observers for practitioners," in *IEEE American Control Conference*, pp. 5183–5188, 2006. 40, 43

[60] Z. Gao, "Active disturbance rejection control: A paradigm shift in feedback control system design," in *IEEE American Control Conference*, pp. 2399–2405, 2006. 43

[61] R. Miklosovic, A. Radke, and Z. Gao, "Discrete implementation and generalization of the extended state observer," in *IEEE American Control Conference*, pp. 2209–2214, 2006. 43

[62] I. D. Landau, R. Lozano, M. M'Saad, and A. Karimi, *Adaptive control: algorithms, analysis and applications.* Springer Science & Business Media, New York, 2011. 46, 47

[63] J.-J. E. Slotine, W. Li, *et al.*, *Applied nonlinear control*, vol. 199. Prentice-Hall Englewood Cliffs, New Jersey, 1991. 46

[64] S. Sastry and M. Bodson, *Adaptive control: stability, convergence and robustness.* Prentice-Hall Advanced Reference Series, New Jersey, 2011. 46

[65] P. Ioannou and J. Sun, *Robust Adaptive Control.* Prentice-Hall, New Jersey, 1996. 46, 47

[66] H. Xu, M. D. Mirmirani, and P. A. Ioannou, "Adaptive sliding mode control design for a hypersonic flight vehicle," in *Journal of guidance, control, and dynamics*, vol. 27, no. 5, pp. 829–838, 2004. 47

[67] K. B. Ariyur and M. Krstic, *Real-time optimization by extremum-seeking control*. John Wiley & Sons, Inc., New York, 2003. 47

[68] M. Krstic, P. V. Kokotovic, and I. Kanellakopoulos, *Nonlinear and Adaptive Control Design*. John Wiley & Sons, New York, 1995. 48, 50, 57, 102

[69] H. Khalil, *Nonlinear Systems*. Prentice Hall, Upper Saddle River, New Jersey, 2002. 53, 58, 98, 105, 117

[70] M.-L. Tseng and M.-S. Chen, "Chattering reduction of sliding mode control by low-pass filtering the control signal," *Asian Journal of control*, vol. 12, no. 3, pp. 392–398, 2010. 53

[71] M. M. Polycarpou and P. A. Ioannou, "A robust adaptive nonlinear control design," in *IEEE American Control Conference*, pp. 1365–1369, 1993. 53

[72] B. Yao, *Adaptive robust control of nonlinear systems with application to control of mechanical systems*. PhD thesis, University of California at Berkeley, 1996. 53

[73] Z.-P. Jiang and L. Praly, "Design of robust adaptive controllers for nonlinear systems with dynamic uncertainties," in *Automatica*, vol. 34, no. 7, pp. 825–840, 1998. 54

[74] R. M. Corless, G. H. Gonnet, D. E. Hare, D. J. Jeffrey, and D. E. Knuth, "On the lambert w function," in *Advances in Computational Mathematics*, vol. 5, no. 1, pp. 329–359, 1996. 56, 57

[75] T. I. Fossen and J. P. Strand, "A tutorial on nonlinear backstepping: Applications to ship control," in *Journal of Modelling, Identification and Control*, vol. 20, no. 2, pp. 83–135, 1999. 61, 62

[76] E. Lavretsky and K. Wise, *Robust and adaptive control: with aerospace applications*. Springer Science & Business Media, New York, 2012. 67, 72

[77] T. E. Gibson, A. M. Annaswamy, and E. Lavretsky, "Improved transient response in adaptive control using projection algorithms and closed loop reference models," in *AIAA Guidance Navigation and Control Conference*, 2012. 67

[78] E. Lavretsky, T. E. Gibson, and A. M. Annaswamy, "Projection operator in adaptive systems," in *arXiv*, 2011. 67, 72

[79] J.-B. Pomet and L. Praly, "Adaptive nonlinear regulation: estimation from the lyapunov equation," in *IEEE Transactions on Automatic Control*, vol. 37, no. 6, pp. 729–740, 1992. 67, 70

[80] R. W. Brockett *et al.*, "Asymptotic stability and feedback stabilization," in *Differential Geometric Control Theory*, vol. 27, no. 1, pp. 181–191, 1983. 74

[81] Y.-l. Liao, L. Wan, and J.-y. Zhuang, "Backstepping dynamical sliding mode control method for the path following of the underactuated surface vessel," in *Procedia Engineering*, vol. 15, pp. 256–263, 2011. 74

[82] K. Do and J. Pan, "Robust and adaptive path following for underactuated autonomous underwater vehicles," in *the American Control Conference*, vol. 3, pp. 1994–1999, 2003. 84, 93

[83] K. D. Do, J. Pan, and Z.-P. Jiang, "Robust and adaptive path following for underactuated autonomous underwater vehicles," in *Ocean Engineering*, vol. 31, no. 16, pp. 1967–1997, 2004. 93, 101

[84] E. Panteley and A. Loria, "Growth rate conditions for uniform asymptotic stability of cascaded time-varying systems," in *Automatica*, vol. 37, no. 3, pp. 453–460, 2001. 93

[85] K. Do, Z. Jiang, and J. Pan, "Robust global stabilization of underactuated ships on a linear course," in *the American Control Conference*, pp. 304–309, 2002. 101

[86] K. Do, Z. Jiang, and J. Pan, "Robust global stabilization of underactuated ships on a linear course: state and output feedback," in *International Journal of Control*, vol. 76, no. 1, pp. 1–17, 2003. 101

[87] R. Skjetne and T. I. Fossen, "Nonlinear maneuvering and control of ships," in *MTS/IEEE OCEANS*, vol. 3, pp. 1808–1815, 2001. 120

[88] H. Sira-Ramírez, "Robust linear output feedback control of a synchronous generator," in *American Control Conference*, pp. 3728–3733, 2011. 142